Sentaro Takahashi *Editor*

Radiation Monitoring and Dose Estimation of the Fukushima Nuclear Accident

Radiation Monitoring and Dose Estimation of the Fukushima Nuclear Accident

Sentaro Takahashi
Editor

Radiation Monitoring and Dose Estimation of the Fukushima Nuclear Accident

Springer Open

Editor
Sentaro Takahashi
Research Reactor Institute
Kyoto University
Sennan-gun, Osaka, Japan

ISBN 978-4-431-54582-8 ISBN 978-4-431-54583-5 (eBook)
DOI 10.1007/978-4-431-54583-5
Springer Tokyo Heidelberg New York Dordrecht London

Library of Congress Control Number: 2013955611

Printed on acid-free paper

Springer is part of Springer Science+Business Media (www.springer.com)

Foreword I

On March 11, 2011, a massive earthquake and the resultant tsunami struck the Tohoku area of Japan, causing serious damage to TEPCO's Fukushima Daiichi Nuclear Power Plant and the release of a significant quantity of radionuclides into the surrounding environment. This accident underlined the necessity of establishing more comprehensive scientific research for promoting safety in nuclear technology. In this situation, the Kyoto University Research Reactor Institute (KURRI) established a new research program called the "KUR Research Program for Scientific Basis of Nuclear Safety" in 2012.

In nuclear safety study in our country, study of the prevention of nuclear accidents might have been encouraged and action might have been lacking to measure nuclear safety from a wider point of view, including the safety measures after the accident or ensuring the safety of residents. A long time is needed for the improvement of the situation, but the social needs for the reinforcement of nuclear safety are considered to increase rapidly. Among the social needs, the advancement of disaster prevention technology for natural disasters such as earthquakes and tsunamis, the reinforcement of measures for the influence of accidents, and the reinforcement of the safety management of spent fuels and radioactive wastes are demanded, not to mention the reinforcement of nuclear reactor safety. Also demanded are the underlying mechanism investigation and accurate assessment for the effect of radiation on the human body and life. As with all premises, detailed inspection and analysis of the cause of the accident, various factors that created the damage serious, and the resulting influence and damage are indispensable.

In the Research Program for the Scientific Basis of Nuclear Safety, an annual series of international symposia was planned along with specific research activities. The first in the series of symposia, entitled "The International Symposium on Environmental Monitoring and Dose Estimation of Residents After Accident of TEPCO's Fukushima Daiichi Nuclear Power Stations," was held on December 14, 2012, concerning the radiological effects of the accident on the public. The purpose of the symposium was to collate data on environmental radioactivity and the

radiation dose on residents, to discuss and verify the data, and to clarify the actual situation of environmental contamination and resultant radiation exposure to residents. The second is planned to be held on November 28, 2013, with the title of "International Symposium on Nuclear Back-end Issues and the Role of Nuclear Transmutation Technology after the Accident of TEPCO's Fukushima Daiichi Nuclear Power Stations."

This book is edited, and some chapters are written, by the members of the KUR Research Program for Scientific Basis of Nuclear Safety. It is expected to contribute to better understanding of the impact of the accident.

On behalf of KURRI, I wish to thank all the contributors to this publication as well as the reviewers who kindly made great efforts to check the scientific accuracy of the manuscript. KURRI also hopes that this publication will promote further progress in nuclear safety research and will contribute to the faster recovery of the people who have suffered damage from the accident.

Kyoto, Japan Hirotake Moriyama

Foreword II

It is inevitable that major disasters such as the nuclear accident at the Fukushima Daiichi nuclear power plant in March 2011, which followed an earthquake and a tsunami, have major impacts on society. These impacts cover many dimensions, such as human, economic, and societal. The *human* dimension can include the loss of relatives and friends as well as that of wider social networks, the impairment of individual health as well as the deterioration of the health status in the population at large, and the restrictions of personal freedom and of the scope of individual development; the *economic* dimension may include the loss of property and of job opportunities; and the *societal* dimension may include the loss of public trust and the development of desperation in a population. All these dimensions have been observed in the population of Japan after the catastrophic events in March 2011.

There is an ethical obligation of science to serve society and to help the people of Japan to better understand what happened, how it happened, and why. This obligation can best be fulfilled by providing sound evidence of the impact of the accident on the population and the environment, including the related health risks and consequences. Although this is a complex undertaking and an ambitious task, there is no alternative. Public trust in science was lost in the aftermath of the accident. Openness and transparency are key issues in this process to regain trust in science.

The United Nation Scientific Committee on the Effects of Atomic Radiation (UNSCEAR) has allocated substantial resources to develop a comprehensive and independent assessment of the accident consequences; the report will be published in fall of 2013. Because of the loss of infrastructure caused by the earthquake and the tsunami, the data needed for a detailed assessment of the environmental situation and the doses to the most exposed members of the public during the early days and weeks after the accident were not available to full satisfaction. There was, and still is, the need to fill the gaps in measurement data by model calculations and to keep the existing uncertainties of the dose and risk assessments as low as reasonably achievable.

The scientific community in Japan regarding radiation-related environmental and health risks has always been at the forefront worldwide. Their scientific contributions toward a better understanding of the current situation are indispensable.

The Kyoto University Reactor Institute (KURRI) has responded in a timely manner to the urgent needs for scientific input by the establishing the "Research Program for Scientific Basis of Nuclear Safety." One of the basic features of the program is to provide a platform for the organization of an annual series of international symposia that address all relevant aspects of the accident development and of its consequences along with identified research activities. The first of this series was organized in December 2012; it focused on all issues related to "Environmental monitoring and dose estimation of residents after accident of TEPCO's Fukushima Daiichi Nuclear Power Stations." The research results presented during the symposium covered a wide spectrum of research activities and documented the state of our knowledge as well as the remaining unknowns and uncertainties, particularly for the early days and weeks after the accident. The discussion of the scientific presentations clearly identified needs for focused scientific work in the years to come. Experience from other emergencies of this nature clearly indicate that a major effort will be needed over extended periods of time to arrive at scientifically sound results that can answer the questions of the population. Two remaining key questions were identified: a better understanding of the source term to the atmosphere during the days and weeks after the accident, and the quantification of releases and the runoff to the ocean.

This publication summarizes the findings of the work presented during the symposium. It contributes toward a better understanding of the overall situation. I hope that it will also contribute to a rapid recovery for the people who have encountered major losses and damages from the accident.

Vienna, Austria Wolfgang Weiss

Preface

The nuclear accident at the Fukushima Daiichi Nuclear Power Plant of the Tokyo Electric Power Company (TEPCO), triggered by the huge earthquake and tsunami in eastern Japan on 11 March 2011, caused serious environmental contamination by the release of radioactive nuclides. Immediately after the accident, monitoring, surveys, and research activities were initiated to estimate the levels of contamination and to take suitable countermeasures, including evacuation, establishment of restricted areas, and decontamination. Not only governmental organizations but also small private groups and even individuals took part in these activities.

The Kyoto University Research Reactor Institute organized an international symposium entitled "Environmental monitoring and dose estimation of residents after accident of TEPCO's Fukushima Daiichi Nuclear Power Stations" in December 2012. In the symposium, the results of a wide range of monitoring and dose assessment activities were reported and discussed. Although the proceedings of the symposium had been published, many people who were interested in this issue, including researchers, staff members of governmental organizations, residents near the accident site, and reporters for the mass media, made strong requests for the publication of a more comprehensive and conclusive book. Those requests have prompted us to publish this book as quickly as possible. All the chapters in the book are based on the latest data and findings, although some of the chapters were adapted from material initially reported at the symposium and then updated.

We invited Prof. Jun Sugimoto, a leading researcher of nuclear reactors and severe nuclear accident, to write a technical review on the outline of the accident at Fukushima. The reader will very easily be able to understand what occurred in the reactor during the early days. Dr. Jiro Inaba kindly wrote a commentary review on the radiation dose estimation. He has devoted his work to establishing a framework of radiation dosage especially as it affects the public, including fetuses and children, as a member of the International Commission of Radiation Protection (ICRP). His review shows the concept of dose assessment with relationship to the actual situation in Fukushima. Following these review articles, a series of scientific reports

presents vital data and findings on radiation surveys of the environment, environmental radioactivity, transfer models and parameters of radioactive nuclides, and dose assessment among residents. These reports contain a wide range of research work carried out in a variety of research activities, from those by large governmental organizations to those by small private groups or individuals. The reports also present data from the early period just after the accident, which are not available elsewhere. The reader thus can find a large collection of valuable and interesting data related to the environmental contamination by radioactive nuclides after the Fukushima accident.

All the chapters in this book were peer-reviewed by specialists in relevant fields, whose names are shown in the List of Cooperators. The editors wish to thank all the authors and the cooperating specialists who worked so hard to publish this book. We hope this volume will serve as both an excellent review and a valuable reference for formulating suitable measures against nuclear accidents and for promoting the science involved in this field.

Osaka, Japan

Sentaro Takahashi
Tomoyuki Takahashi
Hajimu Yamana

Cooperators

Satoshi Fukutani Research Reactor Institute, Kyoto University, Osaka, Japan

Jiro Inaba Radiation Effects Association, Tokyo, Japan

Hirotake Moriyama Research Reactor Institute, Kyoto University, Osaka, Japan

Ken Nakajima Research Reactor Institute, Kyoto University, Osaka, Japan

Kimiaki Saito Japan Atomic Energy Agency, Ibarakim, Japan

Sentaro Takahashi Research Reactor Institute, Kyoto University, Osaka, Japan

Tomoyuki Takahashi Research Reactor Institute, Kyoto University, Osaka, Japan

Shigeo Uchida Research Center of Radiation Protection, National Institute of Radiological Sciences, Chiba, Japan

Wolfgang Weiss United Nations Scientific Committee on the Effects of Atomic Radiation, Vienna, Austria

Hajimu Yamana Research Reactor Institute, Kyoto University, Osaka, Japan

Hiromi Yamazawa Nagoya University, Nagoya, Japan

Satoshi Yoshida Research Center of Radiation Protection, National Institute of Radiological Sciences, Chiba, Japan

Contents

Part VI Source Estimation

Part VII Dose Assessment

Part I
Introduction

Chapter 1
Outline of the Environmental Monitoring of Tepco's Fukushima Daiichi Nuclear Power Plant Accident

Tomoyuki Takahashi

Abstract The Great East Japan Earthquake and the subsequent tsunami caused severe damage to TEPCO's Fukushima Daiichi nuclear power station, and large amounts of radioactive materials were released to the environment. Environmental monitoring data are very important for evaluating radiation exposure and health effects on the public. Therefore, various kinds of environmental monitoring continue to be performed by the Japanese and prefectural government, certain research institutes, or individuals. It is important to collect a wide range of these data to obtain an accurate estimation of the radiation dose.

Keywords Environmental monitoring • Environmental radioactivity • Radiation exposure doses • Radiation survey

1.1 Introduction

The Great East Japan Earthquake and the subsequent tsunami that occurred on March 2011 in the eastern area of Japan caused severe damage to TEPCO's Fukushima Daiichi nuclear power plant (FDNPP). As a result of the core meltdown, a large amount of radioactive material was released from the reactors to the atmospheric and oceanic environment, causing radiation exposure to the public and FDNPP workers. To estimate the effects of the accident, it is necessary to evaluate accurately the levels of radiation exposure resulting from the accident.

T. Takahashi (✉)
Kyoto University Research Reactor Institute,
2-1010, Asashiro-nishi, Kumatori-cho, Osaka 590-0494, Japan
e-mail: tomoyuki@rri.kyoto-u.ac.jp

S. Takahashi (ed.), *Radiation Monitoring and Dose Estimation of the Fukushima Nuclear Accident*, DOI 10.1007/978-4-431-54583-5_1,

1.2 Exposure Pathways

To evaluate the exposure doses resulting from radionuclides released to the environment from the nuclear facilities, it is important to identify the behaviors of radionuclides in the environment. However, the mechanisms affecting the behaviors of radioactive materials are very complicated. They are related to a wide range of research fields, including physics, chemistry, and biology. In addition, the land usage modes, which include forests, urban areas, farm fields, and rice paddy fields, have a great influence on the behavior of radionuclides. The lifestyle of the public, such as their intake of foods, also affects the level of doses.

Figure 1.1 shows major transfer and exposure pathways of the radionuclides released from the nuclear facilities into the atmosphere. In the early stage after an accident, external exposure from the radioactive plume and internal exposure by inhalation of the plume are dominant exposure pathways. When the release of radionuclides from the nuclear plants becomes negligible, external exposure from radionuclides deposited in the soil or on buildings is dominant. Internal exposure by the ingestion of contaminated food may be dominant in areas where the air dose rate is relatively low.

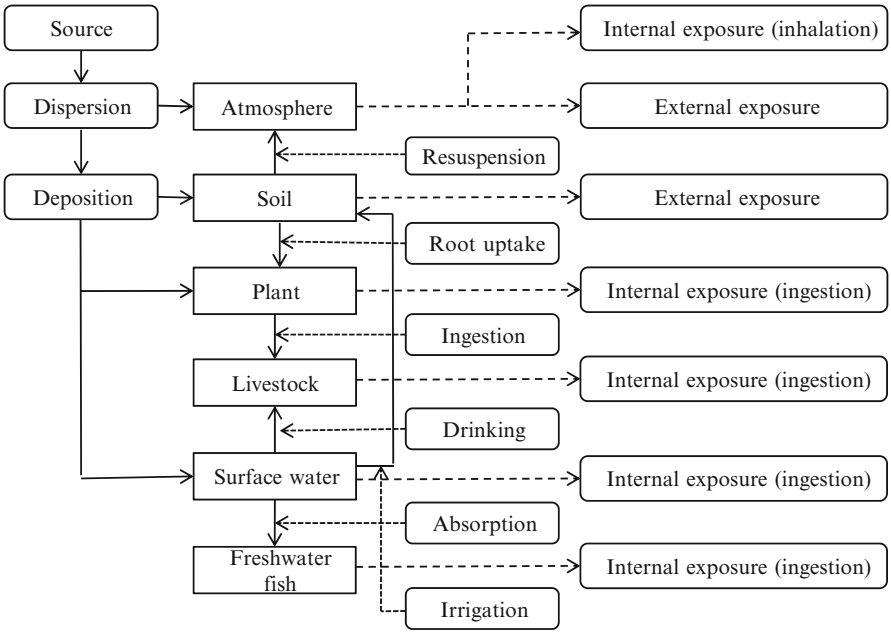

Fig. 1.1 The major transfer pathways and exposure pathways of radionuclides released from nuclear facilities into the atmosphere

Analyses using mathematical models are useful to understand the behavior of radionuclides. Many such models have been developed to predict the behavior of radionuclides in various environmental media and the radiation doses to the public. However, because it is not easy to select suitable models and parameters for a specific situation, environmental monitoring data are very important for evaluating the radiation exposure and health effects on the public.

1.3 Environmental Monitoring

In the early period after the accident, most of the fixed monitoring posts near FDNPP lost their function a a result of the earthquake. Therefore, the Ministry of Education, Culture, Sports, Science and Technology (MEXT) started air dose rate monitoring using monitoring cars [1]. In parallel with such monitoring, a radiation survey on the environment and measurement of the concentration of radionuclides in some environmental media (such as airborne dust, food, drinking water, weeds, groundwater, and soil) was initiated by the Japanese and prefectural governments [1, 2]. Radioiodine, radiocesium, and some other radionuclides were detected in these environmental samples. These monitoring data were utilized for planning measures to protect the public.

Comprehensive environmental monitoring was conducted by MEXT with the cooperation of various universities and research institutes, and distribution maps of radiation dose and soil deposition density were prepared [3]. For example, distribution maps of ambient dose rates based on continuous measurement results through a vehicle-borne survey are shown in Fig. 1.2. This vehicle-borne survey was mainly carried out by the KURAMA system [4]; the details of this system are presented in this book in Chap. 7. The vehicle-borne survey was carried out repeatedly, and distribution maps of ambient dose rates prepared by the survey are used to predict the reduction of dose rates in future [5]. Various kinds of environmental monitoring continue to be conducted by the Japanese and prefectural governments.

Some research organizations or individuals in Japan also carried out environmental monitoring from an early stage after the accident. The "Proceedings of International Symposium on Environmental Monitoring and Dose Estimation of Residents after Accident of TEPCO's Fukushima Daiichi Nuclear Power Stations" [6] include 12 papers on a radiation survey on the environment and 18 papers on environmental radioactivity related to the accident. For example, Iimoto et al. surveyed the environmental status in and around Tokyo immediately after the accident (see Chap. 5 in this book). Zheng et al. investigated the distribution of plutonium isotopes in marine sediments off the coast of Japan before and after the accident (see Chap. 10 in this book). These monitoring data are important and valuable to supplement the large-scale monitoring data and to accurately estimate the radiation dose for the public.

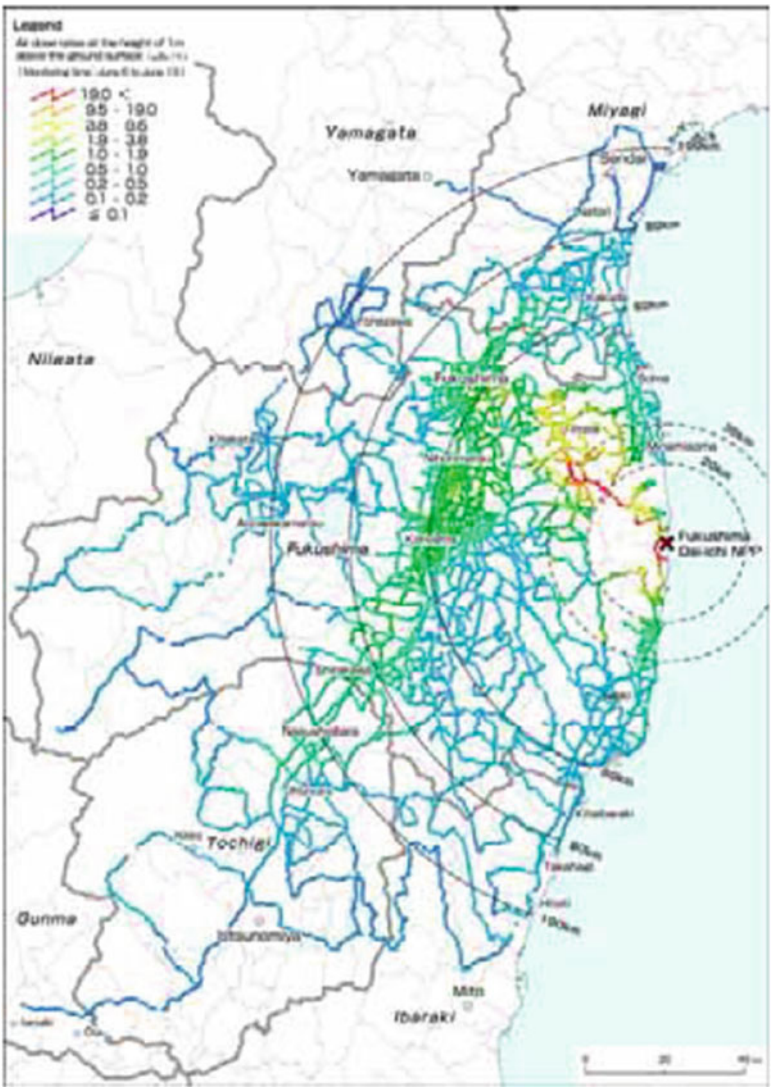

Fig. 1.2 Distribution map of ambient dose rates based on continuous measurement results from vehicle-borne survey [3]

1.4 Conclusion

Environmental monitoring data and analyses conducted using mathematical models are both necessary to accurately evaluate the levels of radiation exposure resulting from the accident. Therefore, it is important to collect a wide range of these data for

an estimation of the radiation dose. In addition, these monitoring data should be preserved as a record of the earthquake and the accident.

References

1. http://radioactivity.nsr.go.jp/en/ (accessed 15 August 2013)
2. http://www.mhlw.go.jp/english/topics/2011eq/index.html (accessed 15 August 2013)
3. Emergency Operation Center, Ministry of Education, Culture, Sports, Science and Technology Agriculture, Forestry and Fisheries Research Council, Ministry of Agriculture, Forestry and Fisheries (2011) Summarized version of the "Results of the Research on Distribution of Radioactive Substances Discharged by the Accident at TEPCO's Fukushima Dai-ichi NPP." http://radioactivity.nsr.go.jp/en/contents/1000/294/view.html
4. Tanigaki M, Okumura R, Takamiya K, Sato N, Yoshino H, Yamana H (2013) Development of a car-borne γ-ray survey system, KURAMA. Nucl Instrum Methods Phys Res A 726:162–168
5. http://www.nsr.go.jp/committee/kisei/data/0016_17.pdf (accessed 15 August 2013) (in Japanese)
6. KUR Research Program for Scientific Basis of Nuclear Safety (2013) Proceedings of international symposium on environmental monitoring and dose estimation of residents after accident of TEPCO's Fukushima Daiichi Nuclear Power Stations

Chapter 2
Outline of the Radiation Dose Estimation of Residents After the Fukushima Daiichi Nuclear Power Plant Accident

Sentaro Takahashi

Abstract The outline of research with relationship to the dose estimation of the residents, which was carried out by a variety of organizations and individuals, is summarized here. This research may be categorized into that for external dose and for internal dose estimation. In addition to the large-scale investigations carried out by governmental organizations, several important studies were carried out by small sectors and individuals.

Keywords Dose estimation • Dose reconstruction • External exposure • Health effects • Internal exposure • Radiation dose

2.1 Introduction

Many residents in the Fukushima Prefecture and neighboring areas were exposed to significant doses of radiation as a result of the radioactive nuclides that were accidentally released from TEPCO'S Fukushima Daiichi nuclear power plant. In the days immediately following the accident, radiation exposure was caused by isotopes of iodine and short-lived radionuclides. As time progressed, radiocesium, that is, cesium-134 and cesium-137, became the major source of radiation. The exposure pathways were external irradiation by radiocesium deposited in the environment and internal irradiation through consumption of foods contaminated with radiocesium.

S. Takahashi (✉)
Kyoto University Research Reactor Institute,
2-1010, Asashiro-nishi, Kumatori-cho, Osaka 590-0494, Japan

Division of Environmental Science and Technology, Faculty of Agriculture,
Kyoto University, Kitashirakawa, Sakyo-ku, Kyoto 606-8502, Japan
e-mail: sentaro@rri.kyoto-u.ac.jp

S. Takahashi (ed.), *Radiation Monitoring and Dose Estimation of the Fukushima Nuclear Accident*, DOI 10.1007/978-4-431-54583-5_2,

Although an accurate estimation of the radiation dose was essential for predicting the health risks to residents and for adopting suitable and effective measures against the radiation risks, it was not easy to achieve an accurate dose assessment for residents because of the complexity of the exposure routes.

Soon after the accident, environmental monitoring of air dose rates and measurements of the concentrations of radioactive nuclides in various environmental materials, including soil, tap water, and food, were widely implemented by the Japanese and local governments, institutes, universities, small groups, and individuals. Some of the results of such monitoring were reported by news media as well as on Internet websites, used for dose estimation for residents, and published in scientific papers. In contrast with this environmental monitoring and these surveys, direct monitoring or measurement of individual radiation doses was not widely carried out in the early stages after the accident. Compared with environmental monitoring, there have not been many attempts to estimate actual radiation doses in the residents, except for large-scale surveys by governmental organizations.

The personal radiation dose is the most important parameter for planning and implementing suitable protective measures. Nevertheless, the attention of the public, governments, and even scientists has mainly been focused on environmental radiation dose and radioactivity, and not particularly on actual radiation dose in individuals, especially in the early stages after the accident. A detailed and easily understandable explanation of the concept of radiation dose assessment is provided in the excellent commentary article by Dr. Inaba in this book (see Chap. 4). In this chapter, we outline the activities performed in an attempt to monitor, measure, or estimate the personal radiation doses of the residents, based mainly on the information presented at the International Symposium on Environmental Monitoring and Dose Estimation of Residents after the Accident of TEPCO's Fukushima Daiichi Nuclear Power Stations, organized by Kyoto University Research Reactor Institute on December 2012 (hereafter referred to as "The Symposium").

2.2 External Dose Estimation

There are two main pathways in external exposure: exposure from a radioactive plume released from nuclear facilities into the atmosphere in the early stages after an accident, and exposure from radionuclides deposited in the surrounding environment, such as land and buildings, after the plume has passed through. A few approaches are generally used to estimate the external radiation doses. A direct and reliable method is personal monitoring with a dosimeter. Personal dosimeters, such as a glass badge and an electric dosimeter, can be used for this purpose. Such direct monitoring is most common for radiation workers in a radiation-controlled area. However, if such direct personal monitoring is not possible, the dose should be estimated using models with some assumptions and environmental monitoring data such as air radiation dose rates.

In the early stages when the radioactive plume was a major source, it was almost impossible to monitor the personal doses of residents directly, and there was no such report in the case of the Fukushima accident. It was speculated that some radiation workers with a personal dosimeter worked with the refugees and were exposed to the radioactive plume. However, personal doses for those radiation workers have not been reported anywhere. In the future, personal dosimeters should be provided to certain public facilities, such as schools and city halls, in specific areas near nuclear facilities such as the emergency planning zone (EPZ), and used for monitoring actual personal radiation doses.

If direct monitoring or measurement of a personal dose is difficult, it may be possible to estimate it using monitoring data (e.g., air radiation dose rates) and analyses of personal behavior, with relatively better accuracy than the estimation of internal doses. The Fukushima Prefecture carried out an estimation of personal doses on a large scale, with the support of the National Institute of Radiological Sciences: this was done as part of the Fukushima Health Management Survey, and 400,000 personal doses were assessed over 4 months, from March to July 2011. This assessment is retrospective; therefore, it is sometimes referred as "dose reconstruction." Detailed data of this assessment are provided at the prefecture's Internet site [1] and are also commented on by Inaba (see Chap. 4).

In the later stages when the deposited radiocesium became the dominant radiation source, some trials began to include the direct monitoring of personal radiation doses, which was handled by local government, groups, and individuals using dosimeters. For example, Fukushima City provided glass badges to 16,223 citizens for 3 months and reported that the cumulative dose of the period was less than 0.2 mSv [2]. In contrast with this large-scale governmental monitoring, some small groups also tried to clarify the actual personal radiation doses locally. Yoshida et al. monitored the personal dose equivalent in local towns in Miyagi Prefecture by using optically stimulated luminescent dosimeters (see Chap. 19). This study provides not only information about the actual radiation doses of the residents, but also scientific explanations of the discrepancy between the personal doses derived from the air dose rates and those measured directly with a personal dosimeter. In Chap. 17, Kinashi et al. report the personal radiation doses of the staff of Kyoto University, who were dispatched to Fukushima to screen the radio-contamination of refugees in the evacuation shelters. This report shows a typical personal radiation dose of a person who stayed in a specific shelter.

Some researchers also estimated personal doses from the environmental monitoring data (e.g., air dose rates), retrospectively and prospectively. Some of these have been reported in this book as well as in the Symposium. Takahara et al. provides an excellent research work on the probabilistic dose assessment of the residents living in contaminated areas (see Chap. 18). Yamamoto et al. measured the air dose rate and estimated the annual dose after the accident in Tochigi Prefecture [3]. Similar assessments had been carried out by Endo et al. for Miyagi Prefecture and by Amano et al. for Chiba Prefecture [4, 5].

2.3 Internal Dose Estimation

Major routes of intake of radionuclides into the human body are by inhalation and oral ingestion. The uptake by inhalation may be categorized into two patterns: inhaled as radioactive gas or particles in the plume, and as particles resuspending from initially deposited sites. The ingestion of foodstuffs and water contaminated with radionuclides is a common route of oral intake, and additionally licking contaminated hands and daily items such as toys becomes a possible intake route, especially for infants and children.

In the early stages after the accident, no attention was paid to internal radiation doses. It seemed that the government intentionally ignored internal exposure. The estimation of internal radiation doses resulting from inhalation of radionuclides is generally complex and difficult, compared with the estimation of external doses. At present, few data and little information are available for estimating the accurate internal doses of each resident resulting from the inhalation of radioactive gases and short-lived radionuclides such as radioiodine in the plume. The National Institute of Radiological Sciences is now making extensive endeavors to reconstruct a system for estimating the internal radiation doses soon after an accident (i.e., a dose reconstruction system). Their interesting and important activities are summarized in Chap. 16 by Kurihara et al.

Radiation exposure of the thyroid is an important issue for human health, especially for children, in the early period after a nuclear accident. Induction of thyroid cancer by the intake of radioiodine in the plume through inhalation had been a major concern because of the Fukushima accident. The Japanese government carried out a screening survey for 1,062 children living near the nuclear plant and reported that no child had an equivalent thyroid dose of more than 50 mSv. Tokonami et al. also measured radioiodine activity in thyroid in situ [6]. Radioiodine activity determined by a whole-body counter in the volunteer workers at the shelter facilities is presented by Kinashi et al. in Chap. 17.

In the later stages after the accident, Fukushima Prefecture started monitoring radiocesium activity in residents by using a whole-body counter. According to their data, 132,011 people were surveyed from 27 July 2011 to 31 March 2013 and only 26 people were estimated to have a committed dose of more than 1 mSv [4, 7].

2.4 Conclusion

The direct monitoring or measurement of personal radiation doses was not carried out sufficiently, especially for internal dose estimation at the early period after the accident, compared with monitoring of radiation dose rates and radioactivity in the environment. The huge numbers of becquerels (Bq) in the environment (kilo, mega, giga) caused severe concern initially, although if these numbers were converted to effective doses, the actual personal radiation doses are not so significant. I wish to

conclude this chapter by stressing that it is important in the future to clarify the personal radiation dose soon after an accident so that suitable and effective protective measures can be undertaken for residents against radiation risks to ensure their safety.

References

1. Fukushima Prefectural, Div. Health Management, http://www.pref.fukushima.jp/imu/kenkou-kanri/250605siryou1-2.pdf
2. Fukushima City, Department of Health and Welfare, http://www.city.fukushima.fukushima.jp/soshiki/71/hkenkou-kanri13051601.html
3. Yamamoto T et al (2012) Measurement of the environmental radiation dose due to the accident at the Fukushima Daiichi Nuclear Power Plant. In: Proceedings of international symposium on environmental monitoring and dose estimation of residents after accident of TEPCO's Fukushima Daiichi Nuclear Power Stations, pp 43–52
4. Endo S et al (2012) Dose rate estimation for northern Miyagi prefecture area in the early stage of the Fukushima Accident. In: Proceedings of international symposium on environmental monitoring and dose estimation of residents after accident of TEPCO's Fukushima Daiichi Nuclear Power Stations, pp 66–70
5. Amano H et al (2012) External and internal radiation doses from the Fukushima Daiichi Nuclear Power Plant accident received by residents of Chiba, Japan. In: Proceedings of international symposium on environmental monitoring and dose estimation of residents after accident of TEPCO's Fukushima Daiichi Nuclear Power Stations, pp 190–193
6. Tokonami S et al (2012) Thyroid doses for evacuees from the Fukushima nuclear accident. Sci Rep 2:507. doi:10.1038/srep00507
7. Fukushima Prefectural, Div. Health Management, http://www.pref.fukushima.jp/imu/wbc/20130628wbc_joukyou.pdf

Part II
Overview

Chapter 3
Accident of Fukushima Daiichi Nuclear Power Plant: Sequences, Fission Products Released, Lessons Learned

Jun Sugimoto

Abstract The nuclear accident that occurred at the Fukushima Daiichi Nuclear Power Plant on March 11, 2011 was caused by the extremely massive earthquake and gigantic tsunami, which resulted in a severe accident that extended over multiple reactors simultaneously. In the present chapter the current status of the accident is described in terms of basic information, sequences of the accident, fission products (FP) released, and lessons learned. Although some details of the accident are still not well known, the sequences, causes, and consequences of the accidents have been basically clarified by the efforts of several investigation committees in Japan. The fission products released to the environment were estimated by the severe accident analysis code, MELCOR, from inside the reactor core, and also by the atmospheric dispersion simulations code, SPEEDI, by coupling with environmental monitoring data in the reverse estimation method from outside the plant. The estimated release amount of ^{131}I is of the order of 120–160 PBq and that of ^{137}Cs is of the order of 8–15 PBq for both estimations. Lessons learned from the accident identified by the investigation committees cover a wide spectrum of insufficient measures, such as for earthquake and tsunami, station blackout, severe accident management, common cause accident at multiple unit site, education and training, chain of command at the accident, disaster prevention, and safety regulation systems. These lessons should be shared all over the world for the higher level of safety assurance of current reactors, and advanced reactors without the need of evacuation in principle should be developed for future.

Keywords Fukushima Daiichi • Severe accident • Fission product • Lessons learned

J. Sugimoto (✉)
Department of Nuclear Engineering, Kyoto University, Kyoto, Japan
e-mail: sugimoto.jun.8u@kyoto-u.ac.jp

S. Takahashi (ed.), *Radiation Monitoring and Dose Estimation of the Fukushima Nuclear Accident*, DOI 10.1007/978-4-431-54583-5_3,

3.1 Introduction

The nuclear accident that occurred at the Fukushima Daiichi Nuclear Power Plant (NPP) of Tokyo Electric Power Co. (TEPCO) on March 11, 2011 was caused by an extremely massive earthquake, the Great East Japan Earthquake, and a gigantic tsunami rarely seen in history, which resulted in the severe accident that extended over multiple reactors simultaneously. Although some details of the accident are still not well known, the sequences, causes, and consequences of the accidents have been basically clarified by the efforts of investigation committees, such as Independent Investigation Commission [1], TEPCO's Investigation Committee [2], National Diet's Investigation Committee [3] and Government's Investigation Committee [4]. The fission products (FPs) released to the environment were estimated by the severe accident analysis code from inside the reactor core, and also by atmospheric dispersion simulation code by coupling with environmental monitoring data in the reverse estimation method from outside the plant. Lessons learned from the accident are identified mostly by those investigation committees, which cover the wide spectrum of insufficient measures in hardware, software, management, and regulation [1–4]. In the present chapter, the current status of the accident is described in terms of basic information, sequences of the accident, estimated fission products released, and lessons learned from the accident.

3.2 Basic Information

The Fukushima Daiichi NPP is located in the towns of Okuma and Futaba, which are in the county of Futaba in Fukushima Prefecture. This NPP consists of six boiling water reactors (BWR) installed, Units 1 through 6, with a total generating capacity of 4,696 MWe (Table 3.1). The reactor model of Unit 1 is BWR3, that of Unit 2 through 4 is BWR4, and that of Unit 5 and 6 is BWR5. The Primary Containment Vessel (PCV) model of Unit 1 through 5 is Mark-1 and that of Unit 6 is Mark-2, respectively. Before the earthquake on March 11, Units 1 through 3 were under operation and Units 4 through 6 were undergoing periodic inspection. Unit 4 was undergoing a major construction for renovations, with all the nuclear fuel in the

Table 3.1 Major characteristics of Fukushima Daiichi Nuclear Power Plant

Unit	1	2	3	4	5	6
Electric output (MWe)	460	784	784	784	784	1,100
Commercial operation	1971/3	1974/7	1976/3	1978/4	1978/4	1979/10
Reactor model	BWR3	BWR4	BWR4	BWR4	BWR	BWR5
PCV model	Mark-1	Mark-1	Mark-1	Mark-1	Mark-1	Mark-2
No. of fuel assemblies in core	400	548	548	548	548	764

reactor pressure vessel (RPV) having already been transferred to the spent fuel pool. More details on the plant specifications and initial and boundary conditions are described in 2].

3.3 Accident Sequences

3.3.1 Before the Tsunami Attack

The Pacific Coast area of eastern Japan was struck off the Tohoku District by the Pacific Ocean Earthquake, which occurred at 14:46 on March 11, 2011. This earthquake occurred in an area where the Pacific plate sinks beneath the North American plate. The magnitude of the earthquake was 9.0, the greatest in Japan's recorded history. Within seconds of the earthquake, the reactor was shut down in all three operating units with the insertion of control rods. The turbo-generators also tripped, and main steam isolation valves closed. All power supplied from a total of six external power supply lines connected to the power plant stopped as a result of damage to the breakers and collapse of the power transmission line tower caused by the earthquake. The earthquake thus disrupted the electrical supply from the grid, which resulted in a loss of offsite power for all six units. As designed, the emergency diesel generators (EDGs) started providing essential power for all safety systems, including the residual heat removal system. Up to the present time, major damage to the reactor facilities that are important for safety functions has not yet been identified [1–4].

3.3.2 After the Tsunami Attack

Fukushima Daiichi was hit by the first enormous tsunami at 15:27 on March 11, and the next enormous wave was around 15:35. The license for the establishment of nuclear reactors at the Fukushima Daiichi was based on the assumption that the maximum design basis tsunami height expected was 3.1 m. The assessment in 2002 based on the "Tsunami Assessment Method for Nuclear Power Plants in Japan" proposed by the Japan Society of Civil Engineers indicated a maximum water level of 5.7 m, and TEPCO raised the height of its Unit 6 seawater pump in response to this assessment. However, the height of the tsunami this time was 14 to 15 m, and all EDGs and the power panels installed in the basements of the reactor buildings and turbine buildings, except one air-cooled diesel generator for Unit 6, were inundated and stopped functioning (Table 3.2): this resulted in a station blackout (SBO) event for Units 1 through 4. All station DC powers (batteries) were also lost at Units 1, 2, and 4 because of the tsunami, but some DC power survived initially at Unit 3. The tsunami also damaged the coolant intake structures, the seawater pumps for

Table 3.2 Summary of damage after tsunami attack

Unit	1	2	3	4	5	6
Operation status	Full-power operation			Under inspection		
Off-site power	×	×	×	×	×	×
Emergency diesel generator	×	×	×	×	×	×
A: Air-cooled	×	×[A]	×	×[A]	×	O[A] ×[A]
Emergency power panel	×	×	×	×	×	O
Normal power panel	×	×	×	×	×	×
DC power source	×	×	O	×	O	O
Seawater cooling pump	×	×	×	×	×	×

auxiliary cooling systems, and turbine and reactor buildings, resulting in a loss of ultimate heat sink for all six units. It took 9 days to restore offsite power to the site.

TEPCO's operators followed their manuals for severe accidents and attempted to secure power supplies to recover equipment within the safety systems, such as core-cooling and water-injection systems, which had automatically started up. However, ultimately power supplies could not be recovered. Because the core-cooling functions using AC power were lost in Units 1 through 3, core-cooling systems without need of AC power were put into operation: the isolation condenser (IC) in Unit 1, reactor core isolation cooling system (RCIC) in Unit 2, and RCIC and high-pressure injection system (HPCI) in Unit 3. Schematics of IC and RCIC systems are shown in Figs. 3.1 and 3.2, respectively. These core-cooling systems, which do not need AC power, stopped functioning thereafter, and were switched to alternative injections of freshwater or seawater by fire-extinguishing lines, using fire engine pumps. In Units 1 through 3, because water injection to each reactor core was impossible to continue for several hours, the nuclear fuels were not covered by water but were exposed to the steam, leading to a core melt situation. It is believed that part of the melted fuel stayed at the bottom of the RPV. The main causes of the damage during the accident are illustrated in Fig. 3.3. More details on the accident sequences of Units 1 through 3 are described in the following sections [3].

3.3.3 Accident Sequence of Unit 1

For Unit 1, the emergency core cooling was provided by isolation condensers (ICs). In the primary side of the IC, steam from the main steam line is condensed and the water is returned to the RPV via the recirculation line (see Fig. 3.1). The secondary side of the IC is cooled by the plant demineralizer, with a minimum water supply for 6 h before makeup is required in the design. However, the ICs for Unit 1 ceased operation within an hour of the SBO event. Because the core cooling was lost relatively early after the SBO, the accident sequence was rather simple. It is presumed that the accident resulted in core melting, RPV failure, and core melt drop on the

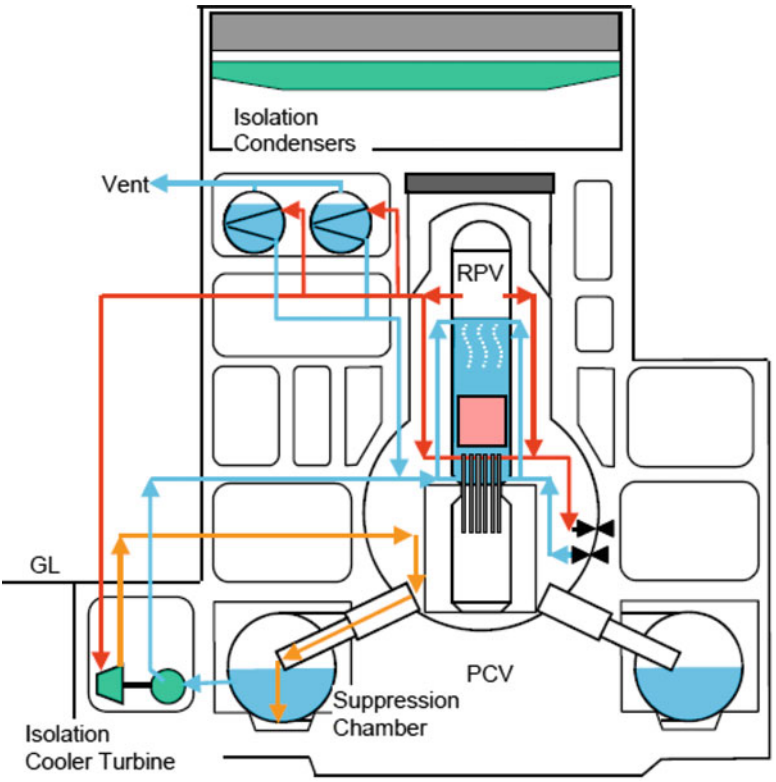

Fig. 3.1 Schematic diagram of isolation condenser (IC). *RPV*, reactor pressure vessel

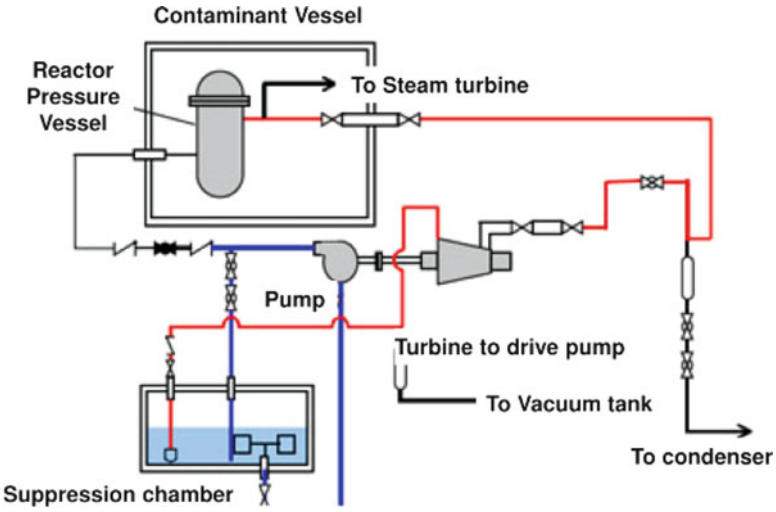

Fig. 3.2 Schematic diagram of reactor core isolation cooling system (RCIC)

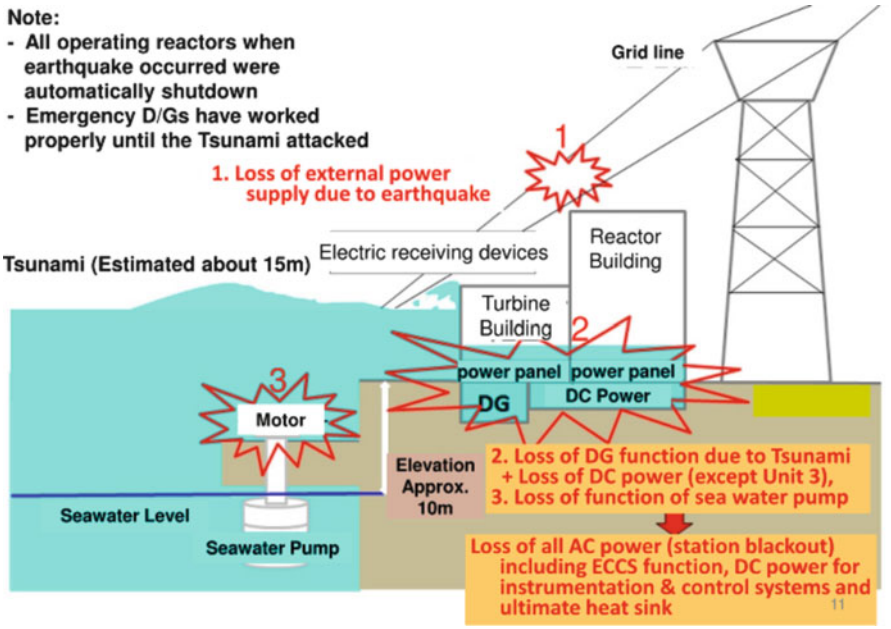

Fig. 3.3 Main causes of damages during the accident

containment vessel floor at the shortest time of the accident sequence. With little core cooling expected in these situations, at about 2.5 h after the SBO, the core water level dropped to the upper core location as a result of overheating of the core, at about 4 h zirconium water chemical reaction heavily progressed, and at about 4.5 h core melt probably initiated. With the progression of the core melt, the core melt temperature increased above 2,500°C; rare gas and volatile fission products, such as iodine, and cesium, were vaporized from the core and were released to the vapor phase in the RPV. It is estimated that RPV failure occurred near the lower head as a result of the relocation of the core melt into the RPV lower plenum. It is estimated that this happened at about 02:45 on March 12 when RPV pressure and containment drywell (D/W) pressure became nearly the same value, as shown in Fig. 3.4; this resulted in releases of high-temperature and high-pressure steam and volatile fission products into the containment D/W from RPV. Because this released steam was much higher in temperature and pressure steam than the design temperature and pressure of the containment vessel, gaskets at the flanges, hatches, airlocks, and penetrations of the containment were degraded, resulting in the loss of leak-tightness of the containment. Hydrogen explosions at Unit 1 and Unit 3 indicate that a large amount of hydrogen along with FPs and steam was released into the reactor building from the containment vessel. FPs released into the reactor building were considered to be released to the environment mostly as a result of the hydrogen explosion.

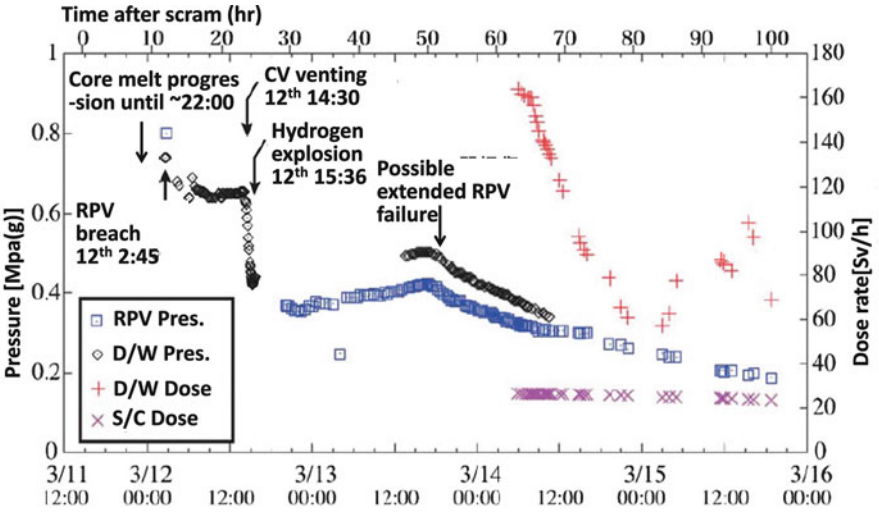

Fig. 3.4 Accident sequence of Unit 1

It is estimated that the most of the core melt dropped on the containment floor at about 04:00 on March 12, and molten core–concrete interaction (MCCI) occurred by abrading the concrete of the containment floor underneath. However, the molten core was finally cooled by the injected cooling water during the accident. It is still quite unknown where and in what state the core debris exists in the containment.

As shown in Fig. 3.4, the pressure of D/W after about 01:00 on March 12 was more than 0.7 MPa, which is much higher than the design pressure of the containment, and this was the critical situation for the containment integrity. At about 14:30 the operators successfully conducted containment suppression chamber (S/C) venting under the poor working conditions. This effort caused drastic decrease of D/W pressure, and containment rupture at the initial stage of the accident could be avoided. However, more than 13 h was required to actually conduct S/C venting. This large delay in S/C venting is one of the reasons that hydrogen explosion and FP release to the environment could not be prevented. Because the pressure of RPV decreased to about 0.8 MPa at about 02:45 on March 12, it was possible to inject water into the RPV by using fire engines. However, it took some more time for preparing the water injection because of the equipment damages and chaos caused by the earthquake and tsunami. The water injection was actually conducted at 05:46 on March 12. The water injection rate was not adequate, only about 1 t/h until about 07:00. However, it is estimated that if this water had not been injected, the core melt would probably have abraded through the containment vessel bottom and the core melt might directly interact with groundwater.

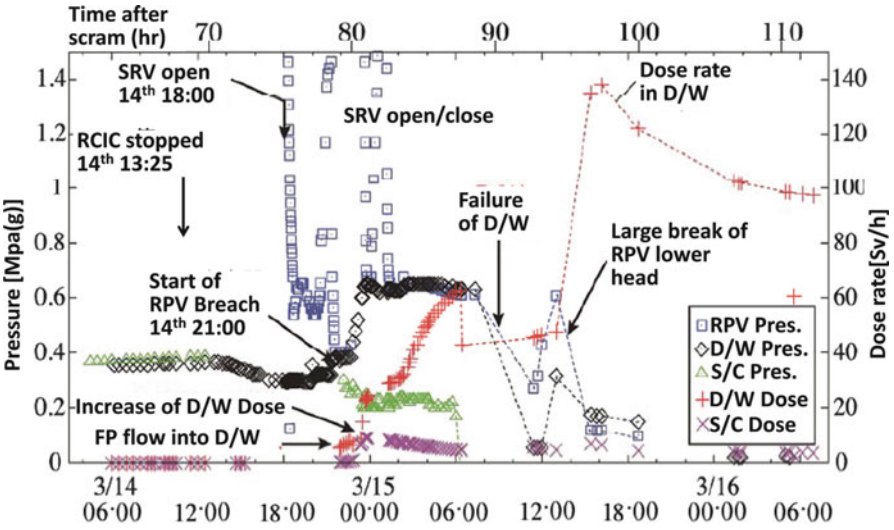

Fig. 3.5 Accident sequence of Unit 2

3.3.4 Accident Sequence of Unit 2

After the SBO, RCIC of Unit 2 was functioning. However, until about 10:00 on March 14, more than 3 h earlier than the RCIC stop time, the water level of the RPV was decreasing and the pressure of RPV was increasing. It is believed that this trend shows that RCIC was losing its core-cooling capability. At the central control room, operators tried to rapidly depressurize RPV by opening the safety relief valves, and it was only possible after 5 to 6 h because of the delay for preparing batteries. The reason of this delay was the immediate chaos caused by the hydrogen explosion at Unit 3, resulting in much time needed to prepare the large amount of batteries. When the depressurization was initiated by opening the safety valves, the RPV water level was almost half of the core. The water level then reached to the bottom of the core, resulting in the loss of water in the core region.

As shown in Fig. 3.5, the increase of D/W pressure initiated after about 19:00 on March 14, and it showed almost the same value as the RPV pressure, which indicates the occurrence of the RPV failure. After the RPV pressure and D/W pressure increased with values similar to each other, they remained at the high values of 0.6 to 0.7 MPa for more than 7 h, which is much higher than the design pressure (0.427 MPa). Around this time, FPs in the RPV were released into D/W, which is indicated by the rapidly increased dose rate in D/W (Fig. 3.5). Through the flanges, hatches, airlocks, and penetrations with gaskets degraded by the high temperature and high pressure of the containment, hydrogen and volatile fission products, such as iodine, and cesium, were released to the reactor building, a similar phenomenon as the hydrogen explosion process in Units 1 and 3. It is believed that the opening

of the blowout panel on the roof of the reactor building caused by the impact of the hydrogen explosion of Unit 3 prevented the occurrence of the hydrogen explosion of Unit 2.

The pressures of D/W and RPV both rapidly decreased from 0.65 MPa from about 07:00 to 11:00 on March 15. Especially, the pressure of D/W decreased to atmospheric pressure. This rapid decrease indicates that a relatively large failure occurred in D/W. It is therefore shows that a large amount of gases including a high level of radioactive materials in D/W was released into the reactor building in a short period because of the loss of containment leak-tightness. Also, sharp synchronized peaks were observed for both RPV and D/W pressures after the immediate decrease of D/W pressure. RPV pressure decreased and then rapidly increased to 0.65 MPa, which is almost before the rapid decrease, and then it rapidly decreased. The peak value of D/W pressure is about half of the RPV pressure spike, but they are almost synchronized and the shape is similar. This rapid increase and decrease of RPV pressure shows that the large amount of steam was generated in a very short period in RPV, and it was released to the D/W side and then released to reactor building through failure location of D/W. It is considered that the large amount of steam generated was the result of direct contact of core melt relocated to the lower plenum of RPV with the remaining water there. It is assumed that a new rupture of relatively large size was formed at the lower head of the RPV. It should be noted that containment venting was tried three times to depressurize the containment, but all attempts were unsuccessful.

3.3.5 Accident Sequence of Unit 3

In Unit 3, RCIC was operated using surviving DC power at 16:03 on March 11 after SBO. This RCIC was stopped at 11:36 on March 12. HPCI was automatically activated by the signal of "RPV low water level" at 12:35 on March 12. After the HPCI operation the PRV pressure, which once reached about 7.5 MPa, decreased to 4.8 MPa at 12:05, and 3.5 MPa at 14:25, 0.8 MPa at about 20:00, and 0.58 MPa at 2:42 on March 13 when HPCI was stopped (Fig. 3.6). The RPV pressure increased again to 4.0 MPa at 1 h and 7.38 MPa at 2 h after HPCI stopped. The RPV pressure rapidly decreased from 7.3 to 0.46 MPa at 8:55 on March 13 from opening of safety relief valves. At the same time, D/W pressure rapidly increased to 0.537 MPa, which is nearly the same as the RPV pressure, because of the inflow of high-temperature and high-pressure coolant. Because the D/W pressure was higher than the design pressure of the containment, 0.427 MPa, containment S/C venting was immediately conducted. D/W pressure decreased rapidly, but the opening of the venting was unstable and the opening began closing in a short time. Opening and closing of the venting were thus iterated five times. During this period RPV pressure and D/W pressure rapidly increased and decreased. Rapid increase of RPV pressure indicates a large amount of steam generation, which implies the existence of the core melt. The rapid decrease of both RPV pressure and D/W pressure clearly

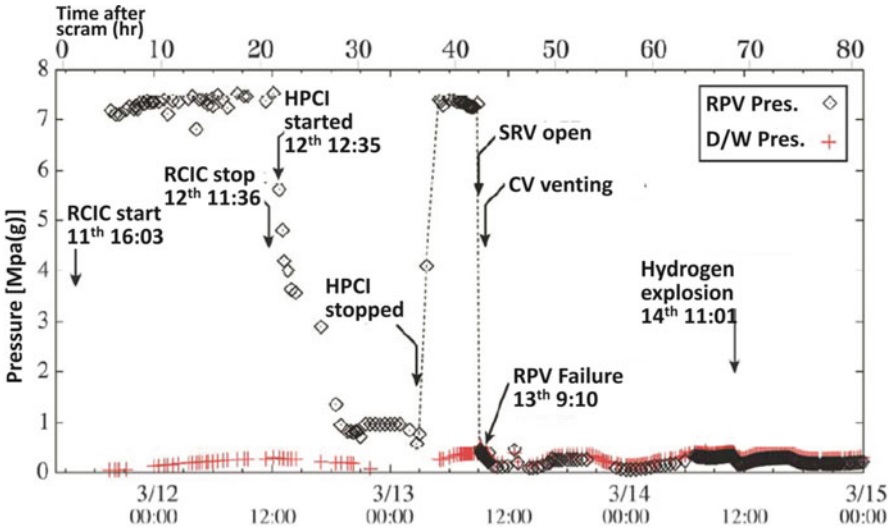

Fig. 3.6 Accident sequence of Unit 3

indicates the effectiveness of the S/C containment venting for the depressurization of the containment. In contrast to Unit 2, the containment pressure of Unit 3 did not remain above 0.6 MPa for a long time because of the multiple depressurizations. Just after the fourth venting at 11:01 on March 14, the hydrogen explosion occurred at the reactor building. This explosion indicates that a large amount of hydrogen along with radioactive materials and steam was released to the reactor building, and the radioactive materials were released to the environment.

3.3.6 Spent Fuel Pools

In Unit 4, all core fuels had been transferred to the spent fuel pool for periodic inspection before the earthquake. The urgent task at the site, along with recovery of the power supply and the continuation of water injection into reactor vessels, was injection of water into the spent fuel pools. In the spent fuel pool in each unit, the water level continued to drop because of evaporation of the water caused by the heat of the spent fuel in the absence of the pool water cooling caused by the loss of power supply. Water injection to the spent fuel pool was conducted by the Self-Defense Forces, the Fire and Disaster Management Agency, and the National Police Agency, using helicopters and water cannon trucks. Concrete pump trucks were ultimately utilized, which led to stable water injection using freshwater from nearby reservoirs after the initial seawater injection. It is confirmed that the water level was never lower than the top of the fuel in any of the pools, and none of the pools suffered any

significant structural damage [2], in contrast to concerns raised during the weeks following the accident. The spent fuel pool, storing 1,500 fuel assemblies, was designed such that the fuel elements would retain integrity for 30 days without active cooling.

3.4 Release of Fission Products

The Nuclear and Industrial Safety Agency (NISA) and the Nuclear Safety Commission (NSC) estimated the total amount of radioactive materials released to the environment. NISA estimated the total discharged amount from reactors on the basis of the analytical results with severe accident analysis code, MELCOR, by Japan Nuclear Energy Safety Organization (JNES) [5, 6], as typically shown in Fig. 3.7. The NSC estimated the amount of nuclides discharged into the atmosphere with the assistance of the Japan Atomic Energy Agency (JAEA) [7, 8] through inverse calculations, based on the data of environmental monitoring and atmospheric diffusion calculation code, SPEEDI, as shown in Fig. 3.8. The estimated values summarized in Table 3.3 range between 1.2 and 1.6×10^{17} Bq for iodine-131 and 8 and 15×10^{16} Bq for cesium-137. Values estimated by TEPCO are also shown in Table 3.3. Estimated release of iodine-131 by TEPCO is about three times larger than values by NISA or NSC. It is also noted that the estimated releases of iodine-131

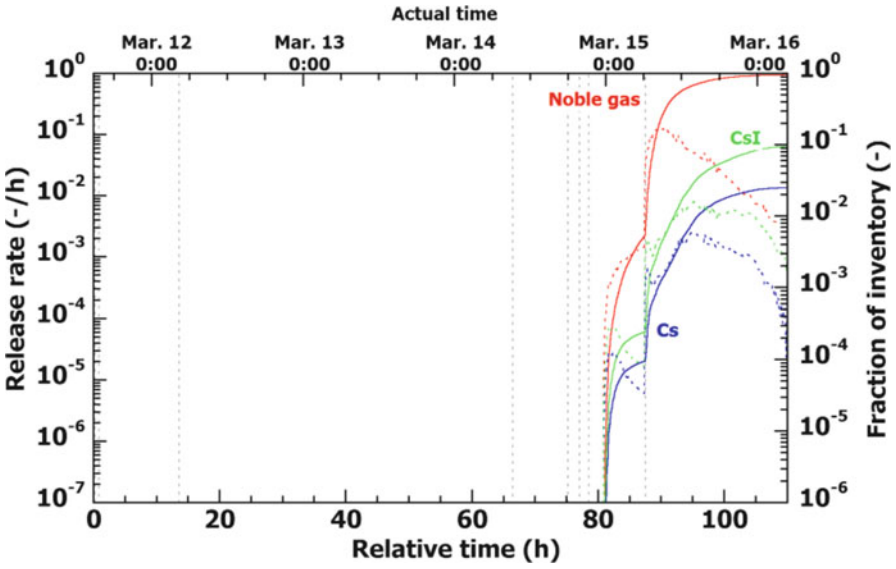

Fig. 3.7 Estimated fission products (FP) release ratio to the environment with MELCOR code (Unit 2). *Solid lines* and *dotted lines* represent cumulative release fraction and release rate, respectively [6]

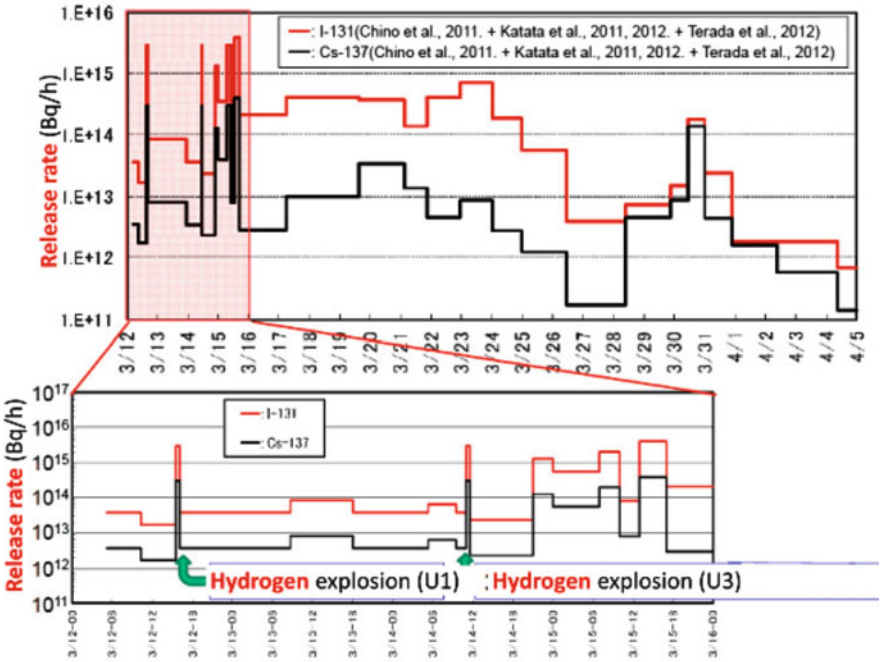

Fig. 3.8 Estimated FP release to the environment with SPEEDI code

Table 3.3 Estimated fission products released to the environment

Organization	^{131}I (10^{15} Bq)	^{137}Cs (10^{15} Bq)
NSC/JAEA (August 2011)[a]	130	11
JAEA (March 2012)[a]	120	9
NISA/JNES (June 2011)[b]	160	15
NISA/JNES (February 2012)[b]	150	8.2
TEPCO (June 2012)[a]	500	10
Chernobyl Accident[a]	1,760	85

[a]Estimated with environmental monitoring data and diffusion analysis (SPEEDI/DIANA, etc.)
[b]Estimated with reactor accident progression analysis (MELCOR)

and cesium-137 of the Chernobyl accident [9] are about one order of magnitude larger and about 6 to 10 times larger than those estimated by NISA and NSC as shown in Table 3.3.

It may be noted that the containment S/C venting is conducted through several meters of water depth in a suppression chamber, and the effectiveness of this pool scrubbing for FP aerosols is usually very high, of the order of 10^3 as a decontamination factor. The estimation of FP release during S/C venting by TEPCO for Units 1 and 3 is not necessarily high compared with other periods [2].

3.5 Lessons Learned

After the accident at Fukushima Nuclear Power Plant, several investigation committees have been established, such as by the Independent Investigation Commission, TEPCO's Investigation Committee, National Diet's Investigation Committee, and Government's Investigation Committee. They have issued investigation reports on the causes of the disaster, major lessons learned from the accident, and recommendations for the future [1–4]. Most of those reports judged that although the accident was triggered by a massive force of nature, it showed existing weaknesses regarding defense against natural hazards, regulatory oversight, and insufficient accident management, emergency response, and emergency training that allowed the occurrence and escalation of the accident [10].

For example, the Independent Investigation Commission [1] mentioned that the Fukushima accident is a "man-made disaster–unprepared nuclear severe accident" because of ambiguous private corporate management by TEPCO under the national nuclear policy. It states that the main cause of the accident is complete lack of crisis management and leadership in both the Government and TEPCO. It also emphasized the utmost importance for resilience to be greatly enhanced for the future. TEPCO's Investigation Committee [2] mentions that enhanced accident measures both in hardware and in software are to be prepared, and recommends that the Government clearly establishes the standards of the emergency offsite center and guidelines of external events that have extremely low probabilities and high consequences. It emphasized the importance of the company-wide enhancement of risk management systems. National Diet's Investigation Committee [3] raises several recommendations, such as monitoring of the nuclear regulatory body by the National Diet, reform of the crisis management system, Government's responsibility for public health and welfare, and development of a system of independent investigation commissions in the National Diet. The Government's Investigation Committee [4] points out several important recommendations, such as establishment of a basic stance for safety measures and emergency preparedness, safety measures regarding nuclear power generation, nuclear emergency response systems, harmonization with international practices in nuclear safety, and continued investigation of the accident causes and damage of the Fukushima accident.

Several measures, such as enhanced power supply capabilities, improved severe accident management policies, and strengthened emergency preparedness capabilities, have already been put in place based on the identified causes and lessons learned from the accident, and some mid-/long-term measures, such as a filtered containment venting system and increased seawall, are being implemented at nuclear power plant sites. Also, it is pointed out that professional leadership in nuclear organizations that manage potentially hazardous activities to maintain the risk to people and the environment as low as reasonably achievable without compromise is of utmost importance, thereby assuring stakeholder trust [10].

The underlying essential lesson will be that a sense of crisis and tension toward a possible severe accident were completely lacking, and groundless overconfidence

against nuclear safety covered all nuclear sectors in Japan. Also it is evident that fully flexible resilience by the maximum use of existing hardware and software with enhanced knowledge, experience, monitors, predictive capability, exercises, and management is the only possible way to effectively cope with "unexpected" events that are largely beyond design base. We should learn these important lessons with humility, share them among all throughout the world, and reflect on them to a future even higher level of safety for current nuclear reactors. Because long-term relocation completely destroys local communities, advanced reactors without the need of evacuation, in principle, should be developed and deployed for the future. Associated important severe accident research items are being systematically identified, for example, by the efforts of the Atomic Energy Society of Japan [11].

Lastly, it may be noted that the Nuclear Regulation Authority (NRA) has been newly established in September 2012, as an independent commission body that solely exercises regulatory authority in the field of nuclear safety and security in Japan. As of July 2013, only 2 units of about 50 units are in operation, although the Government is expecting the restart of the operation of idling nuclear power plants, after satisfying new safety regulation rules [12] in force by the NRA in July 2013, as an important power source.

3.6 Summary

1. Although some details of the accidents of Fukushima Daiichi Nuclear Power Plant are still not well known, the sequences, causes, and consequences of the accidents have been basically clarified by the efforts of several investigation committees established in Japan.
2. The fission products released to the environment were estimated by the severe accident analysis code from inside the reactor core, and also by the atmospheric dispersion simulations code by coupling with environmental monitoring data in the reverse estimation method from outside the plant. The estimated release amount of ^{131}I is of the order of 120–160 PBq, and that of ^{137}Cs is of the order of 8–15 PBq for both estimations.
3. Lessons learned from the accident identified by investigation committees cover a wide spectrum of insufficient measures, such as for earthquake and tsunami, station blackout, severe accident management, common cause accident at multiple unit sites, education and training, chain of command at the accident, disaster prevention, and safety regulation system. These lessons should be shared all over the world for the higher level of safety assurance of current reactors, and advanced reactors without the need of evacuation in principle should be developed for the future.

References

1. Independent investigation commission on the Fukushima daiichi nuclear accident (Feb. 2012) investigation and verification report
2. The Tokyo Electric Power Company Inc. (June 2012) Fukushima nuclear accident analysis report (Final Report)
3. The National Diet of Japan (July 2012) The Official Report of the Fukushima Nuclear Accident Independent Investigation Commission
4. Government of Japan (July 2012) Final report of the investigation committee on the accident at Fukushima nuclear power stations of Tokyo Electric Power Company
5. Nuclear and Industrial Safety Agency (2011) Discharge of radioactive materials to the environment (Chapter VI). Report of Japanese government to the IAEA ministerial conference on nuclear safety
6. Hoshi H et al. (April 2011) Computational analysis on accident progression of Fukushima Daiichi NPS. PSAM topical conference in Tokyo, Japan
7. Chino M et al (2011) Preliminary estimation of release amounts of ^{131}I and ^{137}Cs accidentally discharged from the Fukushima Daiichi Nuclear Power Pplant into the atmosphere. J Nucl Sci Technol 48:1129–1134
8. Terada H et al (2012) Atmospheric discharge and dispersion of radionuclides during the Fukushima Dai-ichi Nuclear Power Plant accident. Part II: Verification of the source term and analysis of regional-scale atmospheric dispersion. J Environ Radioact 112:141–154
9. OECD NEA (1995) The Chernobyl reactor accident source term—development of a consensus view. OECD NEA/CSNI/R(95)24.
10. Kondo S (April 2013) Lessons learned from Fukushima for PSAM community: Leadership and responsibility to assess and inform risk for safety assurance. In: PSAM topical conference in Tokyo, Japan
11. Sugimoto J (July 2013) Important severe accident research issues after accident at Fukushima Daiichi Nuclear Power Station. 21st international conference on nuclear engineering. Chengdu, China
12. Fuketa T (March 2013) Proposed regulatory requirements in Japan. Regulatory Information Conference, Bethesda

Chapter 4
Some Comments on Dose Assessment for Members of the Public After the Fukushima Daiichi NPP Accident

Jiro Inaba

Abstract This chapter describes the importance of dose assessment, either prospectively or retrospectively, for protection of members of the public exposed to radiation after the Fukushima NPP accident. There are three points. The first point is the implication of dose assessment. The International Commission on Radiological Protection (ICRP) has developed a system of radiation protection in which dose is the most important measure of radiological risk. In decision making regarding radiation protection, it is very important to understand the implications of dose assessment and to endeavor suitable protective measures based on the results of dose assessments. The second point is the radiological impact of the Fukushima accident. A large amount of radioactivity was released into the environment, but owing to extensive monitoring and protective measures, doses received by members of the public were fortunately not high, at the level of not causing any immediate health effects. We have much to learn from the accident, which includes (1) establishment of a better strategic system for emergency response, (2) reinforcement of environmental monitoring including in vivo counting of the human body, and (3) enhancement of better communication relevant to the accident. The third point is the effects of radiation exposure of children and infants. The protection of children in the accident aftermath has been a particular concern, and parents were extremely worried about the protection of their offspring. ICRP has provided age-dependent dose coefficients, so it was proposed that UNSCEAR should make the radiation risk of children more clear and that ICRP should revise its recommendation to include radiation protection scheme for children.

J. Inaba (✉)
Radiation Effects Association,
Maruishi-Daini Bldg. 5 F, 1-9-16, Kajichou, Chiyoda-ku, Tokyo 101-0044, Japan
e-mail: zb69jv@bma.biglobe.ne.jp

S. Takahashi (ed.), *Radiation Monitoring and Dose Estimation of the Fukushima Nuclear Accident*, DOI 10.1007/978-4-431-54583-5_4,

Keywords Dose assessment • Dose estimation • Internal dose • External dose • In vivo counting • Environmental monitoring • Infant • Children • Age-dependent dose • Age-dependent risk

4.1 Introduction

On March 11 of 2011, the Great East Japan Earthquake and Tsunami affected the Tohoku District of Japan. In TEPCO's Fukushima Daiichi Nuclear Power Station, the external power supply was lost because of damage to the grid lines caused by the earthquake, and emergency diesel generators were terminated by the tsunami, which eliminated the capability to control radioactivity in reactors and the spent fuel storage pool. Consequently, a large amount of radioactive materials was released into the environment. Immediately after the release there was tremendous difficulty in managing the radioactive materials. It was extremely difficult to maintain communication, to mobilize human resources, and to procure supplies among other areas when addressing the nuclear accident that coincided with a massive natural disaster. Then, environmental radiation monitoring was initiated and various kinds of protective measures were implemented; however, radiation exposure resulted among the residents of Fukushima Prefecture and neighboring areas. Radiation exposure was initially caused by radioisotopes of iodine and short-lived radionuclides and subsequently by radiocesium from both external irradiation and internal irradiation through consumption of foods contaminated with these radionuclides.

Data and information related to dose assessment, such as in air dose rate and the concentration of radioactive materials in various environmental media after the Fukushima accident, have been reported by various organizations and disclosed by news media and the Internet. The International Symposium held on 14 December 2012 by Kyoto University provided an excellent opportunity for the integration of relevant information. Results of dose assessment for various populations have been also reported by various authors. However, no quantified and conclusive results of dose assessment have been reported by the responsible organization so far. The results are still in the process of being finalized for official presentation to the public.

In the present comments, therefore, I start by describing the implication of dose assessment in general, then I will report some results of dose assessment in the Fukushima accident. Finally, I touch on a key point of the present accident, radiation exposure of children, which seems to me extremely important for current radiation protection.

4.2 Implication of Dose Assessment

Ionizing radiation and radioactive materials have always been features of our environment, which means that every one in the world is exposed to a certain level of radiation from natural sources. Moreover, it is unavoidable to receive radiation from artificial sources, including medical use, in present-day life.

Health effects of radiation are caused by the ionization that necessarily changes atoms and molecules, at least transiently, and may thus sometimes damage cells. Ionization is the process by which atoms lose or sometimes gain electrons and thus electrically charged ions. When ionizing radiation passes through matter, energy is imparted to the matter as ions are formed in biological tissues and molecular changes result. If cellular damage does occur and is not adequately repaired, it may prevent the cell from surviving or reproducing, or it may result in viable but modified cells. The damage manifests itself as radiation damage to the organs and tissues of the body. Two outcomes, deterministic effect and stochastic effect, have profoundly different implications for the organism as a whole. The probability of causing the deterministic effect will be zero at a low level of exposure, but above some level of the threshold will increase steeply to unity. Above the threshold the severity of harm will also increase with the level of exposure. The probability of a stochastic effect resulting from radiation usually increases with increments of the level of radiation exposure in a way that is roughly proportional to the level. Thus, dose (the level of exposure) is the most important measure of health risk of radiation exposure.

Radiological protection is concerned with controlling exposure to ionizing radiation so that deterministic effects are prevented and the risk of stochastic effects is limited to acceptable levels. For assessing the "level" of radiation exposures, dosimetric quantities and their units have been developed by ICRP. The fundamental dosimetric quantity in radiological protection is the absorbed dose (Gy, joules per kilogram), the energy absorbed per unit mass. The absorbed dose is defined as the average dose over a tissue or organ of the body. To combine the dosimetric quantities to risk or detriment of radiation exposure, effective dose (Sv) has been developed applying two weighting factors, a radiation weighting factor and tissue weighting factor, to the absorbed dose. The effective dose is the measure of the health risk of radiation exposure; it allows quantification of the extent of exposure of ionizing radiation from both whole-body and partial body irradiations from external radiation sources and from intakes of radionuclides. The estimated doses can be compared with recommended dose limits or reference levels for people who are occupationally exposed and for members of the public.

Radiological protection is a technology to control doses to which individuals may be exposed. ICRP has set out general principles for planning intervention in the case of a radiation emergency in Publication 60 [1]. The current ICRP recommendation extended its guidance on the application of protective measures [2], but it says that the general principle, 'do more good than harm and optimize the protection,' remains valid. Protective measures contain certain levels of nonradiological risks in general. Therefore, in an emergency exposure situation in accidental conditions and in existing exposure situations after an accident, it is extremely important to assess doses as precisely as possible based on a realistic methodology to provide reasonable protective measures such as reasonable allocation of available resources to the cases in emergency. Doses based on realistic methodology can minimize total risk from the exposure and nonradiological risk.

In the study of radiation health effects for radiation protection, it is very important to correctly assess doses each of the affected people receive; however, it is not easy to do so in cases where the exposure occurred in the past and in an emergency

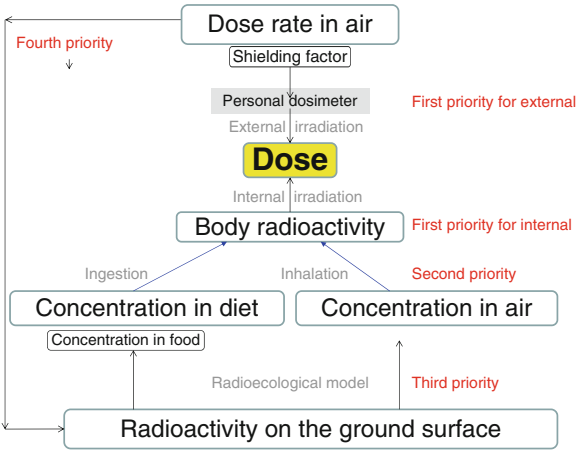

Fig. 4.1 Generic methodology for dose assessment and dose reconstruction

situation. Figure 4.1 shows the generic methods for dose reconstruction. In external exposure, information about the time change of the dose rate in the relevant place is important. In internal exposure, the best information is measured values for radioactivity in the human body; the second priority is radioactivity concentration in food and air. If the information is not available, we have to derive the information from the third-priority data using radioecological models.

In decision making and policy making in the fields related to radiation protection, especially in an emergency situation, it is very important for the competent organization to understand the implication of dose assessments, to appoint a proper person who knows the significance of dose assessment very clearly to a proper position in the system where decision making is done, and to devise suitable protective measures based on the results of dose assessments.

4.3 Radiological Impact of the Fukushima Daiichi Accident

4.3.1 Environmental Monitoring

Immediately after the earthquake the Japanese Government established various systems such as the Nuclear Emergency Response Headquarter to respond to the emergency. The ministry of Education, Culture, Sports, Science and Technology (MEXT) was, and currently the Nuclear Regulation Authority (NRA) is, responsible for environmental monitoring.

The accident at the Fukushima site occurred soon after the occurrence of the natural disasters of the earthquake and tsunami, which caused great difficulties in emergency response including environmental monitoring of the nuclear disaster. For instance, 23 of 24 monitoring posts in Fukushima Prefecture became unavailable, and communication and transportation of necessary resources became very

difficult. In addition, after the loss of external power supply on March 11, TEPCO became unable to perform measurements at monitoring posts and air stack monitors, although these difficulties were resolved gradually.

In spite of the difficulties, nationwide environmental monitoring was started on March 12 by MEXT with assistance from universities and various organizations. Results of daily measurement of air dose rate, radioactivity in fallout at the fixed time, and radioactivity in tap water were reported on news media as well as Internet websites (NRA [3]). Air monitoring was done by MEXT with the help of USDOE, and a map based on air dose rate was prepared. Also, radioactivity in soil, radioactivity in seawater and ocean sediment, and radioactivity of air dust were analyzed. Measurements of foodstuffs were done by the Ministry of Health, Labor and Welfare and measurements of farmland soil and fertilizer by the Ministry of Agriculture, Forestry and Fisheries. The results of these measurements and monitorings were used for decision making of various protective measures such as evacuation and in-house sheltering, the control of consumption and shipping of foodstuffs, as well as for dose assessment. Almost all the monitoring was done periodically, which can provide very useful information for dose assessments.

4.3.2 Dose Assessment

After the Fukushima accident, the public received doses through four major exposure pathways: external dose from radionuclides in the radioactive plume, external dose from radionuclides deposited on the ground, internal dose from inhalation of radionuclides in the radioactive plume, and internal dose from ingestion of radionuclides in food and water. Currently most basic information available for the dose assessment is the gamma dose rate in the air (μSv/h), the density of radioactivity deposited per unit area (Bq/m^2) in areas, and the concentration of radionuclides in soil samples collected (Bq/kg).

Dose assessment for individuals and groups of population is carried out using all available information.

For external dose from the ground, a dose estimation system was developed by NIRS using a time-series set of ambient dose rate maps and individual behavior with help of shielding factors of the house based on personal interview or questionnaire. External doses from a radioactive plume as well as internal dose through inhalation of the radioactive plume are calculated with help of atmospheric dispersion simulation at the time of major release of radioactivity in the affected area.

For internal dose, environmental transfer models of radioactivity from soil to human body were used. The upper soil layer, crops and vegetables, tea, milk and meat, fish and sea products, as well as tap water were important samples. Radioactivity in the total diet rather than an individual food can usually provide better information for dose assessments, although radiological survey of the total diet was not done on a wide scale by the Government after the present accident. Further, radioactivity in human body can provide the best information for dose assessment.

Each step contains some uncertainty, so total uncertainty increases with number of steps. It means that the measured data close to the human body is very important for dose assessment with smaller uncertainty. It is very important, therefore, to emphasize that individual dosimeters for external exposure and in vivo measurements of whole body or thyroid for internal exposure can provide the best information for the dose assessments. In reality, especially in the early stages after an accident, it is not easy to make these measurements, but I think it should be emphasized.

4.3.3 Examples of Dose Assessments in Fukushima Prefecture

4.3.3.1 External Dose

Fukushima Prefecture has been executing a large-scale program, the "Fukushima Health Management Survey." The basic survey in the program is performed to obtain the external radiation dose which residents in Fukushima Prefecture received. A part of the results is shown in Table 4.1. The external dose is calculated by the precise map of air dose rate and the detailed time table for each resident for 4 months from March to July 2011. The total number of residents whose doses were assessed is 420,543 as of the end of March 2013; among them 411,922 are non-radiation workers. Among these non-radiation workers, 99.8 % received doses less than 5 mSv, and the maximum dose was 25 mSv. The higher dose rate can be seen in highly contaminated areas [4].

As already mentioned, the external dose was calculated for just 4 months, which seems to me not long enough to look at the radiological health effect. The doses for 1 year after that accident are expedited, but it is extremely difficult to do now a similar survey on individual behavior in the past. Therefore, it would be required to calculate the 1-year dose using the ecological half-life of radiation that was shown by field monitoring. The ecological half-life of radiation is in general reported to be much shorter than the physical half-life [5].

It was reported that certain local governments distributed personal dosimeters to local residents and obtained information regarding personal dose. It is very important to compare the results of calculation and dosimeter measurement and to validate the present external dose estimation methodology. In this scene, disclosure of the related information is strongly desired.

4.3.3.2 Internal Dose

In the Fukushima Health Management Survey, whole-body counting of the residents in Fukushima Prefecture for radiocesium is also performed and the resulting internal doses were disclosed by Internet. A part of the results is shown in Table 4.2. The committed effective dose is calculated based on the measured value and

Table 4.1 Distribution of external dose estimates received by residents in Fukushima Prefecture during 4 months after the accident (number of persons) [4]

Area	Ken-poku (%)	Ken-chuu (%)	Ken-nan (%)	Aizu (%)	Minami-aizu (%)	So-so (%)	Iwaki (%)	Total (%)
Dose (mSv)								
~1	38,553 (32.2)	59,857 (59.5)	21,237 (91.4)	33,935 (99.6)	3,536 (99.4)	54,236 (77.8)	60,466 (99.2)	271,820 (66.0)
~2	69,709 (58.2)	35,168 (35.0)	1,989 (8.6)	146 (0.4)	22 (0.6)	11,563 (16.6)	436 (0.7)	119,033 (28.9)
~3	11,105 (9.3)	5,337 (5.3)	10 (0.0)	3 (0.0)	0	1,787 (2.6)	19 (0.0)	18,261 (4.4)
~4	388 (0.3)	245 (0.2)	0	1 (0.0)	0	643 (0.9)	3 (0.0)	1,280 (0.3)
~5	35 (0.0)	5 (0.0)	0	0	0	504 (0.7)	0	544 (0.1)
~6	18 (0.0)	2 (0.0)	0	0	0	387 (0.6)	0	407 (0.1)
~7	5 (0.0)	0	0	0	0	222 (0.3)	0	227 (0.1)
~8	1 (0.0)	0	0	0	0	113 (0.2)	0	114 (0.0)
~9	0	0	0	0	0	79 (0.1)	0	79 (0.0)
~10	0	0	0	0	0	42 (0.1)	0	42 (0.0)
~11	0	0	0	0	0	42 (0.1)	0	42 (0.0)
~12	1 (0.0)	0	0	0	0	26 (0.0)	0	27 (0.0)
~13	0	0	0	0	0	14 (0.0)	0	14 (0.0)
~14	0	0	0	0	0	10 (0.0)	0	10 (0.0)
~15	0	0	0	0	0	11 (0.0)	0	11 (0.0)
15~	0	0	0	0	0	11 (0.0)	0	11 (0.0)
Total	119,815 (100.0)	100,614 (100.0)	23,236 (100.0)	34,085 (100.0)	3,558 (100.0)	69,690 (100.0)	60,924 (100.0)	411,922 (100.0)
Maximum	11 mSv	5.9 mSv	2.6 mSv	3.5 mSv	1.8 mSv	25 mSv	3.9 mSv	25 mSv

Table 4.2 Distribution of committed effective dose estimates calculated by whole-body counting of radiocesium in Fukushima Prefecture (number of persons) [7]

Area	Less than 1 mSv	1 mSv	2 mSv	3 mSv
Ken-poku	34,827	2	1	0
Ken-chuu	31,027	0	0	0
Ken-nan	22,822	0	0	0
Aizu	5,270	0	0	0
Minami-aizu	692	0	0	0
So-so	19,673	12	9	2
Iwaki	17,674	0	0	0
Total	131,985	14	10	2

MONDAL 3 developed by NIRS [6] on the ICRP age-dependent biokinetic model for cesium assuming scenarios of a single intake on March 12 and of chronic intake between March 12 and the counting date. From July 2011 to the end of May 2013, 132,011 people were surveyed: among them the internal dose for 131,985 was calculated to be lower than 1 mSv, 14 received 1 mSv, 10 received 2 mSv, and 2 received 3 mSv. Residents received equal to or higher than 1 mSv live in Date City (3), Naraha Town (3), Tomioka Town (1), Kawauchi Village (1), Ookuma Town (4), Futaba Town (6), Namie Town (7), and Iitate Village (1). Date City is in Ken-poku Area and the other towns and villages are in So-so Area (5) [7].

As already mentioned the internal dose from radiocesium is a committed dose at the time of measurement, which means that the dose commitment resulting from intake of radiocesium would be a little different from the committed dose. It is interesting that all the residents whose dose was equal to or higher than 1 mSv were detected before January 2012.

From information collected, the local government of Fukushima Prefecture concluded that the internal dose received by all residents in Fukushima Prefecture was not at a level that can affect human health.

4.3.3.3 Thyroid Dose

Apart from internal dose assessment from radiocesium, that from radioiodine is very difficult because of the short half-lives of the radioactivity as well as tissue distribution of radioiodine. Actually, in the present accident proper information was unavailable regarding internal dose assessment for the thyroid because of various reasons. In the condition of high background radiation, in vivo counting of the thyroid was very difficult. In total, 1,080 children aged 1 year to 15 years old were screened during March 24 to 30, 2011, with conventional ambient dose rate meters. Taking these data into account, it is estimated that the thyroid dose of a 1-year-old is within several tens of mSv and doses of other age groups are lower than that of a 1-year-old child, although a certain extent of uncertainties in these values are unavoidable at present [8].

Currently, to establish methods for estimation of early internal doses to residents, various possible methods are being developed that include methods to draw a more detailed map for radioiodine using the measured data of long-lived radioiodine, ^{129}I, and the radioiodine/radiocesium ratio in various environmental media, as well as atmospheric dispersion simulation with individual behavior.

4.3.4 Some Points Found in the Dose Assessments

The Fukushima accident is attracting attention internationally. The United Nations Scientific Committee on the Effect of Atomic Radiation (UNSCEAR) is one of the UN organizations responsible for scientific review of radiation exposures. In the 60th session of UNSCEAR held in May 2013, scientists discussed the Fukushima accident. Although the discussion is still in the process of finalization of presentation to the General Assembly, they issued a statement [9] concluding that "Radiation exposure following the nuclear accident at Fukushima-Daiichi did not cause any immediate health effects. It is unlikely to be able to attribute any health effects in the future among the general public and the vast majority of workers." And they reported that the exposure of the public including residents of Fukushima Prefecture is low on the whole, leading to correspondingly low risks of health effects later in life. The actions taken to protect the public significantly reduced the radiation exposures that would have otherwise been received.

In general, as UNSCEAR reported, protective actions taken so far in the disaster played important roles in the reduction of doses, but this does not mean that the actions were adequate. It is very important to learn the lessons or points to be improved from the present disaster, even though actions taken can be considered to be adequate, as much as possible.

The followings are some points raised by the author in the field of dose assessment.

(1) Establishment of better strategic systems for emergency response
In an emergency, almost all resources, including human resources, related to the radiation protection easily run short. In this situation the most important thing is to obtain information regarding the dose affected residents would receive. Of course there are cases where lifesaving should proceed, but fortunately, this is generally not the case in the present disaster. Therefore, it is very important to establish a strategic system for emergency response including protective actions based on doses that can be calculated by measurement as well as modeling. If a dose avertable by protective actions can be estimated, it would provide better information regarding the choise of protective action. In an emergency with limited resources, it is important to compromise, for instance, the number of cases of monitoring or measurement and their quality. For this purpose, the concept of the representative person developed by ICRP [10] can be used.

(2) Reinforcement of environmental monitoring including in vivo counting of the human body
Environmental monitoring can provide essential information for radiation protection. Especially, in vivo counting of the human body can provide good information for dose assessments. However, resources for monitoring are usually limited, and moreover monitoring devices can easily be contaminated. In the present disaster, great difficulties were experienced in dose assessment for children's thyroid levels by short-lived radioiodines because in vivo counting was not performed in a precise way. This experience revealed the importance of dose assessment as well as the importance of implementation of measurement in a timely manner.

(3) Enhancement of better communication relevant to the accident
In the present accident, important information was not always provided to residents and local communities in affected areas in a timely manner. The same thing can be said in the field of dose assessments. MEXT seems for me to have a tendency to disclose information with high accuracy rather than information in a timely manner with less accuracy. In an emergency situation, it is very important to harmonize the accuracy and the timing or speed of communication. Information on dose or radioactivity, with which the public are not familiar, should be added by sufficient explanation; otherwise, rumors can spread and people's concerns can grow unreasonably as time passes.

In the end of May 2013, WHO published a report [11] on the radiological impact for the Fukushima disaster, but the risk estimation relied on rather old doses based on measurements available by mid-September 2011 [12]. It is likely that sufficient information had not been provided by the Japanese government to WHO. Actually, as already described, doses received by residents are not yet finalized as of the end of August 2013.

4.4 Effects of Radiation Exposure of Children

One of the characteristics of the Fukushima Daiichi Accident is the fact that people are very much concerned about the impact of radiation exposure on children.

The protection of children in the accident aftermath has been of particular concern, and parents are extremely worried about the protection of their offspring. They are suspicious that the levels of dose applied for the protection of the population as a whole do not provide sufficient safety for their offspring. The doubt may have been amplified by the natural tendency of human beings to be sensitive about children and infants. I believe that it is the time for UNSCEAR to start efforts to provide a clear summary of the current information on radiation risk of children and infants and for ICRP to start efforts for revision of their recommendation to include a radiation protection scheme for children.

ICRP has developed a radiation protection scheme for three categories of exposed individuals: workers in occupational exposure, members of the public in public exposure, and patients in medical exposure. ICRP seems to consider that the

children are included in one of these categories and that a definite ICRP document with recommendations specifically dedicated to the protection of children and infants is not needed at present.

Because of anatomical and physiological differences, radiation exposure has a different impact on children compared with adults. UNSCEAR had started a general review of these differences before the Fukushima-Daiichi accident; its conclusions on this subject are expected to be finalized soon.

4.4.1 Radiation Dose of Children

There are differences in the doses received by children and adults from exposure to the same distribution of radioactive material in the environment, for example, when there are elevated levels of radionuclides on the ground. So far, ICRP has not provided age-dependent dose conversion coefficients for the members of the public [13].

Very recently ICRP organized a task group on Age-dependent Dose Conversion Coefficients for External Exposures to Environmental Source in Committee 2. The objectives of the group are to provide age-dependent dose conversion coefficients for the members of the public that are applicable to the situation where a large amount of radionuclides are released from nuclear facilities to the environment as in the present accident.

If radionuclides are ingested or inhaled, the presence of radionuclides in one organ in the human body can give higher radiation doses to another organ because the organs of children are in closer proximity to one another than those of adults. In addition, both metabolism and physiology depend on age, which also affects the biokinetics and concentrations of radionuclides in different organs and thus the dose to those organs for a given intake.

For internal exposure, the necessity for internationally accepted dose coefficients for members of the public became particularly evident after the Chernobyl reactor accident. An ICRP report entitled “Age-dependent doses to members of the public from intake of radionuclides: Part 1” was published as ICRP Publication 56 [14]. The report provided age-dependent dose coefficients (Sv/Bq) as organ equivalent dose and effective dose per unit intake of radionuclides. Then, Parts 2 to 5 were published [15–18]. Moreover, dose coefficients for embryo and fetus, as well as dose coefficients for infants through mother’s breast milk, have been published as ICRP reports [19, 20]. These dose coefficients were successfully used for the internal dose assessments for the residents in the Fukushima disaster.

4.4.2 Radiosensitivity of Children

In contrast to radiation doses, age-dependent radiosensitivity has been treated in the current ICRP recommendations rather lightly [2]. In the 1990 recommendations of the ICRP it was reported that the total risk determined as the sum of the individual

organ risks differs by a factor of about 3 for young (0–19 years) versus older (20–64 years) age groups [1]. For the development of radiation protection in the current ICRP recommendation, the average detriments for ages 18–64 years at exposure were used for workers and those for ages 0–85 years were used for the public.

After radiation exposure, children are reported to be more radiosensitive for about 30 % of tumor types when compared with adults. These types include leukemia and thyroid, skin, and brain cancer. They have the same sensitivity as adults when it comes to 25 % of tumor types such as kidney and bladder, and are less sensitive than adults when it comes to 10 % of tumor types including lung cancer.

For effects that are bound to occur after high doses, UNSCEAR [9] concluded that, as seen with carcinogenesis, there are some instances in which childhood exposure poses more risk than adult exposure (e.g., for effects in the brain, cataracts, and thyroid nodules). There are other instances where the risk appears to be about the same (e.g., neuroendocrine system and effects in the kidneys), and there are a few instances where children's tissues are more resistant (lung, immune system, marrow, and ovaries).

4.4.3 Effective Dose Adjusted by Age Weighting Factor for Radiation Protection

Radiation exposure means the process of being exposed to radiation or radionuclides, and the significance of exposure is determined by the resulting radiation dose. Thus, dose can be considered a quantitative expression of risk of radiation exposure. In protecting individuals from the harmful effects of radiation, it is the control of radiation doses that is important, no matter what the source.

The ICRP's system of radiological protection aims primarily to protect human health. It is to manage and control exposure to radiation so that deterministic effects are prevented and risk of stochastic effects is reduced to the extent reasonably achievable.

In view of the uncertainties surrounding the values tissue weighting factors and the estimate of detriment, currently the ICRP considers it appropriate for radiological protection purposes to use age- and sex-averaged tissue weighting factors and numerical risk estimates.

However, quantitative information on the age-dependent risk coefficients of radiation exposures can be now considered to be available. Actually, WHO [11] has calculated health risk for various age groups. To control exposure so that the risk is reduced to an extent we have to develop a measure applicable to all age groups. As described previously, age-dependent dose coefficients have been already provided by ICRP. Now, it is needed for the ICRP to prepare a new report on the age-dependent radiation risks, and then to develop a new system of radiation protection for the general public to include radiation protection scheme for children based on the age-dependent radiation risks. I think there are two approaches: development of new radiological protection criteria for children, and development of a new effective dose adjusted by age weighting factors.

4.5 Discussion

This chapter is concerned with radiation exposure of members of the public. Other than the public, nearly 25,000 workers including TEPCO employees and contractors were also involved in the accident. Doses for workers were controlled, so no radiation-related deaths or acute effects have been observed among them. A small number of workers were highly exposed, but it is unlikely that excess cases of thyroid cancer caused by radiation exposure would be detectable. Special health examinations will be given to workers with exposures above 100 mSv.

The assessment regarding radiological effects on plants and animals was performed by UNSCEAR, and its secretary concluded that the exposures of organisms in the environment are unlikely to cause anything more than transient harm to their populations [9]. The issue is important for the environment, so detailed studies should be continued.

The experience from the 1986 Chernobyl accident has shown us that apart from any direct impact on physical health, the social and societal effects, and their associated health consequences in the affected population, are very important [21]. In this chapter, I have emphasized the importance of dose as a measure of radiation risk in radiation protection. It was reported, however, that the social and societal effects as well as their associated health consequence are not directly related to the dose. Now, we have to realize the importance of the sufficient explanation of the meaning of dose. Nevertheless, I would like to emphasize the importance of dose assessments both for practical purposes of radiation protection and for scientific goals such as epidemiological studies and radiological risk analysis.

References

1. ICRP (1991) 1990 Recommendations of the International Commission on Radiological Protection. ICRP Publication 60. Ann ICRP 21(1-3):1–201
2. ICRP (2007) The 2007 recommendations of the International commission on radiological protection. ICRP Publication 103. Ann ICRP 37 (2-4)
3. Nuclear Regulation Authority (2013) http://radioactivity.nrs.go.jp/ja
4. Fukushima Prefecture (2013) http://www.pref.fukushima.jp/imu/kenkoukanri/25605siryou1-2.pdf
5. Pröhl G, Ehlken S, Fiedler I, Kirchner G, Klemt E, Zibold G (2006) Ecological half-lives of ^{90}Sr and ^{137}Cs in terrestrial and aquatic ecosystems. J Environ Radioact 91:41–72
6. Ishigure N, Matsumoto M, Nakano T, Enomoto H (2004) Development of software for internal dose calculation from bioassay measurements. Radiat Protect Dosim 109:235–242
7. Fukushima Prefecture (2013) http://www.pref.fukushima.jp/imu/wbc/20130628wbc_joukyou.pdf

8. Kim E, et al (2012) Screening survey on thyroid exposure for children after the Fukushima Daiichi Nuclear Power Station Accident. In: Proceedings of the 1st NIRS symposium on reconstruction of early internal dose, NIRS, Chiba
9. UNSCEAR (2013) http://wwwunis.unvienna.org/unis/en/pressrels/2013/unisin475.html
10. ICRP (2006) Assessing dose to the representative person for the purpose of radiation protection of the public. ICRP Publication 101. Ann ICRP 346 (3)
11. World Health Organization (WHO) (2013) Health risk assessment from the nuclear accident after the Great East Japan Earthquake and tsunami based on a preliminary dose estimation. World Health Organization
12. World Health Organization (WHO) (2012) Preliminary dose estimation from the nuclear accident after the Great East Japan Earthquake and Tsunami. World Health Organization
13. ICRP (1996) Conversion coefficients for use in radiological protection against external radiation. ICRP Publication 74. Ann ICRP 26 (3/4)
14. ICRP (1989) Age-dependent doses to members of the public from intake of radionuclides: Part 1. ICRP Publication 56. Ann ICRP 20 (2)
15. ICRP (1993) Age-dependent doses to members of the public from intake of radionuclides: Part 2. ICRP Publication 67. Ann ICRP 23(3/4)
16. ICRP (1995) Age-dependent doses to members of the public from intake of radionuclides: Part 3. ICRP Publication 69. Ann ICRP 25 (1)
17. ICRP (1995) Age-dependent doses to members of the public from intake of radionuclides: Part 4. ICRP Publication 67. Ann ICRP 25 (3/4)
18. ICRP (1996) Age-dependent doses to members of the public from intake of radionuclides: Part 5. ICRP Publication 72. Ann ICRP 26 (3/4)
19. ICRP (2001) Dose to the embryo and embryo/fetus from intake of radionuclides by the mother. ICRP Publication 88. Ann ICRP 31 (1-3)
20. ICRP (2004) Doses to infants from ingestion of radionuclides in mother's milk. ICRP Publication 95. Ann ICRP 34 (3/4)
21. United Nations Scientific Committee on the Effects of Atomic Radiation (UNSCEAR) (2008) Sources and effects of ionizing radiation. UNSCEAR 2008 Report Volume 2, Annex D. United Nations Scientific Committee on the Effects of Atomic Radiation

Part III
Radiation Survey of the Environment

Chapter 5
Environmental Radiation Status In and Around Tokyo Immediately After the TEPCO Fukushima Dai-ichi Nuclear Power Plant Disaster

Takeshi Iimoto, Hirofumi Fujii, Seiichi Someya, Sadao Iizumi, Takao Ebisawa, Seiichi Hirose, Etsuko Furuta, Keiji Kusama, Norio Nogawa, Hiroshi Mitani, Masao Kamiko, Natsumaro Kutsuna, Yasuhiro Watanabe, and Takahiko Suzuki

Abstract An example of environmental radiation status in and around Tokyo immediately after the TEPCO Fukushima Dai-ichi Nuclear Power Plant (NPP) disaster is introduced. The east part of the Metropolis of Tokyo and northwest of Chiba Prefecture are located about 200–250 km south from the NPP. The local governments in the area have officially surveyed the environmental radiation status after the disaster in response to numerous requests from their citizens. The radiation surveillance by local governments has been conducted and technically guided by the radiation protection specialists. The two main goals of the surveillance are (1) to measure the ambient radiation dose (microsieverts per hour) at all the schoolyards, public parks, and representative measuring points selected by the local government, and (2) to measure the specific radioactivity (becquerels per kilogram) of drinking

T. Iimoto (✉) • N. Nogawa • H. Mitani • M. Kamiko • N. Kutsuna • Y. Watanabe • T. Suzuki
The University of Tokyo, 7-3-1 Hongo, Bunkyo-ku, Tokyo 113-8654, Japan
e-mail: iimoto.takeshi@mail.u-tokyo.ac.jp

H. Fujii
National Cancer Center Hospital East, Kashiwa, Japan

S. Someya
Kashiwa City Local Government, Kashiwa, Chiba, Japan

S. Iizumi
Nagareyama City Local Government, Nagareyama, Chiba, Japan

T. Ebisawa • S. Hirose
Bunkyo Ward Local Government, Tokyo, Japan

E. Furuta
Ochanomizu University, Tokyo, Japan

K. Kusama
Japan Radioisotope Association, Tokyo, Japan

S. Takahashi (ed.), *Radiation Monitoring and Dose Estimation of the Fukushima Nuclear Accident*, DOI 10.1007/978-4-431-54583-5_5,

water and local food items. In parallel with these movements, radiation experts in the University of Tokyo also organized a special correspondence team to survey the environmental radiation status immediately after the nuclear disaster. These activities and related data are introduced in this chapter.

Keywords Ambient radiation dose • Chiba • Specific radioactivity • Tokyo

5.1 Introduction

Kashiwa City and Nagareyama City are located in the northwest part of Chiba Prefecture in the metropolitan area of Tokyo, Japan. These cities are located roughly 200 km southward from the TEPCO Fukushima Dai-ichi Nuclear Power Plant (NPP). Bunkyo ward in Tokyo is at a distance of 220 km south of the NPP. The office location and other detailed information of these three cities are listed in Table 5.1.

These local governments have officially surveyed the environmental radiation status immediately after the disaster in response to requests from their citizens. The radiation surveillance in this area has been conducted and technically guided by radiation protection specialists.

The University of Tokyo is also located mainly in the metropolitan area of Tokyo, Japan. This university owns three main campuses: the Hongo campus and the Komaba campus are located in the middle-eastern part of the Metropolis of Tokyo, and the Kashiwa campus is located in the northwestern part of Chiba Prefecture. The distance between the NPP and the three campuses ranges from about 200 to 250 km. Immediately after the nuclear disaster, the university organized a special corresponding team to survey the environmental radiation status in the site of the university. The team consists of about 20 members and includes mostly radiation protection specialists or technical experts of the university specialized in radiation measurement. This project is not research oriented; rather, the purpose is to provide, in the absence of related information, the actual data on environmental radiation immediately after the accident. This information had been continuously provided both to the university community members and to the public through a website.

Table 5.1 Location, area, and population of the cities as of April 1, 2012

City name	Prefecture	Office location (-°-′-″)	Area (km^2)	Population
Kashiwa City	Chiba	35-52-05N 139-58-35E	114.9	404,252
Nagareyama City	Chiba	35-51-31N 139-54-9E	35.28	166,493
Bunkyo ward	Tokyo	35-42-29N 139-45-9E	11.31	201,079

This chapter provides the background status and technical information on the related activities together with the estimated environmental radiation data at that time.

5.2 Monitoring Activity and Data of Local Governments

5.2.1 External Exposure

5.2.1.1 Targets and Methods

Main targets of the surveillance at the northwest of Chiba prefecture are the ambient radiation dose (μSv h^{-1}, microsieverts per hour) at all the schoolyards, public parks, and representative measuring points selected by the local governments. This activity has been based on the decision of a local forum of six cities including the two cities of Kashiwa and Nagareyama as the "Conference on Radiation Countermeasures in the Tohkatsu Area (CRCT)" [1].

The ambient dose equivalent rate around the Tohkatsu area, northwest of Chiba, was elevated after the accident, as already mentioned. The public strongly requested their local governments to monitor the ambient dose equivalent rate precisely and officially. In addition, many questions, requests for consultation, and feelings of fear assaulted the local governments. Six local governments (Kashiwa, Nagareyama, Matsudo, Noda, Abiko, and Kamagaya) in the Tohkatsu area decided to establish a new organization, CRCT, to solve the total situation officially and in cooperation. The CRCT started its official activity on June 8, 2011, after a preparation period of about 1 month. A chair of the conference is the mayor of Kashiwa City. Three specialists of radiation protection, radiation measurement, and medical science in the radiation field are also involved in the conference as supporting members for its activity. We think this is a preparation step or first step toward the real stakeholder engagement and involvement procedure in local governments for the optimization of protection. ICRP Publication 111 [2] recommends "(71) Authorities should facilitate the setting-up of local forums involving representatives of the affected population and relevant experts (e.g., health, radiation protection, agriculture authorities, etc.). These forums will allow gathering and sharing of information and favor a common assessment of the effectiveness of strategies driven by the population and the authorities."

Based on the guideline determined by the CRCT, the ambient dose rate has been monitored in the cities of Kashiwa and Nagareyama. The latest dose distribution data at the height of 5 cm (for identifying contaminated areas), 50 cm (for dosimetry of children), and 100 cm (for adults) from the ground in the cities can be seen against the background of a Google map on the government web pages. Monitoring targets are all schoolyards (nursery schools, kindergartens, child centers, elementary schools, and high schools), parks and sports grounds, the exterior

of local government institutions, bus terminals, city streets, city pools, and around sewage adjustment ponds and waste disposal sites. These sites are monitored by energy-response compensation gamma survey meters with NaI(Tl) or CsI(Tl) scintillation detectors. These survey meters are also selected based on the CRCT guideline. The monitoring frequency for each investigation point was more than once monthly. These monitoring activities have also been conducted by Bunkyo ward in Tokyo.

The local governments distributed one (or two) electric personal dose meter(s) to all the public/private schools in Kashiwa City and Nagareyama City. The purpose was to announce the monthly dose of children for their routine activities to the citizens, and to determine an actual annual dose based on the measured results; this is representative of a child's personal dose, not the ambient dose. Unfortunately, at the early stages the citizens tended to worry about the effects of an extremely small area's high contamination, a so-called micro hot spot. The cities would like to do a quantitative analysis to show the actual level of the exposure dose around the micro hot spot rather than a qualitative explanation. Electric personal dose meters in each school were given to a representative staff member, and the meters were worn at the chest height of a typical child. The personal dose meter was operated all day long (24 h). At nights and on holidays the dose meters were placed in rooms of the schools.

5.2.1.2 Data and Information

The following data are major results of activities conducted by the three local governments as described in the earlier section.

The ambient radiation dose in the cities has been surveyed since around May 2011. The highest value of the ambient radiation dose was 0.65 μSv h^{-1} in Kashiwa City, 0.58 μSv h^{-1} in Nagareyama City and 0.22 μSv h^{-1} in Bunkyo ward at the height of 1 m from the ground among all the monitoring points. These values include the natural background dose rate (0.04–0.08 μSv h^{-1}).

Figure 5.1 shows an example of annual average dose at schools in Kashiwa City measured by personal dose meters from September 1, 2011 to August 31, 2012. The data recorded in this project have been announced on the official website in the city every month. This activity and information greatly reduced the number of questions or requests for consultations from citizens living around the "micro hot spot" area.

5.2.2 Internal Exposure

5.2.2.1 Targets and Methods

Local governments were strongly encouraged to monitor the specific radioactivity (Bq kg^{-1}, becquerels per kilogram) of local food and drinking water under the present popular policy of "Local Production for Local Consumption" in Japan.

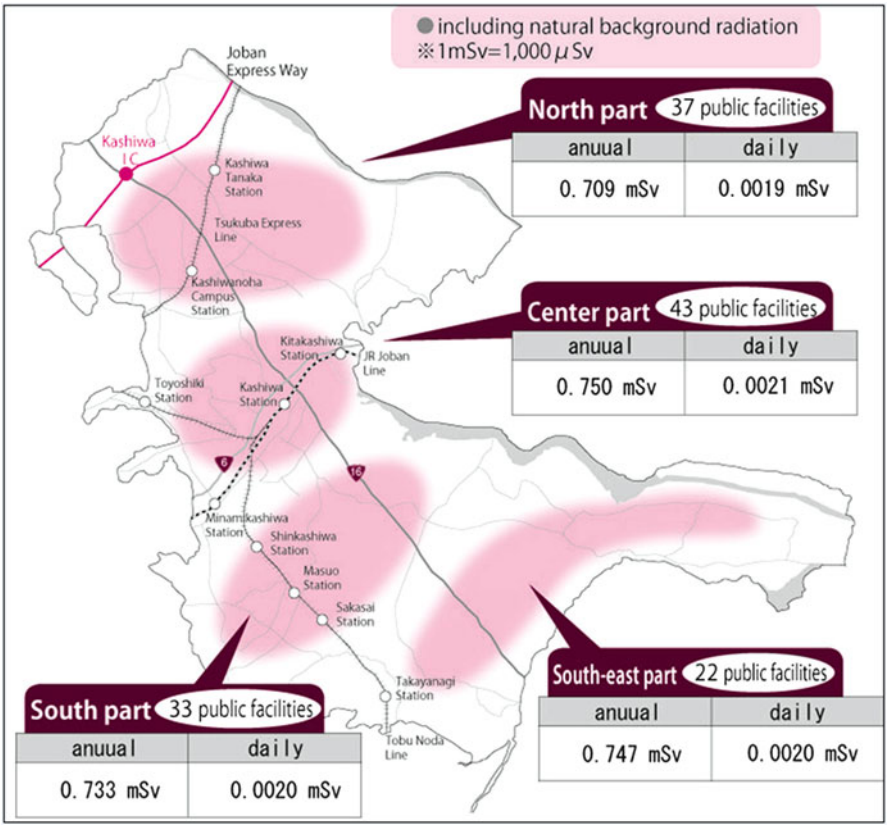

Fig. 5.1 Annual average dose at schools in Kashiwa City measured by personal dose meters from September 1, 2011 to August 31, 2012. Kashiwa City is located in the northwest part of Chiba Prefecture in the metropolitan area of Tokyo, Japan, roughly 200 km to the south of the TEPCO Fukushima Dai-ichi Nuclear Power Plant

In parallel with the national survey and the relating prefectures' survey, the three cities have been continuing to monitor various materials and to announce the results to their citizens. The target materials are school lunch and food items, local food items, tap water, and supplied water, water in school or public pools, waste disposal, etc. For example, the actual lunch supplied for 1 week in each school was monitored by a Ge semiconductor or NaI(Tl) scintillation spectroscopy system.

The sampling procedures of local food items are as follows: for example, in Kashiwa City, (1) the types of food to be monitored from the representative four areas of the city are discussed and selected among agricultural cooperatives, farmers, and city officers; (2) city officers ask the selected farmers for basic information on these food items, for example, the planting season; and (3) local food items are sampled, weighed, and passed on to monitoring rooms. The food samples are then measured by a NaI(Tl) scintillation spectroscopy system (a 15-min measurement with a 500-ml Marinelli beaker, where the minimum detectable limit concentration

Table 5.2 Specific radioactivity of service water in Nagareyama purification plant in April, 2011

Date in April 2011	22	23	24	25	26	27	28	29	30
Bq kg^{-1} of ^{131}I	–	110	–	33	14	–	ND	ND	ND

–, no data
ND, less than lower detectable limit concentration

is estimated as 6 Bq kg^{-1}). As of the end of August 2012, about 800 local food samples have been monitored using this procedure in Kashiwa City. These data have been reported on the city website as well as in a bimonthly report in the public relations magazine of the local government.

Nagareyama City and Bunkyo ward have also monitored their food materials and opened all data to the public similarly.

5.2.2.2 Data and Information

The following data are major results of activities conducted by the three local governments as described in the earlier section.

The specific radioactivity of the drinking water and of the local food items has been surveyed since March 2011 and since April 2011, respectively, for example in Nagareyama City. As of March 23, 2011, only one sample of service water showed 110 Bq kg^{-1} of ^{131}I; no water sample other than this has been found to exceed the limits until now, 2013, as shown in Table 5.2.

The highest specific radioactivity was 831 Bq kg^{-1} of $^{134+137}$Cs, measured for a flat Japanese mushroom that was cultivated on Japanese oak logs, which were sampled in Nagareyama City on November 16, 2011. This was detected during the monitoring carried out for Chiba Prefecture. In addition, the radioactivity levels of an outdoor bamboo shoot and a flat mushroom also temporarily exceeded the acceptable limits for the specific concentration of food items. These were also detected by Chiba Prefecture. According to the monitoring results for Nagareyama City, disaster-induced specific radioactivity of all surveyed food items (excluding the items listed above) was found to be below the limits for intake dose (see Tables 5.3 and 5.4).

In Kashiwa City, about 800 samples of the local food items, which were grown and circulated in the city as of the end of August 2012, have been checked using a NaI(Tl) scintillation spectroscopy system. An outdoor bamboo shoot sampled in the city on April 9, 2012 showed 170 Bq kg^{-1} as the specific radioactivity of $^{134+137}$Cs. In addition, a crucian carp sampled in Teganuma Lake on June 23, 2012 showed 241 Bq kg^{-1}. Specific radioactivity of all surveyed samples, other than these three, has been below the limits.

In Bunkyo ward, no water sample supplied to the city has exceeded the national limits for intake dose, based on the monitoring at their local purification plants. The specific radioactivity of school lunches was also surveyed four times (in December

Table 5.3 Specific radioactivity ($^{134+137}$Cs) of local food items in Nagareyama City, measured *after* April 13, 2012

Bq kg^{-1}	<25	>25, <50	>50, <100	>100<
Number of items	269	4	0	0

This monitoring was carried out by the Nagareyama City local government

Table 5.4 Specific radioactivity ($^{134+137}$Cs) of local food items in Nagareyama City, measured *before* April 13, 2012

Bq kg^{-1}	<20	>20, <500	>500
No. of items	203	2	0

This monitoring is carried out by the Nagareyama City local government

2011, and May, July, and September 2012) by the local government. Thus far, 162 sets of school lunches in the city have been checked using a Ge spectroscopy system. The highest specific radioactivity of $^{134+137}$Cs was detected as 2.5 Bq kg^{-1} in a school lunch and 15.4 Bq kg^{-1} in milk, which were recorded in December 2011.

5.3 Monitoring Activity and Data of the University of Tokyo

5.3.1 Targets and Methods

The two primary targets of the surveillance were (1) the ambient radiation dose (μSv h^{-1}) and (2) the specific radioactivity (Bq kg^{-1}) of rainwater and of soil around the surface of the ground, which was used to show the level of contamination.

To measure the ambient dose, well-calibrated NaI(Tl) scintillation survey meters of the energy compensation type were used. The elevations at which measurements were performed were adequately selected as 1 m (for the standard height of adults in the Kashiwa campus and the Hongo campus), or 15 m for the airborne radioactivity survey in the Komaba campus.

To measure the specific radioactivity of soil, NaI(Tl) scintillation and/or Ge semiconductor spectroscopy systems were used. Soil materials were sampled from the surface of the ground, from a layer between 0 and 1 cm depth (for surface layer target method) or from a layer between 0 and 5 cm depth (for standard target method). The sampled soil was weighed and measured as is (without being dried). Specific radioactivity of samples of rainwater was also measured. The ambient dose data had been reported every day on the website. In addition, the data had been published in the portal site magazine of the university. Soil contamination data were reported occasionally and periodically.

5.3.2 Data and Information

Since the morning of March 15, 2011, continuous survey of the ambient radiation dose rate has been officially performed at the selected representative locations on the campus sites. The first peak dose of 0.72 μSv h^{-1} was observed around 2:30 pm on March 15, 2011, in the Kashiwa campus, and the second peak dose of 0.80 μSv h^{-1} was observed around 11:00 am on March 21, 2011, when the first rain fell after the NPP accident. The elevation at which these measurements were performed was 1 m above the ground.

The large reduction of ambient radiation dose rate was observed after 20 days following March 21, 2011, and afterward the ambient radiation dose gradually reduced until the continuous surveillance ended at the end of March 2012. At that time, the representative ambient dose rates of the campuses were measured to be about 0.23 μSv h^{-1} for the Kashiwa campus and about 0.11 μSv h^{-1} for the Hongo campus (at 1 m above the ground). These measured values included the natural background dose rate.

Area distribution of ambient radiation dose was measured at 1,516 points with a distance of 6 m between them in the site of the Kashiwa campus from October 10 to November 10, 2011. At the elevation of 1 m above the ground, the average dose rate was 0.3 μSv h^{-1}, and more than 80 % of measurements yielded values less than 0.35 μSv h^{-1}. Some measurement spots where the radiation dose indicated more than 0.6 μSv h^{-1} at the elevation of 1 m and more than 1.0 μSv h^{-1} at the elevation of 5 cm have been decontaminated, following the corresponding plan determined by the Kashiwa local government. These spots were found in drainage pathways, such as rain gutters and underneath downspouts. After the contaminated surface soil was removed, the observed radiation dose at the elevation of 5 cm above the ground dropped by about 70–80 % from the level of the predecontamination values.

From March 13, radiation experts in the Komaba campus had started measuring the ambient radiation dose rate. An automatic ambient radiation monitoring system was installed about 15 m above the ground. During the measurement period, the maximal level of the ambient radiation dose rate in the Komaba campus was about 0.52 μSv h^{-1}, observed at 7:00 pm on March 15, 2011. By the end of April 2011, the radiation dose rate at the elevation of 15 m was reduced almost to the same level as the natural background radiation (0.05–0.06 μSv h^{-1}).

As of mid-April 2011, 0.2–0.35 kBq kg^{-1} of ^{131}I and 1.0–1.5 kBq kg^{-1} of $^{134+137}Cs$ were measured in soil samples in the Kashiwa campus using the standard target method. On March 29, 2011, 7.8 kBq kg^{-1} of ^{131}I and 2.7 kBq kg^{-1} of $^{134+137}Cs$ were measured in soil samples in the Hongo campus using the surface layer target method. On March 22, 2011, 3.2 kBq l^{-1} of ^{131}I and 0.18 kBq l^{-1} of $^{134+137}Cs$ were measured in a rainwater sample on the Hongo campus site.

Box 5.1 indicates a member list of the special corresponding team appointed to survey the environmental radiation status in the University of Tokyo. We wish to express our sincere gratitude to the members for their enormous contribution in the related activity.

Box 5.1 Members of the special corresponding team appointed to survey the environmental radiation status in the University of Tokyo

T. Iimoto, N. Nogawa, K. Tao, S. Higaki, Y. Koike, N. Kosaka, T, Suzuki, A. Kobashi, M. Tanikawa, K. Tanoi, M. Hirota, Y, Yie, K. Nozawa, H. Mitani, N. Kutsuna, T. Watanabe, K. Kamiko, Y. Watanabe, Y. Kamimura, and Staffs of Division for Environment, Health and Safety and Staffs of Environment, Health and Safety Department.

5.4 Conclusion

An example outline of the environmental radiation status in and around Tokyo immediately after the nuclear disaster of the TEPCO Fukushima Dai-ichi NPP has been presented. The background status and technical information of the related measuring activities and the estimated data were introduced, focusing on activities of three local governments and the University of Tokyo.

Kashiwa City and Nagareyama City are now continuing monitoring of environmental radiation and operating their decontamination program following the local government policies. Their newest data can be checked and traced through their official website.

References

1. Iimoto T, Fujii H, Oda S, Nakamura T, Hayashi R, Kuroda R, Furusawa M, Umekage T, Ohkubo Y (2012) Measures against increased environmental radiation dose by the Tepco Fukushima Dai-ichi NPP accident in some local governments in the Tokyo metropolitan area: focusing on examples of both Kashiwa and Nagareyama cities in Chiba prefecture. Radiat Prot Dosim 152(1–3):210–214. doi:10.1093/rpd/ncs224
2. Annals of the ICRP, ICRP Publication 111. Application of the commission's recommendations to the protection of people living long-term contaminated areas after a nuclear accident or a radiation emergency (2009) ISSN 0146-6453, ISBN 978-0-7020-4191-4, 39(3)

Chapter 6
Radiation Survey Along Two Trails in Mt. Fuji to Investigate the Radioactive Contamination Caused by TEPCO's Fukushima Daiichi Nuclear Plant Accident

Kazuaki Yajima, Kazuki Iwaoka, and Hiroshi Yasuda

Abstract Mt. Fuji is located approximately 300 km southwest of TEPCO's Fukushima Daiichi Nuclear Power Plant. We performed the radiation survey along two main Mt. Fuji's trails from 04:30 to 18:30 on July 9, 2011. We climbed Yoshida trail from Fuji-Subaru Line fifth station (2,300 m in altitude) to Yoshida-Subashiri top (3,720 m in altitude) and descended Subashiri trail from the Yoshida-Subashiri top to Subashiri new fifth station (2,000 m in altitude) on foot while measuring gamma rays. The dose rate 1 m above ground as measured using a NaI(Tl) scintillation survey meter was within the range from 0.03 to 0.05 μSv/h throughout our measuring trip. We used a NaI(Tl) scintillation spectrometer for gamma-ray pulse height spectra measurement. The gamma-ray pulse height spectra obtained at least 2,500 m in altitude on both Yoshida and Subashiri trails showed the peaks of two radioactive cesium isotopes (^{134}Cs and ^{137}Cs) and natural radioactive nuclides. It was confirmed that a radioactive plume released from the Fukushima Daiichi Nuclear Power Plant had arrived at least 2,500 m above sea level of Mt. Fuji.

Keywords Dose rate • Plume • Radiation survey • Radioactive contamination

K. Yajima (✉) • K. Iwaoka
National Institute of Radiological Sciences,
4-9-1, Anagawa, Inage-ku, Chiba 2638555, Japan
e-mail: k_yajima@nirs.go.jp

H. Yasuda
National Institute of Radiological Sciences,
4-9-1, Anagawa, Inage-ku, Chiba 2638555, Japan

United Nations Scientific Committee on the Effects of Atomic Radiation,
Vienna International Centre, PO Box 500, Vienna 1400, Austria

S. Takahashi (ed.), *Radiation Monitoring and Dose Estimation of the Fukushima Nuclear Accident*, DOI 10.1007/978-4-431-54583-5_6,

6.1 Introduction

A large amount of radioactive materials was released in the environment as a result of the TEPCO Fukushima Daiichi Nuclear Power Plant (NPP) accident caused by the Great East Japan Earthquake that occurred on March 11, 2011. The spread of the radioactive contamination had become a concern just after the accident. Mt. Fuji, which is 3,776 m above sea level and the highest mountain in Japan, is located approximately 300 km southwest of TEPCO's Fukushima Daiichi NPP. Because an environmental radiation monitoring level in Shizuoka City, which is approximately 50 km southwest from Mt. Fuji, rose on March 15 and 21–22, 2011, it is estimated that the radioactive plume released by TEPCO's

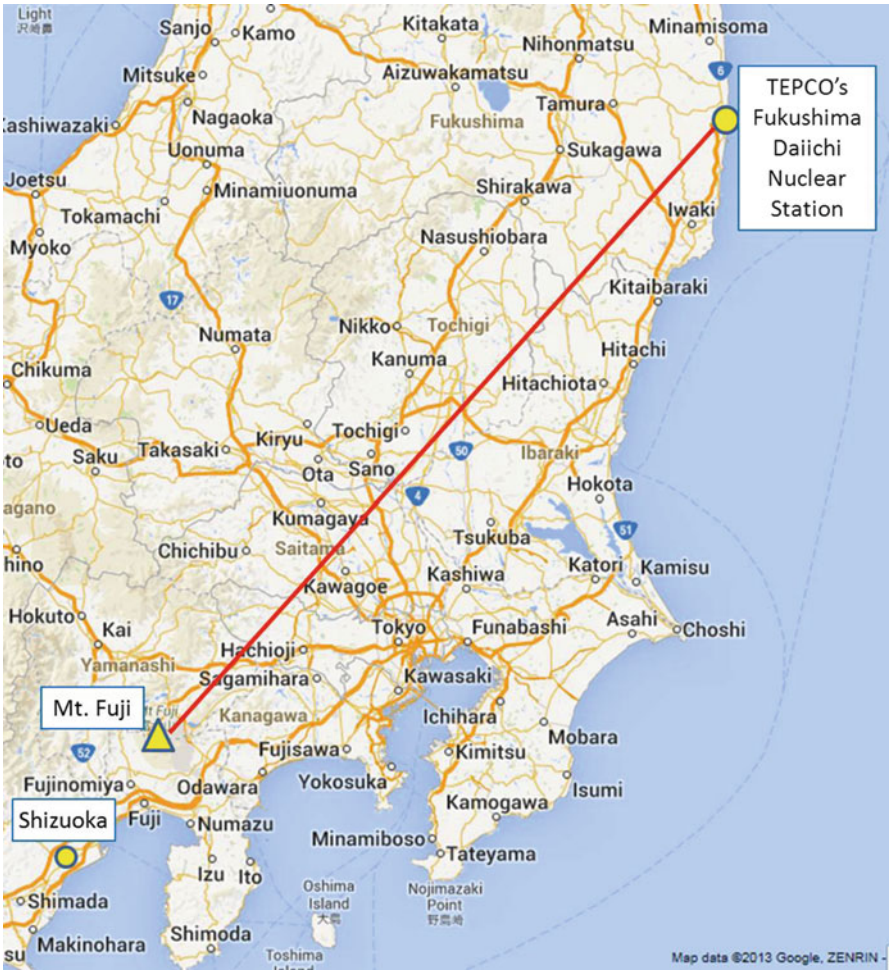

Fig. 6.1 Location of TEPCO's Fukushima Daiichi Nuclear Plant, Mt. Fuji, and Shizuoka City

Fukushima Daiichi Nuclear Power Station arrived around Mt. Fuji at those times [1]. Figure 6.1 shows the locations of TEPCO's Fukushima Daiichi Nuclear Station, Mt. Fuji, and Shizuoka City.

Climbing Mt. Fuji is a very popular leisure activity and its trails are crowded with many climbers every summer. Thus, to reveal the radioactive contamination level of Mt. Fuji's trails before the summer season began, we performed the radiation survey along two main Mt. Fuji trails.

6.2 Measurements

The measurements were carried out from 04:30 to 18:30 on July 9, 2011. We climbed the Yoshida trail from the Fuji-Subaru Line fifth station 2,300 m above sea level to the top of Yoshida-Subashiri 3,720 m above sea level and descended Subashiri trail from the Yoshida-Subashiri top to the Subashiri-guchi new fifth station at 2,000 m above sea level on foot while measuring gamma-ray dose rate and pulse height spectra. A trace of our measuring trip at Mt. Fuji is shown in Fig. 6.2.

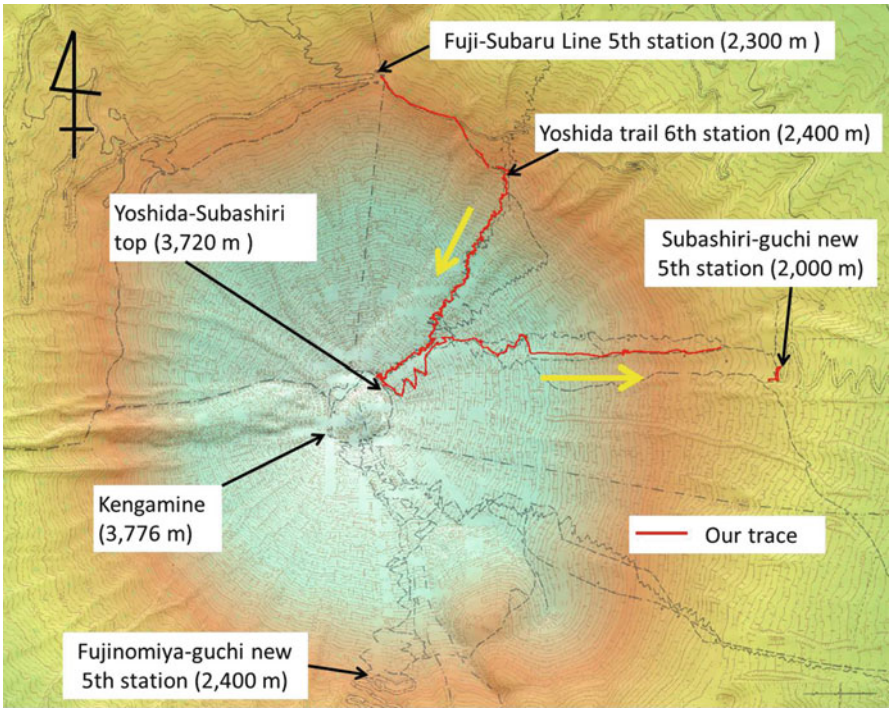

Fig. 6.2 A trace of our measuring trip at Mt. Fuji on July 9, 2011. We started from Fuji-Subaru line fifth station at 04:30 and reached Subashiri-guchi new fifth station at 18:30

Fig. 6.3 Two of the authors on the measuring trip around Yoshida trail sixth station. The probe of the NaI(Tl) survey meter was set to an altitude of 1 m from the ground for dose rate measurements

The dose rate was measured using a NaI(Tl) scintillation survey meter (Aloka, TCS-172B; Hitachi Aloka Medical, Tokyo, Japan). The authors at times stopped moving and read the indicated values of the survey meter at a height of 1 m from the ground on the trail. A NaI(Tl) scintillation spectrometer (EMF211; EMF Japan, Osaka, Japan) with a tablet-size personal computer and an external power supply battery was used for gamma-ray pulse height spectrum measurements. The authors performed the 1-min repetition measurement, putting the spectrometer in a bag pack through the measuring trip. One scene of the measuring trip taken around the Yoshida trail sixth station 2,400 m above sea level is shown in Fig. 6.3.

6.3 Results and Discussions

The measured dose rates ranged from 0.03 to 0.05 μSv/h throughout our measuring trip. As a result, it was found that the dose rates of the Yoshida trail and the Subashiri trail in Mt. Fuji were at nominal background levels. These two trails are located on the northeastern side of Mt. Fuji. There are two other major trails in Mt. Fuji. One is Fujinomiya trail, located on the south side of Mt. Fuji, and the other is Gotemba trail, on the southeastern side of Mt. Fuji. Arrival direction to Mt. Fuji and the horizontal expanse of the radioactive plume released from TEPCO's Fukushima Daiichi NPP have not been investigated yet. However, we assume that the dose rates of the Fujinomiya trail and Gotemba trail were in the same range (nominal background

level) as the Yoshida and Subashiri trails because a difference in the degree of radioactive contamination is not seen around the Mt. Fuji area from the result of the airborne monitoring survey at an altitude less than 2,000 m by the Ministry of Education, Culture, Sports, Science and Technology (MEXT) [2].

Figure 6.4a–h shows the gamma-ray pulse height spectra given as the integration of the ten consecutive measurements (corresponding to 10-min collection time) measured at (a) the Fuji-Subaru Line fifth station, 2,300 m above sea level, (b) the Yoshida trail sixth station, 2,400 m above sea level, (c) the middle of the Yoshida trail, 2,500 m above sea level, (d) the middle of the Yoshida trail, 3,000 m above sea level, (e) the middle of the Yoshida trail, 3,400 m above sea level, (f) the Yoshida-Subashiri top, 3,720 m above sea level, (g) the middle of the Subashiri trail, 2,500 m above sea level, and (h) the Subashiri new fifth station at 2,020 m above sea level, respectively. The spectra measured at less than 2,500 m above sea level showed the peaks of two radioactive cesium isotopes (^{134}Cs and ^{137}Cs) and natural radioactive nuclides. The peaks of ^{134}Cs and ^{137}Cs could not be identified in spectra that were measured more than 2,500 m above sea level.

It was confirmed that a radioactive plume released from TEPCO's Fukushima Daiichi NPP had arrived at least 2,500 m above sea level at Mt. Fuji. The ground surface is often above rain clouds on a high mountain such as Mt. Fuji. Therefore, we comment that the radioactive materials might hardly be deposited in the soil because it was dry, although the radioactive plume arrived at places more than 2,500 m above sea level. The airborne monitoring survey by MEXT has not provided data in mountain areas greater than 2,000 m in altitude because of difficulty in making flights. Therefore, it is hoped that our data become valuable information for the evaluation of the vertical distribution of the radioactive plume released by the Fukushima nuclear accident.

6.4 Conclusion

We performed a radiation survey along two main Mt. Fuji trails on July 9, 2011. The measured dose rates were within the range from 0.03 to 0.05 μSv/h throughout our measuring trip, which were nominal background levels. From the results of these gamma-ray pulse height spectrum measurements, it was confirmed that a radioactive plume released from TEPCO's Fukushima Daiichi NPP had arrived at least 2,500 m above sea level at Mt. Fuji.

Acknowledgments The authors thank the staff of the NPO "Valid Utilization of Mt. Fuji Weather Station" for their kind advice about our Mt. Fuji climbing.

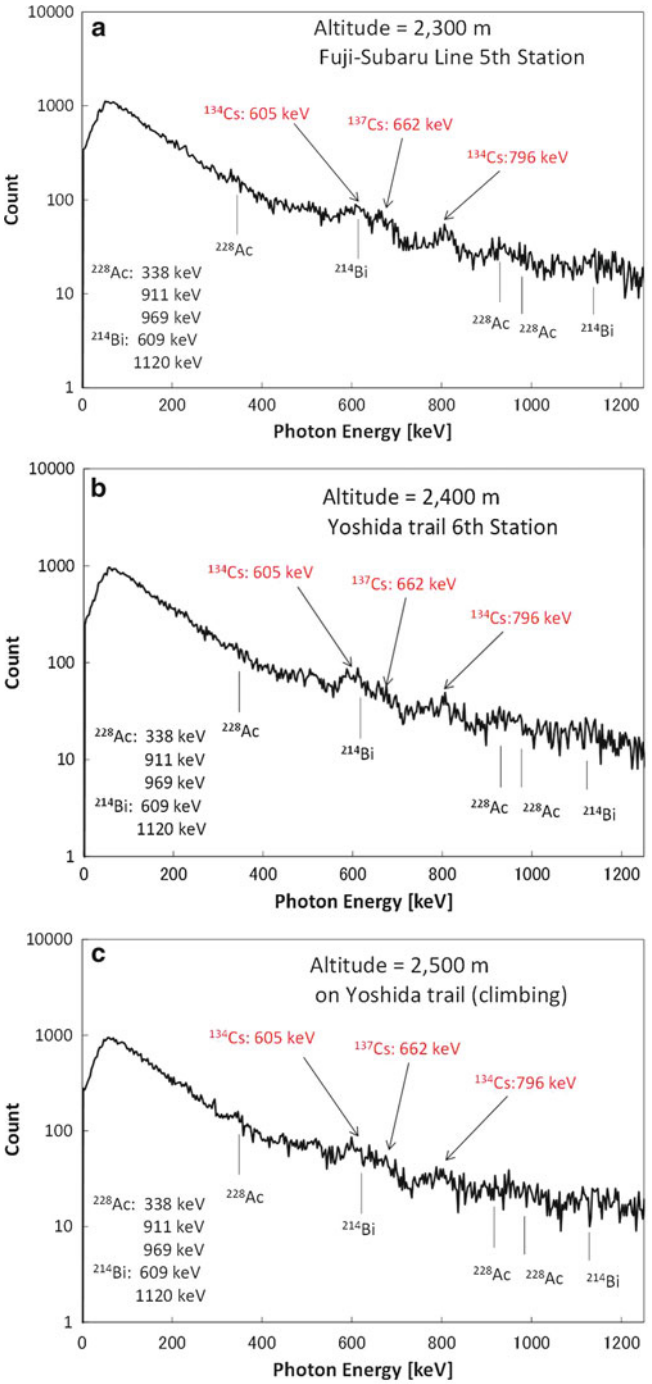

Fig. 6.4 **a**–**h** Gamma-ray pulse height spectra measured using a NaI(Tl) scintillation spectrometer on Mt. Fuji's trails

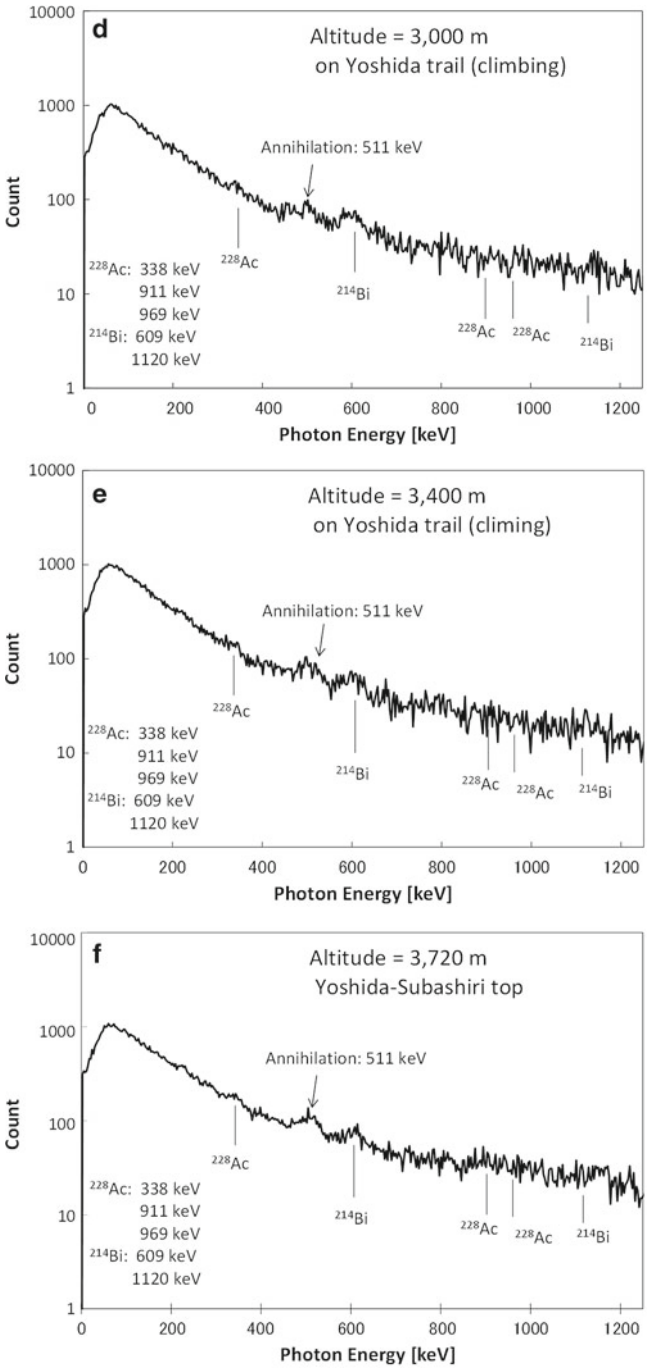

Fig. 6.4 (continued)

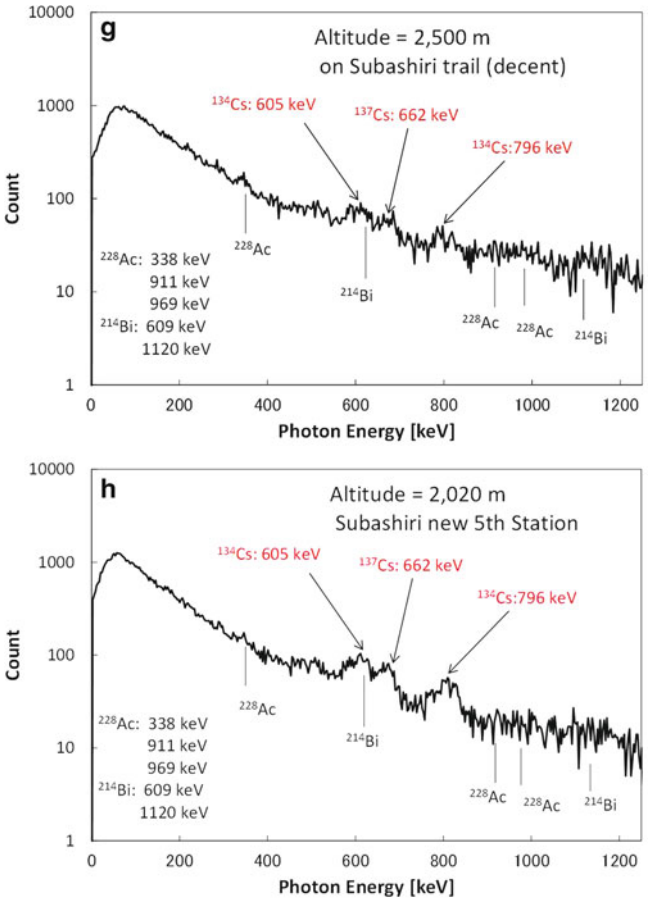

Fig. 6.4 (continued)

References

1. Shizuoka Prefecture website (in Japanese) (2013) http://www.pref.shizuoka.jp/kinkyu/1fmonitoring/documents/110311-0831-1fruikei.pdf. Accessed 26 July 2013
2. Ministry of Education, Culture, Sports, Science and Technology (MEXT) (2013) Results of airborne monitoring survey by MEXT in Iwate, Shizuoka, Nagano, Yamanashi, Gifu, and Toyama Prefectures, and revision of the past airborne monitoring results by reflecting the influences of natural radionuclides. http://radioactivity.nsr.go.jp/en/contents/4000/3177/24/1270_111114.pdf. Accessed 26 July 2013

Chapter 7
Development of a Carborne Survey System, KURAMA

Minoru Tanigaki

Abstract A carborne survey system named KURAMA (Kyoto University RAdiation MApping system) has been developed for the establishment of air dose rate maps in Fukushima and the surrounding area as a response to the nuclear accident at the TEPCO Fukushima Daiichi Nuclear Power Plant. KURAMA is a γ-ray survey system with Global Positioning System (GPS) and up-to-date network technologies developed for the primary use of carborne surveys. The monitoring data tagged by GPS location data are shared with remote servers over the cloud network, then processed by servers for a real-time plot on Google Earth and other various purposes. Based on the success of KURAMA, KURAMA-II, an improved version of KURAMA with better handling and ruggedness, was developed for autonomous operation in public vehicles. About 200 KURAMA-II systems now serve for continuous monitoring in living areas by local buses as well as the periodic monitoring in Eastern Japan by the Japanese government. The outline and present status of KURAMA and KURAMA-II are introduced.

Keywords γ-Ray • Air dose rate • Carborne survey • Fukushima Daiichi Nuclear Power Plant • Mapping • Radiometry

M. Tanigaki (✉)
Research Reactor Institute, Kyoto University, 2-1010 Asashironishi, Kumatori, Osaka 590-0494, Japan
e-mail: tanigaki@rri.kyoto-u.ac.jp

S. Takahashi (ed.), *Radiation Monitoring and Dose Estimation of the Fukushima Nuclear Accident*, DOI 10.1007/978-4-431-54583-5_7,

7.1 Introduction

The magnitude 9 earthquake in Eastern Japan on 11 March 2011 and the following massive tsunami caused a serious nuclear disaster at the Fukushima Daiichi nuclear power plant, which Japan had never experienced before. Huge amounts of radioactive isotopes were released in Fukushima and the surrounding prefectures.

In such nuclear disasters, air dose rate maps are quite important to take measures to handle the incident, such as assessing the radiological dose to the public, making plans for minimizing public exposure, or establishing procedures for environmental reclamation. The carborne γ-ray survey technique is known to be an effective method to make air dose rate maps [1]. In this technique, continuous radiation measurement with location data throughout the subject area is performed by one or more monitoring cars equipped with radiation detectors. Unfortunately, the existing monitoring system did not work well in the disaster. Such monitoring cars tend to be multifunctional; thus, it is too expensive to own multiple monitoring cars in a prefecture. Fukushima was such a case, and worse, both the only monitoring car and the data center were contaminated by radioactive materials released by the hydrogen explosions of the nuclear power plant. Monitoring cars owned by other prefectures were then collected, but these monitoring cars were too heavy to drive on the roads in Fukushima, which were heavily damaged by the earthquake. Thus, daily measurements of the air dose rate in the whole area of Fukushima were eventually performed by humans. The measuring personnel drove around more than 50 fixed points in Fukushima Prefecture twice a day by sedan cars, and they measured the air dose rate of each point by portable survey meters. Airborne γ-ray surveys were performed by the Ministry of Education, Culture, Sports, Science and Technology of Japan (MEXT) and the United States Department of Energy, but difficulties in arrangements for the aircraft and their flight schedules prevented immediate and frequent surveys in the areas of interest.

KURAMA and its successor KURAMA-II were developed to overcome such difficulties in radiation surveys and to establish air dose rate maps during the present incident. KURAMA and KURAMA-II were designed based on consumer products, enabling much in-vehicle apparatus to be prepared within a short period. KURAMA/KURAMA-II realize high flexibility in the configuration of data-processing hubs or monitoring cars with the help of cloud technology. In the present chapter, an outline of KURAMA/KURAMA-II as well as their applications are presented.

7.2 KURAMA

KURAMA [2] is a γ-ray survey system with Global Positioning System (GPS) and up-to-date network technologies developed for the primary use of carborne surveys. The system outline of KURAMA is shown in Fig. 7.1.

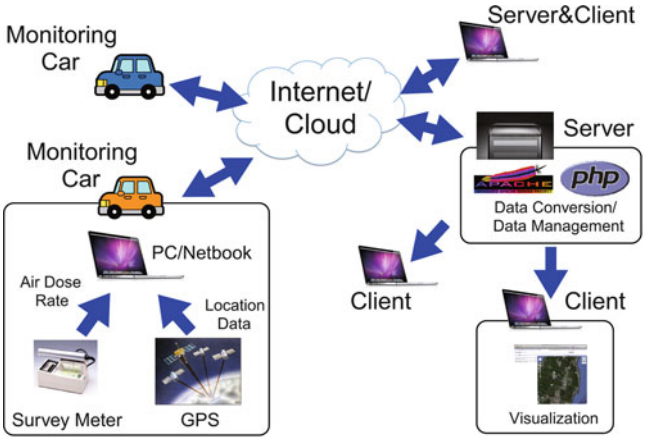

Fig. 7.1 KURAMA system. Monitoring cars and servers are connected over the Internet by cloud technology

An in-vehicle unit of KURAMA consists of a conventional NaI scintillation survey meter with an appropriate energy compensation, an interface box for the analog voltage output of the detector to a USB port of a PC, a GPS unit, a laptop PC, and a mobile Wi-Fi router (Fig. 7.2). Its simple and compact configuration allows users to set up an in-vehicle unit in a common automobile. The software of the in-vehicle part is developed with LabVIEW. The radiation data, collected every 3 s, are tagged by the respective location data obtained by the GPS and stored in a csv file. The csv files updated by respective monitoring cars are simultaneously shared with remote servers by Dropbox over a 3G network, differing from other typical carborne survey systems in which special telemetry systems or storage media are used for data collection. With this feature, anyone can set up their own "Data Center" anywhere so long as a conventional Internet connection and a PC with Dropbox are available. This kind of flexibility should be required in the disasters such as the present situation because the carborne system owned by Fukushima Prefecture was eventually halted as a result of the shutdown of the data center by the disaster.

Once the radiation data in csv format are shared with remote servers, the data file is processed or analyzed by servers in various ways, including the real-time display on Google Earth in client PCs (Fig. 7.3).

KURAMA has served for monitoring activities in Fukushima and surrounding prefectures employed by the Fukushima prefectural government and the Ministry of Education, Culture, Sports, Science and Technology in Japan (MEXT). The team of Fukushima prefectural government makes precise radiation maps of major cities in Fukushima Prefecture mainly for "Hot Spots" search [3], whereas MEXT performed carborne surveys in eastern Japan [4], including the Tokyo metropolitan area (Fig. 7.4).

Fig. 7.2 The in-vehicle part is compactly composed of mostly commercial components: (*1*) GPS unit, (*2*) 3G mobile Wi-Fi router, (*3*) MAKUNOUCHI, (*4*) NaI survey meter, (*5*) PC

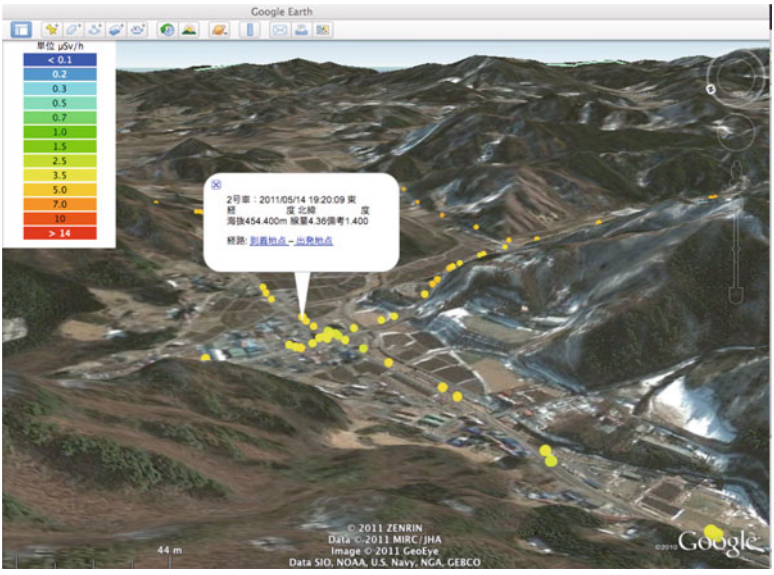

Fig. 7.3 Data are simultaneously plotted on Google Earth. The color of each dot represents the air dose rate at the respective point

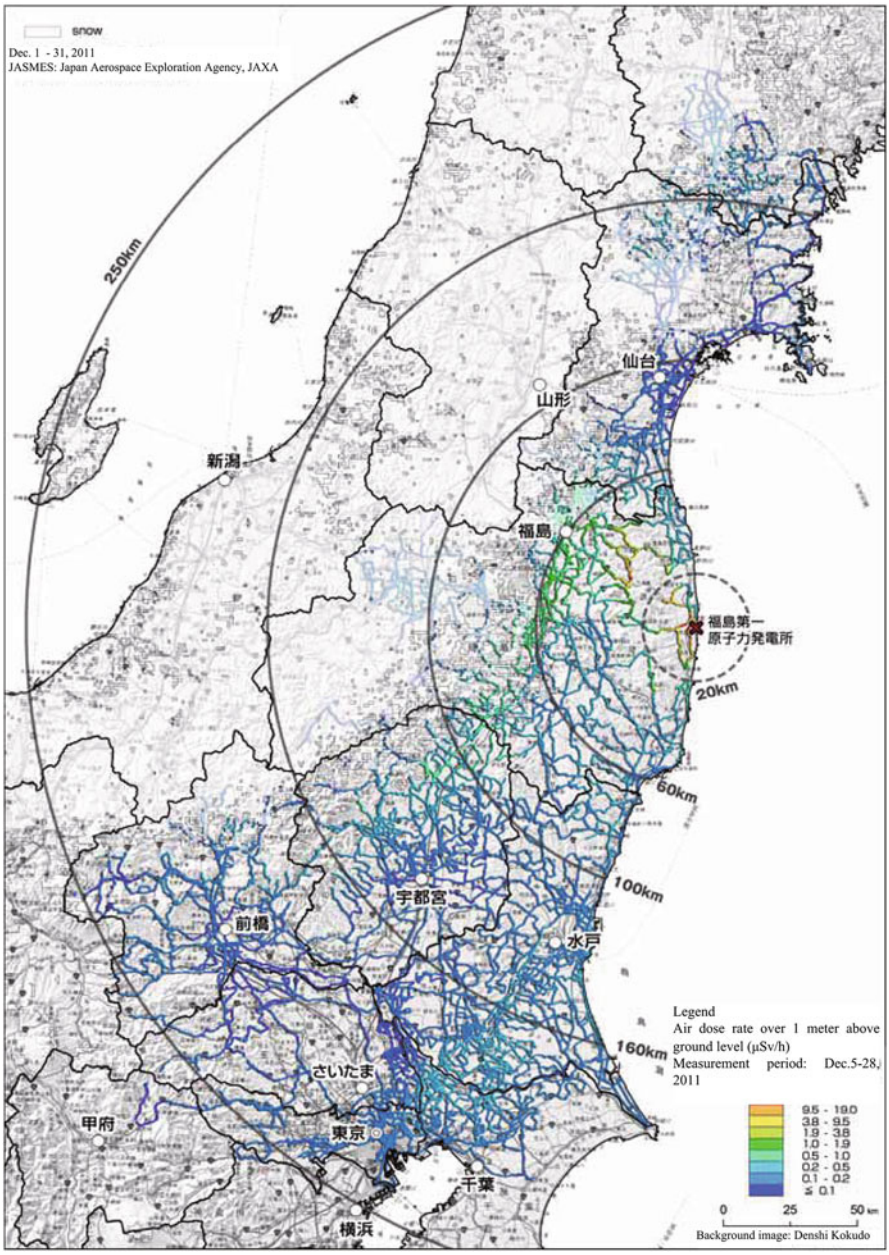

Fig. 7.4 Air dose rate mapped by KURAMA in December 2011 [4]. MEXT performed the first and second carborne surveys in East Japan by KURAMA in June and December 2011, respectively

7.3 KURAMA-II

Long-term (several decades) and detailed surveillance of radiation are required in residential areas that are exposed to the radioactive materials. Such monitoring can be realized if moving vehicles in residential areas such as buses, delivery vans, or bicycles for mail delivery have KURAMA onboard. KURAMA-II is designed for such purposes.

KURAMA-II is based on the architecture of KURAMA, but the in-vehicle part is totally redesigned (Fig. 7.5). The platform is based on CompactRIO series of National Instruments to obtain better durability, stability, and compactness. The radiation detection part replaces the conventional NaI survey meter with a Hamamatsu C12137 detector [5], a CsI detector characterized as its compactness, high efficiency, direct ADC output, and USB bus power operation. The direct ADC output enables obtaining γ-ray energy spectra during the operation. The mobile network and GPS functions are handled by a Gxxx 3G series module for CompactRIO by SEA [6].

The software for KURAMA-II is basically the same code as that of the original KURAMA, thanks to the good compatibility of LabVIEW over various platforms. Additional developments are employed in several components such as device control software for the newly introduced C12137 detector and Gxxx 3G module, the startup and initialization sequences for autonomous operation, and the file transfer protocol.

For the file transfer protocol, a simple file transfer protocol based on RESTful was developed because Dropbox does not support VxWorks, the operating system

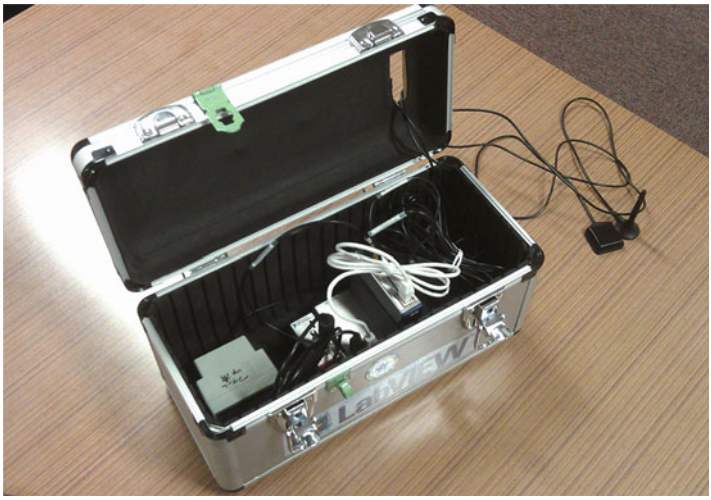

Fig. 7.5 In-vehicle unit of KURAMA-II. A CsI detector and a CompactRIO are compactly placed in a tool box 34.5×17.5×19.5 cm in size

Fig. 7.6 KURAMA-II during field test on a city bus

of CompactRIO. In this protocol, a chunk of data as a time-stamped file in csv format is produced for every three measuring points. The size of a chunk is typically about 400 bytes. Then, every chunk is transferred to a remote "gateway server" by the POST method. The gateway server combines received chunks to the data file, which is shared by remote servers using Dropbox as did the original KURAMA.

Even though the present transfer protocol works well, the existence of the "gateway server" can be a bottleneck in this data collection scheme. National Instruments is now developing a cloud service named "Technical Data Cloud" [7], which natively supports CompactRIO. This service can be one of the alternatives of Dropbox for KURAMA-II.

A field test on a city bus has been carried out since December 2011 in collaboration with Fukushima Kotsu, one of the largest bus operators in Fukushima Prefecture (Fig. 7.6). City buses are suitable for continuous monitoring purposes because of their fixed routes in the center of residential areas, and their routine operations. Up to now, this field test has been basically successful. The present file transfer protocol successfully manages data transmission under the actual mobile network. Several minor problems in hardware and software were found and fixed during this test, and stable operation has continued for more than a year.

7.4 Current Status and Future Prospects

Based on the success in the field test on city buses in Fukushima City, the region of this field test has been extended to other major cities in Fukushima Prefecture since January 2013, i.e., Koriyama City, Iwaki City and Aizuwakamatsu City. Five KURAMA-II in-vehicle units are deployed for this test, and the results are

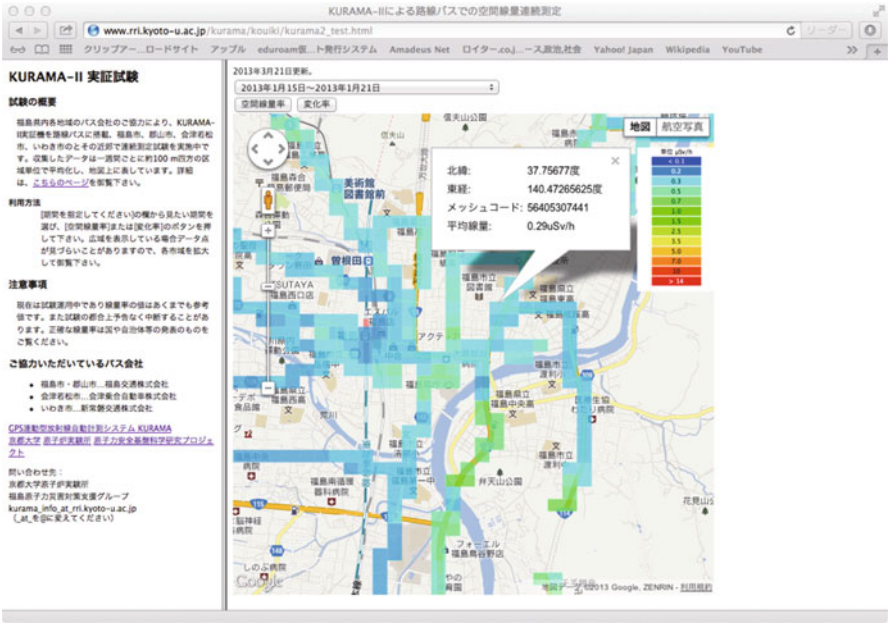

Fig. 7.7 Results of field tests on city buses are released to the public on a weekly basis. Averaged data are shown in every one-eighth grid square defined by the Statistics Bureau of the Ministry of Public Management, Home Affairs, Posts and Telecommunications

summarized and released to the public from the website [8] on a weekly basis (Fig. 7.7). In Fukushima City, around 30 additional KURAMA-II units will soon be deployed for minute mapping as well as the follow-up survey of distribution of air dose rate over the course of time.

The autonomous operation feature of KURAMA-II enables extended measurements of air dose rate with less effort. MEXT conducted a carborne survey for a month in March 2012 in which 100 KURAMA-II were leased to municipalities in eastern Japan [9]. KURAMA-II were placed in sedan cars of municipalities and the cars were driven around by ordinary staff members of the municipalities who did not have special training in radiation measurement. The survey was successful and proved the performance and scalability of the KURAMA-II system. Now this survey is conducted periodically by MEXT and the nuclear regulatory agency (NSR), which is the successor of the radiation monitoring of the present incident (Fig. 7.8).

CompactRIO is designed for applications in harsh environments and limited space. Therefore, KURAMA-II can be used for other than carborne surveys (Fig. 7.9). For example, KURAMA-II is loaded on a motorcycle: this is intended not only for attachment to motorcycles used for mail delivery, but also for monitoring in regions where conventional cars cannot be driven, such as the narrow paths between rice fields or those through forests. Also, KURAMA-II with a DGPS unit is about to be used for precise mapping by walking in rice fields, orchards, parks, and playgrounds in Fukushima Prefecture.

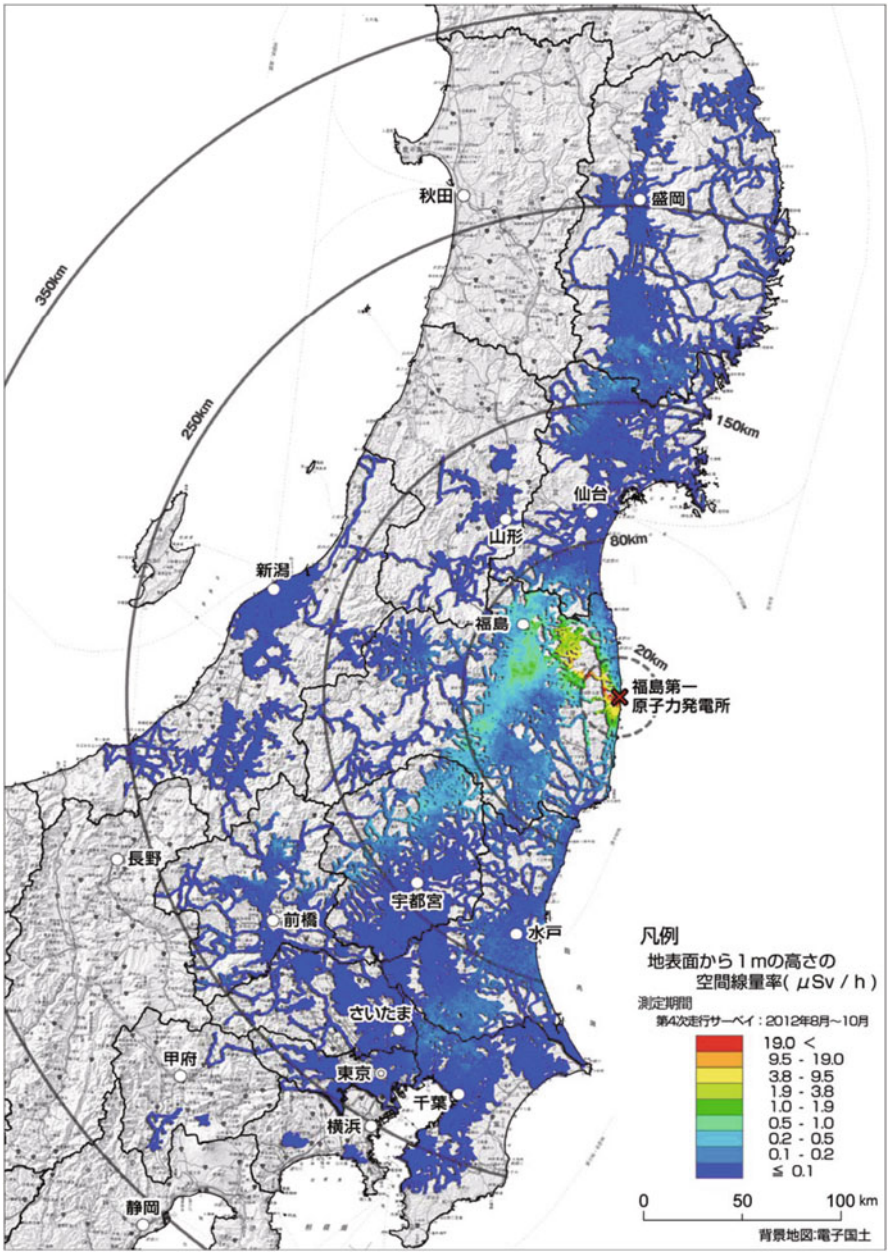

Fig. 7.8 Map of air dose rates on roads measured by KURAMA-II in periodic survey conducted by NSR between August and October 2012 [10]

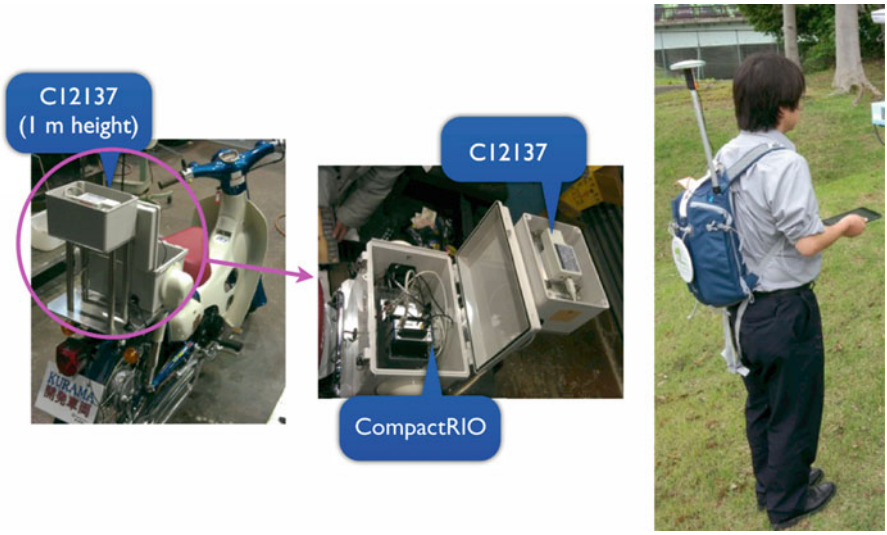

Fig. 7.9 KURAMA-II for bicycle survey (*left and middle*) and walking survey (*right*). All are the basically the same hardware and software configuration with different installations. In the case of the walking survey, the existing GPS part is replaced with DGPS for better precision of positioning the measurements

Acknowledgments The author is grateful to Dr. Mizuno, Mr. Abe, Mr. Koyama, and staff members of the KURAMA operation team at the Fukushima prefectural government for the continuous support for field tests of KURAMA in Fukushima. The author thanks Dr. Ito of ICR, Kyoto University, Prof. Maeno of Graduate School of Science, Kyoto University, and staff members of the KURAMA field test team of RRI, Kyoto University for their contribution to the test operation in Fukushima. The development of KURAMA-II is adopted by "Japan recovery grant program" from National Instruments Japan. Field tests of KURAMA-II on city buses are supported by Fukushima Kotsu Co. Ltd., Shin Joban Kotsu Co. Ltd., and Aizu Noriai Jidosha Co. Ltd. The author is indebted to Mr. and Mrs. Takahashi and the staff members at Matsushimaya Inn, Fukushima, for their heartwarming hospitality during the activities in Fukushima regardless of their severe circumstances resulting from the earthquake and the following nuclear accident.

References

1. Guidelines for Radioelement Mapping Using Gamma Ray Spectrometry Data, IAEA-TECDOC-1363, International Atomic Energy Agency, 2003, p. 40
2. Tanigaki M, Okumura R, Takamiya K, Sato N, Yoshino H, Yamana H (2013) Development of a car-borne γ-ray survey system, KURAMA. Nucl Instrum Methods Phys Res A 726:162–168
3. http://www.pref.fukushima.jp/j/soukoukekka.htm (in Japanese)

4. Press Release, Results of Continuous Measurement of Air Dose Rates through a Vehicle-borne Survey by MEXT (as of December 2011). 21 March 2012, MEXT, http://radioactivity.mext.go.jp/en/contents/5000/4688/view.html
5. http://www.hamamatsu.com/jp/ja/product/category/3100/4012/4134/C12137/index.html (in Japanese)
6. http://www.sea-gmbh.com/en/products/compactrio-products/sea-crio-modules/radio-technology/gxxx-3g/
7. http://www.ni.com/tdc/
8. http://www.rri.kyoto-u.ac.jp/kurama/kouiki/kurama2_test.html (in Japanese)
9. http://radioactivity.nsr.go.jp/en/contents/6000/5637/24/338_Suv_091218_e.pdf
10. Saito K (2013) Studies on the precise distribution and trends of air dose rate on the road by using carborne survey technique—the introduction of the progress of the third distribution study. http://www.jaea.go.jp/fukushima/kankyoanzen/tyouki-eikyou/giji/08/pdf/8-2-1.pdf (in Japanese). February 2013

Chapter 8
Radiation Measurement in East Japan in 2011 After the Fukushima Nuclear Accident

Takumi Kubota, Jun-ichi Hori, Nobuhiro Sato, Koichi Takamiya, Tomoko Ohta, and Yasunori Mahara

Abstract Air dose rates were measured inside a car with an ion chamber detector across Fukushima Prefecture from March 19 to 22, 2011. The dose rate along the Tohoku Expressway ranged from 2 to 6 μSv/h. Relatively high values were obtained around Nihonmatsu City. The dose rate dipped to an exceptionally low value inside a tunnel to what was probably the normal background value before the Fukushima nuclear accident. The dose rate in Fukushima City ranged from 2 to 9 μSv/h. High values were obtained in the center of the city. The dose rates along the Banetsu Expressway and in Samegawa Village located in the Abukuma highlands were very low at 1.5–3 and 1 μSv/h, respectively. During our stay in Fukushima, external and internal exposure was evaluated at 0.1 and 0.0327 mSv, respectively.

A commercially available GM-tube detector calibrated with a ^{137}Cs standard source was used to determine the status of environmental radioactive contamination caused by the Fukushima nuclear accident. The calibration was achieved with a quadratic correction function for dose rates up to 4 μSv/h. The calibrated GM-tube detector was used for measuring air dose rates and ground surface contamination in East Japan. Measurements were taken inside a car and a bullet train as well as outdoors from March to August 2011. The dose rates measured inside a vehicle along the Tohoku Expressway (in May) and in the Tohoku Shinkansen (in August) were as much as 1.0 and 0.25 μSv/h, respectively. The measurement results agreed well with the official data obtained using a NaI scintillation counter, demonstrating that a calibrated GM-tube detector can be an effective tool for measuring radioactivity.

T. Kubota (✉) • J.-i. Hori • N. Sato • K. Takamiya
Research Reactor Institute, Kyoto University, Kumatori, Osaka 590-0494, Japan
e-mail: t_kubota@rri.kyoto-u.ac.jp

T. Ohta
Hokkaido University, Sapporo, Hokkaido 060-8628, Japan

Y. Mahara
Kyoto University, Kyoto 615-8246, Japan

S. Takahashi (ed.), *Radiation Monitoring and Dose Estimation of the Fukushima Nuclear Accident*, DOI 10.1007/978-4-431-54583-5_8,

Keywords Air dose rate • GM-tube detector • Ion chamber detector • Mobile radiation survey • Surface contamination

8.1 Introduction

As a result of the Great East Japan Earthquake, a large amount of radioactive material was accidentally released from the Fukushima Daiichi Nuclear Power Plant (NPP). The Fukushima nuclear accident required radiation screening and medical support for refugees and residents from a very early stage. As one of these activities, we traveled to Fukushima Prefecture to perform radiation screening. The air dose rate inside a car was measured during the trip. The external and internal exposure during our stay in Fukushima for the screening activity was also measured. The measurement results are described in this report.

Many reports concerning radioactivity [1–3], including surface contamination, radioactive concentration, and air dose rate, were published by researchers, mass media outlets, and the government. Additional information was obtained and published by some members of the general population who used commercially available detectors, mainly Geiger Mueller tube (GM-tube) detectors, without calibration. However, these detectors often exhibited a considerable amount of interindividual variability, and the measurement results sometimes caused unnecessary confusion. In this study, a calibrated GM-tube detector was used for measuring radioactivity in East Japan, and the measurement results were compared with official data provided by the Japanese government.

8.2 Materials and Methods

Two commercially available detectors, a GM-tube detector and an ion chamber detector, were in-house calibrated. The GM-tube detector ("Radiation Alert Inspector+," SE International, which is co-owned by International Medcom) was calibrated using a standard ^{137}Cs radioactive source (#JDSR9518; 1.47×10^{-12} C kg/s at 1 m, 0.225 μSv/h at 1 m), which provided dose rates of 3.6, 0.9, and 0.4 μSv/h at distances of 0.25, 0.50, and 0.75 m from the source, respectively. The ion chamber detector (Aloka ICS-313) was calibrated with a standard ^{226}Ra radioactive source (85 μSv/h at 1 m). During the calibration, the detector and the radioactive source were placed on a 1-m-high plastic table.

The calibrated ion chamber was used to measure dose rate (μSv/h) inside a car throughout our following radiation screening activity. On March 19, 2011, we left Kumatori Town, Osaka, in the morning and arrived at Iizaka Onsen in Fukushima City that night; on March 20, we departed from Fukushima City and arrived at Nakoso High School in Iwaki City (southeast part of Fukushima Prefecture) for radiation screening, and then returned to Fukushima City that night; on March 21 and 22,

we departed from Fukushima City and traveled to Shirakawa City (southern part of Fukushima Prefecture) and Samegawa Village (only March 21), and then returned to Fukushima City that night; finally, on March 23 we returned to Kumatori Town by bus, airplane, and train. Except for the last day, we traveled by the same delivery cargo van on all other days.

The calibrated GM-tube detector measured the dose rate just above the ground surface and at a height of 1 m from the ground surfaces. The locations and dates of the radioactive measurements were as follows: Ueno Park in Tokyo on March 30, 2011; the Tohoku Expressway from Tochigi to Miyagi on May 26, 2011; the Tohoku Shinkansen bullet train from Saitama to Koriyama, Fukushima in August 2011; and Namie and its surrounding area in Fukushima in August 2011.

The resulting personal external and internal exposure in radiation screening activity was evaluated by a glass dosimeter (Chiyoda Technol) and by MONDAL with results from a NaI scintillation whole-body counter (detector size: $8''\Theta \times 4''$t), respectively. In whole-body counting, the measuring time was 10 min and the detection limits of ^{131}I and ^{137}Cs were 20 and 500 Bq, respectively. During this activity, we wore new masks every morning to avoid internal exposure, and the radioactivity of masks was measured for 3,600 s with two GE semiconductor detectors (Princeton Gamma-Tech IGC3019 and Seiko EG&G 7600–0001). The radioactivity of masks was defined as the average value calculated from the two calibration equation for a thin membrane filter of 50-mm diameter and a charcoal filter of 60-mm diameter and 20-mm thickness to take into account the effect of solid angle and then corrected for decay to the day when masks were used. The detection limits of ^{132}Te, ^{131}I, ^{134}Cs, ^{136}Cs, and ^{137}Cs were 0.3, 0.3, 0.4, 0.7, and 0.4 Bq, respectively.

8.3 Results and Discussion

8.3.1 Calibration

The GM-tube detector measured the radiation fields regulated by the ^{137}Cs standard radioactive source. Measurements were taken ten times every minute. The background air dose rate measured using a NaI scintillation counter was 0.09 μSv/h; this value was added to the air dose regulated from the standard source. The temporal change in the measurement is presented in Table 8.1. The measurement values barely approached a certain value correlated with the actual air dose rate, in contrast to the values obtained using the scintillation counter, and their variation coefficient decreased with the air dose rate. The GM-tube detector used here showed an instrument reading with a maximum error of ±20 %.

The GM-tube detector was calibrated with certified values from 0.09 to 3.69 μSv/h to obtain the following calibration equation:

$$Y = -0.0409X^2 + 0.9238X - 0.0264$$

Table 8.1 Temporal change in instrument reading

Certified value (μSv/h)	Instrument reading									
	#1	#2	#3	#4	#5	#6	#7	#8	#9	#10
0.09	0.149	0.161	0.125	0.089	0.143	0.113	0.119	0.119	0.107	0.089
0.49	0.527	0.539	0.569	0.581	0.461	0.611	0.640	0.575	0.706	0.539
0.99	1.132	1.220	1.114	1.246	1.084	1.192	1.090	1.060	1.282	1.330
3.69	5.431	5.250	5.238	5.413	5.335	5.262	5.262	4.708	5.244	5.112

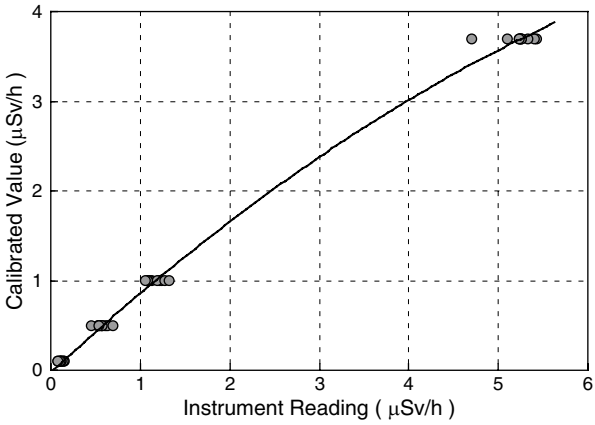

Fig. 8.1 Calibration of a GM-tube detector

where Y and X represent the calibrated value and the instrument reading, respectively. Figure 8.1 clearly shows the calibration equation as a quadratic rather than a linear function. The fact that the function is convex upward suggests that the GM-tube detector would underestimate the radiation fields at higher air dose rate conditions.

8.3.2 Air Dose Rate

8.3.2.1 Along Tohoku Expressway

During the screening activity, we traveled on the Tohoku Expressway in Fukushima Prefecture five times. The change of air dose rates is shown in Fig. 8.2. The dose rates obtained on March 19 were low, and they increased with time. The degree of increment, however, fluctuated greatly. It seemed that radioactive materials released still wafted over and were not yet strongly adsorbed into the ground. At the Adatara service area in Motomiya City around 7:00 p.m. on March 19, we observed the following dose rate change: the initial value was 2 μSv/h, it peaked at 4 μSv/h, and finally decreased to 2.7 μSv/h. This short-period change might have shown that a small radioactive plume had passed over. A radioactive peak seemed to have formed

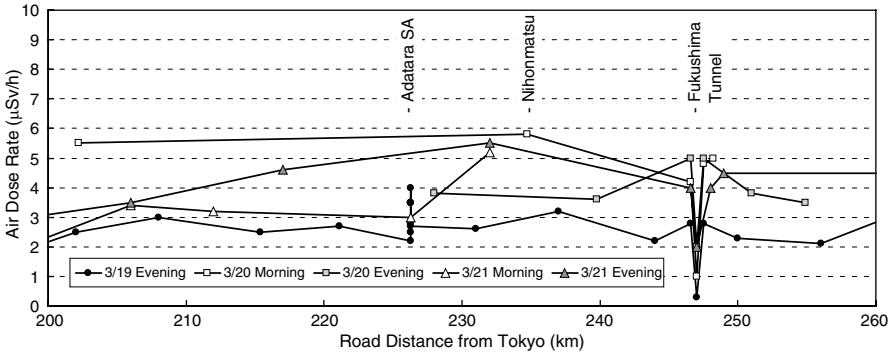

Fig. 8.2 Change in air dose rate along Tohoku Expressway

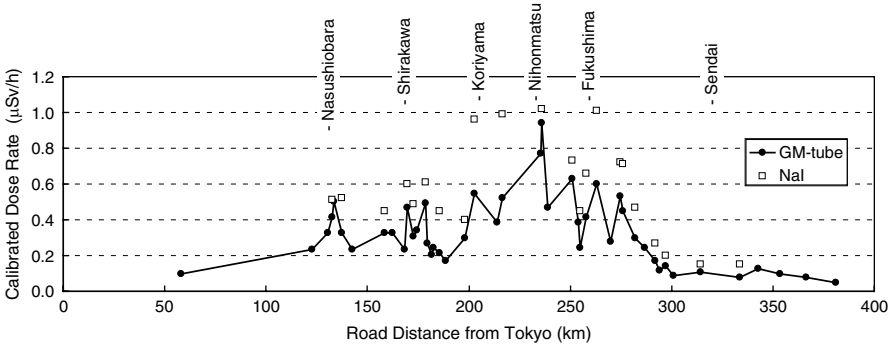

Fig. 8.3 Dose rate inside a car along the Tohoku Expressway. *Closed circles* and *open squares* indicate data from the Geiger Mueller tube (GM-tube) measurements and official material, respectively

around Nihonmatsu where a high air dose rate on the expressway was reported in May 2011 by the Fukushima Prefecture government [4]. The dose rate dipped inside the Fukushima tunnel, about 900 m in length, through Mt. Atago in Fukushima City. Although dose rates inside the long tunnel rapidly decreased because of the negligible direct radioactive deposition, these values gradually increased with time as the result of transit of contaminated traffic and air.

The calibrated dose rates obtained inside a car along the Tohoku Expressway on May 26, 2011, are shown in Fig. 8.3. A peak dose rate of 0.94 μSv/h was recorded at Nihonmatsu City, which is 55 km from the Fukushima Daiichi NPP and is the nearest point to the plant on the Tohoku Expressway. A similar measurement was carried out using a NaI scintillation counter on May 22, 2011; this was part of the official data published by the Fukushima Prefecture government [4]. The results of the long-distance mobile radiation survey (shown in Fig. 8.3) indicate that both measurements provide comparable results, except for three points in Fukushima and Koriyama City, and that they validate the use of calibrated GM-tube counting.

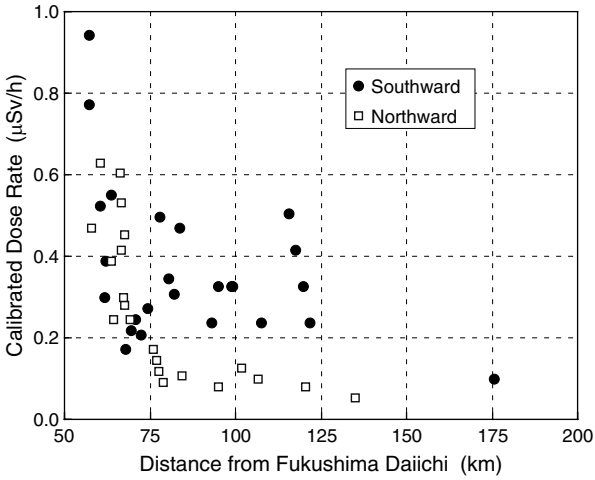

Fig. 8.4 Measure of contamination based on distance from Fukushima Daiichi Nuclear Power Plant (NPP)

Table 8.2 Comparison of dose rate between in Tohoku Shinkansen and on the Tohoku Expressway

Location	Calibrated dose rate (μSv/h)	
Nasushiobara	0.50	0.20
Shirakawa	0.47	0.15
Koriyama	0.55	0.25
Date	May 2011	August 2011
Route	Tohoku Expressway	Tohoku Shinkansen

A comparison of dose rate trends north and south of Nihonmatsu City (Fig. 8.4) provided the status of the radioactive contamination spread in the environment. Both trends show a similar decrease up to 75 km. Different trends, however, are shown from 75 to 125 km. The values obtained in the northern location decreased to a certain constant value, defined here as the background value. In contrast, the values obtained in the southern location are two to five times higher than the background value and exhibit some small peaks, which could be considered hot spots. These trends indicate that larger amounts of radioactive material were widespread in the southern location.

8.3.2.2 Tohoku Shinkansen

The results of measurements carried out in August 2011 aboard the Tohoku Shinkansen (bullet train), which runs almost parallel to the Tohoku Expressway, are listed in Table 8.2. The dose rates obtained in the Shinkansen decreased to 40 % of those obtained along the expressway in May 2011. According to "Extension Site of the Distribution Map for Radiation Dose" [5], the radiation dose at three locations decreased from a range between 0.5 and 1.0 μSv/h to a range between 0.2 and

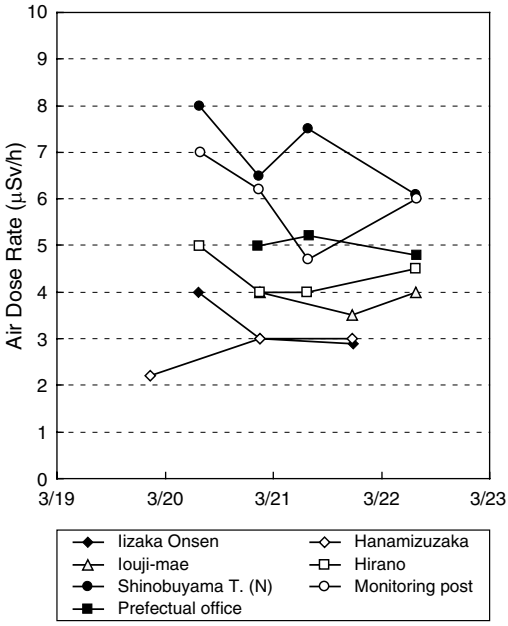

Fig. 8.5 Temporal variation of radiation dose rate in Fukushima City

0.5 μSv/h in the same period. The same decreasing tendency suggests the validity of using a calibrated GM-tube for radiation dose measurement in a rapidly moving vehicle at a speed of around 200 km/h.

8.3.2.3 Fukushima City

In Fukushima City as well as on the Tohoku Expressway, air dose rates measured several times on the same street between the Prefectural office (center of Fukushima City) and Iizaka Onsen (northern part of the city) are shown in Fig. 8.5. The dose rate in the center of the city was higher, and the highest values were obtained at the north end of the Shinobuyama tunnel, about 700 m in length through Mt. Shinobuyama (altitude 275 m). The distance between the prefectural office and Iizaka Onsen is about 9 km, and they are located 60 and 64 km from the Fukushima Daiichi NPP, respectively. In spite of similar distances from Fukushima Daiichi, a large variation in the air dose rate at these locations was observed. Further, a dip in the air dose rates inside the Shinobuyama tunnel was observed: the rates were 6–8 μSv/h at both ends and decreased to 1.5–2 μSv/h at the center of the tunnel.

8.3.2.4 Across Fukushima Prefecture

We made a round trip to Iwaki City on March 20. The temporal change in the air dose rate is shown in Fig. 8.6. The rates along the Banetsu Expressway and in Iwaki

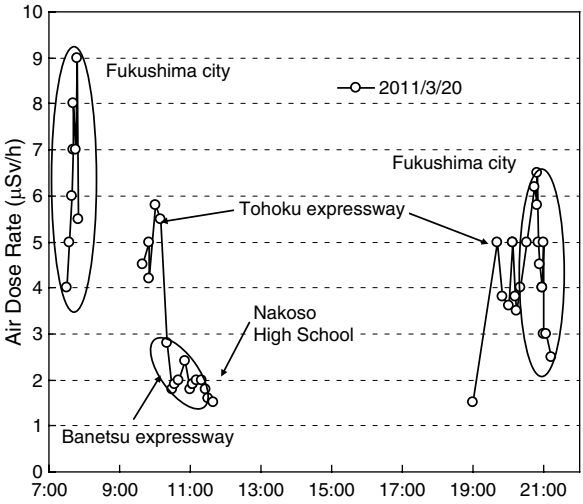

Fig. 8.6 Change in air dose rate on 1 day of screening activity

City were considerably lower than those along Tohoku Expressway and in Fukushima City as already described. This trend across Fukushima Prefecture agreed with the results from airborne monitoring in April 2011 [6], which would suggest the distribution of contamination (mainly radioactive cesium) had roughly stabilized since March 20 at the latest.

Screening activity was conducted in Samegawa Village and Shirakawa City on March 21 and 22, and their dose rates were approximately 1 and 2 μSv/h, respectively. Low air dose rates were obtained on both the Banetsu Expressway and in Samegawa Village in the Abukuma highlands. The Abukuma highlands served as a barrier to the diffusion of the radioactive plume released from the Fukushima Daiichi NPP [7]. Consequently, the plume streamed along the basin at the foot of the highland where Fukushima City and Tohoku Expressway are located and high radioactive contamination was detected.

8.3.3 Surface Contamination

The instrument readings (uncalibrated value) obtained near the ground surface in and around Ueno Park, 2 weeks after the nuclear accident, are shown in Fig. 8.7. Some of the values obtained are beyond the calibration value, and hence, the original instrument reading is adopted. The measurement values and the width of their distribution increased in the following order: park ground, road asphalt, and street gully. The removal of several millimeters of the surface of park ground provided a decrease in the measured dose rate by a factor of 2–4, which showed that radioactive material contaminated only the park ground surface and barely penetrated deeper. The nature of the ground surface affected the measurement values, although all the

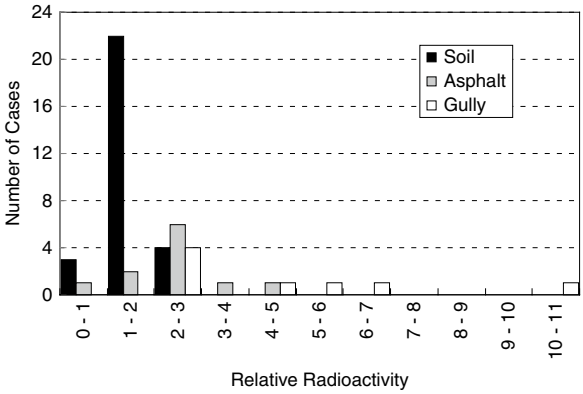

Fig. 8.7 Amount of relative radioactivity (instrument reading indicated in μSv/h) obtained near the ground surface

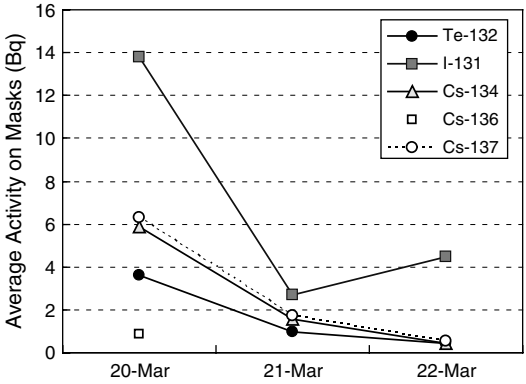

Fig. 8.8 Average activity on masks used during screening activity

monitoring locations were very close to each other. Our observation discovered "hot spots" where radioactive material would accumulate with fine soil particles from its original deposit location owing to wind and rain.

A measurement of ground surface was conducted at two points in August 2011 in Namie town, which is located about 30 km northwest of the Fukushima Daiichi NPP. The result values were 54 and 175 μSv/h (uncalibrated), which are 10–100 times higher than the results obtained at Ueno Park on March 30, 2011. In other words, serious contamination was observed.

8.3.4 Radiation Exposure

The radioactivity of the masks used on each day is shown in Fig. 8.8. Among detected nuclides, only ^{136}Cs was found in masks used on March 20 with ^{131}I showing a slightly different trend, and the radioactivity decreased faster than their own physical half-lives, which was caused by the difference in location of screening

activity and time spent outdoors. During this screening activity, the effective dose (external exposure) was 0.1 mSv, and the committed effective dose (internal exposure) was 0.0327 mSv.

8.4 Conclusion

A GM-tube detector was calibrated with a standard cesium-137 (^{137}Cs) source and used for measuring radioactive contamination from the Fukushima Daiichi Nuclear Power Plant. The GM-tube detector used in this study was calibrated up to 4 μSv/h based on a quadratic equation. This GM-tube detector yielded the same result as a NaI scintillation counter, and its practical use was validated under calibration.

Air dose rates were measured in Fukushima City, Iwaki City, Shirakawa City, and Samegawa Village and along the Tohoku and Banetsu Expressways during our screening activity in Fukushima Prefecture from March 19 to 22, 2011. Those rates in Fukushima City were highest, followed by those along Tohoku Expressway, whereas those in Samegawa Village and along Banetsu Expressway (both located in the Abukuma highlands) were relatively low. This radioactive distribution agreed with the MEXT reports consisted of airborne monitoring in April 2011. The radioactivity on masks used and the external and internal exposure was substantially low.

Acknowledgement We thank the Matsushimaya Ryokan staff for their support despite difficulties following the Great East Japan Earthquake and the subsequent nuclear accident. We thank Mr. Yukihiro Mizuochi for measuring the dose rates. This work was supported by KUR Research Program for Scientific Basis of Nuclear Safety.

References

1. Hirose K (2012) 2011 Fukushima Dai-ichi nuclear power plant accident: summary of regional radioactive deposition monitoring results. J Environ Radioact 111:13–17
2. Ohta T et al (2012) Prediction of groundwater contamination with ^{137}Cs and ^{131}I from the Fukushima nuclear accident in the Kanto district. J Environ Radioact 111:38–41
3. Tagami K et al (2011) Specific activity and activity ratios of radionuclides in soil collected about 20 km from the Fukushima Daiichi Nuclear Power Plant: radionuclide release to the south and southwest. Sci Total Environ 409:4885–4888
4. Fukushima prefecture government. http://www.pref.fukushima.jp/nuclear/info/pdf_files/H230615.pdf (in Japanese)
5. Japan Atomic Energy Agency, Distribution Map for Radiation Dose. http://ramap.jaea.go.jp/map/
6. MEXT. http://www.mext.go.jp/component/english/__icsFiles/afieldfile/2011/05/10/1304797_0506.pdf
7. Katata G et al (2012) Numerical reconstruction of high dose rate zones due to the Fukushima Dai-ichi Nuclear Power Plant accident. J Environ Radioact 111:2–12

Part IV
Environmental Radioactivity

Chapter 9
Distribution of Plutonium Isotopes in Marine Sediments off Japan Before and After the Fukushima Dai-ichi Nuclear Power Plant Accident: A Review

Wenting Bu, Jian Zheng, Qiuju Guo, Keiko Tagami, and Shigeo Uchida

Abstract A large amount of radionuclides was released into the atmosphere and directly discharged into the ocean as a consequence of the Fukushima Dai-ichi Nuclear Power Plant (FDNPP) accident. The possible actinides, especially plutonium contamination in the ocean from the nuclear accident, attracted general public and scientific concern. In this review, we summarize studies of the distribution of Pu isotopes in the marine sediments off Japan before and after the FDNPP accident to assess possible Pu contamination from the nuclear accident. Our results suggested that there was no detectable additional Pu injection from the FDNPP accident in the marine environment 30 km off the FDNPP 1 year after the accident. The detectable Pu isotopes originated from global fallout and the Pacific Proving Ground close-in fallout.

Keywords FDNPP • Marine sediments • Plutonium isotopes

W. Bu
State Key Laboratory of Nuclear Physics and Technology,
School of Physics, Peking University, Beijing, China

Research Center of Radiation Protection, National Institute
of Radiological Sciences, Chiba, Japan

J. Zheng (✉) • K. Tagami • S. Uchida
Research Center of Radiation Protection, National Institute
of Radiological Sciences, Chiba, Japan
e-mail: jzheng@nirs.go.jp

Q. Guo (✉)
State Key Laboratory of Nuclear Physics and Technology,
School of Physics, Peking University, Beijing, China
e-mail: qjguo@pku.edu.cn

S. Takahashi (ed.), *Radiation Monitoring and Dose Estimation of the Fukushima Nuclear Accident*, DOI 10.1007/978-4-431-54583-5_9,

9.1 Introduction

On March 11, 2011, the Fukushima Dai-ichi Nuclear Power Plant (FDNPP) was hit and damaged by a magnitude 9.0 earthquake in the Northwest Pacific about 130 km off the northeast coast of Japan and the following gigantic tsunami. As a result, large amounts of radionuclides were released into the atmosphere and directly discharged into the sea. More than 70 % of the released radionuclides were deposited over the North Pacific Ocean [1]. Studies concerning the fission products, such as ^{131}I and radiocesium, were carried out intensively after the nuclear accident. However, information about actinides, especially the plutonium (Pu) isotopes, is limited.

Pu isotopes are of public and scientific interest because they are characterized by radiotoxicity and strong chemical toxicity. They contribute much to the long-term dose for humans because of their relatively long half-lives (^{238}Pu, 87.7 years; ^{239}Pu, 24,110 years; ^{240}Pu, 6,561 years; ^{241}Pu, 14.4 years). Investigating the characterization of Pu isotopes in marine sediments is important for purposes of environmental monitoring and radiotoxicity assessment. Moreover, Pu isotopes are considered as new geochemical tracers for the study of oceanic processes, such as sedimentation and particle scavenging, and the isotopic composition of Pu (^{240}Pu/^{239}Pu) has been used as an important fingerprint for environmental radioactive source identification [2–5].

Abnormal atom ratios of ^{240}Pu/^{239}Pu and ^{241}Pu/^{239}Pu, and activity ratios of ^{241}Pu/$^{239+240}$Pu and ^{238}Pu/$^{239+240}$Pu, have been reported in surface soil and litter samples in the 20- to 30-km zone around the FDNPP [6, 7], suggesting the atmospheric release of Pu isotopes from the nuclear accident. For the marine environment, in previous studies [8, 9] we investigated the distribution of Pu isotopes in marine sediments collected in the Pacific Ocean, 30 km off the FDNPP site, from July 2011 to July 2012 after the nuclear accident. Sakaguchi et al. [10] determined Pu concentration in seawaters in the Pacific, 50 km off the FDNPP, and they observed no significant amount of extra components from the nuclear accident. However, possible long-term Pu contamination from the nuclear accident in the marine environment, especially in the Japanese near-coastal (within 30 km) marine environment, remains unknown because so far no information on Pu isotopes in the released radioactive liquid and in the FDNPP near-coastal marine environment is available.

Pu isotopes are particle reactive and can be easily incorporated into the sediments in the marine environment. Radiocesium (^{134}Cs and ^{137}Cs) released from the FDNPP accident was detected in sinking particles collected from the deep sea in the Western North Pacific 1 month after the accident [11]. The sediment–water distribution coefficient of Pu is two orders of magnitude higher than that of Cs [12]. Thus, Pu could be more easily incorporated into the sediments, and Pu distribution in the marine sediments could give direct information about Pu contamination in the marine environment.

In this review, we first summarize studies about the distribution of Pu isotopes in the marine sediments off Japan before and after the FDNPP accident. Then, we compare the results to assess possible contamination by Pu from the FDNPP accident. Perspectives about future research are presented as well.

9.2 Distribution of Pu Isotopes in the Marine Sediments off Japan Before the Accident

During past decades, the distribution of Pu isotopes in the Western North Pacific and its marginal seas have been studied intensively because of the potential application of Pu isotopes as geochemical tracers for oceanic processes and source identification of radioactive contamination. Before the FDNPP accident, Pu isotopes in the Western North Pacific off Japan originated from global fallout and the oceanic current-transported Pacific Proving Ground (PPG) close-in fallout. Global fallout Pu has been characterized by a $^{240}Pu/^{239}Pu$ atom ratio of 0.18 and a $^{241}Pu/^{239}Pu$ atom ratio of 0.0011 [13]. (For all the values discussed in this study, ^{241}Pu decay corrections have been made to March 11, 2011.) However, the PPG close-in fallout has higher Pu isotopic composition values ($^{240}Pu/^{239}Pu$ atom ratio, 0.30–0.36; $^{241}Pu/^{239}Pu$ atom ratio, ~0.0020) [14–17].

In our previous study [9], we determined the characterization of Pu isotopes in the sediments collected in seven Japanese estuaries facing the Pacific before the accident. Here, we summarized $^{239+240}Pu$ activity and $^{240}Pu/^{239}Pu$ atom ratios in the surface sediments in the marine environment off Japan, as presented in Fig. 9.1. $^{239+240}Pu$ activity was relatively low, especially for the Japanese river estuary sandy sediments, which ranged from 0 to 1 mBq g^{-1}. The highest concentration (5.81 mBq g^{-1}) of $^{239+240}Pu$ activity was reported in the surface sediment of Sagami Nada [18]. This high concentration was suggested to be caused by additional inputs of Pu from land origins (by rivers and by winds, followed by bioturbation) and the enhanced particle scavenging of transported PPG-source Pu [18, 21].

Studies on ^{241}Pu in the marine sediments off Japan before the nuclear accident are limited. Yamamoto et al. [22] determined Pu isotopes in the sediments in the Japan Sea and found that ^{241}Pu activity ranged from 4.5 to 7.5 mBq g^{-1}, which was similar to the results observed by Zheng and Yamada [21] in a sediment core collected from Sagami Bay. The Japanese government investigated Pu isotopes in the surface sediments off Japan and reported ^{241}Pu activities less than 3.3 mBq g^{-1} [23]. However, as a result of the influence of the PPG close-in fallout, high ^{241}Pu activities (up to 19–33 mBq g^{-1}) were observed in the sediment near Bikini Atoll [24].

$^{240}Pu/^{239}Pu$ atom ratios in the Japanese near-coastal surface sediments ranged from 0.17 to 0.27 (Fig. 9.1). Almost all the values were generally higher than the value of global fallout (0.18), except in the marine sediments in Northern Japan, where global fallout was the dominant source. Comparison of $^{240}Pu/^{239}Pu$ atom ratios in the marine sediments in Japanese river estuaries with global fallout and PPG close-in fallout values is shown in Fig. 9.2. For the eastern estuaries facing the North Pacific, the average $^{240}Pu/^{239}Pu$ atom ratio was 0.231. The high $^{240}Pu/^{239}Pu$ atom ratios clearly indicated the mixing of global fallout Pu and PPG close-in fallout Pu in the marine environment before the FDNPP accident. For the vertical distribution of $^{240}Pu/^{239}Pu$ atom ratios in sediment cores, high $^{240}Pu/^{239}Pu$ atom ratios,

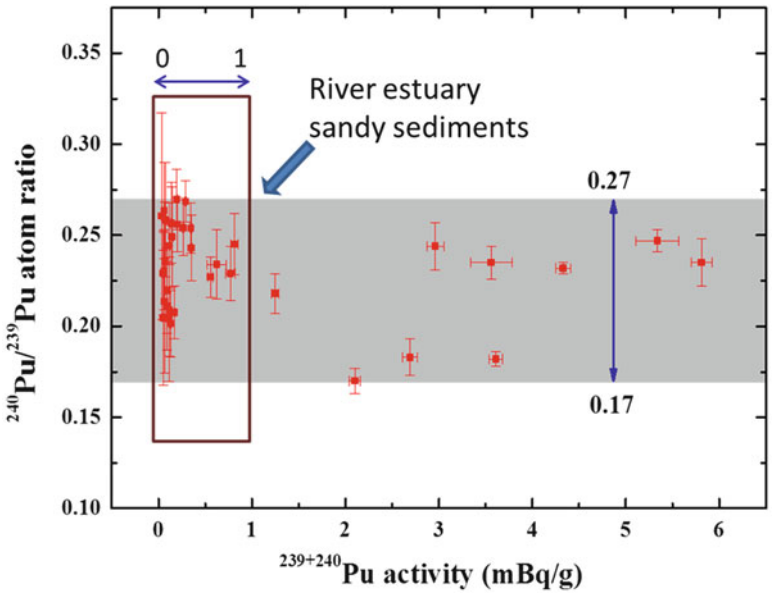

Fig. 9.1 $^{239+240}$Pu activities and ^{240}Pu/^{239}Pu atom ratios in Japanese near-coastal marine sediments (0–2 cm). (Data from the literature [9, 18–20])

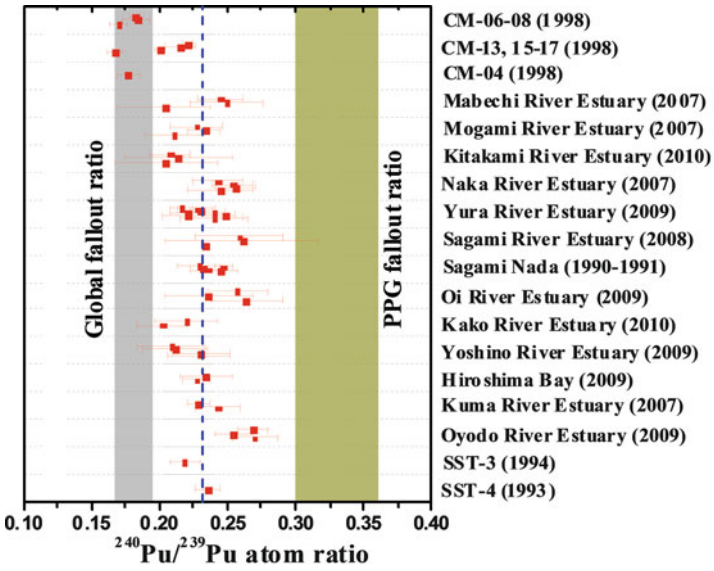

Fig. 9.2 The ^{240}Pu/^{239}Pu atom ratio distribution in surface sediments of Japanese river estuaries [9]

up to 0.30–0.33, have been found in the deeper layer (>5 cm) sediments from Okinawa Trough and Sagami Bay [25–27]. The high $^{240}Pu/^{239}Pu$ atom ratio in the deeper layer sediment could be caused by earlier deposition of PPG close-in fallout Pu isotopes.

From the reported results about the vertical distribution of Pu activities and atom ratios in the marine sediments in the Western North Pacific off Japan before the accident, we conclude that $^{239+240}Pu$ activity and $^{240}Pu/^{239}Pu$ atom ratio in the upper layer (<5 cm) sediments ranged from 0.02 to 5.38 mBq g^{-1} and 0.15 to 0.28, respectively. For the deeper layer (>5 cm), the $^{240}Pu/^{239}Pu$ atom ratio could reach 0.30–0.33 because of the influence of earlier deposition of PPG close-in fallout Pu. Inventories of Pu in the sediments varied significantly because the bottom topography and sediment dynamics in different sea areas are different. These results can be regarded as background data for Pu distribution in the marine sediments before the FDNPP accident.

9.3 Distribution of Pu Isotopes in the Marine Sediments off Japan After the Accident

To assess the impact of the Fukushima nuclear accident on possible Pu contamination in the marine environment, sediment core samples were collected in the Western North Pacific 30 km off the FDNPP during several cruises from July 2011 to July 2012 after the nuclear accident. The sampling information for each location is shown in Table 9.1. Pu distribution in surface sediments and sediment cores has been investigated [8, 9]. Results for $^{239+240}Pu$ activity in the surface sediments, inventory-weighted $^{240}Pu/^{230}Pu$ atom ratios, and $^{239+240}Pu$ inventories for each sample station are presented in Fig. 9.3.

Table 9.1 Sampling information about the sediment cores collected in the western North Pacific off the Fukushima Dai-ichi Nuclear Power Plant (FDNPP) site after the nuclear accident

Sample	Cruise	Sampling time	Water depth (m)	Location
MC1	MR 11-05	18 July 2011	1,327	36°28.97′N, 141°29.93′E
MC5	MR 11-05	19 July 2011	141	37°35.01′N, 141°30.95′E
ES2	KH 11-07	17 July 2011	2,200	37°4.00′N, 142°16.00′E
ES4	KH 11-07	18 July 2011	5,400	37°53.00′N, 143°35.00′E
ES5	KH 11-07	18 July 2011	7,300	37°47.00′N, 143°54.00′E
FS1	KH 11-07	2 August 2011	150	37°20.00′N, 141°25.00′E
F1	MR 12-02	7 July 2012	1,322	36°29.09′N, 141°30.01′E

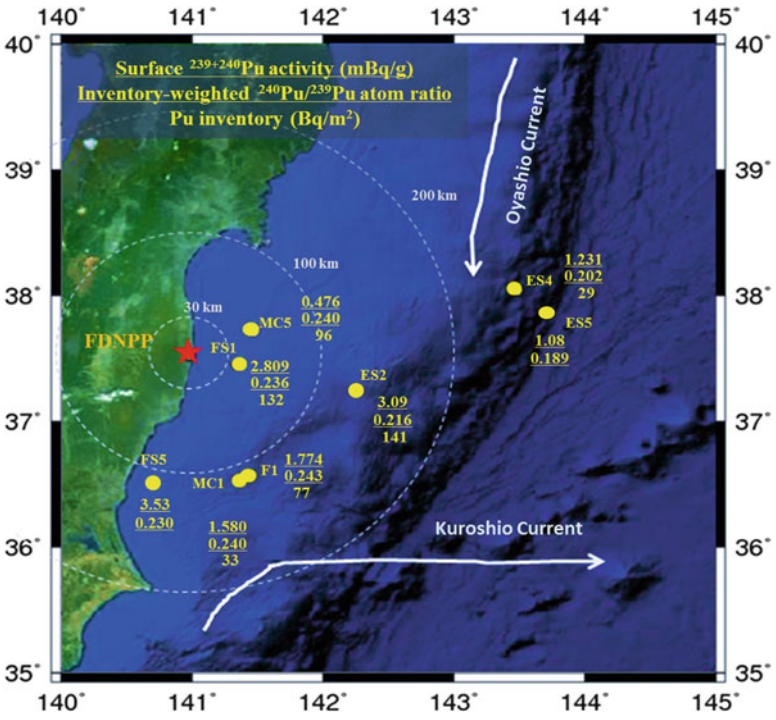

Fig. 9.3 Plutonium (Pu) distribution in the marine sediments 30 km off the Fukushima Dai-ichi Nuclear Power Plant (FDNPP) site after the nuclear accident. (Data from references [8, 9])

9.3.1 Distribution of Pu Activities and Pu Inventories

Zheng et al. [8] reported Pu isotopic concentration in the surface sediments; the surface $^{239+240}$Pu activities ranged from 0.48 to 3.53 mBq g^{-1}. Bu et al. [9] investigated the vertical distribution of Pu isotopes in sediment cores. $^{239+240}$Pu activities for all the surface sediments collected after the nuclear accident were less than 4 mBq g^{-1}, typically less than the background upper limit data (5.81 mBq g^{-1}) before the accident. Activity of ^{241}Pu in the investigated sediments was found to be quite low, most values being below the detection limit of 2 mBq g^{-1}.

The inventories of Pu in the sediment cores ranged from 29 to 141 Bq m^{-2}. High Pu inventories have been commonly reported in the coastal sediments in the Western North Pacific and its marginal seas. For example, Pu inventories in the Southern Okinawa Trough were extremely high (201–693 Bq m^{-2}) [25]. For the Japan Sea and Okhotsk Sea, Pu inventories ranged from 5.7 to 241 Bq m^{-2} and from 81 to 271 Bq m^{-2}, respectively [27]. Therefore, isotopic composition information should be combined with the inventory to reach a more reliable conclusion.

9.3.2 *Pu Atom Ratios*

The $^{240}Pu/^{239}Pu$ atom ratios in the surface sediments were between 0.188–0.255, and for all the sediment cores collected after the accident, $^{240}Pu/^{239}Pu$ atom ratios ranged from 0.188 to 0.293 [8, 9], typically higher than the global fallout value (0.18). $^{240}Pu/^{239}Pu$ atom ratios in the upper layers of the sediment cores showed nearly uniform distribution patterns, whereas for the sediment cores of MC1, FS1, and F1, the ratios increased from a definite depth. The higher $^{240}Pu/^{239}Pu$ atom ratios (>0.25) could be attributed to the presence of the PPG close-in fallout Pu.

As shown in Fig. 9.3, the inventory-weighted $^{240}Pu/^{239}Pu$ atom ratios for the sediment cores ranged from 0.189 to 0.243. The $^{240}Pu/^{239}Pu$ atom ratios for ES4 and ES5, which are located northeast of the FDNPP site, were lower than the values for the other stations. As the ES4 and ES5 stations are in the pathway of the Oyashio Current, they received more global fallout Pu than did the other stations investigated. The inventory-weighted $^{240}Pu/^{239}Pu$ atom ratio values were significantly lower than the reported values (>0.30) for the FDNPP accident-released Pu [6] but typically in the background range before the nuclear accident.

The $^{241}Pu/^{239}Pu$ atom ratio observed in the surface sediments ranged from 0.0012 to 0.0016, almost two orders of magnitude lower than the values (>0.1) derived from the FDNPP accident [6]. As mentioned in Sect. 9.2, global fallout of Pu is characterized by a $^{241}Pu/^{239}Pu$ atom ratio of 0.0011 and PPG close-in fallout has a $^{241}Pu/^{239}Pu$ atom ratio ~0.0020 [13, 16, 17]. The $^{241}Pu/^{239}Pu$ atom ratios in the Fukushima surface sediments were between the global fallout value and the PPG close-in fallout value. These results suggested that ^{241}Pu in the Fukushima surface sediment originated from global fallout and PPG close-in fallout.

9.4 Sources of Pu Isotopes in Marine Sediments in the Western North Pacific off Japan

9.4.1 *Influence of the FDNPP Accident on Pu Distribution*

FDNPP-derived Pu has been characterized by high atom ratios of $^{240}Pu/^{239}Pu$ (0.303–0.330) and $^{241}Pu/^{239}Pu$ (0.103–0.135) [6]. Although the $^{240}Pu/^{239}Pu$ atom ratios in the sediments after the FDNPP accident were higher than the global fallout value, these values cannot be simply explained as the influence of the FDNPP accident because higher $^{240}Pu/^{239}Pu$ atom ratios were observed in a wide range of sea areas in the Western North Pacific before the accident as the result of the influence of PPG close-in fallout. Comparison of $^{240}Pu/^{239}Pu$ atom ratio and $^{239+240}Pu$ activity for the marine sediments in the Western North Pacific before and after the accident is shown in Fig. 9.4. All the data observed after the FDNPP accident were in the

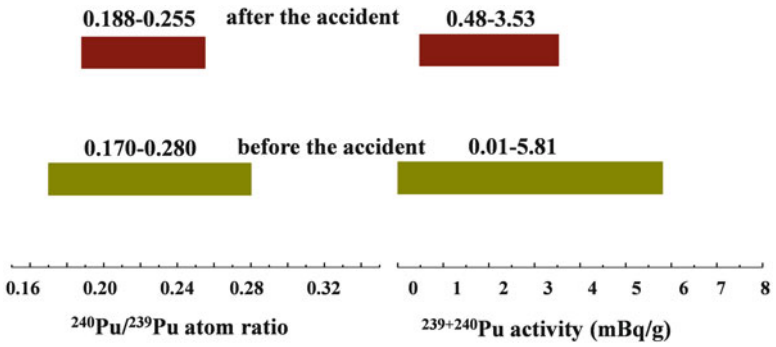

Fig. 9.4 Comparison of $^{239+240}$Pu activities (mBq g^{-1}) and ^{240}Pu/^{239}Pu atom ratios in the marine sediments off Japan before and after the FDNPP accident. (Data for Pu isotopes in the marine sediments after the FDNPP accident cited from references [8, 9])

background range before the accident. In the deeper layer sediments, higher ^{240}Pu/^{239}Pu atom ratios (>0.25) were observed, which could be explained as the earlier deposition of PPG close-in fallout Pu, considering the sediment depth. Therefore, it can be concluded that no extra Pu injection from the FDNPP accident has been detected in the marine sediments in the Western North Pacific 30 km off the FDNPP site after the nuclear accident.

The data on the distribution of ^{241}Pu provide further support to this conclusion. The ^{241}Pu/^{239}Pu atom ratios in the Fukushima surface sediments were two orders of magnitudes lower than the values derived from the FDNPP accident. The ^{241}Pu/^{239}Pu atom ratios were between the global fallout value and the PPG close-in fallout value, thus further implicating global fallout and PPG close-in fallout source contributions to the investigated regions.

9.4.2 Resolving Global Fallout and PPG Close-In Fallout Pu

Because two sources (global fallout and PPG close-in fallout) of Pu contamination in the marine sediments off Fukushima are identified, a simple two-end-member mixing model was used to calculate the relative contributions:

$$Y = \frac{(Pu)_P}{(Pu)_G} = \frac{(R_G - R_S)(1 + 3.66R_P)}{(R_S - R_B)(1 + 3.66R_G)}, \tag{9.1}$$

where (Pu) is the $^{239+240}$Pu activity, R represents the ^{240}Pu/^{239}Pu atom ratio, and the subscripts P, G, and S refer to PPG close-in fallout, global fallout, and measured sediment samples, respectively. The inventory-weighted percentages of the PPG close-in fallout in each sediment core can be calculated by Eq. (9.1).

The results showed that Pu in the sediment cores from the PPG contributed 16–43 % to the total Pu contamination [9]. The contribution of PPG close-in fallout Pu at ES4 station is 16 %, lower than the values (38–43 %) for the other stations. As discussed before, ES4 is located at the pathway of the Oyashio Current, which brought a large amount of global fallout Pu to that region. The contribution of PPG close-in fallout Pu in other stations is almost the same as the reported value (41 %) in CM-03 at the same sea area before the accident [27], suggesting there was no significant variability for the distribution of Pu isotopes in the marine sediments off the FDNPP site before and after the nuclear accident.

9.5 Perspectives for Future Study

We compared the distribution of Pu isotopes in the marine sediments before and after the FDNPP accident. From this comparison, we could not identify any additional Pu injection from the FDNPP accident into the marine environment outside the 30-km zone after the accident. The Pu isotopes originated from global fallout and PPG close-in fallout. Recently, Perianez et al. [28] simulated the migration of the possible released Pu from the FDNPP accident in the Pacific Ocean, and they concluded that because of the low mobility of Pu in marine environment, if any Pu contamination from the FDNPP accident occurred in the sea, it would remain in an area very close to the FDNPP site. Therefore, the distribution of Pu isotopes in the marine sediments off the Fukushima Prefecture coast needs continuous investigation to reach a more comprehensive conclusion. We suggest that the following topics should be considered in future studies:

1. Expansion of the investigating intensity and area for the Pu distribution in the marine sediments off the Fukushima coast, especially for the marine sediments within the 30-km zone.
2. Fractionation of Pu in marine sediments to understand the mobility and bioavailability of Pu.
3. Investigation of Pu distribution and isotopic composition in seawater after the accident.
4. Study of Pu concentrations in marine biota to estimate the long-term dose influence of the FDNPP accident and to strengthen public confidence in the safety of seafood.

Acknowledgments This work was jointly supported by the Kakenhi Grant in Aid for Scientific Research on Innovative Areas (24110004) and the National Natural Science Foundation of China (A050507). Wenting Bu thanks the China Scholarship Council for offering a scholarship (20126010102) for supporting his Ph.D. study.

References

1. Yoshida N, Kanda J (2012) Tracking the Fukushima radionuclides. Science 336:1115–1116
2. Muramatsu Y, Uchida S, Tagami K, Yoshida S, Fujikawa T (1999) Determination of plutonium concentration and its isotopic ratio in environmental materials by ICP-MS after separation using and extraction chromatography. J Anal At Spectrom 14:859–865
3. Muramatsu Y, Ruhm W, Yoshida S, Tagami K, Uchida S, Wirth E (2000) Concentrations of ^{239}Pu and ^{240}Pu and their isotopic ratios determined by ICP-MS in soils collected from the Chernobyl 30-km zone. Environ Sci Technol 34:2913–2917
4. Zheng J, Yamada M (2006) Plutonium isotopes in settling particles: transport and scavenging of Pu in the Western Northwest Pacific. Environ Sci Technol 40:4103–4108
5. Ketterer ME, Watson BR, Matisoff G, Wilson CG (2002) Rapid dating of recent aquatic sediments using Pu activities and ^{240}Pu/^{239}Pu as determined by quadrupole inductively coupled plasma mass spectrometry. Environ Sci Technol 36:1307–1311
6. Zheng J, Tagami K, Watanabe Y, Uchida S, Aono T, Ishii N, Yoshida S, Kubota Y, Fuma S, Ihara S (2012) Isotopic evidence of plutonium release into the environment from the Fukushima DNPP accident. Sci Rep 2:304. doi:10.1038/srep00304
7. Yamamoto M, Takada T, Nagao S, Koike T, Shimada K, Hoshi M, Zhumadilov K, Shima T, Fukuoka M, Imanaka T, Endo S, Sakaguchi A, Kimura S (2012) An early survey of the radioactive contamination of soil due to the Fukushima Dai-ichi Nuclear Power Plant accident, with emphasis on plutonium analysis. Geochem J 46:341–353
8. Zheng J, Aono T, Uchida S, Zhang J, Honda MC (2012) Distribution of Pu isotopes in marine sediments in the Pacific 30 km off Fukushima after the Fukushima Daiichi nuclear power plant accident. Geochem J 46:361–369
9. Bu WT, Zheng J, Aono T, Tagami K, Uchida S, Zhang J, Guo QJ, Yamada M (2013) Vertical distribution of plutonium isotopes in marine sediment cores off the Fukushima coast after the Fukushima Dai-ichi nuclear power plant accident. Biogeosci 10:2497–2511
10. Sakaguchi A, Kadokura A, Steier P, Tanaka K, Takahashi Y, Chiga H, Matsushima A, Nakashima S, Onda Y (2012) Isotopic determination of U, Pu and Cs in environmental waters following the Fukushima Daiichi nuclear plant accident. Geochem J 46:355–360
11. Honda MC, Kawakami H, Watanabe S, Saino T (2013) Concentration and vertical flux of Fukushima-derived radiocesium in sinking particles from two sites in the Northwestern Pacific ocean. Biogeosci 10:3525–3534
12. IAEA (2004) Sediment distribution coefficients and concentration factors for biota in the marine environment, vol 422, Technical reports series. International Atomic Energy Agency, Vienna, pp 10–12
13. Kelley JM, Bond LA, Beasley TM (1999) Global distribution of Pu isotopes and ^{237}Np. Sci Total Environ 237(238):483–500
14. Buesseler KO (1997) The isotopic signature of fallout plutonium in the North Pacific. J Environ Radioact 36:69–83
15. Muramatsu Y, Hamilton T, Uchida S, Tagami K, Yoshida S, Robison W (2001) Measurement of ^{240}Pu/^{239}Pu isotopic ratios in soils from the Marshall Islands using ICP-MS. Sci Total Environ 278:151–159
16. Yamamoto M, Ishiguro T, Tazaki K, Komura K, Ueno K (1996) ^{237}Np in hemp-palm leaves of Bontenchiku for fishing gear used by the fifth Fukuryu-maru: 40 years after “Bravo”. Health Phys 70:744–748
17. Lachner J, Christl M, Bisinger T, Michel R, Synal HA (2010) Isotopic signature of plutonium at Bikini Atoll. Appl Radiat Isot 68:979–983
18. Zheng J, Yamada M (2004) Sediment core record of global fallout and Bikini close-in fallout Pu in Sagami Bay, Western Northwest Pacific Margin. Environ Sci Technol 38:3498–3504
19. Liu ZY, Zheng J, Yamada M, Pan SM, Kawahata H (2011) Plutonium characteristics in sediments of Hiroshima Bay in Seto Inland Sea in Japan. J Radioanal Nucl Chem 288:911–917

20. National Institute of Radiological Sciences (2010) Report on biospheric assessment for waste, pp 29–30 (in Japanese)
21. Zheng J, Yamada M (2008) Isotopic dilution sector-field inductively coupled plasma mass spectrometry combined with extraction chromatography for rapid determination of ^{241}Am in marine sediments: a case study in Sagami Bay, Japan. J Oceanogr 64:541–550
22. Yamamoto M, Yamauchi Y, Chatani K, Igarashi S, Komura K, Ueno K (1990) Fallout ^{237}Np, Pu isotopes and ^{241}Am in lake and sea sediments from the coastal area of the sea of Japan. Radiochim Acta 51:85–95
23. MEXT (2008) Environmental radiation database. http://www.kankyo-hoshano.go.jp/08/ers_lib/ers_abs53.pdf
24. Lee SH, Povinec PP, Wyse E, Pham MK, Hong GH, Chung CS, Kim SH, Lee HJ (2005) Distribution and inventories of ^{90}Sr, ^{137}Cs, ^{241}Am and Pu isotopes in sediments of the Northwest Pacific Ocean. Mar Geol 216:249–263
25. Lee SY, Huh CA, Su CC, You CF (2004) Sedimentation in the Southern Okinawa trough: enhanced particle scavenging and teleconnection between the Equatorial Pacific and Western Pacific margins. Deep Sea Res I 51:1769–1780
26. Wang ZL, Yamada M (2005) Plutonium activities and ^{240}Pu/^{239}Pu atom ratios in sediment cores from the East China sea and Okinawa trough: sources and inventories. Earth Planet Sci Lett 233:441–453
27. Zheng J, Yamada M (2006) Determination of Pu isotopes in sediment cores in the sea of Okhotsk and the NW Pacific by sector field ICP-MS. J Radioanal Nucl Chem 267:73–83
28. Perianez R, Suh KS, Min BII M (2013) Should we measure plutonium concentration in marine sediments near Fukushima? J Radioanal Nucl Chem doi: 10.1007/s10967-013-2422-1

Chapter 10
Time Trend Change of Air Dose Rate on Paved Areas in Fukushima City After the Fukushima Daiichi NPP Accident

Sin-ya Hohara, Masayo Inagaki, Hirokuni Yamanishi, Genichiro Wakabayashi, Wataru Sugiyama, and Tetsuo Itoh

Abstract The Kinki University Atomic Energy Research Institute investigated radioactive contamination resulting from the Fukushima Daiichi Nuclear Power Plant accident in urban areas of Fukushima City, Fukushima Prefecture, Japan. Activity measurement of the surface soil and a survey of the dose rate distribution in urban areas were performed. From the results of this research, dose rate changes in paved areas became clear, and gradients of the dose rate decrease for different paving materials were measured and analyzed.

Keywords Activities • Distribution • Dose rate

10.1 Introduction

On March 11, 2011, the Tohoku Region Pacific Coast Earthquake and the subsequent tsunami occurred, causing the Fukushima Daiichi Nuclear Power Plant (Fukushima Daiichi NPP) accident. As a result of the failure of the NPP's coolant systems, hydrogen explosions occurred that released radioactive materials to the general environment [1–6].

The released radioactive materials were dispersed as radioactive plumes over wide ranges of the Tohoku and Kanto regions. These radioactive plumes were deposited to grounds, building surfaces, and other substrates through several processes. Several surveys tried to measure the contamination in general environments [1–6].

S.-y. Hohara (✉) • M. Inagaki • H. Yamanishi • G. Wakabayashi • W. Sugiyama • T. Itoh
Kinki University Atomic Energy Research Institute,
3-4-1 Kowakae, Higashi-Osaka City, Osaka 577-8502, Japan
e-mail: hohara@kindai.ac.jp

S. Takahashi (ed.), *Radiation Monitoring and Dose Estimation of the Fukushima Nuclear Accident*, DOI 10.1007/978-4-431-54583-5_10,

The Kinki University Atomic Energy Research Institute (Kinki University AERI) has conducted research in the Fukushima area since the middle April of 2011 [6]. Two types of measurement were conducted: the measurement of the activity of radioactive materials in surface soils and the measurement of dose rate distributions in urban areas. From these measurements, it became clear that the concentration of radioactive materials that had dispersed from the Fukushima Daiichi NPP decreased faster than the physical half-lives of the radioactive materials themselves in the urban parts of the Fukushima Naka-Dori area.

In this chapter, the methods used and some of the results of the measurements are presented.

10.2 Methods

Kinki University AERI researched radioactive materials at Fukushima station (East Japan Railway Company) neighborhoods, which is located at the center of the downtown of Fukushima city. This place is 60 km from the Fukushima Daiichi NPP in a northwestern direction. The dose rate in the downtown area was more than ten times greater than the published environmental background dose rate [6, 9].

Two types of research were undertaken in this work: the first was a dose rate survey, and the other was an activity measurement for surface soils in the urban area. The measurement area of the dose rate survey and the surface soil sampling point for activity measurement are shown in Fig. 10.1. These places are in a 1-km neighborhood, because quantities of fallen radioactive materials in a unit square footage and ratios of radioactive nuclides were thought to be similar in these research locations. Both studies have continued since April 2011.

The methods of the two studies are described in the following sections.

10.2.1 Measurement of the Radioactivity in Surface Soils

Surface soils have been collected since April 2011. Figure 10.2 shows a photograph of the soil sampling location. Soil samples were collected from a 30×30 cm^2 area and a ground depth of 1 cm with a scoop at the center of the ground (Fig. 10.2). The collected soils were mixed and packed in U-8 sample cases at the sampling place. These samples were measured with a high pure germanium detector at Kinki University AERI in Osaka that was calibrated with a standard volume source, and the measured gamma spectrum was analyzed using the nuclide library of ORTEC EG&G. Measurement time was 1,800 s for each sample. The data include a summing effect correction and a self-shielding effect correction.

Fig. 10.1 Map of the research area in Fukushima City. *Red line*, research area for a dose rate measurement; *blue point*, sampling point of surface soils for a specific activity measurement

Fig. 10.2 Photograph of soil sampling point taken April 17, 2011. Soil samples were taken at the center of this ground

10.2.2 Dose Rate Distribution Survey

In this measurement, a GPS-linked NaI(Tl) scintillation counter [7] was used to simultaneously record the dose rates and location. The GPS-linked NaI(Tl) scintillation counter includes three components: the first component is the radiation detection unit, which uses a NaI(Tl) survey meter (TCS-171; Hitachi-Aloka Medical) and a microcomputer board (CQ-V850; ESP); the second component is the GPS receiver unit, which uses a USB-linked GPS receiver (UMGPS/MF; IODATA; GPS receiver chip, SiRF StarIII); and the last component is a data acquisition unit, an Ultra-Mobile PC (FM-V BIBLO LOOX U/ C30; Fujitsu). The radiation detection unit and the GPS receiver unit are linked to the data acquisition unit where dose rate and GPS data are saved. The data acquisition software was developed and built using the Visual C#/ .NET Framework (Microsoft).

The whole system was put in a portable bag with the detection head of the radiation detector positioned 50–60 cm above ground, and the measurement was taken while walking at a speed of about 100 m/min. The height of the radiation detector was determined from the limits of the detector equipment.

In the research area, there are some typical areas paved with different materials. Figure 10.3 shows a cushion paving area, Fig. 10.3b is a block paving area, and

Fig. 10.3 Sites for dose rate distribution measurement photographed July 17, 2011: cushion paving area (**a**), block paving area (**b**), and normal asphalt paving area (**c**). Dose rates were measured by walking at the center of the walkway

Fig. 10.3c is a normal asphalt paving area. Dose rates were measured with walking at the center of the walkway in the photographs.

10.3 Results

10.3.1 Measurement of the Radioactivity in Surface Soils

Results of the measurements ranging from April 2011 to July 2012 have already been published [6, 8, 9]. Almost all the radioactive nuclides from the Fukushima Daiichi NPP decayed to approximately background levels by the middle of 2011, except for ^{134}Cs and ^{137}Cs. Figure 10.4 shows a time trend of ^{137}Cs activity in ratios for the April 17, 2011 sample. Figure 10.4 shows a radical decrease between September 2011 and October 2011 as a result of water exposure of the sampling place by a typhoon [No. 15 (2011), named Roke]. It is surmised that the water exposure carried away thickly contaminated surface soils from the place, bringing lightly contaminated muds. After a few months, an increase is seen between April 2012 and May 2012 because of the change of sampling soil type. Until April 2012, I sampled sand-type soil that is similar to the ground surface soil before the water exposure. Since May 2012, I sampled mud-type soil that is presumed to have come with water exposure. With this change, ^{137}Cs activity increased. Furthermore, the ^{137}Cs activity decreased drastically again between January 2013 and February 2013. In this period, decontamination of the sampling point was carried out by Fukushima City, and as a result the ^{137}Cs activity decreased.

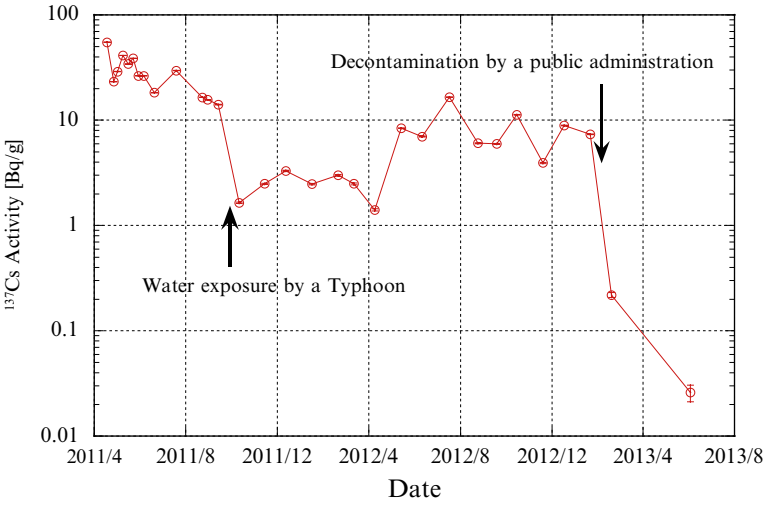

Fig. 10.4 Time trend change of ^{137}Cs activity of surface soil samples. *Horizontal axis*, date; *vertical axis*, specific activity; *circles*, measured activities

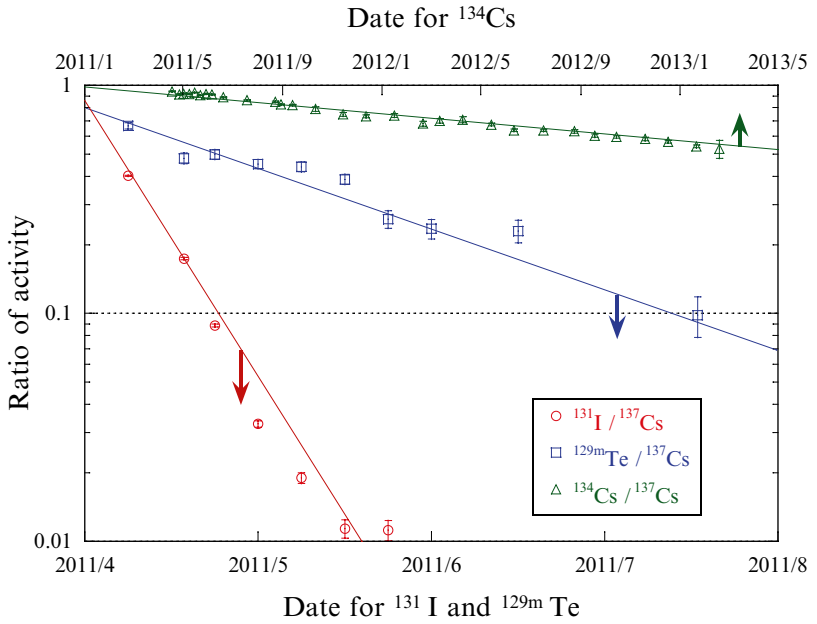

Fig. 10.5 Ratios of activity. *Vertical axis*, ratio in activity for ^{137}Cs; *upper horizontal axis*, date for ^{134}Cs/^{137}Cs ratio; *lower horizontal axis*, date for ^{131}I/^{137}Cs and ^{129m}Te/^{137}Cs ratio. *Circles* show ^{131}I/^{137}Cs activity ratios, *squares* show ^{129m}Te/^{137}Cs activity ratios, and *triangles* show ^{134}Cs/^{137}Cs activity ratios. ^{131}I and ^{129m}Te decreased following their physical half-lives

The data show that activity of ^{137}Cs was in a decreasing trend with time and the gradient of the trend was faster than the physical half-life of ^{137}Cs decay.

For more detailed analysis, activity ratios of other radioactive nuclides for ^{137}Cs activity are shown in Fig. 10.5. From this result, the ratios of radioactive nuclides are following their physical half-lives, which means the radioactive nuclides moved together with ^{137}Cs in the general environment after the fallout.

10.3.2 Dose Rate Distribution Survey

Some of the earlier results of this measurement have been published [6, 8, 9], showing dose rate distributions in the urban part of the Fukushima Naka-Dori area had changed. The change in the dose rate in paved areas (with time) is described in this chapter.

A characteristic dose rate distribution change (Fig. 10.6) is shown by dose rate distributions of the Fukushima station neighborhood close to the soil sampling point. Figure 10.6a shows the dose rate distribution on April 17, 2011, and Fig. 10.6b shows the dose rate distribution on October 13, 2012.

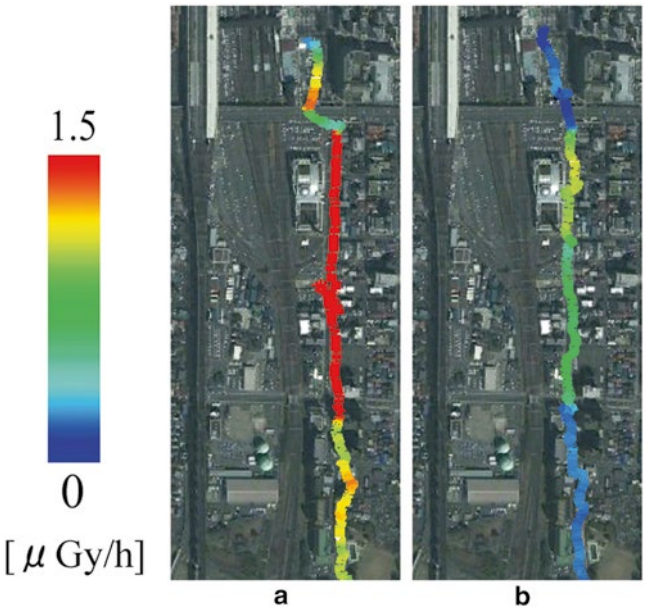

Fig. 10.6 Dose rate distributions in Fukushima City. *Lines* indicate the survey route and their *color* the measured dose rate on April 17, 2011 (**a**) and October 13, 2012 (**b**)

The dose rate on October 13, 2012 was lower than that on April 17, 2011 (Fig. 10.6), and the dose rate distribution became much clearer on October 13, 2012. The higher dose rate areas (Fig. 10.6b) were where the streets were paved with cushion, the average dose rate areas were where the streets were paved with blocks, and the lower dose rate areas were where the streets were paved with normal asphalt (Fig. 10.7). The dose rates of these three points decreased with time (Fig. 10.7). The dose rate decreasing rate appears different among the three points in Fig. 10.7.

For more detailed analysis, I compared measured dose rates with calculated dose rates. The calculated dose rate trends were determined as follows.

The air dose rate at Fukushima city is composed of the environmental background dose rate and the dose rate of radioactive materials from Fukushima Daiichi NPP, as shown in Eq. (10.1), where D_{calc} is the calculated dose rate, D_{BG} is the environmental background, and D_{RM} is the dose rate from the radioactive materials from Fukushima Daiichi NPP.

$$D_{calc} = D_{BG} + D_{RM}. \tag{10.1}$$

Background dose rate at Fukushima City was set at 0.044 (μGy/h), calculated from total background dose rate, 0.075 (μGy/h) [=8.6 (μR/h)] [10], and cosmic muon dose rate, 0.031 (μGy/h). The muon dose rate is calculated from 0.031 (μSv/h) at sea level [11] and a height correction equation [11]. The conversion from Sv to

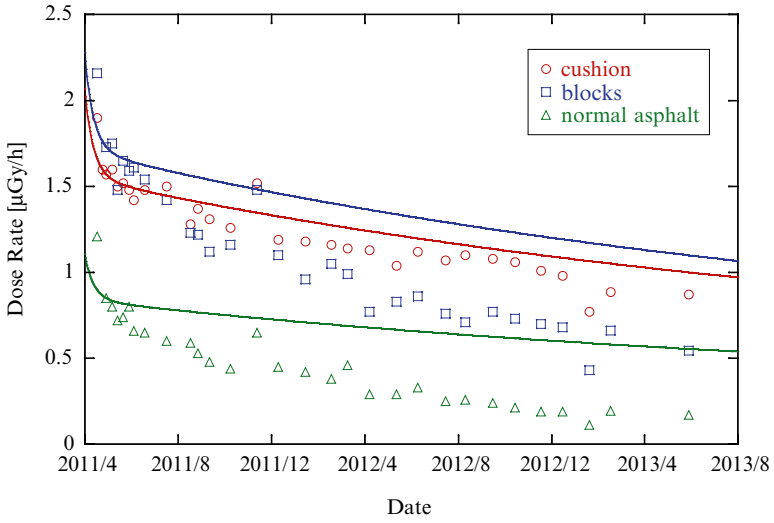

Fig. 10.7 Time dependence of the dose rate for different paving materials. *Horizontal axis* is date and *vertical axis* is dose rate. *Circles* show measured dose rates at the cushion-paved area, *squares* show measured dose rates at the block-paved area, and *triangles* show measured dose rates at the normal asphalt-paved area; *solid lines* show calculated dose rates

Gy was executed with a muon radiation weighting factor, 1.0. Time trend of dose rate from the radioactive materials was calculated from elapsed time from a normalization date, activities of the detected radioactive materials measured in previous studies [6, 8, 9], and the air kerma-rate constant as shown in Eq. (10.2), where A is normalization constant, i is a number of detected radioactive materials measured in the previous work, C_i is air kerma-rate constant [12], SA_i is activity in the surface soil [6], λ_i is a decay constant, and t is elapsed time from the normalization date.

$$D_{RM} = A \cdot \sum_i C_i \cdot SA_i \cdot \exp\left(-\lambda_i \cdot t\right), \tag{10.2}$$

From this formula, the dose rate changes that do not include movement of the radioactive materials can be estimated. A relative decay effect for dose rate change can be estimated from a sum of products of C_i and SA_i. Absolute changes can be set up by the normalization with a measured dose rate. The normalization constant A was determined from the measured dose rate at each point on a normalization date. In this analysis, the normalization date is April 29, 2011, because the consecutive dose rate measurement for the same places shown in Fig. 10.3 started at April 29, 2011. The calculated results are shown as solid lines in Fig. 10.7.

Some differences between calculated and measured dose rates are found in Fig. 10.7. The measured dose rates become smaller than calculated dose rates in all three points with time, and the difference in blocks area looks larger than the

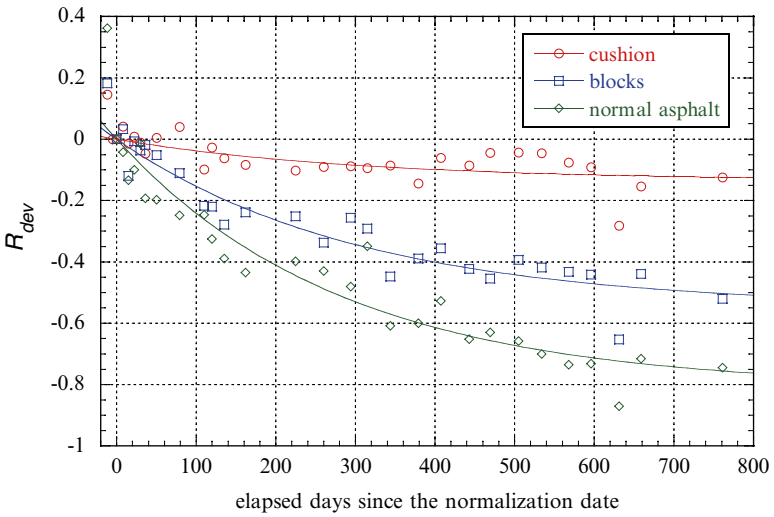

Fig. 10.8 Ratios of the deviations between measured and calculated dose rates for different paving materials. *Horizontal axis* is elapsed dates since the normalization date; *vertical axis* is a ratio of the deviations between measured and calculated dose rates; *circles* show the ratio at the cushion-paved area; *squares* show the ratio at the block-paved area; *triangles* show the normal asphalt-paved area

difference in cushion area. The dose rate differences between calculated and measured were changed to ratios for a calculated net dose rate as shown in Eq. (10.3) to compare decreasing trends.

$$R_{dev} = \left(D_{meas} - D_{calc}\right) / D_{RM}. \tag{10.3}$$

R_{dev} is the ratio for a calculated net dose rate and D_{meas} is a measured dose rate (Fig. 10.8). The decrease in gradient of the cushion-paved area was smallest, and the gradient of the normal asphalt-paved area was largest of the three areas (Fig. 10.8). The ratios for elapsed time were fitted with Eq. (10.4), where k is fixation ratio and r is a decreasing constant to estimate the effect of fixed radioactive materials.

$$R_{dev} = k \cdot \left\{\exp\left(-r \cdot t\right) - 1\right\}. \tag{10.4}$$

k describes a ratio of the fixed radioactive materials and r describes a gradient of the decrease. Fitted lines are shown as solid lines in Fig. 10.8, which show different gradients and saturation values. k and r for each point are shown in Table 10.1. The fixation ratio of the cushion area dose rate is highest and that of the normal asphalt area is lowest in the three points.

From these analyses, it became clear that the dose rates on paved areas decrease faster than the physical decay of radioactive nuclides that were speculated to come

Table 10.1 Fixation rate and decreasing constant for different paving materials

Paving material	Cushion	Blocks	Normal asphalt
k	0.13 ± 0.05	0.55 ± 0.06	0.81 ± 0.08
r	0.0033 ± 0.0027	0.0033 ± 0.0008	0.0035 ± 0.0008

from the Fukushima Daiichi NPP, and the decreasing trends are correlated with the paving materials.

This phenomenon is believed to occur by capture activity differences of the paving materials for radioactive materials.

10.4 Conclusion

Kinki University AERI conducted two studies on the radioactive contamination derived from the Fukushima Daiichi NPP in urban areas of Fukushima City since April 2011. One of these measurements was activities of surface soils and the other a survey of dose rate distributions. The results presented herein demonstrate that the dose rate distribution changed with time and that the dose rate distributions in paved areas have different characteristics for different paving materials.

This phenomenon is estimated to occur by capture activity differences of the paving materials for radioactive materials. More detailed studies are needed to acquire evidence of the mechanisms of the phenomenon.

References

1. Matsumura H, Saito K, Ishioka J, Uwamino Y (2011) Diffusion of radioactive materials from Fukushima Daiichi nuclear power station obtained by gamma-ray measurements on expressways. Trans At Energy Soc Jpn 10:152–162
2. Sanami T, Sasaki S, Iijima K, Kishimoto Y, Saito K (2011) Time variations in dose rate and gamma spectrum measured at Tsukuba city, Ibaraki, due to the accident of Fukushima Daiichi nuclear power station. Trans At Energy Soc Jpn 10:163–169
3. Naganawa H, Kumazawa N, Saitoh H, Yanase N, Mitamura H, Nagano T, Kashima K, Fukuda T, Yoshida Z, Tanaka S (2011) Removal of radioactive cesium from surface soils solidified using polyion complex rapid communication for decontamination test at Iitate-mura in Fukushima prefecture. Trans At Energy Soc Jpn 10:227–234
4. Sakamoto F, Ohnuki T, Kozai N, Igarashi S, Yamasaki S, Yoshida Z, Tanaka S (2012) Local area distribution of fallout radionuclides from Fukushima Daiichi nuclear power plant determined by autoradiography analysis. Trans At Energy Soc Jpn 11:1–7

5. Tagawa A (2012) Effects of ground surface decomination on the air radiation dose rate results of a decomination trial at a playground lot in a Fukushima residential area. Trans At Energy Soc Jpn 11:111–117
6. Hohara S, Inagaki M, Kojima K, Yamanishi H, Wakabayashi G, Sugiyama W, Itoh T (2011) Survey of living environmental land contaminated with radioactive materials due to Fukushima Daiichi nuclear plant accident. Trans At Energy Soc Jpn 10:145–148
7. Hohara S, Ito S. Development of a portable natural background-radiation measurement system equipped with global positioning function and its application. Annual report of Kinki University Atomic Energy Research Institute, vol 45, pp 1–10. Kinki University Atomic Energy Research Institute, 2008.
8. Hohara S, Inagaki M, Yamanishi H, Wakabayashi G, Sugiyama W, Itoh T. Survey of radioactive contamination in urban distracts of Naka-Dori Area due to Fukushima-Daiichi Nuclear Plant Accident. Annual report of Kinki University Atomic Energy Research Institute, vol 48, pp 11–21. Kinki University Atomic Energy Research Institute, 2011.
9. Hohara S, Inagaki M, Yamanishi H, Wakabayashi G, Sugiyama W, Itoh T (2012) Survey of radioactive contamination in Fukushima Naka-Dori region, Fukushima, Japan. In: Progress in nuclear science and technology: proceedings of 12th international conference on radiation shielding, Nara, Japan, 2–7 Sept 2012 (printing)
10. Abe S, Fujitaka K, Abe M, Fujimoto K (1981) Extensive field survey of natural radiation in Japan. J Nucl Sci Technol 18:21–45
11. UNSCEAR (2008) Reports, Sources and effects of ionizing radiation, United Nations Scientific Committee on the Effects of Atomic Radiation (2008)
12. Radioisotope data book, 11th edn. Japan Radioisotope Association (2011)

Chapter 11
Observation of Radionuclides in Marine Biota off the Coast of Fukushima Prefecture After TEPCO's Fukushima Daiichi Nuclear Power Station Accident

Tatsuo Aono, Yukari Ito, Tadahiro Sohtome, Takuji Mizuno, Satoshi Igarashi, Jota Kanda, and Takashi Ishimaru

Abstract Monitoring and surveying of radioactivity in seawater and biota in the marine environment off the coast of Fukushima Prefecture in the Pacific Ocean are important for understanding the dispersion of artificial radionuclides after the TEPCO Fukushima Daiichi Nuclear Power Station (FD1NPS) accident. Marine biota were collected in the coastal area off Fukushima Prefecture after this accident to investigate the radioactivity of ^{134}Cs, ^{137}Cs, and ^{110m}Ag in marine biota, including not only fish and shellfish but also benthos. It is well known that ^{108m}Ag, one of the radioactive isotopes of Ag, was observed in some kinds of squid and octopus before this accident. As a result, ^{110m}Ag was observed in many kinds of marine biota off the coastal area of Fukushima. It is suggested that rapid change in the radioactivity in seawater, resuspension of particles from sediments, and food chain effects led to high radionuclide activities in the marine biota after this accident.

Keywords ^{110m}Ag • ^{134}Cs • ^{137}Cs • Marine organisms

T. Aono (✉)
Fukushima Project Headquarters, National Institute of Radiological Sciences, Anagawa 4-9-1, Inage, Chiba 263-8555, Japan
e-mail: t_aono@nirs.go.jp

Y. Ito • J. Kanda • T. Ishimaru
Department of Ocean Sciences, Tokyo University of Marine Science and Technology, Konan 4-5-7, Minato, Tokyo 108-0075, Japan

T. Sohtome • T. Mizuno
Fukushima Prefecture Fisheries Experimental Station, Matsushita 13-2, Shimokajoro, Onahama, Iwaki, Fukushima 970-0316, Japan

S. Igarashi
Fukushima Prefecture Fisheries Experimental Station, Matsushita 13-2, Shimokajoro, Onahama, Iwaki, Fukushima 970-0316, Japan

Fukushima Prefecture Sea-Farming Association, Iino 4-3-1, Tyuohdai, Iwaki, Fukushima 970-8044, Japan

S. Takahashi (ed.), *Radiation Monitoring and Dose Estimation of the Fukushima Nuclear Accident*, DOI 10.1007/978-4-431-54583-5_11,

11.1 Introduction

Monitoring and surveying of radioactivity in seawater, sediments, and biota in the marine environment in the Pacific Ocean around Eastern Japan are important for understanding the dispersion of artificial radionuclides after the Tokyo Electric Power Company (TEPCO) Fukushima Daiichi Nuclear Power Station (FD1NPS) accident. The activities of $^{134}Cs + ^{137}Cs$ in seawater were observed to be more than 10 kBq/L around FD1NPS at the end of March 2011 and have recently decreased gradually to 1–2 mBq/L, approaching the pre-accident levels [1]. On the other hand, higher activities of $^{134}Cs + ^{137}Cs$ in sediments have been reported off the coast area of Fukushima Prefecture in the Pacific Ocean [2]. It is necessary that radioactivity in marine biota, including not only fish and shellfish but also the benthos, be monitored continuously as it is well known that marine biota accumulate and concentrate elements and radionuclides in their bodies [3]. The activities of radionuclides in marine biota off Fukushima, including plankton and benthos, are investigated to determine the variation in radioactivity. The observed artificial gamma-emitting radionuclides in marine biota include not only ^{134}Cs and ^{137}Cs but also ^{110m}Ag. Artificial radionuclides such as ^{134}Cs, ^{137}Cs, ^{141}Ce, ^{144}Ce, ^{103}Ru, ^{106}Ru, and ^{110m}Ag were reported in Mediterranean seagrass after the Chernobyl accident [4]. However, ^{141}Ce, ^{144}Ce, ^{103}Ru, and ^{106}Ru were not observed in the fallout after this accident [5]. Most marine biota, aside from benthos, contained no observable ^{110m}Ag a year after the accident, as the activities of the short half-life radionuclide decrease with time, rather than being discharged by metabolic activity in the biota. $^{134}Cs + ^{137}Cs$ activity in marine biota was classified into three types, either tending to gradually decrease with time, or showing considerable variation, or being less than the detection limit of activity [6]. The aims of the present study were to examine the temporal and spatial changes in radioactivity in marine biota and to survey the contamination after this accident.

11.2 Materials and Methods

Marine biota samples were collected with a plankton net, dredge sampler, and trawl during cruises of T/S *Umitaka-maru*, T/S *Shinyo-maru*, and some research and fishing vessels. After being classified into species and weighed, each sample was dried with a vacuum drying machine, homogenized, and packed into a plastic container (U-8). Radioactivity was determined by gamma-ray spectrometry using a HPGe detector (GX-2019; Canberra). The radionuclide activities of biota in the sampling date were calculated with the correction of the decay and the coincidence-summing of ^{134}Cs. Detection limits of ^{134}Cs, ^{137}Cs, and ^{110m}Ag were estimated within 1 and 0.5 Bq/kg [wet weight (wet wt)], respectively.

11.3 Results and Discussion

Radionuclide activity in the marine biota off Onahama (Fukushima) that are used as foodstuffs, measured on June 21, 2011 and December 20, 2011, is shown in Tables 11.1 and 11.2. Radionuclide activity in marine biota (plankton and benthos, etc.) off Fukushima in the Pacific Ocean is shown in Table 11.3. The radioactivity of $^{134}Cs + ^{137}Cs$ in marine products ranged from 15 to 132 Bq/kg (wet wt) in June 2011 and from less than 1 to 135 Bq/kg (wet wt) in December 2011. ^{110m}Ag activity was not detected in fishes collected in December 2011, although this activity was observed in the viscera of squid, crab, and fish collected in June 2011. It is considered that the activity of ^{110m}Ag in fish and plankton gradually decreased with time because the half-life of ^{110m}Ag is 249.8 days. However, no cesium radioactivity was observed in squid and crab. It is well known that Mollusca and Crustacea concentrate silver in their visceral parts. After the accident, ^{110m}Ag was observed from fallout in the eastern area of Japan in April and May 2011 [2]. ^{110m}Ag added to seawater tends to be rapidly scavenged to the sediments because the solubility of silver in seawater is extremely low. The bottom-dwelling biota such as shellfish and benthos had high activities of Cs and Ag 1 year after the accident. Comparison of weight and radioactivity in each part of the marine organisms is shown in Fig. 11.1. The ratios of cesium activity in the various parts of marine organisms are similar to their weight ratios. The average cesium activity in seawater was 0.20 Bq/L in June 2011, which gradually decreased to 0.03 Bq/L in December 2011 around the sampling area [7]. Cesium activity in seawater decreased to a low ten times during 6 months, and then activity in marine organisms was also reduced. On the other hand, the decrease of ^{110m}Ag activity in mollusks could be observed to be almost that of the physical half-life time. It is thought the decrease of activity of these radionuclides in marine organisms depends on differences in the mechanisms of accumulation and metabolism.

The CR [concentration ratio = activity in biota (Bq/kg (wet wt))/activity in seawater (Bq/kg or Bq/L)] is usually represented in term of the concentration in biota relative to that of seawater for modeling purposes. This value of cesium in marine organisms was calculated with the activity of cesium in seawater (Fig. 11.2). CR of cesium (CR-Cs) in marine organisms ranged from 2.6E+1 in the muscle part of squid to 1.0E+4 in clam viscera. Large differences in CR-Cs in different parts of marine organisms were not observed. These values were higher than the reported CR of fish, crustaceans, mollusks, and macroalgae in TRS-422, 1.0E+2, 5.0E+1, 6.0E+1, and 5.0E+1, respectively [8]. CR in plankton was also calculated with the activity of cesium in seawater collected around the sampling area during this monitoring period. These resulting values ranged from 5.8E+1 to 7.8E+2, and were higher than the Cs-CR values (2.0E+1–4.0E+1), but also similar to the Cs-K_d value in TRS-422 [8]. It was suggested that the rapid change in radioactivity in seawater and the resuspension of particles from the sediments led to high CRs of Cs after the accident.

Table 11.1 Activities of radionuclides in marine organisms used as foodstuffs off Onahama (Fukushima) on June 21, 2011

Name of biota						
Marine products	English name	Genus, species	Measured parts	^{134}Cs (Bq/kg-wet wt)	^{137}Cs (Bq/kg-wet wt)	^{110m}Ag (Bq/kg-wet wt)
Fish	Japanese anchovy	*Engraulis japonica*	Whole body	10.1 ± 0.1	10.8 ± 0.1	<0.5
Fish	Pacific cod	*Gadus macrocephalus*	Whole body[a]	27.5 ± 0.3	30.2 ± 0.5	<0.5
			Muscle (edible portion)	37.9 ± 0.2	41.8 ± 0.3	<0.5
			Viscera	15.1 ± 0.1	16.3 ± 0.2	1.2 ± 0.1
			Bony parts	24.9 ± 0.2	27.2 ± 0.4	<0.5
Fish	Fat greenling	*Physiculus maximowiczi*	Whole body[a]	30.5 ± 0.4	33.4 ± 0.5	<0.5
			Muscle (edible ortion)	42.3 ± 0.2	46.2 ± 0.3	<0.5
			Viscera	11.0 ± 0.1	11.8 ± 0.1	0.6 ± 0.03
			Bony parts	35.3 ± 0.3	39.0 ± 0.4	<0.5
Fish	Pointhead flounder	*Hippoglossoides dubius*	Whole body[a]	63.3 ± 0.9	68.8 ± 1.3	<0.5
			Muscle (edible portion)	137.0 ± 0.9	148.9 ± 1.2	<0.5
			Viscera	22.5 ± 0.2	24.3 ± 0.3	<0.5
			Bony parts	18.4 ± 0.1	20.2 ± 0.2	<0.5
Fish	Rikuzen sole	*Dexistes rikuzenius*	Whole body[a]	13.2 ± 0.2	14.1 ± 0.3	0.8 ± 0.1
			Muscle (edible portion)	13.5 ± 0.1	14.7 ± 0.2	<0.5
			Viscera	17.6 ± 0.2	18.8 ± 0.2	5.3 ± 0.1
			Bony parts	11.6 ± 0.1	12.2 ± 0.2	<0.5
Squid	Bobtail squid	Sepioida	Whole body[a]	5.4 ± 0.1	5.7 ± 0.1	37.6 ± 0.2
			Muscle (edible portion)	2.5 ± 0.1	2.7 ± 0.1	2.9 ± 0.1
			Viscera	8.0 ± 0.1	8.6 ± 0.1	70.7 ± 0.2
Squid	Japanese common squid	*Todarodes pacificus*	Whole body[a]	10.6 ± 0.1	11.5 ± 0.2	24.9 ± 0.3
			Muscle (edible portion)	10.6 ± 0.1	11.5 ± 0.1	1.5 ± 0.03
			Viscera	10.6 ± 0.1	11.3 ± 0.1	92.8 ± 0.3
Crab	Snow crab	*Chionoecetes opilio*	Soft tissue[b]	7.2 ± 0.1	7.8 ± 0.2	3.4 ± 0.1

[a]Whole-body activity was weighted as average with that in all parts

[b]Activity was calculated with those in muscle and viscera parts because that in the shell part of crab was not determined

Table 11.2 Radionuclide activity in marine organisms used as foodstuffs off Onahama (Fukushima) on December 20, 2011

Name of biota						
Marine products	English name	Genus, species	Measured parts	^{134}Cs (Bq/kg-wet wt)	^{137}Cs (Bq/kg-wet wt)	^{110m}Ag (Bq/kg-wet wt)
Algae	Arame	*Eisenia bicyclis*	Whole body	16.4 ± 0.3	20.9 ± 0.4	1.9 ± 0.1
Fish	Greeneyes	*Chlorophthalmus albatrossis*	Whole body[a]	11.9 ± 0.3	15.1 ± 0.4	<0.5
			Muscle (edible portion)	12.1 ± 0.3	15.2 ± 0.5	<0.5
			Viscera	14.0 ± 0.4	18.2 ± 0.7	<0.5
			Bony parts	10.9 ± 0.2	14.5 ± 0.3	<0.5
Fish	Slime flounder	*Microstomus achne*	Whole body[a]	1.7 ± 0.1	2.3 ± 0.2	<0.5
			Muscle (edible portion)	1.5 ± 0.1	2.1 ± 0.2	<0.5
			Viscera	2.9 ± 0.1	3.8 ± 0.2	<0.5
			Bony parts	1.4 ± 0.1	1.7 ± 0.1	<0.5
Squid	Japanese squid	*Loliolus* (*Nipponololigo*) *japonica*	Whole body[a]	<1	<1	4.2 ± 0.1
			Muscle (edible portion)	<1	<1	4.6 ± 0.1
			Viscera	<1	<1	43.3 ± 0.7
			Eyeball	<1	<1	6.9 ± 0.1
			Cartilage	<1	<1	15.1 ± 0.9
Squid	Spear squid	*Loligo bleekeri*	Whole body[a]	<1	<1	2.4 ± 0.2
			Muscle (edible portion)	<1	<1	<0.5
			Viscera	<1	<1	12.4 ± 0.4
			Eyeball	<1	<1	1.7 ± 0.1
			Cartilage	<1	1.1 ± 0.1	<0.5
Crab	Snow crab	*Chionoecetes opilio*	Whole body[b]	<1	<1	3.1 ± 0.1
			Muscle (edible portion)	<1	<1	2.2 ± 0.1
			Viscera	<1	<1	11.1 ± 0.2
Shellfish	Sakhalin surf clam	*Pseudocardium sachalinense*	Whole body[c]	58.9 ± 1.1	76.3 ± 1.8	19.0 ± 0.7
			Muscle (edible portion)	16.8 ± 0.3	20.5 ± 0.5	4.8 ± 0.2
			Mantle	108.4 ± 1.6	142.1 ± 2.6	29.7 ± 1.0
			Viscera	23.7 ± 0.5	29.5 ± 0.8	31.7 ± 0.6

[a]Whole-body activity was weighted as average with that in all parts

[b]Whole-body activity was calculated with those in muscle and viscera parts, as that in the shell part of crab was not determined

[c]Whole-body activity was calculated with those in muscle, mantle, and visceral parts, as that in the shell parts of shellfish was not determined

Table 11.3 Radionuclide activity in marine biota (plankton and benthos) off Fukushima in the Pacific Ocean

Date	Location								Depth (m)	Name of biota			Measured part	^{134}Cs (Bq/kg-wet wt)	^{137}Cs (Bq/kg-wet wt)	^{110m}Ag (Bq/kg-wet wt)
	Latitude				Longitude					Marine products	English name	Genus, species				
2011/7/6	36	55	2	N	141	0	0	E		Plankton			Whole	2.7±0.2	2.9±0.2	1.6±0.1
2011/7/6	36	55	2	N	141	25	92	E		Plankton			Whole	2.2±0.9	2.4±1.2	0.9±0.1
2011/7/14	37	5	0	N	140	59	10	E	7	Crustacea	Mysidacea		Whole	24.1±0.4	26.4±0.6	15.5±0.3
2011/8/17	37	4	58	N	140	59	19	E	7	Crustacea	Mysidacea		Whole	41.3±0.5	46.7±0.7	7.0±0.2
2011/9/5	37	5	8	N	140	59	56	E	10	Crustacea	Mysidacea		Whole	31.0±0.5	34.8±0.7	15.0±0.3
2011/11/1	37	4	30	N	141	9	18	E	26	Plankton (mesh size of net, 330 μm)			Whole	32.2±0.8	37.1±1.1	<1
2012/4/25	37	50	0	N	141	6	0	E	28	Plankton (mesh size of net, 330 μm)			Whole	22.2±1.1	31.5±1.3	<1
2011/10/22	36	55	2	N	141	0	0	E	40	Polychaeta	Polychaetes		Whole	146.8±3.8	181.5±5.7	11.6±1.5
2011/10/22	36	55	2	N	141	0	0	E	40	Sea urchin		*Echinocardium cordatum*	Whole	271.0±5.6	311.4±8.5	<1
2011/10/22	36	55	2	N	141	0	0	E	40	Starfish		*Distolasterias nipon*	Whole	5.6±0.3	7.0±0.4	8.3±0.3
2011/10/22	36	55	2	N	141	0	0	E	40	Starfish	Northern Pacific seastar	*Asterias amurensis*	Whole	3.4±0.3	4.7±0.4	16.0±0.4
2011/10/22	36	55	2	N	141	0	0	E	40	Sea slug	Opisthobranchia Spengel	*Philine argentata*	Whole	17.2±0.4	20.6±0.5	21.8±0.4

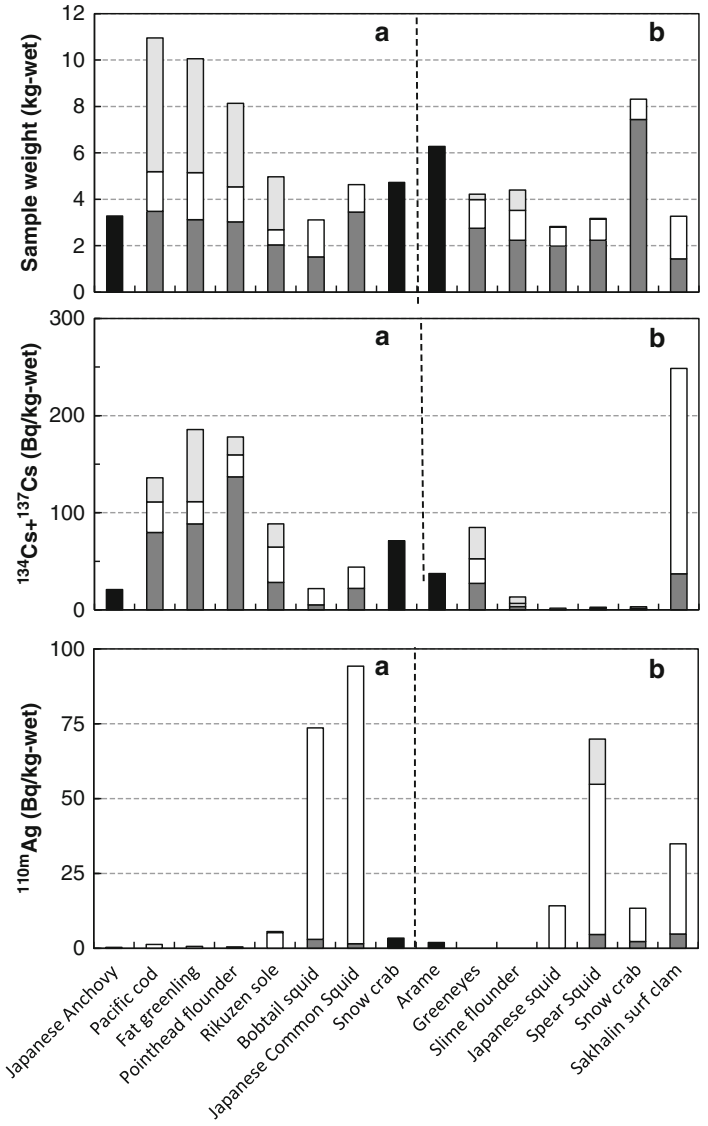

Fig. 11.1 Comparison of weight and radioactivity in each part of the marine organisms. *Black bars*, whole body; *gray bars*, muscle (edible parts); *open bars*, viscera; *light gray bars*, bony parts. Samples were collected in June (**a**) and December (**b**), 2011

11.4 Conclusion

The activities of ^{134}Cs, ^{137}Cs, and ^{110m}Ag in marine biota off the coast of Fukushima Prefecture in the Pacific Ocean were investigated a year after the FD1NPS accident. ^{110m}Ag could be observed in many marine biota after this accident, although it is

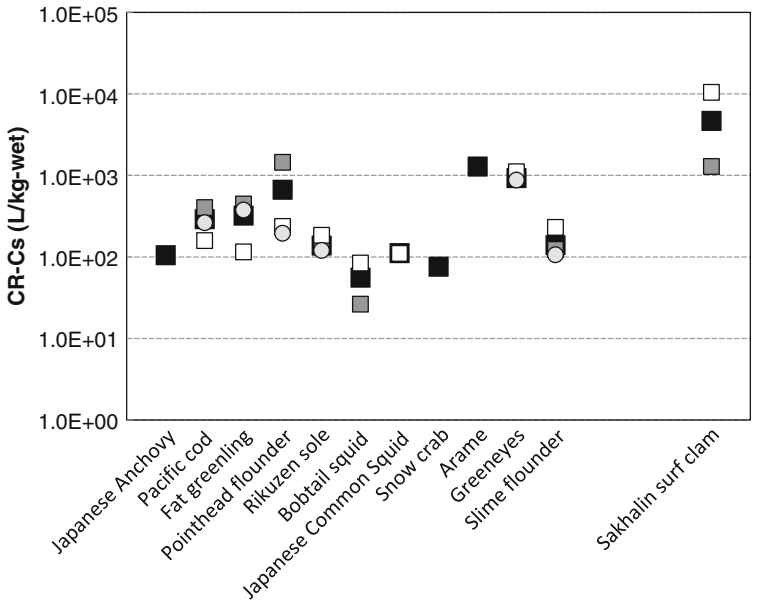

Fig. 11.2 Concentration ratio of cesium (*CR-Cs*) in each part of the marine organisms. *Black squares*, whole body; *gray squares*, muscle (edible parts); *open squares*, viscera; *open circles*, bony parts

well known that Mollusca and Crustacea concentrate silver in the visceral parts. Finally, it was suggested that the CR fluctuations in plankton is a result of both radioactivity in seawater and sediment resuspension.

Acknowledgements Sampling would not have been possible without the field support provided by the T/S *Umitaka-maru*, T/S *Shinyo-maru*, and some research and fishing vessels. Part of the sample treatment support was provided by staff members of the National Research Institute of Fisheries Science, Fisheries Research Agency. This work was partly supported by Health Labour Sciences Research Grant and MEXT Grant-in-Aid for Scientific Research on Innovative Areas (24110004).

References

1. Aoyama M, Tsumune D, Hamajima Y (2012) Distribution of ^{137}Cs and ^{134}Cs in the North Pacific Ocean: impacts of the TEPCO Fukushima-Daiichi NPP accident. J Radioanal Nucl Chem doi:10.1007/s10967-012-2033-2
2. MEXT (2012) http://radioactivity.mext.go.jp/old/ja/monitoring_around_FukushimaNPP_sea_marine_soil/2012/03/1350_031518.pdf. Accessed Nov 2012

3. Kasamatsu F (1999) Marine organisms and radionuclides with special reference to the factors affecting concentration of ^{137}Cs in marine fish. Radioisotopes 48:266–282 (in Japanese)
4. Calmet D, Charmasson S, Gontier G (1991) Chernobyl radionuclides in the Mediterranean seagrass *Posidonia oceanica*, 1986–1987. J Environ Radioact 13:157–173
5. MEXT (2012) http://radioactivity.mext.go.jp/ja/contents/6000/5731/24/194_1_H2305data_0713.pdf. Accessed Nov 2012
6. Fisheries Agency (2012) Inspection on radioactivity in fisheries products. http://www.jfa.maff.go.jp/j/sigen/gaiyou/index.html. Accessed Nov 2012 (in Japanese)
7. Oikawa S, Takata H, Watabe T, Misonoo J, Kusakabe M (2013) Distribution of the Fukushima-derived radionuclides in seawater in the Pacific off the coast of Miyagi, Fukushima, and Ibaraki Prefectures, Japan. Biogeosciences 10:5031–5047
8. IAEA (1985) Sediment distribution coefficients and concentration factors for biota in the marine environment, vol 422, Technical reports series. International Atomic Energy Agency, Vienna

Part V
Transfer Models and/or Parameters

Chapter 12
Evaluating Removal of Radionuclides from Landfill Leachate Using Generally Practiced Wastewater Treatment Processes

Nao Kamei-Ishikawa, Ayumi Ito, and Teruyuki Umita

Abstract Some amounts of the radionuclides released in the nuclear accident at the Fukushima Daiichi Nuclear Power Plant are transferred to wastes such as sewage sludge ash and municipal waste ash. Among these wastes, those that contain less than 8,000 Bq/kg radiocesium are being disposed in controlled landfill sites that have been in use since before the accident. At the landfill sites, a leachate treatment system is generally used, and there are no specific treatment steps for removal of radionuclides. In this study, the stable element concentrations of the relevant radionuclides in the leachate and treated water at each treatment step were determined to evaluate the radionuclide removal at each step. Target elements in this study were Cs, Co, Mn, Ni, and Sr. More than 93.9 % of the Co, Mn, Ni, and Sr present in the leachate could be removed at the alkali removal step by precipitation; however, Cs could not be removed by any of the treatment processes.

Keywords Cesium • Cobalt • Fractionation • Landfill leachate • Leachate treatment • Manganese • Nickel • Stable isotopes • Strontium

12.1 Introduction

Radionuclides such as ^{134}Cs, ^{137}Cs, ^{90}Sr, and $^{239+240}$Pu, which were released to the environment in the nuclear accident at the Fukushima Daiichi Nuclear Power Plant, have been found in bottom ash and fly ash of incinerated wastes produced in

N. Kamei-Ishikawa (✉) • T. Umita
Department of Civil and Environmental Engineering, Iwate University,
Ueda 4-3-5, Morioka, Iwate 020-8551, Japan
e-mail: naoki@iwate-u.ac.jp

A. Ito
Department of Frontier Materials and Function Engineering, Graduate School of Engineering,
Iwate University, Ueda 4-3-5, Morioka, Iwate 020-8551, Japan

S. Takahashi (ed.), *Radiation Monitoring and Dose Estimation of the Fukushima Nuclear Accident*, DOI 10.1007/978-4-431-54583-5_12,

Fukushima Prefecture, Japan [1]. ^{134}Cs and ^{137}Cs have been found in sewage sludge produced in a wide area of northern and eastern Japan [2]. The Japanese government divides wastes into three types, depending on radiocesium concentration in the waste, and each type has its own disposal methods [3]. For the waste with the lowest level of radiocesium concentrations (<8,000 Bq/kg), controlled landfill sites can be used as the disposal place. The radiocesium concentrations in sewage sludge ash produced in Iwate Prefecture have been lower than 8,000 Bq/kg; therefore, these ashes have been disposed in a controlled landfill site that has been used since before the nuclear accident.

Controlled landfill sites have leachate treatment systems. Although leachate characteristics depend on the individual sites, generally leachate has high alkalinity and contains a high organic matter content and a large amount of suspended solids [4]. To remove these contaminants, several types of treatment steps are used: coagulation-flocculation, chemical precipitation, membrane filtration, activated carbon adsorption, biological treatment, and ion-exchange treatment [5]. However, the extent of removal of any radionuclides present in the leachate by existing treatment steps is not clear.

The objective of this study was to evaluate radionuclide removal from the leachate sampled at a controlled landfill site. Stable elements were analyzed as analogues of the radionuclides. The main elements studied were Co, Cs, Mn, Ni, and Sr; their radionuclides (^{58}Co, ^{60}Co, ^{134}Cs, ^{137}Cs, ^{54}Mn, ^{59}Ni, and ^{63}Ni) were actually detected or expected to be found in environmental samples collected after the nuclear accident [6].

12.2 Materials and Methods

12.2.1 Sample Collection

Samples were collected from the Iwate Clean Center landfill site in Iwate Prefecture, Japan. The site is separated into two blocks: block I (landfill capacity, 50,300 m^3) and block II (landfill capacity, 75,000 m^3). Block I is now closed, whereas more than half of the landfill capacity of block II remains available. Major wastes buried in the landfill site have been combustion residue (26,000 t), glass, concrete, and ceramic (25,000 t), and inorganic sludge (10,000 t).

A flow sheet of the leachate treatment system that indicates sampling points is shown in Fig. 12.1. Leachates from blocks I and II are mixed in the regulating reservoir. Samples were taken after the following steps: regulating reservoir (raw leachate, RL); alkali removal step using sodium carbonate (AR); biological treatment step (BT); membrane filtration step (MF); activation carbon adsorption step (AC); and chelating and zeolite adsorption step (effluent water, EW). Samples were taken in July, September, and December 2012 at all locations, except for the AC, which was only sampled in September and December. Zeolite adsorption for radiocesium

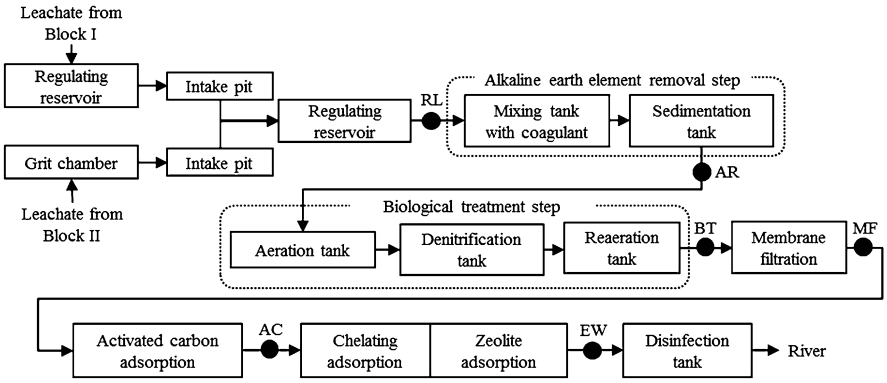

Fig. 12.1 Leachate treatment system with sampling points (*filled circles*)

adsorption was added to the process from May 2012. There is a pH regulating tank after each step.

The precipitate in the sedimentation tank at the AR step was collected in December to determine the distribution between liquid phase and solid phase (precipitates) for each element.

12.2.2 Determination of Characteristics of Samples

Chemical characteristics of the samples were determined. The pH was measured with a pH meter (HM-25R; TOADKK). Suspended solids (SS) were determined in duplicate by the standard method [7]. Total organic carbon content (TOC) was determined three times using a TOC analyzer (TOC-V; Shimadzu).

Concentration analyses of the target elements (Cs, Sr, Co, Ni, and Mn) and major elements were based on standard methods for examination of wastewater [7]. These analyses were done in triplicate. First, 100 mL of sample was digested with 1 mL concentrated HNO_3 and 0.5 mL concentrated HCl, and then evaporated on a hot plate at around 120 °C. Next, deionized water was added to the sample to make a solution volume of 100 mL. The sample solution was filtered through a 0.45-μm membrane filter. Element concentrations in the filtrate were measured using an inductively coupled plasma (ICP) mass spectrometer (iCAP Qs; Thermo) and ICP atomic emission spectrometer (Shimadzu, ICPE-9000). Standard solutions were purchased from Merck Chemicals (CertiPUR series). No contaminations of the analyzed elements were found in a processed blank.

The precipitate collected in the sedimentation tank at the AR step was also analyzed to determine concentrations of each element in the solid phase in the precipitate as already described.

12.2.3 Determination of Physical and Chemical Forms of the Target Elements in Raw Leachate

Filtration and ion-exchange methods were used to determine three fractions of each element in RL sample: particulate, cationic, and anionic fractions. The particulate fraction was the solid phase retained by filtration through a 0.45-μm membrane filter. The filtrate was used for further fractionation.

Two types of ion-exchange resins, an anion-exchange resin (AER) (IRA402BL; Amberlite) and a cation-exchange resin (CER) (IR120B-Na; Amberlite), were used to determine the ion species of each element in the filtrate. A preliminary experiment confirmed that the cations of the target elements were retained by CER but not by AER.

After passing through the 0.45-μm membrane filter, the filtrate was passed through the AER or CER resin column separately. Each column eluent was analyzed for the element concentrations using the ICP mass spectrometer. The cation form fraction or the anion form fraction was the fraction that passed through the AER or CER, respectively.

12.3 Results and Discussion

12.3.1 Characteristics of the Samples

Table 12.1 shows SS, TOC, and pH in each sample. SS in the RL sample had a wide variation. Sediments in one of the two intake pits were moved to another pit during the pit maintenance between July and September; therefore, the turbidity in the pit in September was the highest, causing a wide variation of SS. More than 84 % of the SS in the RL was removed at the AR step, and then after the BT step, more than 93 % of the SS in the RL was removed. On the other hand, TOC was lowered after the MF step.

Table 12.1 Suspended solids (SS), total organic carbon (TOC), and pH in samples

	SS (mg/L)			TOC (mg/L)			pH		
	Max	Min	Mean	Max	Min	Mean	Max	Min	Mean
RL	281	77	182	23	15	18	7.4	7.2	7.3
AR	15	5.3	11	23	10	15	10.0	8.3	9.2
BT	5.0	1.6	3.1	30	12	18	7.7	7.2	7.5
MF	1.3	<0.4	0.9	8.2	1.8	5.7	7.1	6.7	6.9
AC	1.2	<0.1	0.7	3.5	2.3	2.9	6.9	6.9	6.9
EW	2.2	<0.4	1.2	5.1	3.7	4.3	7.1	6.8	7.0

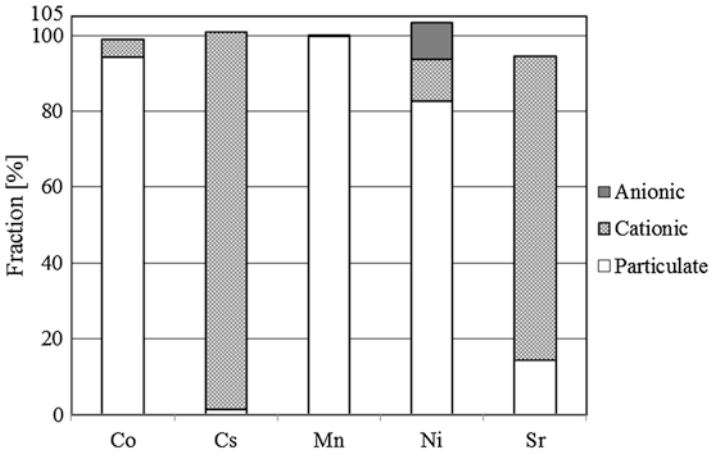

Fig. 12.2 Element fractionation in the raw leachate (RL) sample

12.3.2 Element Fractionation in the Raw Leachate Sample

For the RL sample collected in December, concentrations of Co, Cs, Mn, Ni, and Sr were 13.4, 3.3, 1,810, 87.7, and 3,960 μg/L, respectively. The distribution of the element concentrations in each fraction were obtained as shown in Fig. 12.2. The filtration and ion exchange were carried out with good recovery ratios ranging from 94.6 % to 103 %. More than 82 % of the Co, Ni, and Mn was present in the particulate fraction. Mn exists as brown-colored Mn_3O_4 when it is incinerated at temperatures higher than 800 °C [8]. Because waste is generally incinerated above 800 °C and the color of the suspended solid was brown in the RL sample, Mn should be present as Mn_3O_4. Some Ni was in anionic form (9.5 %) and slightly more in cationic form (11 %). Ni is present as Ni^{2+} in the water environment [9], and it is also combined with organic matter [10, 11]. Organic matter has several functional groups such as phenolic, carboxyl, and carbonyl [12]. The leachate filtrate contained 13.8 mg/L dissolved organic carbon. Therefore, a part of the Ni in the leachate could be combined with dissolved organic matter and then exist in anionic form.

Cationic forms were dominant for Cs and Sr (Fig. 12.2). Most of the Cs and Sr would be present as Cs^+ and Sr^{2+} under the pH and Eh conditions [9]. The principal form of Cs in municipal waste fly ash was suggested to be CsCl, which has high solubility [11]; this was attributed to the fact that the extraction ratios of Cs from five municipal waste fly ash samples ranged from 64 % to 89 % [13]. In contrast, extraction ratios of Cs from the municipal solid waste incinerator bottom ash and sewage sludge ash were less than 5.6 % and 2.7 %, respectively [13, 14]. Therefore, Cs in the leachate was from municipal waste fly ash, and the insoluble forms of Cs could not move downward with the leachate. For Sr, insoluble fractions were around 25 % in municipal waste fly ash and bottom ash and more than 40 % in sewage sludge ash [13], which implied that Sr in the leachate could originate from different types of waste.

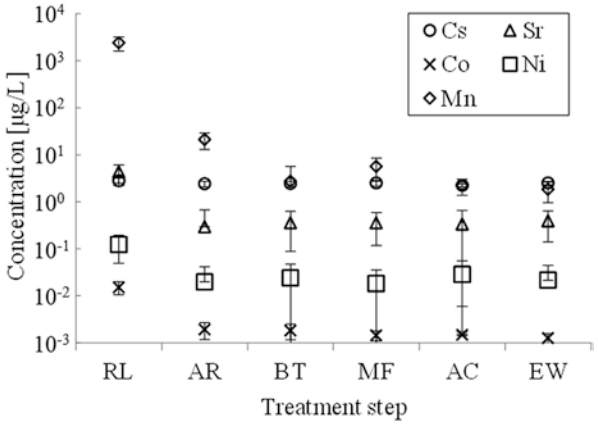

Fig. 12.3 Element concentrations in samples at each treatment step. *Error bars* show the standard deviation of three replicates

12.3.3 Element Concentration in Samples at Each Treatment Step

Figure 12.3 shows the element concentrations in samples at each treatment step. Co, Mn, Ni, and Sr concentrations in RL were lowered at the AR step. The removal rates at the AR step for Co, Mn, Ni, and Sr were 87.3 %, 99.1 %, 83.9 %, and 93.2 %, respectively. However, Cs concentration was not changed at any treatment steps.

As already described, except for Cs, all the target elements were removed from the RL at the alkali removal step. To obtain the degree of precipitation, the distribution coefficient (K_d) for each element was calculated by the following equation:

$$K_d = C_{solid} / C_{liquid}$$

where C_{solid} is an element concentration in the solid phase (precipitate) and C_{liquid} is an element concentration in the liquid phase (AR sample). Table 12.2 shows the K_d values for the target and major elements of the precipitate at the AR step. At this step, Na_2CO_3 was added as a reagent for removing alkalinity. Na concentration was 1.5 g/L in the RL and then rose to 2.2 g/L, which implied at least 1.5×10^{-2} mol/L CO_3^{2-} ion was added at the AR step. Ca and Sr had high K_d values and were present mostly as cationic forms in the RL sample. The solubility products of $CaCO_3$ and $SrCO_3$ are quite low ($10^{-8.3}$ for Ca and 10^{-10} for Sr) [15]; therefore, these elements in the RL must be precipitated by the following reactions:

$$Na_2CO_3 + Ca^{2+} \rightarrow CaCO_3 \downarrow + 2Na^+$$

$$Na_2CO_3 + Sr^{2+} \rightarrow SrCO_3 \downarrow + 2Na^+$$

Table 12.2 K_d values of the precipitate at the alkali removal (AR) step for each element

	K_d (L/kg)
Co	1,456 ± 111
Cs	67 ± 4
Mn	20,549 ± 3,304
Ni	1,215 ± 72
Sr	1,530 ± 101
Ca	5,015 ± 280
K	1.9 ± 0.4
Mg	90 ± 14.8
Rb	3.4 ± 1.0

In addition, particulate fraction could be coprecipitated by the increasing pH at the AR step, which would explain why Co, Mn, and Ni also had high K_d values.

Although the zeolite adsorption step introduced for Cs adsorption was not effective for Cs removal, Takano et al. [16] succeeded in developing a radiocesium removal treatment system from a leachate in a general waste disposal landfill site, and in fact, the system has been introduced to a landfill site in Gunma Prefecture [16]. At the Iwate Clean Center landfill site, use of zeolite was begun in an adsorption tower in May 2012, and the zeolite had not been exchanged by the collection of the last samples in the present study (December 2012). Adsorption sites on the zeolite must be occupied by not only Cs but also other major cations such as K and Ca. K, especially, which is most like Cs with similar chemical properties, had a concentration in the AC that was 1.5×10^5 times higher than the Cs concentration. From this fact, little Cs could be adsorbed by the zeolite. Consequently, frequent changing of zeolite or introduction of another new type of treatment system may be necessary for effective Cs removal.

12.4 Conclusions

In this study, the possibility of radionuclide removal from landfill leachate was evaluated by using generally practiced leachate treatment processes. As a result, more than 93.9 % of the Co, Mn, Ni, and Sr present in the RL could be removed at the alkali removal step by coprecipitation or precipitation as carbonate. Cs could not be removed by any treatment steps, even though there was a zeolite adsorption step. Cs removal can be achieved by frequently exchanging the zeolite in the zeolite adsorption tank. However, because that will generate more wastes and increase costs, it is necessary to adopt another treatment step for Cs removal.

Acknowledgments This work was partly supported by JSPS KAKENHI Grant Number 12014030.

References

1. Ministry of the Environment (2012) Additional information of 13th Commission of safety assessment for disaster waste disposal. http://www.env.go.jp/jishin/index.html#haikibutsu. Accessed 9 July 2013 (in Japanese)
2. Ministry of Land, Infrastructure, Transport and Tourism (2013) Measurements of radioactive concentrations in sewage sludge etc. http://www.mlit.go.jp/mizukokudo/sewerage/mizukokudo_sewerage_tk_000211.html. Accessed 9 July 2013 (in Japanese)
3. Ministry of Land, Infrastructure, Transport and Tourism (2011) The approach to immediate handling of secondary byproducts of water and sewage treatment in which radioactive materials were detected. http://www.nsr.go.jp/archive/nisa/english/press/2011/09/en20110909-2-2.pdf. Accessed 9 July 2013
4. Rowe PK, Quigley RM, Brachman RWI et al (2004) Barrier systems for waste disposal facilities. E&FN Spon, London
5. Kurniawan TA, Lo WH, Chen GYS (2006) Physico-chemical treatments for removal of recalcitrant contaminants from landfill leachate. J Hazard Mater 129:80–100
6. WHO (2012) Preliminary dose estimation from the nuclear accident after the 2011 Great East Japan Earthquake and Tsunami. WHO, Geneva
7. Japan Sewage Works Association (1997) Wastewater examination method, vol 2. Japan Sewage Works Association, Tokyo (in Japanese)
8. Greenwood NN, Earnshaw A (1997) Chemistry of the elements, 2nd edn. Butterworth-Heinemann, Oxford
9. Pourbaix M (1974) Atlas of electrochemical equilibria in aqueous solutions. National Association of Corrosion Engineers, Houston
10. Mellis EV, Cruz MC, Casagrande JC (2004) Nickel adsorption by soils in relation to pH, organic matter and iron oxides. Sci Agric 61:190–195
11. NITE (2008) Risk assessment of chemical substances, vol 69. National Institute of Technology and Evaluation, Tokyo (in Japanese)
12. Kumada K (2001) Chemistry of soil organic matter. Japan Scientific Societies Press, Tokyo (in Japanese)
13. NIES (2012) Appropriate waste disposal in terms of radionuclides behavior, technical data. National Institute of Environmental Studies, Tsukuba (in Japanese)
14. Tsushima I, Ogoshi M, Yamashita H et al (2013) Behavior of radioactive cesium in wastewater treatment plants and dissolution test of contaminated sewage sludge. J Jpn Soc Water Environ 36:23–28 (in Japanese)
15. Charlot G, Sone K (1974) Chemical reactions in solution. Kyoritsu Shuppan, Tokyo (in Japanese)
16. Takano T, Tamura Y, Nishizaki Y et al (2012) Radiocesium removal from leachate in general waste disposal using zeolite. Tishiseisou 65:218–222 (in Japanese)

Chapter 13
Studies on Radiocesium Transfer in Agricultural Plants in Fukushima Prefecture

Takashi Saito, Yasukazu Suzuki, Shigeto Fujimura, and Hirofumi Tsukada

Abstract After the Fukushima Daiichi Nuclear Power Plant (Tokyo Electric Power Company) accident occurred in March 2011, the concentration of radiocesium in brown rice produced in several areas of Fukushima Prefecture has exceeded a provisional regulation value. Therefore, we attempted research on decreasing the radiocesium concentration in agricultural plants.

To decrease the concentration of radiocesium in brown rice, we investigated the effect of the application of potassium fertilizer in rice paddy fields on the root uptake of radiocesium. The soil-to-brown-rice transfer factor of radiocesium decreased with an increase in exchangeable K_2O in the soil, suggesting that the application of

T. Saito (✉)
Agro-environment Division, Fukushima Agricultural Technology Centre,
116 Shimonakamichi, Takakura-Aza, Hiwada-machi, Koriyama, Fukushima 9630531, Japan
e-mail: saito_takashi_01@pref.fukushima.lg.jp

Y. Suzuki
Agro-environment Division, Fukushima Agricultural Technology Centre,
116 Shimonakamichi, Takakura-Aza, Hiwada-machi, Koriyama, Fukushima 9630531, Japan

Graduate School of Horticulture, Chiba University, 648 Matudo, Matudo-shi,
Chiba 2718510, Japan

S. Fujimura
Agro-environment Division, Fukushima Agricultural Technology Centre,
116 Shimonakamichi, Takakura-Aza, Hiwada-machi, Koriyama, Fukushima 9630531, Japan

NARO Tohoku Agricultural Research Center, 50 Harajukuminami, Arai, Fukushima-shi,
Fukushima 9602156, Japan

H. Tsukada
Fukushima Future Center for Regional Revitalization, Fukushima University,
1 Kanayagawa, Fukushima, Fukushima 9601296, Japan

Department of Radioecology, Institute for Environmental Sciences, 1-7 Ienomae,
Obuchi, Rokkasho, Kamikita-gun, Aomori 0393212, Japan

S. Takahashi (ed.), *Radiation Monitoring and Dose Estimation of the Fukushima Nuclear Accident*, DOI 10.1007/978-4-431-54583-5_13,

potassium fertilizer is an effective countermeasure to reduce the radiocesium concentration in brown rice.

We examine the possibility of decontamination by means of phytoremediation. Four species of plants were sown. The highest removal percentages of ^{137}Cs were obtained in amaranth (0.093 %) and sunflower (0.038 %) in the light-colored Andosol and gray lowland soils, respectively. This result indicates that it is difficult to remove radiocesium from contaminated soil by means of phytoremediation.

Keywords Brown rice • Exchangeable K_2O • Phytoremediation • Radiocesium • Soil • Soil-to-brown-rice transfer factor

13.1 Objective

The magnitude 9.0 earthquake and the subsequent large tsunami that occurred on March 11, 2011, caused extensive damage to coastal areas in Tohoku, Japan. In particular, the cooling system of the Fukushima Daiichi Nuclear Power Plant [Tokyo Electric Power Company (TEPCO) FNPP] collapsed from the tsunami in excess of 10 m, which resulted in several explosions in the four reactors of the plant. Large amounts of radioactive materials, mainly noble gas, ^{131}I, ^{134}Cs, and ^{137}Cs, were released into the atmosphere, and consequently agricultural land and forests in Eastern Japan were contaminated. Radiocesium ($^{134}Cs + ^{137}Cs$) is an important radionuclide that can be used for the assessment of radiation exposure to the public because it has a long half-life (^{134}Cs, 2.06 years; ^{137}Cs, 30.2 years), high transferability, and wide distribution in the environment. Because of their long half-lives, there is concern that radiocesium ($^{134}Cs + ^{137}Cs$) will remain on the surface of agricultural land and persist for a long time [1, 2]. Therefore, we have started monitoring of radiocesium in soil collected from agricultural land in Fukushima Prefecture from March 2011. Based on these data, Nuclear Emergency Response Headquarters showed planting areas of rice in all regions, except a 20-km exclusion zone and the deliberate evacuation zone (DEZ) in Fukushima Prefecture in 2011. However, the brown rice produced in some areas in northern part of Fukushima prefecture exceeded the provisional regulation value for agricultural crops at the times (>500 Bq kg^{-1}). Consequently, the planting of rice crops for the year 2012 had been restricted in that area. The present studies show investigation of radiocesium transfer in the agricultural plants.

13.2 Effect of Potassium Application on Root Uptake of Radiocesium in Rice

To decrease radiocesium uptake in brown rice from the contaminated fields, we examined the effect of using potassium fertilizer on the radiocesium uptake in brown rice.

Rice plants (*Oryza sativa*) were cultivated in the five experimental paddy fields in the northern area in Fukushima Prefecture, which was contaminated with radiocesium, in 2011. Soils and rice plants were collected from five points in each experimental field at harvest time. The mean concentration of radiocesium at soil depths of 0–5, 5–10, and 10–15 cm was 5,800, 3,200 and 1,800 Bq kg^{-1} dry weight (DW), which was not uniformly distributed, even during plowing before cultivation. The concentration of radiocesium in each field at the depth of 0–5 cm showed approximately threefold variation.

The concentration of radiocesium in brown rice from five rice paddy fields was 231 ± 135 (52–485) Bq kg^{-1} fresh weight (FW), and the values were different in each collecting point. The soil-to-plant transfer factor is a simple but important parameter that can be used to estimate the concentrations of radionuclides in plants. The transfer factor generally shows a very wide range of variation. The transfer factor of soil-to-brown rice collected from a pair of soil and brown rice samples at each point was in the range of 0.0075–0.11, which was more than one order of magnitude different. Tsukada et al. and Komamura and Tsumura reported that the geometric mean of the soil-to-plant transfer factor of polished rice in rice paddy fields, which were determined by the fallout depositions derived from the nuclear weapons tests, as 0.0016 and 0.0030, respectively [3, 4]. The observed values, which were determined in the same or nearby fields, were higher than previously reported values. The difference may be attributed to nonuniform distribution of radiocesium in the available fractions because of the early stage of the aging periods after deposition onto the soil.

Potassium is an important essential element in plant physiology, and it is supplemented by the application of fertilizers to agricultural soils. There was a high correlation ($r = 0.88$) between the soil-to-brown-rice transfer factor of radiocesium and the exchangeable K_2O in the soil (Fig. 13.1). Other researchers have reported that the transfer factor of ^{137}Cs decreased with increasing concentrations of potassium in soils [5–7]. Kato [8] also reported that the soil-to-plant transfer factor of radiocesium decreased with increasing concentrations of exchangeable K_2O in soils. Further, the soil-to-brown-rice transfer factor of radiocesium also decreased from 0.074 to 0.024 with the application of potassium fertilizer through top dressing. Hence, it is clear that the application of potassium fertilizer reduces the concentration of radiocesium in brown rice.

13.3 Phytoremediation of Radiocesium in Different Soils Using Cultivated Plants

Following the nuclear power plant disaster, more than 90 % of the radionuclides were distributed in the upper 6 cm of the soil column in wheat fields, and within 4 cm of the surface in rice paddies, orchards, and cedar forests [9]. It is well known that radiocesium is adsorbed into the soil and binds strongly to clay. As a result, it is difficult to reduce the contamination level in the soil. It was reported that phytoremediation using rice plants in a paddy field was also difficult [10]. We examined the

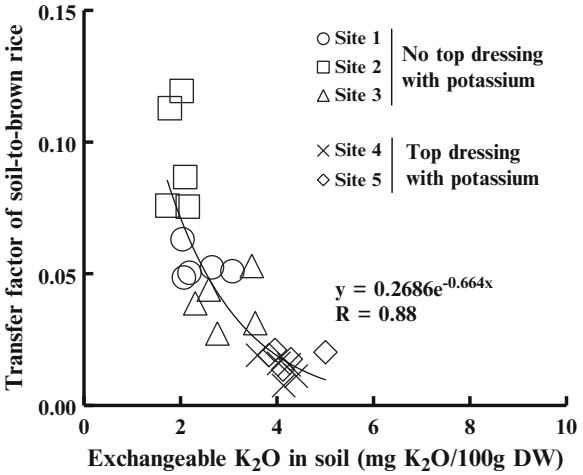

Fig. 13.1 Relationship between transfer factor of soil to brown rice and exchangeable K_2O in the soil

Table 13.1 Yield of four plants cultivated in light-colored andosol and gray lowland soil

Cultivated soil type	Plant	Yield					
		Leaf	Stem	Flower	Root	Whole body	Aboveground of plant
Light-colored andosol	Amaranth	0.15 ± 0.05	0.51 ± 0.02	0.58 ± 0.12	0.18 ± 0.03	1.43 ± 0.19	1.25 ± 0.19
	Buckwheat	0.33 ± 0.04	0.57 ± 0.10	0.79 ± 0.13	0.16 ± 0.06	1.86 ± 0.27	1.69 ± 0.22
	Sorghum	0.55 ± 0.07	1.11 ± 0.18	–	0.24 ± 0.02	1.91 ± 0.20	1.66 ± 0.18
	Sunflower	0.13 ± 0.04	0.28 ± 0.01	0.13 ± 0.01	0.03 ± 0.01	0.57 ± 0.05	0.54 ± 0.05
Gray lowland soil	Amaranth	0.28 ± 0.01	0.30 ± 0.01	0.58 ± 0.02	0.09 ± 0.01	1.24 ± 0.02	1.16 ± 0.02
	Buckwheat	0.16 ± 0.01	0.28 ± 0.01	0.49 ± 0.03	0.04 ± 0.00	0.98 ± 0.03	0.94 ± 0.03
	Sorghum	0.91 ± 0.03	1.58 ± 0.10	–	0.42 ± 0.06	2.91 ± 0.14	2.49 ± 0.13
	Sunflower	0.29 ± 0.05	0.50 ± 0.08	0.05 ± 0.00	0.04 ± 0.00	0.87 ± 0.13	0.84 ± 0.13

Sampling from September 6–13, 2011

possibility of decontamination by means of phytoremediation using four agricultural plants such as sunflower (*Helianthus annuus* L.), amaranth (*Amaranthus* L.), sorghum (*Sorghum bicolor*), and buckwheat (*Fagopyrum esculentum*) in upland fields.

The total yields of biomass cultivated in the light-colored Andosol and gray lowland soil is shown in Table 13.1. The biomass of the sorghum in the gray lowland soil (2.91 kg dry weight m^{-2}) was five times higher than that of buckwheat cultivated in the light-colored Andosol, and the gray lowland soil was within a factor of 2.

Table 13.2 Concentration of ^{137}Cs in plant components (Bq kg^{-1} dry weight)

Cultivated soil type	Plant	Concentration of plant component					
		Leaf	Stem	Flower	Root	Whole body	Aboveground of plant
Light-colored andosol	Amaranth	184 ± 57.7	49 ± 31.6	57 ± 11.0	113 ± 48.4	50 ± 4.9	79 ± 15.8
	Buckwheat	104 ± 26.4	9 ± 0.1	33 ± 10.7	150 ± 9.9	22 ± 1.9	37 ± 5.4
	Sorghum	72 ± 8.4	25 ± 12.5	–	156 ± 9.9	21 ± 4.1	42 ± 9.4
	Sunflower	152 ± 28.7	46 ± 7.4	23 ± 2.5	142 ± 119.1	68 ± 9.1	48 ± 6.4
Gray lowland soil	Amaranth	157 ± 10.9	11 ± 3.8	38 ± 7.5	29 ± 12.6	84 ± 14.2	51 ± 5.6
	Buckwheat	41 ± 3.5	8 ± 1.3	34 ± 3.6	38 ± 2.6	43 ± 5.0	21 ± 2.5
	Sorghum	41 ± 7.4	5 ± 1.4	–	35 ± 8.7	58 ± 7.4	18 ± 4.1
	Sunflower	231 ± 4.7	30 ± 8.7	11 ± 2.3	39 ± 13.9	65 ± 11.6	69 ± 11.6

Decay correction was done at harvest time, 2011; average ± SD ($n = 3$)

Sorghum had the highest biomass in both the light-colored Andosol and the gray lowland soil.

The concentration of ^{137}Cs in the soil among the fields was 1,300–2,000 Bq kg^{-1} dry weight. The concentration of ^{137}Cs in the plant components is indicated in Table 13.1. Among the components, the leaves exhibited the highest concentration of ^{137}Cs, except sorghum cultivated in the light-colored Andosol. The concentration of ^{137}Cs in the roots, including adhered soil particles, was relatively similar among the plants cultivated in each soil. However, the concentration of ^{137}Cs in the stem differed approximately fivefold among the plants. The ^{137}Cs concentration in the aboveground part of the plant was 36.7–78.9 Bq kg^{-1} dry weight in the light-colored Andosol and 18.0–69.1 Bq kg^{-1} dry weight in the gray lowland soil (Table 13.2).

The total content of ^{137}Cs in the biomass among the four plants was 19.8–132 Bq m^{-2} cultivated in the light-colored Andosol and 17.6–79.8 Bq m^{-2} cultivated in the gray lowland soil. The content in amaranth and sunflower was the highest in the light-colored Andosol and the gray lowland soil, respectively.

The removal percentage of ^{137}Cs, which is defined as the ratio of the total content of ^{137}Cs in the plant biomass (20–154 Bq m^{-2}) to that in the cultivated soil of 0–15 cm depth (154,000–247,000 Bq m^{-2}), was 0.015–0.109 % for the light-colored Andosol and 0.008–0.039 % for the gray lowland soil. The removal percentage of ^{137}Cs for aboveground parts, excluding the root part, was 0.013–0.093 % for the light-colored Andosol and 0.007–0.038 % for the gray lowland soil. The highest values of the aboveground parts were obtained in amaranth (0.093 %) and sunflower (0.038 %) in the light-colored Andosol and the gray lowland soil, respectively (Table 13.3). The ratio of the removal of radiocesium from the surface soil to that of the cultivated biomass, that is, sunflower, amaranth, sorghum, and buckwheat, was negligible. This result indicates that it is difficult to remove radiocesium from contaminated soil by means of phytoremediation.

Table 13.3 Removal percentage of ^{137}Cs by cultivated plant

Cultivated soil type	Plant	Soil (Bq m^{-2})	^{137}Cs content		Removal percentages (%)	
			Whole body	Aboveground of plant	Whole body	Aboveground of plant
Light-colored andosol	Amaranth	154,000 ± 61,000	91 ± 12.1	61 ± 15.7	0.109 ± 0.039	0.093 ± 0.032
	Buckwheat	158,000 ± 21,000	154 ± 22.0	132 ± 20.8	0.015 ± 0.001	0.013 ± 0.001
	Sorghum	208,000 ± 11,000	110 ± 10.4	70 ±21.0	0.056 ± 0.030	0.033 ± 0.023
	Sunflower	175,000 ± 64,000	24 ± 4.2	20 ±1.2	0.059 ± 0.029	0.036 ± 0.007
Gray lowland soil	Amaranth	209,000 ± 42,000	84 ± 25.8	80 ±12.2	0.024 ± 0.004	0.023 ± 0.003
	Buckwheat	247,000 ± 18,000	49 ± 10.6	48 ±5.8	0.008 ± 0.002	0.007 ± 0.002
	Sorghum	201,000 ± 12,000	60 ± 13.6	45 ±12.2	0.030 ± 0.007	0.022 ± 0.005
	Sunflower	216,000 ± 20,000	20 ± 4.3	18 ±4.4	0.039 ± 0.009	0.038 ± 0.009

Decay correction was done at harvest time, 2011; average ± SD (n = 3)

References

1. Tsukada H, Takeda A, Nakao A (2012) Vertical distribution and physicochemical form of fallout ^{137}Cs in an allophanic andisol acidified by long-term fertilizer application. Pedologist 55:435–441
2. Tanaka K, Takahashi Y, Sakagichi A, Umeo H, Hayakawa S, Tanida H, Saito T, Kanai Y (2012) Vertical profiles of iodine-131 and cesium-137 in soils in Fukushima Prefecture related to the Fukushima Daiichi nuclear power station accident. Geochem J 46:73–76
3. Tsukada H, Hasegawa H, Hisamatsu S, Yamasaki S (2002) Transfer of ^{137}Cs and stable Cs from paddy soil to polished rice in Aomori, Japan. J Environ Radioact 59:351–363
4. Komamura M, Tsumura A (1994) The transfer factors of long-lived radionuclides from soil to polished rice measured by ICP-MS. Radioisotopes 43:1–8 (in Japanese, with English abstract)
5. Kuhn W, Handl J, Schuller P (1984) The influence of soil parameters on ^{137}Cs^{+}-uptake by plants from long-term fallout of forest clearings and grassland. Health Phys 46(5):1083–1093
6. van Bergeijk KE, Noordijk H, Lembrechts J, Frissel MJ (1992) Influence of pH, soil organic matter content on soil-to-plant transfer of radiocesium and strontium as analyzed by a non-parametric method. J Environ Radioact 15:265–276
7. Wang CJ, Lai SY, Wang JJ, Lin YM (1997) Transfer of radionuclides from soil to grass in northern Taiwan. Appl Radiat Isot 48:301–303
8. Kato N (2012) Countermeasures to reduce radiocaesium contamination in paddy rice, soybean and cabbage. In: International science symposium on combating radionuclide contamination in agro-soil environment, Fukushima, Japan, 8–10 March 2012, pp 317–318
9. Ohno T, Muramatsu Y, Miura Y, Oda K, Inagawa N, Ogawa H, Yamazaki A, Toyama C, Sato M (2012) Depth profiles of radioactive cesium and iodine released from the Fukushima Daiichi nuclear power plant in different agricultural fields and forests. Geochem J 46:287–295
10. Tsukada H, Takeda A, Hasegawa H (2008) Uptake and distributions of ^{90}Sr and ^{137}Cs in rice plants. In: 16th Pacific basin nuclear conference, Aomori, Japan, October 13–18 (Paper ID P16P1121)

Part VI
Source Estimation

Chapter 14
Investigation of Uncertainty in the Release Rates of ^{131}I and ^{137}Cs from Fukushima Dai-ichi NPS Estimated from Environmental Data

Shigekazu Hirao, Hironori Hibino, Takuya Nagae, Jun Moriizumi, and Hiromi Yamazawa

Abstract It is an urgent task to estimate the release rate of airborne radionuclides and its uncertainty for the assessment of internal and external dose to the public from the Fukushima Dai-ichi Nuclear Power Station accident. We estimated the release rates of ^{131}I and ^{137}Cs by using a method commonly used in the previous studies for the source term estimation. This study investigated the sensitivity of the estimated release rate to the deposition parameters. It was found that the dry deposition velocity had only minor significance on the estimated release rate, predominately because of the inherently small contribution to total deposition when wet deposition occurred. The scavenging coefficient, on the other hand, showed a substantial effect on the estimated release rate. The release rate estimated with the small scavenging coefficient could be larger than that with the large scavenging coefficient when the calculated deposition was small because of weak rainfall intensity and the short travel time of the plume in the rainfall area. In contrast, the large scavenging coefficient also resulted in a large estimated release rate when the calculated deposition was small because heavy rainfall caused substantial depletion of the plume before the plume reached sampling sites. Adoption of a scavenging coefficient three times larger could result in increases of 10 and 21 fold in the estimated release rates of ^{131}I and ^{137}Cs, respectively, at maximum.

Keywords Release rate estimation • ^{131}I • ^{137}Cs • Sensitivity analysis • Atmospheric dispersion model • Environmental monitoring data

S. Hirao (✉) • H. Hibino • T. Nagae • J. Moriizumi • H. Yamazawa
Department of Energy Engineering and Science, Nagoya University,
Furo-cho, Chikusa-ku, Nagoya 4648603, Japan
e-mail: s-hirao@ees.nagoya-u.ac.jp

S. Takahashi (ed.), *Radiation Monitoring and Dose Estimation of the Fukushima Nuclear Accident*, DOI 10.1007/978-4-431-54583-5_14,

14.1 Introduction

During the accident at the Fukushima Daiichi Nuclear Power Station (FDNPS), the released airborne radionuclides spread out over the Kanto and Tohoku regions and consequently caused land surface contamination. Assessment of radiological dose to the public requires information on the spatial and temporal evolution of the atmospheric transport of the radionuclides, land surface contamination, and radioactive composition. The most reliable information is environmental monitoring data. Although in the early phase of the accident atmospheric concentrations were measured, the spatial coverage of the measurements was too coarse to delineate the evolution of the radioactive plume and its radioactive composition.

Airborne measurements were made by the Ministry of Education, Culture, Sports, Science and Technology (MEXT) in collaboration with the U.S. Department of Energy [1]. This work provided the distribution of land surface contamination for the medium- and long-lived radionuclides of ^{134}Cs and ^{137}Cs. The atmospheric dispersion and deposition of short-lived radionuclides, such as ^{131}I, which are important to evaluate radiological doses, still have a large uncertainty. In this situation, atmospheric dispersion simulations can play an important role of evaluating the atmospheric transport of radioactive plumes when source term information, such as release rates of radionuclides, is available.

To estimate the release rates, environmental monitoring data have been used with atmospheric dispersion models in several studies [2–5]. All studies with inverse methods indicate similar temporal variations in the atmospheric release rate of ^{131}I and ^{137}Cs despite of the use of different sets of monitoring data and atmospheric dispersion models. According to these studies, the release began in the morning of 12 March 2011, the largest release occurred on 15 March, and during other periods the releases were one to two orders of magnitude smaller than that on 15 March. Although this similarity implies the reliability of the estimated release rates, the uncertainties in the estimated release rate have not been discussed sufficiently. In our previous study, the uncertainty was preliminary estimated to be approximately a factor of 3 because of errors in the modeling of deposition processes [5]. In the absence of extensive environmental monitoring data, evaluation of the uncertainty of the source term is a difficult task. In these cases, the uncertainty of the source term can typically be evaluated by a sensitivity analysis of parameters that might affect the source term [6]. The purpose of this study is to estimate the release rates of ^{131}I and ^{137}Cs and their uncertainties. We investigated the sensitivity of the estimated release rates to the deposition parameters, that is, the dry deposition velocity and the washout coefficient. The analysis was conducted first with a simplified meteorological condition, and second with an under-realistic meteorological condition during the period of March 2011 that was calculated by a meteorological model.

14.2 Methods

14.2.1 Release Rate Estimation

Estimation of the release rate is based on the principle that the atmospheric dispersion model can calculate a spatial distribution of relative values of deposition rates on the ground although their absolute values are unknown. According to this principle, the ratio of deposition rate to the release rate can be assumed to be the same for both measurements and calculations as follows:

$$\left(\frac{Q_{\mathrm{r}}}{S_{\mathrm{r}}}\right)_{t,i} = \left(\frac{Q_{\mathrm{m}}}{S_{\mathrm{m}}}\right)_{t,i}, \tag{14.1}$$

where S_{m} is the release rate used for model calculation (Bq h^{-1}), Q_{r} is the measured deposition rate (Bq m^{-2} day^{-1}), and Q_{m} is the calculated deposition rate (Bq m^{-2} day^{-1}). The subscripts t and i denote the sampling time and sampling point, respectively. The release rate was estimated with Eq. (14.1) by solving it for S_{r} (Bq h^{-1}). To estimate a release rate at the time when discharged into the atmosphere, a release time was determined by calculating a fractional contribution that represents how much of the release during a unit-time period contributes to each sampling time and sampling point. The contributions were determined by using a series of calculations with an atmospheric dispersion model for every 12-h continuous release. The calculation for each release was carried out until the released radionuclides went out of the calculation domain.

Equation (14.1) does not strictly hold, primarily because of errors in the atmospheric dispersion calculation. For a given time, there might be more than two different release rate values estimated from independent monitoring data. In this case, a geometric mean was applied to estimate a single value for the time.

14.2.2 Atmospheric Dispersion Model

A Lagrangian particle random-walk model (LPRM) [7] coupled with a nonhydrostatic atmospheric dynamic model, MM5 [8], was used to calculate the dispersion of the radioactive plume released from FDNPP. MM5 calculates the three-dimensional wind field and the vertical diffusion coefficient. Radioactive decay, dry deposition, and wet deposition were calculated using LPRM. Iodine-131 and cesium-137 were modeled as passive tracers with half-lives of 8.04 days and 30 years, respectively. Dry and wet depositions were parameterized in terms of a dry deposition velocity and a washout (or scavenging) coefficient, respectively.

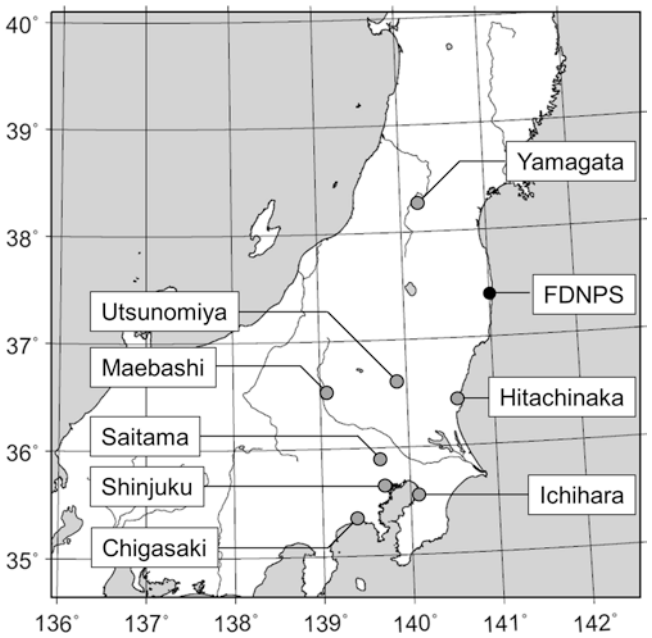

Fig. 14.1 Location of deposition measurement site on calculation domain

As a standard pair of these removal parameters, according to [9], the dry deposition velocity, V_d, was set to be 1.0 mm s^{-1} and the scavenging coefficient, Λ, was expressed as $\Lambda = \alpha(I/I_0)^{\beta}$, where I is the precipitation intensity, $I_0 = 1.0$ mm h^{-1}, $\alpha = 8.0 \times 10^{-5}$ s^{-1}, and $\beta = 0.8$. Dry deposition velocity and α can vary within a range of approximately 0.1–10 mm s^{-1} and 10^{-6}–10^{-3} s^{-1}, respectively, depending on the physicochemical characteristics of the nuclides, gas–particle partitioning, and particle-size distribution of aerosols (see [10, 11] for an overview). The removal parameters were changed by a factor of 3 in the sensitivity analysis.

14.2.3 Environmental Monitoring Data

To estimate the release rate, this study used the daily deposition measured at Chigasaki, Hitachinaka, Ichihara, Maebashi, Saitama, Sinjuku, Utsunomiya, and Yamagata with a 24-h sampling time from 18 March 2011 by MEXT [12]. The sampling sites are plotted in Fig. 14.1. The following criteria were set for data selection to eliminate the influence of resuspended radionuclides: the deposition rate of ^{131}I and ^{137}Cs is greater than 5.0×10^2 and 1.0×10^2 Bq m^{-2} day^{-1}, respectively. Altogether, 56 measured deposition rates of ^{131}I and ^{137}Cs were adopted in this study.

14.2.4 Calculation Condition

The calculation domain of the atmospheric dispersion was a 600-km square with a 6-km depth above the ground to cover most of Tohoku and Kanto Regions. The same physical processes of MM5 as the previous study [5] were used. For initial and boundary conditions and the four-dimensional data assimilation of the meteorological fields, the JRA-25 reanalysis data provided by Japan Meteorological Agency (JMA) and Central Research Institute of Electric Power Industry (CRIEPI) were used. Topography and land-use data were obtained from the United States Geological Survey global database. The radar-AMeDAS precipitation analysis data from JMA were used for the precipitation intensity in the wet deposition calculation. The MM5 calculation was conducted for the period from 09 Japanese Standard Time (JST), 8 March to 00 JST, 1 April. The dispersion of ^{131}I and ^{137}Cs from FDNPS started at 15 JST, 17 March and ended at 00 JST, 1 April. The release height was set to be 15 m above the ground. A constant release rate of 1 TBq h^{-1} was assumed.

14.3 Results and Discussion

14.3.1 Simplified Meteorological Condition

Before carrying out simulations with the calculated meteorological variables from MM5, this study conducted a series of preliminary simulations with a set of simplified meteorological conditions, that is, a uniform and constant wind field of 1 m s^{-1}, horizontally uniform but vertically varying vertical eddy diffusivities based on the calculated values of MM5, and prescribed intensities of uniform precipitation. The LPRM was the same as the main simulations. The purpose of these simulations is to discuss dependency of deposition and air concentration on deposition parameters.

The results are shown in Figs. 14.2 and 14.3. The dependency of dry deposition on the deposition velocity is quite simple. The dry deposition rate from the plume monotonously decreases with travel time, which is the elapsed time from release, mainly from horizontal and vertical diffusion causing air concentration decreases (Fig. 14.2a). The dry deposition rate for the 0.3 mm h^{-1} case is about 11.4 % of that for the 3 mm h^{-1} case at the travel time of 6 h. This ratio is almost same with the ratio of deposition velocities, but slightly modified by the change in the air concentration. The concentration for the 3 mm h^{-1} case is about 88 % of that of the 0.3 mm h^{-1} case (Fig. 14.2b). These results imply that the dry deposition process does not significantly reduce the amount of radioactivity in air within a period of several hours.

The dependency of wet deposition on the scavenging coefficient is somewhat complicated (Fig. 14.3a). A larger scavenging coefficient does not always cause greater deposition. Among the four cases, the largest scavenging coefficient, which corresponds to the rain intensity of 6.6 mm h^{-1}, resulted in the largest wet deposition

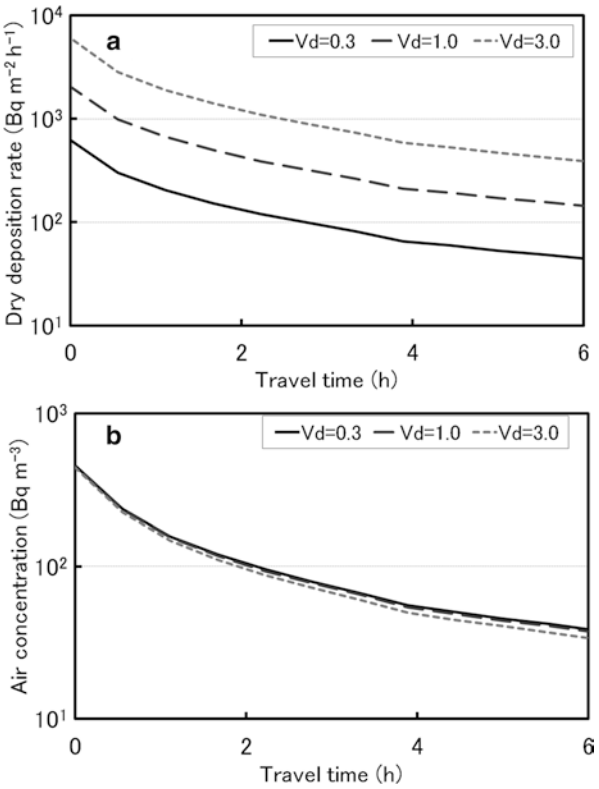

Fig. 14.2 Variation of the calculated values of (**a**) dry deposition rate and (**b**) air concentration with travel time. Dry deposition velocities, V_d, are 0.3, 1.0, and 3.0 mm s^{-1}

only in the first 0.6 h from the release. The wet deposition of this case becomes the smallest after a travel time of 1.7 h. On the other hand, the wet deposition in the case with the smallest scavenging coefficient (rain intensity of 0.37 mm h^{-1}) is the largest among the four cases after the travel time of 3.9 h. This complicated result is caused by the substantial depletion of the plume by scavenging (Fig. 14.3b). In the cases with large scavenging coefficient, the air concentration rapidly decreases with travel time.

14.3.2 Actual Meteorological Condition

14.3.2.1 Release Rate Estimation

The release rates of ^{131}I and ^{137}Cs were estimated for every 12-h time segment during 19 to 23 March and 25 and 29 to 30 March with their geometric standard deviations as shown in Fig. 14.4. Release rate could not be estimated for the period during which there was no measured deposition. The geometric standard deviation could not be calculated for the time segments in which only one monitoring datum was

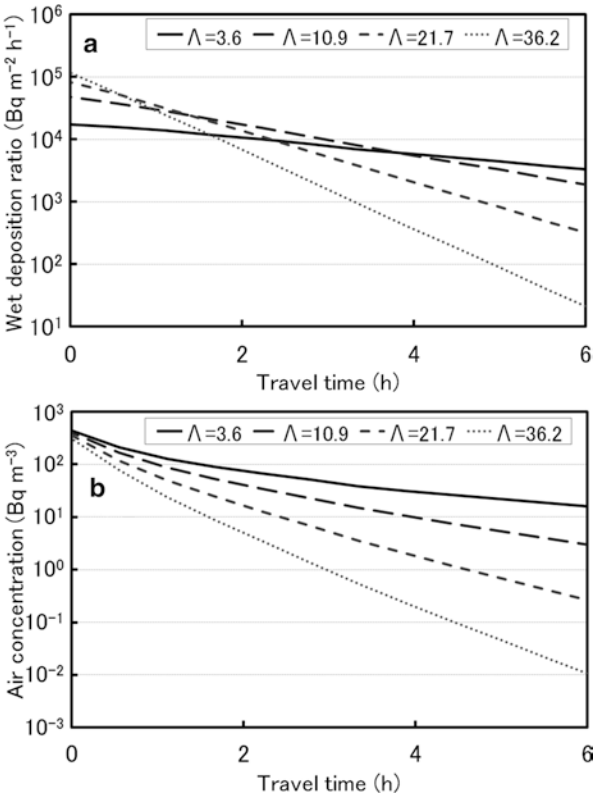

Fig. 14.3 Variation of the calculated values of (**a**) wet deposition rate and (**b**) air concentration with travel time. Scavenging coefficients, Λ, are 3.6, 10.9, 21.7, and 36.2×10^{-5} s^{-1}, which correspond to rain intensities of 0.37, 1.47, 3.48, and 6.60 mm h^{-1}, when the scavenging coefficient is expressed as $\Lambda = 8.0 \times 10^{-5} (I/I_0)^{0.8}$ in s^{-1}

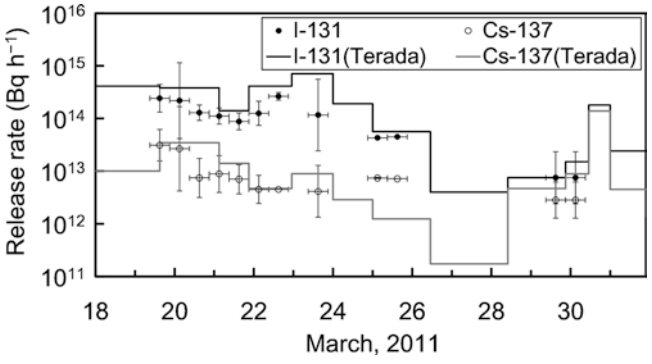

Fig. 14.4 Temporal change in the estimated release rate of ^{131}I and ^{137}Cs. *Lateral bars* on plots show the release duration 6 s of 12 h. *Vertical bars* show geometric standard deviations of the estimated release rate. *Closed* and *open circles* indicate the estimated values. *Black* and *gray lines* indicate the values estimated by Terada et al. [4]

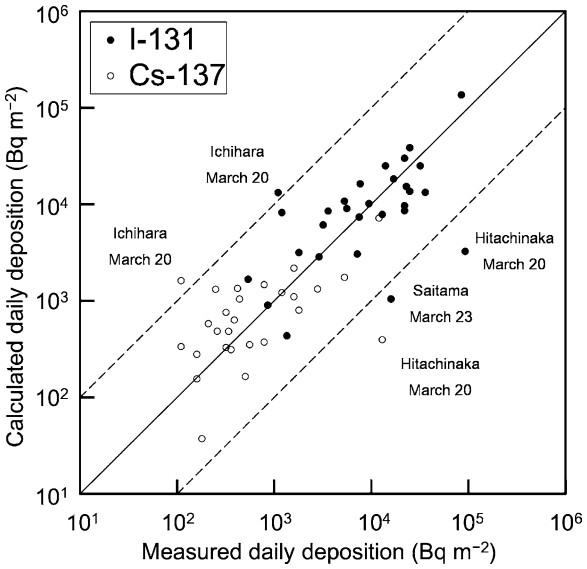

Fig. 14.5 Comparison of measured and calculated daily deposition using estimated release rate of ^{131}I and ^{137}Cs

available. The estimated release rate of ^{131}I was 2.4×10^{14} Bq h^{-1} in the afternoon of 19 March and showed a slight decrease during the following few days. A large increase in release rate was evaluated to have occurred from the afternoon of 22 March to the morning of 23 March to reach the release rate of 2.6×10^{14} Bq h^{-1}. After this day, the release of ^{131}I gradually decreased to the release rate of 7.5×10^{13} Bq h^{-1} on 30 March. For ^{137}Cs, the release rate was 2.7–3.1 $\times 10^{13}$ Bq h^{-1} from the afternoon of 19 March to the morning of 20 March and maintained in the range of 2.8–8.8 $\times 10^{12}$ Bq h^{-1} during the following days. The estimated release rates imply that the release of ^{131}I decreased during March whereas that of ^{137}Cs remained unchanged significantly.

Figure 14.4 also represents the temporal change of the release rate of ^{131}I and ^{137}Cs estimated by Terada et al. [4]. Although the release rates estimated in this study are smaller than the Terada values, the temporal changes are consistent with those of Terada. The difference of our estimated values compared to Terada's values are that the decrease of the release rate in the period from 20 to 21 March starts earlier and the temporal change in the release rate of ^{137}Cs is more moderate.

Scatter diagrams of the daily deposition of ^{131}I and ^{137}Cs of the calculated values using the estimated release rate and of measured values from 18 March to 31 March are shown in Fig. 14.5. For both nuclides, a good correlation was found between the calculated and measured values. The percentages of the calculated values that are within factors of 2 and 5 of the measured values are 55 % and 86 % for ^{131}I and 48 % and 89 % for ^{137}Cs, respectively. The calculated daily depositions showed large underestimation at Hitachinaka on 20 March and Saitama on 23 March and large overestimation at Ichihara on 20 March by a factor of more than 10 of the measured values. The pairs of measured and calculated daily deposition values at these sites resulted in large geometric standard deviations of the release rate in the morning of

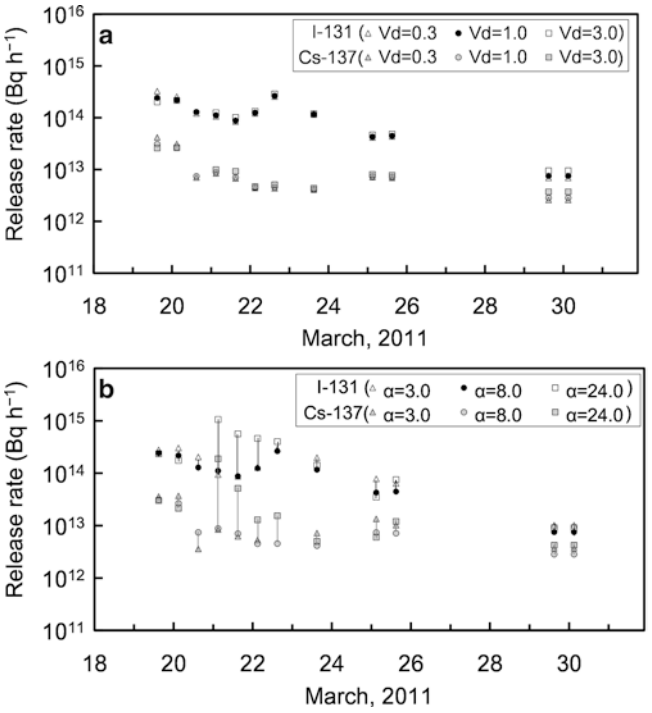

Fig. 14.6 Sensitivity of estimated release rate of ^{131}I and ^{137}Cs to (**a**) dry deposition velocity and (**b**) scavenging coefficient. Dry deposition velocities, V_d, are 0.3, 1.0, and 3.0 mm s^{-1} and α are 3.0, 8.0, and 24.0 × 10^{-5} s^{-1}, when the scavenging coefficient is expressed as $\Lambda = \alpha(I/I_0)^{0.8}$

20 March and 23 March (Fig. 14.4). Errors of the atmospheric dispersion model could lead to a large uncertainty in the calculated deposition. However, the error does not propagate seriously to the estimated release rate because the release rate in one time segment was estimated by several pairs of measured and calculated daily deposition values.

14.3.2.2 Sensitivity Analysis on Deposition Parameters

The changes in the estimated release rates with the change in V_d from the standard value 1.0–0.3 and to 3.0 mm s^{-1}, and in α from the standard value 8.0 × 10^{-5} to 3.0 × 10^{-5} and to 2.4 × 10^{-4} s^{-1}, are shown in Fig. 14.6a and 14.6b, respectively. To investigate the sensitivity to the deposition parameters, we calculated the ratio of the estimated release rate to that for the standard deposition parameters.

The ratios for $V_d = 0.3$ mm s^{-1} varied in the range of 0.9–1.3 for both nuclides. For $V_d = 3.0$ mm s^{-1}, the ratios varied in the range of 0.8–1.3 for both nuclides, indicating that the estimated release rates for ^{131}I and ^{137}Cs vary only by a factor of 1.1–1.3 when the dry deposition velocity is changed by a factor of approximately 3.

Slightly larger release rates were estimated for 19 March and 29 March by using the smaller dry deposition velocity because the plume on this day did not experience rain and dry deposition was dominant. This result is consistent with the discussion for the dry deposition in the previous section. The estimated release rates in the period from 20 to 25 March were not substantially affected by dry deposition velocity because wet deposition processes dominated the deposition.

During the period from 19 to 20 March, the plume was transported to Kanto region after being once transported over the Pacific Ocean. In general, dry deposition velocity over the sea surface is considered to be smaller than that on land surfaces. If horizontally homogeneous dry deposition is assumed in the estimation of release rate, which might be an overestimation of dry deposition over sea surface, and hence underestimation of air concentration and dry deposition at the place of observation, the release rates could be overestimated. However, this effect is not serious, as shown in Fig. 14.2.

In the case of the scavenging coefficient, the ratios for $\alpha = 3.0 \times 10^{-5}$ s^{-1} varied in the range of 0.9–1.8 for ^{131}I and 0.5–1.8 for ^{137}Cs. For $\alpha = 2.4 \times 10^{-4}$ s^{-1}, the ratios varied in the range of 0.8–9.6 for ^{131}I and 0.8–21.3 for ^{137}Cs. A scavenging coefficient three times larger resulted in increases of 10 and 21 fold in the estimated release rate for ^{131}I and ^{137}Cs, respectively, at maximum. Sensitivity to the scavenging coefficient was considerably larger than that to the dry deposition velocity.

For the period from 19 March to the morning of 20 March and the morning of 25 March, the release rates estimated with the small scavenging coefficient were larger than the release rate with the large scavenging coefficient, which is likely because the calculated deposition was small as a result of the weak rainfall intensity and the short travel time in the rainfall area. This tendency is also consistent with the results of the wet deposition for a short travel time discussed in the previous section. In contrast, the release rates in the period from 21 to 22 March showed a high sensitivity to scavenging coefficient because there was heavy rainfall in the Kanto Region where the plume was transported. The large estimated release rate can be attributed to the depletion of plume when it traveled over Kanto Region, causing lessr deposition on the area where the plume passed later. This tendency is depicted in Fig. 14.2, in which the wet deposition rates decrease more rapidly with time if the scavenging coefficient is larger. Except for these periods, the sensitivity analysis showed no systematic tendency.

14.4 Conclusion

The present study estimated the release rate of ^{131}I and ^{137}Cs during March 2011 and showed the results of the sensitivity analysis of the release rate to the deposition parameters. To estimate the release rate, the method applied is based on a simple inverse method by combining the measured daily deposition of ^{131}I and ^{137}Cs with regional range atmospheric dispersion calculations.

The present study showed that the release rates were reasonably estimated by using the measured daily depositions. It was found that the dry deposition velocity

had only minor significance on the estimated release rate, predominately as a result of the inherently small contribution to total deposition when wet deposition occurred. The scavenging coefficient, on the other hand, showed a substantial effect on the release rate estimation. A three times larger scavenging coefficient resulted in increases of 10 and 21 fold in the estimated release rate for ^{131}I and ^{137}Cs, respectively, at maximum. The uncertainties of the release rate estimated by the inverse method might be large when the plume is transported through the rainfall area. It can be suggested that a more realistic parameterization of wet deposition processes is needed to refine the release rate estimation from environmental data.

Acknowledgments This work was partly supported by JSPS KAKENHI grant number 24110002. We thank JMA and CRIEPI for the JRA-25/JCDAS dataset.

References

1. MEXT (2011) Results of the 2nd airborne monitoring by the Ministry of Education, Culture, Sports, Science and Technology and the U.S. Department of Energy. http://radioactivity.nsr.go.jp/en/contents/4000/3180/view.html. Accessed 26 Aug 2013
2. Chino M, Nakayama H, Nagai H et al (2011) Preliminary estimation of release amounts of ^{131}I and ^{137}Cs accidentally discharged from the Fukushima Daiichi nuclear power plant into the atmosphere. J Nucl Sci Technol 48:1129–1134
3. Stohl A, Seibert P, Wotawa G et al (2012) Xenon-133 and cesium-137 releases into the atmosphere from the Fukushima Dai-ichi nuclear power plant: determination of the source term, atmospheric dispersion, and deposition. Atmos Chem Phys 12:2313–2343
4. Terada H, Katata G, Chino M et al (2012) Atmospheric discharge and dispersion of radionuclides during the Fukushima Dai-ichi nuclear power plant accident. Part II: Verification of the source term and analysis of regional-scale atmospheric dispersion. J Environ Radioact 112:141–154
5. Hirao S, Yamazawa H, Nagae T (2013) Estimation of release rate of iodine-131 and cesium-137 from the Fukushima Daiichi nuclear power plant. J Nucl Sci Technol 50:139–147
6. Bocquet M (2011) Parameter field estimation for atmospheric dispersion: application to the Chernobyl accident using 4D-Var. Q J R Meteorol Soc 138:664–681
7. Hirao S, Yamazawa H (2010) Release rate estimation of radioactive noble gases in the criticality accident at Tokai-Mura from off-site monitoring data. J Nucl Sci Technol 47:20–30
8. Grell GA, Dudhida J, Stauffer DR (1994) A description of the fifth-generation Penn State/NCAR mesoscale model (MM5). NCAR Tech Note NCAR/TN-389+STR, National Center for Atmospheric Research (NCAR)
9. Baklanov A, Sørensen JH (2001) Parameterisation of radionuclide deposition in atmospheric long-range transport modelling. Phys Chem Earth (B) 26:787–799
10. George AS (1980) Particle and gas dry deposition: a review. Atmos Environ 14:983–1011
11. Sportisse B (2007) A review of parameterizations for modelling dry deposition and scavenging of radionuclides. Atmos Environ 41:2683–2698
12. MEXT (2011) Reading of environmental radioactivity level by prefecture. http://radioactivity.nsr.go.jp/en/list/194/list-201103.html. Accessed 26 Aug 2013

Chapter 15
Source Term Estimation of ^{131}I and ^{137}Cs Discharged from the Fukushima Daiichi Nuclear Power Plant into the Atmosphere

Haruyasu Nagai, Genki Katata, Hiroaki Terada, and Masamichi Chino

Abstract It is urgent to assess the radiological dose to the public resulting from the month-long discharge of radioactive materials into the atmosphere from the Fukushima Daiichi Nuclear Power Plant accident in Japan in March 2011. To do this task, computer simulations on the dispersion of radioactive materials in the environment are useful. However, the source term essential to computer simulations was not available. Thus, the Japan Atomic Energy Agency has been trying to estimate the source term of iodine and cesium discharged to the atmosphere. As the first step, the source term was preliminary estimated by coupling environmental monitoring data with atmospheric dispersion simulations. The release rates and total amounts of ^{131}I and ^{137}Cs discharged into the atmosphere were estimated for the period from 12 March to 5 April, 2011. Then, detailed analysis on the local atmospheric dispersion around the Fukushima Daiichi Nuclear Power Plant was carried out, revealing the formation process of high dose rate zones in a northwest direction from the plant. With this and further analyses for the early phase of the accident, the release rates and total amounts of ^{131}I and ^{137}Cs discharged into the atmosphere were reestimated for the period from 12 to 15 March 2011. Finally, the validity of the revised source term was examined by comparing daily and monthly surface deposition (fallout) over land in eastern Japan between measurements and outputs from the regional-scale atmospheric dispersion simulation.

Keywords ^{131}I • ^{137}Cs • Atmospheric dispersion simulation • Fukushima Daiichi Nuclear Power Plant accident • Monitoring data • Release rate • Source term estimation • SPEEDI • WSPEEDI

H. Nagai (✉) • G. Katata • H. Terada • M. Chino
Japan Atomic Energy Agency, 2-4 Shirane, Shirakata, Tokai-mura,
Naka-gun, Ibaraki 319-1195, Japan
e-mail: nagai.haruyasu@jaea.go.jp

S. Takahashi (ed.), *Radiation Monitoring and Dose Estimation of the Fukushima Nuclear Accident*, DOI 10.1007/978-4-431-54583-5_15,

15.1 Introduction

The Fukushima Daiichi Nuclear Power Plant (FNPP1) accident in Japan triggered by the magnitude 9.0 earthquake and resulting tsunami on 11 March 2011 caused a month-long discharge of radioactive materials into the atmosphere. It is urgent to assess the radiological dose to the public resulting from this release. To do this task, the spatial and temporal distribution of radioactive materials in the environment needs to be determined. The Japan Atomic Energy Agency (JAEA) has been conducting this task by using both environmental monitoring data and computer simulation on the dispersion of radioactive materials in the environment. However, the source term, which is essential to computer simulations, for example, nuclides, release rates, and duration, was not available, although it was expected to be provided from a stack monitor or a reactor behavior analysis. Thus, JAEA has been trying to estimate the source term of iodine and cesium discharged from the FNPP1 into the atmosphere.

As the first step, the source term of radioactive materials discharged into the atmosphere was preliminary estimated by coupling environmental monitoring data with atmospheric dispersion simulations under the assumption of unit release rate (1 Bq h^{-1}) in cooperation with the Nuclear Safety Commission of Japan (NSC) [1]. The atmospheric dispersion models used for this task were the System for Prediction of Environmental Emergency Dose Information (SPEEDI) network system operated by the Ministry of Education, Culture, Sport, Science and Technology (MEXT) and the Worldwide version of SPEEDI (WSPEEDI) developed by JAEA. The calculation domain of SPEEDI was a 100-km-square area with 1-km resolution, including the dust sampling points by MEXT in Fukushima Prefecture. For additional dust sampling data obtained beyond SPEEDI's calculation domain (Tokai-mura and Chiba City), calculations by WSPEEDI (390 × 570 km area with 3-km resolution) were used. The release rates and total amounts of ^{131}I and ^{137}Cs discharged into the atmosphere were estimated for the period from 12 March to 5 April 2011.

By using the preliminary estimated source term, detailed analysis on the local atmospheric dispersion around the FNPP1 has been carried out using WSPEEDI. The formation process of the high dose rate zone in a northwest direction from the plant was investigated by reconstructing the atmospheric dispersion of radionuclides during the period from 15 to 16 March 2011 [2]. In the reconstruction of the event, revisions of dispersion calculations were repeated by changing conditions of meteorological data assimilation and modifying the source term, respectively, until the simulation results of meteorological field and air dose rate became consistent with most of the measurements. The simulation results revealed that two significant releases, from 07:00 to 10:00 JST and from 13:00 to 17:00 JST on 15 March, were necessary to reproduce the spatial distribution and temporal changes of measured air dose rates. [Note that Japanese Standard Time (JST = UTC + 9 h) is used in this chapter.]

With the foregoing and further analyses for the early phase of the accident from 12 to 14 March, 2011 [3], the release rates and total amounts of ^{131}I and ^{137}Cs discharged into the atmosphere were reestimated for the period from 12 to 15 March 2011. The validity of the revised source term was also examined by comparing daily and monthly surface deposition (fallout) over land in eastern Japan between measurements and outputs from the regional-scale atmospheric dispersion simulation by WSPEEDI [4].

In this chapter, our studies on the source term estimation of radioactive materials discharged to the atmosphere during the Fukushima Daiichi nuclear power plant accident are summarized.

15.2 Method

15.2.1 Reverse Estimation Method

The method applied in this study is a reverse estimation of source term by coupling environmental monitoring data with atmospheric dispersion simulations under the assumption of unit release rate (1 Bq h^{-1}). Release rates of radionuclides (Bq h^{-1}) were obtained mainly by comparing measured air concentrations of radionuclides with the dilution factors, which are equal to the air concentrations at sampling points calculated under the assumption of unit release rate. Even when air concentration data are not available, the release rates can also be estimated by comparing measured air dose rates from radionuclides in the plume or on the ground surface with calculated rates derived from simulations with unit release rate, assuming the composition of radionuclides. According to the condition of available monitoring data, we used the following three methods.

Method 1: Release rates are obtained as the ratio of measured to calculated air concentrations of nuclide i at the sampling points, as follows:

$$Q_i = \frac{M_i}{C_i} \tag{15.1}$$

where Q_i is the release rate (Bq h^{-1}) of nuclide i when discharged into the atmosphere, M_i the measured air concentration (Bq m^{-3}) of nuclide i, and C_i the dilution factor (h m^{-3}) of nuclide i, which is equal to the air concentration calculated under the assumption of a unit release rate. This method of using the data of air concentrations is more reliable than the following methods described next because it does not require an assumption for the composition of radionuclides.

Method 2: When air concentration data were not available, release rates were estimated by comparing observed spatial patterns of air dose rates from radionuclides

on the ground surface (i.e., ground-shines) with calculated rates. First, the spatial pattern of the observed air dose rate from ground-shines was reproduced by WSPEEDI assuming a unit release rate. Then, the conversion factor, which is equal to the release rate (Bq h^{-1}), was multiplied to the calculated contour values so that the absolute values of the calculation become similar to the measurements.

Method 3: When neither the dust sampling nor offsite air dose rate data were obtained around FNPP1, release rates were estimated by combining the data of air dose rates observed at the boundary of FNPP1, the leeward of the nuclear reactors, with isopleths of those derived from the Gaussian plume model [5] under the assumption of a unit release rate (1 Bq h^{-1}). The method required data on the wind speed, the atmospheric stability, the release height, the downwind distance from the release point, the effective gamma energy of the nuclides, and the composition of the major radionuclides.

15.2.2 Environmental Monitoring Data

For the preliminary source term estimation [1], environmental monitoring data on air concentrations of nuclides (hereafter, dust sampling data) were mainly used. Iodine of gaseous and particulate conditions was expected to be sampled according to the guideline for environmental radiation monitoring from NSC [6], which recommends using dust samplers with a charcoal cartridge. The data used in the estimation are from the websites of MEXT [7], the Japan Chemical Analysis Center (JCAC) [8], and JAEA [9]. Figure15.1 shows the locations of the dust sampling and the sampling period, which are thought to capture the plumes. Air dose monitoring data from MEXT indicate that the atmospheric release of radionuclides in the daytime of March 15 caused a large amount of ground deposition and resulting high dose rates in the sector to the northwest of the plant. However, because no dust sampling data were available in the daytime of March 15, the release rates of ^{131}I and ^{137}Cs in this period were estimated from the comparison of measured air dose rate pattern caused by ground-shine with the calculated rate, after the plume moved away from this region.

In the detailed analysis on local atmospheric dispersion around the FNPP1 during the period from 15 to 16 March 2011 [2], meteorological data of wind speed and direction observed at surface weather stations around FNPP1 were used for data assimilation of meteorological calculation. In addition, the data of wind speed and direction at the ground surface at FNPP1 and at the top of stack at 120-m height at Fukushima Daiichi Nuclear Power Plant (FNPP2) obtained from the Ministry of Economy, Trade and Industry (METI) [10] were used to correct wind fields around the plant. To estimate the release rates and to validate the simulation results, we used the data of airborne [11] and ground-level monitoring in Fukushima [12–14], Ibaraki [15–17], and Tochigi Prefectures [18].

In the reestimation of the source term for the early phase of the accident from 12 to 14 March 2011 [3], the dust sampling data from the early phase of the accident

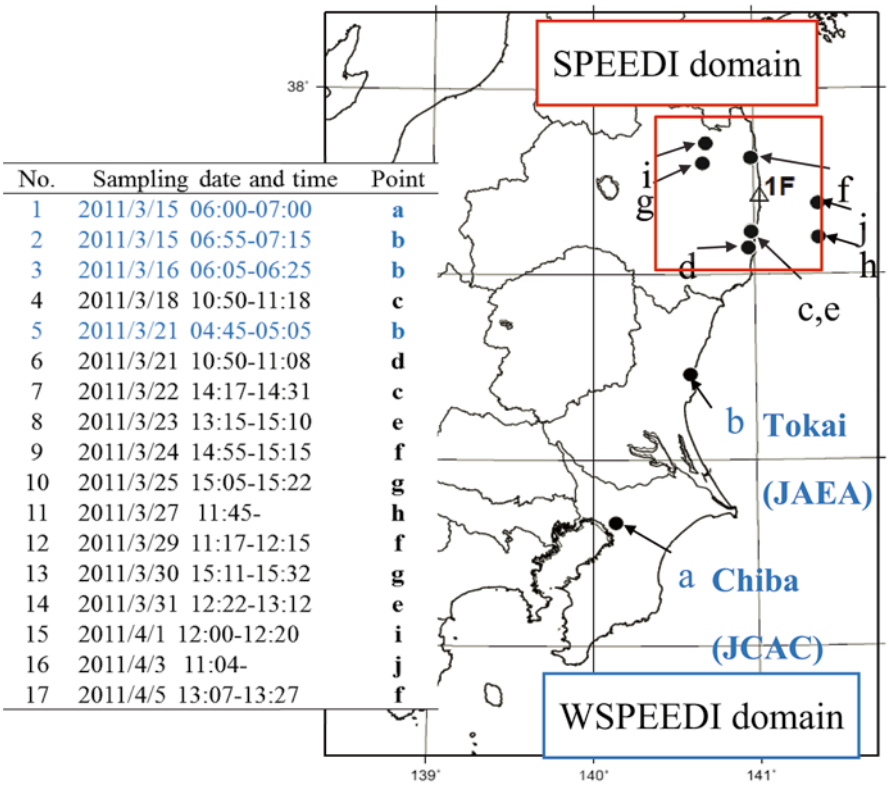

No.	Sampling date and time	Point
1	2011/3/15 06:00-07:00	a
2	2011/3/15 06:55-07:15	b
3	2011/3/16 06:05-06:25	b
4	2011/3/18 10:50-11:18	c
5	2011/3/21 04:45-05:05	b
6	2011/3/21 10:50-11:08	d
7	2011/3/22 14:17-14:31	c
8	2011/3/23 13:15-15:10	e
9	2011/3/24 14:55-15:15	f
10	2011/3/25 15:05-15:22	g
11	2011/3/27 11:45-	h
12	2011/3/29 11:17-12:15	f
13	2011/3/30 15:11-15:32	g
14	2011/3/31 12:22-13:12	e
15	2011/4/1 12:00-12:20	i
16	2011/4/3 11:04-	j
17	2011/4/5 13:07-13:27	f

Fig. 15.1 Locations of the dust sampling and the sampling period (JST) used for the preliminary source term estimation. The symbol (*1 F*) indicates the Fukushima Daiichi nuclear power plant and the square around 1 F is the SPEEDI calculation domain

were obtained from METI [19]. For estimation of the major release during the afternoon of 12 March, the measurements of air dose rate by monitoring cars from 06:00 to 15:00 JST on 13 March [19] were used because no dust sampling data were available. To compare the calculated air dose rate with observed rate, the equivalent gamma dose rate (Sv h^{-1}) shown in most of the data was assumed to be equal to the air absorbed gamma dose rate (Gy h^{-1}). To validate the estimated source term, the ground-level observations for the air dose rate in Fukushima [12–14] and Ibaraki Prefectures [15, 17] were used for comparison to calculations made by WSPEEDI.

In the validation of the source term by the regional-scale atmospheric dispersion simulation [4], observational data of daily and monthly surface deposition (fallout) and air concentrations of ^{131}I and ^{137}Cs sampled in Japan [20] were used for verification and refinement of the source term. The sampling period for daily surface deposition was 24 h starting from 09:00 JST on each day and the sampling was carried out using bulk samplers. Hereafter, the daily surface deposition on 18 March, for example, means the one from 09:00 JST on 18 March to 09:00 JST on 19 March. All prefectures in the simulation domain have one monitoring point for

daily and monthly surface deposition, except for Fukushima and Shizuoka Prefectures, where monthly surface deposition was observed at a different point from the daily point. Observations of daily surface deposition started on 18 March at 45 monitoring points except in Fukushima and Miyagi Prefectures. The measurement was not conducted in Miyagi Prefecture, and was started later on 27 March at the sampling sites in Fukushima Prefecture, because of earthquake damage. The monthly surface deposition measurements in Miyagi Prefecture are also not available for similar reasons. In addition, the map of the surface deposition of ^{137}Cs observed by airborne monitoring [21] was used for comparisons of the spatial pattern of cumulative surface ^{137}Cs deposition from calculations with that observed. To refine the initial source term, dust sampling data at FNPP2 [22], Tokai [23], and Setagaya [24] were used.

15.2.3 Atmospheric Dispersion Simulation

For the preliminary source term estimation [1], the SPEEDI [25] was used for calculating air concentrations and dose rates. The simulation results were furnished from NSC for the purpose of the source term estimation. Atmospheric dispersions of radionuclides were simulated by successive uses of the meteorological prediction model PHYSIC and the Lagrangian particle dispersion model PRWDA21 in SPEEDI; detailed descriptions of these models are given in the literature [26]. In addition, to utilize dust sampling data obtained beyond SPEEDI's calculation domain as points a (Chiba City) and b (Tokai-mura) in Fig. 15.1, WSPEEDI [27] was used. WSPEEDI was also used in the detailed analysis of the local atmospheric dispersion [2], reestimation of the source term for the early phase of the accident from 12 to 14 March, 2011 [3], and validation of the source term by the regional-scale atmospheric dispersion simulation [4].

WSPEEDI has been constructed by expanding the function of SPEEDI with a combination of nonhydrostatic meso-scale atmospheric model MM5 [28] and Lagrangian particle dispersion model GEARN [29]. MM5 is a community model having many users all over the world and is used for the official weather forecast by some countries. It has many useful functions such as nesting calculations, 4-D data assimilation, and many options of parameterizations for cloud microphysics, cumulus cloud, planetary boundary layer (PBL), radiation, and land surface scheme. The Lagrangian particle dispersion model GEARN calculates the atmospheric dispersion of radionuclides by tracing the trajectories of a large number (typically a million) of marker particles discharged from a release point. The horizontal model coordinates are the map coordinates, and the vertical coordinate the terrain-following coordinate (z*-coordinate). By using the meteorological field predicted by MM5, it calculates the movement of each particle affected by both advection caused by mean wind and subgrid-scale turbulent eddy diffusion. GEARN also has a function of nesting calculation for two domains corresponding to the MM5 nested domains. Two nested domains of GEARN are calculated concurrently by different

executables on parallel computers, and marker particles that flow out and in across the boundary of inner domain are exchanged between domains. A part of the radioactivity in the air is deposited on the ground surface by turbulence (dry deposition) and precipitation (wet deposition). These processes are modeled as follows. The decrease in radioactivity from dry deposition is calculated for each particle by using the dry deposition velocity (simply set as 0 m s^{-1} for noble gases, 3×10^{-3} m s^{-1} for iodine, and 10^{-3} m s^{-1} for the other nuclides without consideration of chemical form and particle size) based on the typical value for short vegetation [30]. The decrease in radioactivity of each particle by wet deposition is calculated by the scavenging coefficient, calculated at each grid cell for any nuclides except for noble gases from the precipitation intensity for convective and nonconvective rains predicted by MM5. The air concentration in each Eulerian cell averaged over an output time interval and total surface deposition accumulated during the time interval are calculated by summing up the contribution of each particle to the cell. The radioactive decay is calculated at each time step and integrated in both air concentration and surface deposition calculations, although decay chains are not considered. The radiological doses are calculated by multiplying the air concentration and deposition by conversion factors [31]. The performance of this model system was evaluated by its application to the field tracer experiment over Europe, ETEX [32] and Chernobyl nuclear accident [29, 33, 34].

15.2.4 Reconstruction of Local Atmospheric Dispersion Process

By using the preliminary estimated source term, detailed analysis on the local atmospheric dispersion around the FNPP1 has been carried out by WSPEEDI. The for - mation process of the high dose rate zone in the northwest direction from the plant, which was clarified by aerial monitoring carried out after 16 March [1], was investigated by reconstructing the atmospheric dispersion of radionuclides during the period from 15 to 16 March 2011 [2]. Three nested domains (domain-1, 100 ×100 grids with 9-km resolution; domain-2, 130 ×190 grids with 3-km resolution; domain-3, 190 × 190 grids with 1-km resolution) were used for MM5 calculation, and GEARN used two inner domains of MM5. Major radioactive species of ^{131}I, ^{132}I (^{132}Te), ^{134}Cs, and ^{137}Cs (radioactivity ratio, 1:2:0.1:0.1 assumed based on air sampling data at Tsukuba [35]) were considered in the calculation. GEARN code was modified temporarily to treat ^{132}I as a ^{132}Te progeny nuclide, and radioactive equilibrium between ^{132}Te and ^{132}I is assumed. The dry deposition velocity in GEARN was also modified to have a fivefold larger value at grids with forested land surface considering the particle capture efficiency of a tall canopy [36]. In the reconstruction of the event, revisions of MM5 and GEARN calculations were repeated by changing conditions of meteorological data assimilation and modifying the source term, respectively, until the simulation results of meteorological field and air dose rate mostly reproduced the measurements (Fig. 15.2).

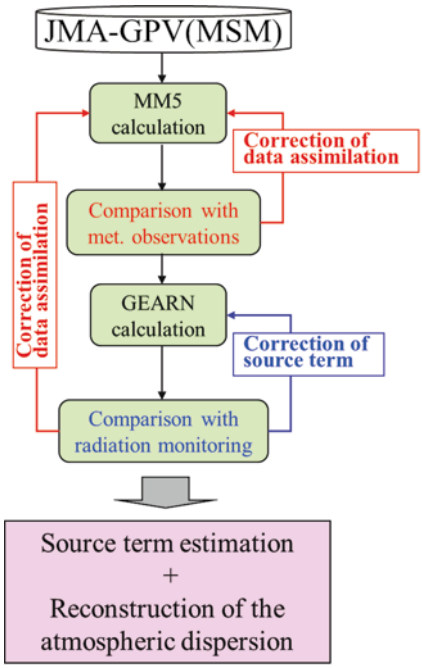

Fig. 15.2 Calculation method for the source term estimation and reconstruction of local atmospheric dispersion process

15.2.5 Radionuclides

As described in the previous subsection, the compositions of the radionuclides [^{131}I, ^{132}I (^{132}Te), ^{134}Cs, and ^{137}Cs] are required for the calculation of dose rates when the data of air dose rates are used to estimate release rates. From 05:00 JST on March 12 to 00:00 JST on March 15, the fixed value of 0.1, determined from available datasets [19, 23], was used for the activity ratio of ^{137}Cs to ^{131}I. The concentration of ^{134}Cs was given to be equal to that of ^{137}Cs based on the same datasets. Although the activity ratio of ^{132}Te to ^{131}I varied widely from 0.1 to 3 in the datasets, the overall values ranged from 1.9 to 2.5 on 12 March, and later on, gradually decreased to 1.0. Considering this tendency, the activity ratios of ^{132}Te to ^{131}I were set to 2.0 until 16:00 JST on March 12, and 1.3 from 16:00 JST on March 12 to 21:30 JST on March 14.
In addition to the activity ratio of deposited nuclides, the activity ratio of the radioactive noble gas, ^{133}Xe, to ^{131}I is also needed for calculations using Method 3. Because there were no available environmental data for ^{133}Xe near the site, the release rate of 4.0×10^{15} Bq h^{-1} was used for ^{133}Xe, as estimated by the severe accident analysis for Unit 3 of FNPP1 [37]. Although other nuclides such as ^{136}Cs, ^{133}I, and ^{129m}Te were also observed at the monitoring points in and around FNPP1 [23, 38], gamma air dose rates of these radionuclides calculated from both air concentration data and their effective energies were relatively small compared with those for the major radionuclides of ^{131}I, ^{132}I (^{132}Te), ^{134}Cs, and ^{137}Cs. Thus, the other radionuclides except for major radionuclides were neglected in the estimation of source term.

15.3 Results and Discussion

15.3.1 Preliminary Source Term Estimation

The release rates and total amounts of ^{131}I and ^{137}Cs discharged into the atmosphere were estimated for the period from 12 March to 5 April 2011 in the preliminary source term estimation [1]. Then, total release amounts were estimated by the time integration of release rates. Figure 15.3 shows the temporal variation in release rates of ^{131}I and ^{137}Cs. The results of source term estimation are as follows. Here, the first release rate estimated from the dust sampling data on the morning of 15 March at JCAC, Chiba-city, is assumed to continue from the occurrence of accidental release from Unit 1, 10:00 JST on 12 March to 23:00 JST on 14 March. The significant release, 10^{16} Bq h^{-1} of ^{131}I, occurred on 15 March. Concerning the duration for the release rate of 10^{16} Bq h^{-1} of ^{131}I in the daytime of March 15, which is critical to the total release amounts, several trial simulations of atmospheric dispersion were carried out with various release duration. The results indicated that the plume released during the period from about 12:00 to 15:00 JST March 15 flowed northwestward and resulted in high dose rates from wet deposition in the nighttime of that day. From 16 March, the release rates of ^{131}I were estimated to be rather constant, on the order of 10^{14} Bq h^{-1}, until 24 March. The release rates had decreased with small day-to-day variations to the order of 10^{11} to 10^{12} Bq h^{-1} of ^{131}I in the beginning of April. The release rate of ^{137}Cs was derived based on the radioactivity ratios of ^{131}I to ^{137}Cs from dust sampling data and had a similar trend with fluctuations of the ^{131}I/^{137}Cs ratio in the range from 1 to 100. The total amounts of ^{131}I and ^{137}Cs discharged into the atmosphere from 12 March to 6 April were estimated to be approximately 1.5×10^{17} and 1.3×10^{16} Bq, respectively. On 12 April 2011, the NSC announced that the total amounts of ^{131}I and ^{137}Cs discharged into the atmosphere in the same period were 1.5×10^{17} Bq and 1.2×10^{16} Bq as preliminary values [39], based on our research. The slight difference of the total amount of ^{137}Cs from this chapter results from the revision of the activity ratio of ^{131}I and ^{137}Cs based on additional environmental data.

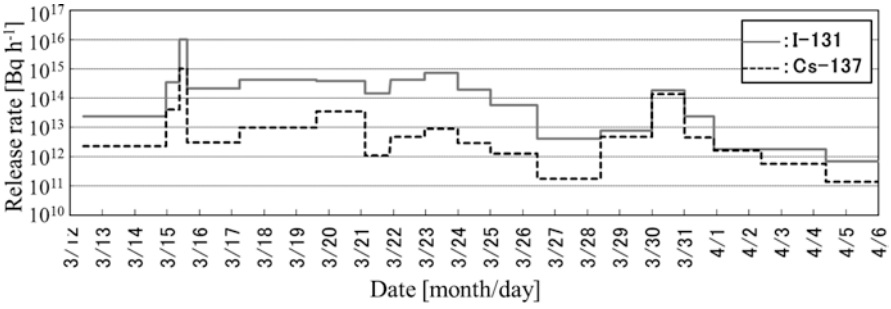

Fig. 15.3 Temporal variation in the preliminary estimated release rates of ^{131}I and ^{137}Cs. *Solid* and *dashed lines* show release rates of ^{131}I and ^{137}Cs, respectively. Japanese standard time (*JST*) is used

15.3.2 Detailed Analysis on the Local Atmospheric Dispersion Process

The formation process of the high dose rate zone in a northwest direction from the plant [11] was investigated by reconstructing the atmospheric dispersion of radionuclides during the period from 15 to 16 March 2011 [2]. The simulation results revealed that two significant releases, 3×10^{15} Bq h^{-1} of ^{131}I from 07:00 to 10:00 JST and 4×10^{15} Bq h^{-1} of ^{131}I from 13:00 to 17:00 JST on 15 March, were necessary to reproduce the spatial distribution and temporal changes of measured air dose rates (Fig. 15.4). Increases in air dose rates at the monitoring posts at the southwest and west directions from the plant were caused by the high-concentration plume released in the morning. The plume encountered the rainband that covered the west and central areas of Fukushima Prefecture and caused some amount of wet deposition around the middle area of Fukushima Prefecture. A southeasterly wind carried the plume discharged in the afternoon to the northwest of the plant. The precipitation covering the northern part of Fukushima scavenged this high-concentration plume and produced a significant amount of surface deposition at the region northwest of the plant. The dry deposition was dominant in the southwest region of the plant where no rainfall area appeared during the passage of the plume. It gradually decreased with distance from the plant, that is, with the decrease of ground-level concentration from atmospheric dispersion. In contrast, the wet deposition dominated the high dose rate zones in the northwest region of the plant and the middle area of Fukushima Prefecture. These results indicate that wet deposition plays an important role in the formation of wide and heterogeneous high dose rate zones. It corresponds to the prior observational study on the Chernobyl nuclear accident considering that the geographic pattern of deposited ^{137}Cs was closely related to that of rainfall [40].

15.3.3 Reestimation of Source Term for the Early Phase of the Accident

The source term of ^{131}I and ^{137}Cs in the early phase of the FNPP1 accident from 12 to 14 March was estimated as shown in Fig. 15.5 [3]. The release was assumed to start at 05:00 JST on 12 March, just before the increases in air dose rate at the main gate in FNPP1 were observed. In the present study, release rates for the six periods from 05:00 JST on 12 March to 00:00 JST on 15 March (Nos. 1–5 and 8; Fig.15.5) were estimated from environmental data. Four of them (Nos. 1, 2, 4, and 8; Fig. 15.5) were estimated by comparing dust sampling data with calculation results. The estimation methods based on the air dose rates in and around FNPP1 were applied to the remainder of the periods (Nos. 3 and 5; Fig. 15.5) because no dust sampling data were available. The release duration of each estimated release rate was determined by dividing the period from the previous one at the middle time point

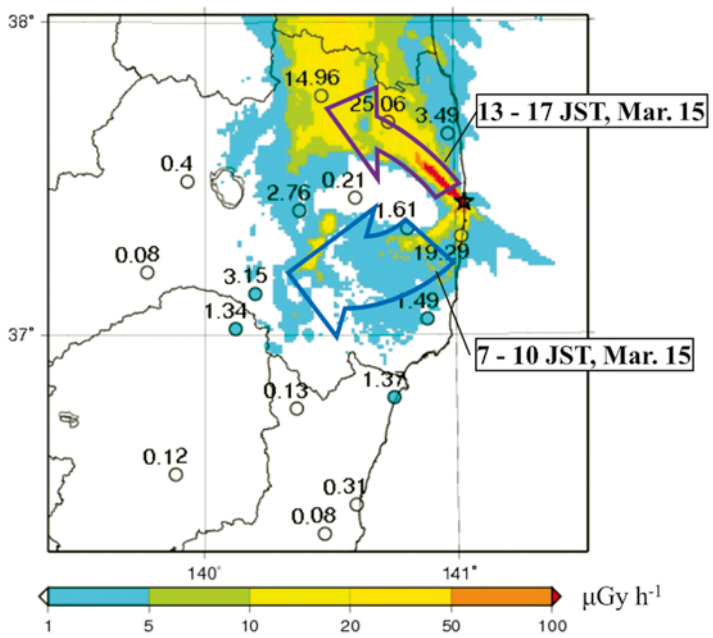

Fig. 15.4 Distribution of air dose rate by calculation (*shaded area*) and monitoring (*circles* with values, μG h^{-1}) at 21 JST on 16 March and movements of plumes (*arrows*) discharged from 07:00 to 10:00 JST on 15 March and from 13:00 to 17:00 JST on 15 March

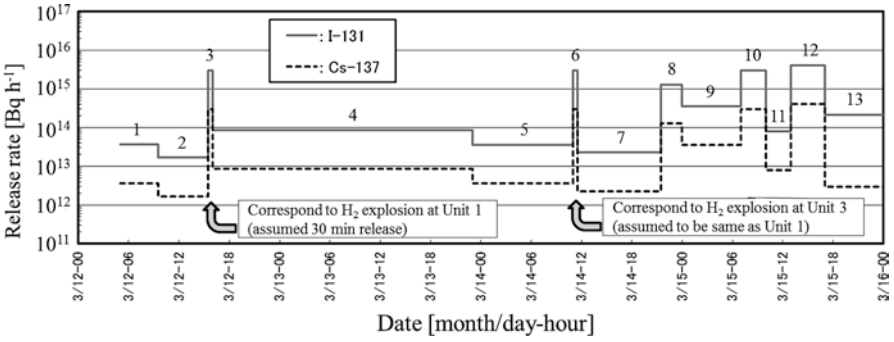

Fig. 15.5 Temporal variation in release rates of ^{131}I and ^{137}Cs reestimated for the early phase of the accident from 12 to 14 March. *Solid* and *dashed lines* show release rates of ^{131}I and ^{137}Cs, respectively. Japanese standard time (*JST*) is used

between the times when the release rates were estimated. The value of 30 min was assumed for the release duration for hydrogen explosions at Units 1 and 3. Some values of release rates estimated by the previous studies [1] (Nos. 7, 9, and 13; Fig. 15.5) and [2] (Nos. 10–12; Fig. 15.5) are included. The major releases of ^{131}I

greater than 10^{15} Bq h^{-1} were estimated during the afternoon of 12 March after the hydrogen explosion at Unit 1 and late at night on 14 March. The possible major release during the hydrogen explosion of Unit 3 at 11:00 JST on 14 March could not be estimated because the plume flowed to the Pacific Ocean on the northwesterly wind. Thus, the same value of release rate estimated for the hydrogen explosion of Unit 1 (i.e., 3.0×10^{15} Bq h^{-1}) was assumed for this period. For other time periods before 21:30 JST on 14 March, estimated release rates of ^{131}I had values between 1.7×10^{13} and 8.4×10^{13} Bq h^{-1}, which were similar to our preliminary estimated values.

The spatial pattern of surface deposition of ^{137}Cs and increases in air dose rates observed at the monitoring posts around FNPP1 were generally reproduced by WSPEEDI using the estimated release rates. The simulation results indicate that the amount of dry deposition of the high-concentration plume discharged during the afternoon of 12 March was clearly smaller than that of the total deposition from the afternoon to the evening of 15 March, which formed the highest dose rate zone in the northwest region of FNPP1 [21]. The results indicate that air dose rates largely increased in the south-southwest region of the site by dry deposition of the high-concentration plume discharged from the night of 14 March 14 to the morning of 15 March.

15.3.4 Validation of Source Term by the Regional-Scale Atmospheric Dispersion Simulation

The regional-scale atmospheric dispersion and surface deposition of ^{131}I and ^{137}Cs released from the FNPP1 from 05:00 JST on 12 March to 00:00 JST on 1 May 2011 were simulated over eastern Japan using WSPEEDI. In this simulation, the source term, which was estimated in previous studies primarily using observed air concentrations of radionuclides and air dose rates over land around FNPP1, was verified and refined on the basis of its agreement of calculated daily surface deposition with measurements [4]. For the period from 03:00 to 21:00 JST on 21 March, the ^{131}I/^{137}Cs activity ratio was determined from dust sampling data at different points from those used for the release rate of ^{131}I in the preliminary source term estimation [1] because of the lack of ^{137}Cs measurements. This change caused the ^{137}Cs deposition to be underestimated in the Kanto region on 21 and 22 March by setting a lower release rate of ^{137}Cs, although good agreement was seen for ^{131}I. Considering the range of observed ^{131}I/^{137}Cs activity ratios (from 1.5 to 19.1) in the 12 sampling datasets at FNPP2 [22], Tokai [23], and Setagaya [24] from 06:00 to 22:00 JST on 21 March, we modified the ^{131}I/^{137}Cs activity ratio from 131 in the preliminary source term to 10. We also added new release rates for the period from 21:00 JST on 29 March to 11:00 JST on 30 March, estimated using the dust sampling data at FNPP2 [22], which were not used in the preliminary source term estimation [1]. The release rate of ^{131}I was estimated to be 1.5×10^{13} Bq h^{-1} and the ^{131}I/^{137}Cs activity ratio was 1.7. The value of the ^{131}I/^{137}Cs activity ratio of 4.9 obtained from the dust sampling data

Table 15.1 Release start time, release duration, release rates of ^{31}I and ^{137}Cs, ^{131}I/^{137}Cs radioactivity ratio, and release height for the period from 05:00 JST on 12 March and 00:00 JST on 1 May 2011

No.	Start time (JST)	Duration (h)	^{131}I (Bq h^{-1})	^{137}Cs (Bq h^{-1})	^{131}I/^{137}Cs	Height (m)
1	2011/3/12 05:00	4.5	3.7E+13	3.7E+12	10	20
2	2011/3/12 09:30	6.0	1.7E+13	1.7E+12	10	120
3	2011/3/12 15:30	0.5	3.0E+15	3.0E+14	10	100 (volume)
4	2011/3/12 16:00	31.0	8.4E+13	8.4E+12	10	120
5	2011/3/13 23:00	12.0	3.6E+13	3.6E+12	10	120
6	2011/3/14 11:00	0.5	3.0E+15	3.0E+14	10	300 (volume)
7	2011/3/14 11:30	10.0	2.3E+13	2.3E+12	10	20
8	2011/3/14 21:30	2.5	1.3E+15	1.3E+14	10	120
9	2011/3/15 00:00	7.0	3.5E+14	4.0E+13	8.8	120
10	2011/3/15 07:00	3.0	3.0E+15	3.0E+14	10	20
11	2011/3/15 10:00	3.0	8.0E+13	8.0E+12	10	20
12	2011/3/15 13:00	4.0	4.0E+15	4.0E+14	10	20
13	2011/3/15 17:00	37.0	2.1E+14	3.0E+12	70	20
14	2011/3/17 06:00	57.0	4.1E+14	1.0E+13	41	20
15	2011/3/19 15:00	36.0	3.8E+14	3.5E+13	11	20
16	2011/3/21 03:00	18.0	1.4E+14	1.4E+13	10	20
17	2011/3/21 21:00	26.0	4.1E+14	4.7E+12	87	20
18	2011/3/22 23:00	25.0	7.1E+14	8.9E+12	80	20
19	2011/3/24 00:00	24.0	1.9E+14	2.9E+12	66	20
20	2011/3/25 00:00	35.0	5.6E+13	1.2E+12	45	20
21	2011/3/26 11:00	47.0	4.0E+12	1.7E+11	23	20
22	2011/3/28 10:00	35.0	7.5E+12	4.7E+12	1.6	20
23	2011/3/29 21:00	14.0	1.5E+13	8.8E+12	1.7	20
24	2011/3/30 11:00	13.0	1.8E+14	1.4E+14	1.3	20
25	2011/3/31 00:00	22.0	2.4E+13	4.5E+12	5.3	20
26	2011/3/31 22:00	35.0	1.8E+12	1.6E+12	1.1	20
27	2011/4/02 09:00	48.0	1.8E+12	5.8E+11	3.1	20
28	2011/4/04 09:00	80.0	7.0E+11	1.4E+11	4.9	20
29	2011/4/07 17:00	150.0	7.0E+11	3.5E+11	2.0	20
30	2011/4/13 23:00	409.0	7.0E+11	1.8E+11	4.0	20

Volume sources with the sizes of $(x, y, z) = (100, 100, 100\,\text{m})$ and $(100, 100, 300\,\text{m})$ were assumed for hydrogen explosions at unit 1 (No. 3) and 3 (No. 6), respectively [4]. Japanese standard time (JST) is used

on 5 April was simply assumed to continue until 00:00 JST on 1 May. This assumption caused underestimation of the daily surface deposition of ^{137}Cs after 6 April, although the calculated ^{131}I deposition showed relatively good agreement. In the refined source term, the ^{131}I/^{137}Cs activity ratios after 6 April were modified to be 2.0 from 17:00 JST on 7 April to 23:00 JST on 13 April and to be 4.0 from 23:00 JST on 13 April to 00:00 JST on 1 May on the basis of the mean values from the measured air concentration data sampled at Tokai [23]. As a result, the release rates of ^{131}I and ^{137}Cs discharged into the atmosphere were refined as in Table 15.1, and those for the period from 12 March to 5 April are shown in Fig. 15.6.

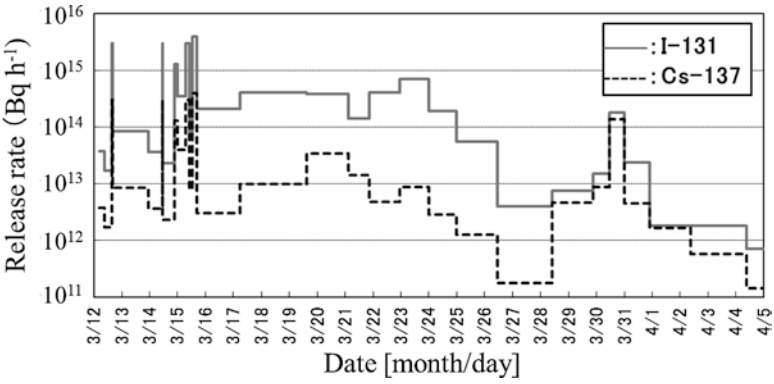

Fig. 15.6 Temporal variation in the refined release rates of ^{131}I and ^{137}Cs for the period from 12 March to 5 April 2011. *Solid* and *dashed lines* show release rates of ^{131}I and ^{137}Cs, respectively. Japanese standard time (*JST*) is used

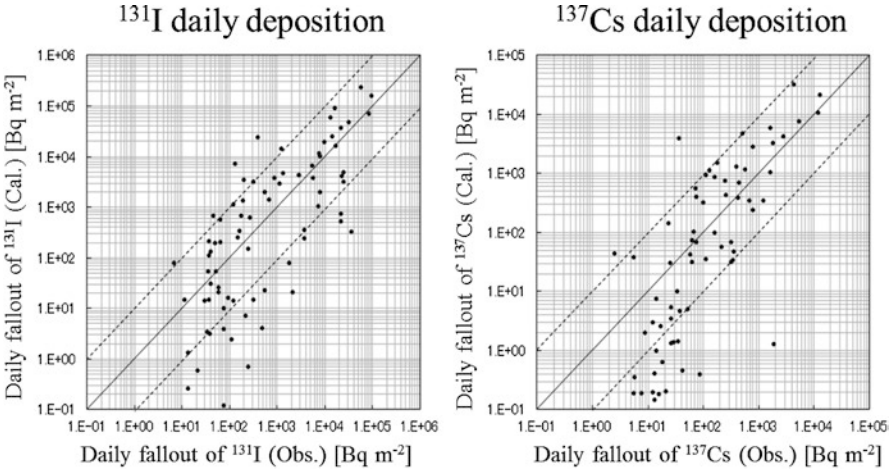

Fig. 15.7 Scatter diagrams of the daily surface deposition of ^{131}I and ^{137}Cs comparing measurements and calculations for the period from 18 to 31 March. *Solid lines* show 1:1 lines; the areas between two *dashed lines* indicate the bands within a factor of 10

Daily surface deposition of ^{131}I and ^{137}Cs calculated using the refined source term agreed better with the measurements than those using the preliminary source term. Scatter diagrams and statistics of the daily surface deposition of ^{131}I and ^{137}Cs for calculations and for measurements from March 18 to 31 are shown in Fig. 15.7 and Table 15.2, respectively. In Table 15.2, FA2, FA5, and FA10 denote the percentage of calculations that are within factors of 2, 5, and 10 of the measurements, respectively.

Table 15.2 Statistics of the daily surface deposition of ^{131}I and ^{137}Cs for calculations and for measurements from March 18 to 31, 2011

Radionuclides	FA2 (%)	FA5 (%)	FA10 (%)	Correlation coefficients
^{131}I	22.4	48.7	65.8	0.75
^{137}Cs	26.5	48.5	70.6	0.72

The values of FA2, FA5, and FA10 denote the percentage of calculations within factors of 2, 5, and 10 of the measurements, respectively [4]

Using the refined source term, the calculation reproduced daily and monthly surface deposition distributions over land in eastern Japan, without apparent biases toward under- or overestimation. Therefore, it is concluded that the source term over the period when the plume flowed over land in Japan is reasonable, although the source term during the period when the plume flowed and deposited over the ocean could not be verified in this study.

15.3.5 Formation Processes of ^{137}Cs Deposition over Eastern Japan

The analysis of the regional-scale atmospheric dispersion was carried out using the estimated source term [4]. It suggested that the present surface deposition distribution of ^{137}Cs over eastern Japan, observed by airborne monitoring [21], was produced mainly by the following events (Fig. 15.8):

- Dry deposition in the northeastern coastal area of Miyagi Prefecture on 12 March
- Wet and dry deposition in Fukushima Prefecture and the north of Tochigi and Gunma Prefectures on 15 March
- Dry deposition in the north of Ibaraki Prefecture on 15 March and, possibly, dry and wet deposition on 16 March
- Wet deposition in the area from the south of Iwate Prefecture to the northwest of Miyagi Prefecture on 20 March
- Wet deposition in the Kanto region, especially in the area from the south of Ibaraki Prefecture to the northwest of Chiba Prefecture, from 21 to 23 March

A general feature is that the areas corresponding to a large amount of wet deposition were distributed heterogeneously far from FNPP1, as well as around FNPP1, whereas the areas corresponding to a large amount of dry deposition were mainly located near FNPP1. However, the ratio of dry deposition to the total was relatively high not only near FNPP1, but also in the northeastern coastal area of Miyagi Prefecture, because of dry deposition on 12 March, and in the north of Ibaraki Prefecture from dry deposition on 15 and 16 March.

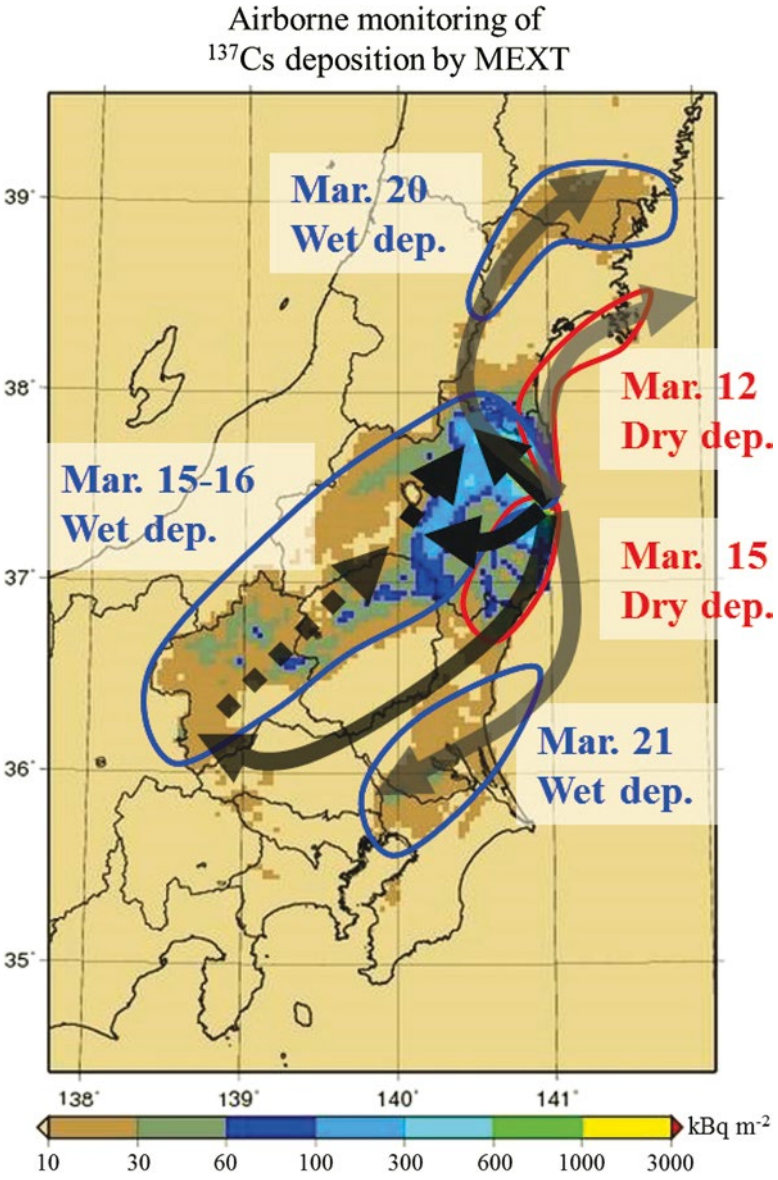

Fig. 15.8 Formation process of surface deposition distribution of ^{137}Cs over eastern Japan. Shaded area show the surface deposition of ^{137}Cs made from the airborne monitoring data by MEXT (MEXT 2011c). *Arrows and enclosed areas* show the movements of major plumes and dominant deposition processes and dates (JST), respectively, causing the measured ^{137}Cs deposition

15.4 Conclusions

To assess the radiological dose to the public resulting from the month-long discharge of radioactive materials into the atmosphere from the Fukushima Daiichi Nuclear Power Plant accident, the source term is essential for computer simulations on the dispersion of radioactive materials in the environment. The Japan Atomic Energy Agency has been trying to estimate the source term of iodine and cesium discharged to the atmosphere in the studies on the preliminary source term estimation [1], detailed analysis on the local atmospheric dispersion [2], reestimation of source term for the early phase of the accident [3], and validation of source term by the regional-scale atmospheric dispersion simulation [4]. As the result of these studies, the release rates of ^{131}I and ^{137}Cs discharged into the atmosphere were estimated for the period from 12 March to 1 May 2011 (Table 15.1); those for the period from 12 March to 5 April are shown in Fig. 15.6. The total amounts of ^{131}I and ^{137}Cs discharged into the atmosphere in this period were 1.2×10^{17} and 8.8×10^{15} Bq, respectively.

These studies on the source term estimation of radioactive materials discharged to the atmosphere from the Fukushima Daiichi Nuclear Power Plant had been carried out within 1 year after the accident using limited monitoring data and plant information. In these analyses, some limitation of WSPEEDI was also found in the utilization of simple dry and wet deposition processes. The results indicated that more sophisticated deposition processes considering chemical form and particle-size distribution of radionuclide are necessary to better reconstruct the measured surface deposition pattern [41]. New data, for example, the special distribution of ^{131}I deposition by airborne monitoring [42], have been reported after our source term estimation studies were made. Thus, more accurate and detailed source term estimation can be expected by using these additional data and the upgraded WSPEEDI with improved deposition processes.

References

1. Chino M, Nakayama H, Nagai H, Terada H, Katata G, Yamazawa H (2011) Preliminary estimation of release amounts of ^{131}I and ^{137}Cs accidentally discharged from the Fukushima Daiichi nuclear power plant into atmosphere. J Nucl Sci Technol 48:1129–1134
2. Katata G, Terada H, Nagai H, Chino M (2012) Numerical reconstruction of high dose rate zones due to the Fukushima Dai-ichi Nuclear Power Plant accident. J Environ Radioact 111:2–12
3. Katata G, Ota M, Terada H, Chino M, Nagai H (2012) Atmospheric discharge and dispersion of radionuclides during the Fukushima Dai-ichi Nuclear Power Plant accident. Part I: Source term estimation and local-scale atmospheric dispersion in early phase of the accident. J Environ Radioact 109:103–113

4. Terada H, Katata G, Chino M, Nagai H (2012) Atmospheric discharge and dispersion of radionuclides during the Fukushima Daiichi Nuclear Power Plant accident. Part II: Verification of the source term and regional-scale atmospheric dispersion. J Environ Radioact 112: 141–154
5. Taki M, Kobayashi H, Suzuki T, Shimizu I (1990) Isopleths if surface air concentration and surface air absorbed dose rate due to a radioactive cloud released from a stack. JAERI-M-90-206 (in Japanese with English abstract)
6. Nuclear Safety Commission of Japan (NSC) (2010) The guideline for environmental radiation monitoring. http://www.nsc.go.jp/shinsajokyo/pdf/100327_kankyo_monita.pdf. (in Japanese)
7. Ministry of Education, Culture, Sports Science and Technology (MEXT) (2011) Readings of dust sampling. http://radioactivity.mext.go.jp/en/list/200/list-1.html. Accessed 4 May 2012
8. Japan Chemical Analysis Center (JCAC) (2011) http://www.jcac.or.jp/lib/senryo_lib/taiki_kouka.pdf. Accessed 18 Nov 2011 (in Japanese)
9. Okura T, Oishi T, Taki M, Shibanuma Y, Kikuchi M, Akino H, Kikuta Y, Kawasaki M, Saegusa J, Tsutsumi M, Ogose H, Tamura S, Sawahata T (2012) Emergency monitoring of environmental radiation and atmospheric radionuclides at nuclear science research institute, JAEA Following the accident of Fukushima Daiichi nuclear power plant, JAEA-Data/Code 2012–010, Japan Atomic Energy Agency (available online)
10. Ministry of Economy, Trade and Industry (METI) (2011) http://www.meti.go.jp/press/20110316001/20110316001-2.pdf. Accessed 18 Nov 2011 (in Japanese)
11. Ministry of Education, Culture, Sports Science and Technology (MEXT) and U.S. Department of Energy (DOE) (2011) MEXT and DOE airborne monitoring. http://www.mext.go.jp/english/incident/1304796.htm. Accessed 22 July 2011
12. Fukushima Prefecture (2011) http://www.pref.fukushima.jp/j/20-50km0315-0331.pdf. Accessed 18 Nov 2011 (in Japanese)
13. Fukushima Prefecture (2011) http://www.pref.fukushima.jp/j/7houbu0311-0331.pdf. Accessed 18 Nov 2011 (in Japanese)
14. Tokyo Electric Power Company (TEPCO) (2011) Radiation dose measured in the Fukushima Daini nuclear power station. http://www.tepco.co.jp/en/nu/fukushima-np/f2/index-e.html. Accessed 18 Nov 2011
15. Ibaraki Prefecture (2011) http://www.pref.ibaraki.jp/20110311eq/radiation.html. Accessed 18 Nov 2011
16. Ibaraki Prefectural Environmental Radiation Monitoring Center (2011) http://www.houshasen-pref-ibaraki.jp/earthquake/doserate_past.html. Accessed 21 July 2011
17. Japan Atomic Energy Agency (JAEA) (2011) Transition of radiation rates measured at environmental monitoring posts of the sites of JAEA. http://www.jaea.go.jp/english/jishin/e-monitor.pdf. Accessed 18 Nov 2011
18. Tochigi Prefecture (2011) http://www.pref.tochigi.lg.jp/kinkyu/documents/20110312-18.pdf. Accessed 21 July 2011
19. Ministry of Economy, Trade and Industry (METI) (2011) http://www.meti.go.jp/press/2011/06/20110603019/20110603019.html. Accessed 18 Nov 2011 (in Japanese)
20. Ministry of Education, Culture, Sports Science and Technology (MEXT) (2011) Reading of radioactivity level in fallout by prefecture. http://radioactivity.mext.go.jp/en/list/194/list-1.html. Accessed 4 May 2012
21. Ministry of Education, Culture, Sports Science and Technology (MEXT) (2011) MEXT and DOE airborne monitoring. http://radioactivity.mext.go.jp/en/list/203/list-1.html. Accessed 4 May 2012
22. Tokyo Electric Power Company (TEPCO) (2011) http://www.tepco.co.jp/en/press/corp-com/release/index1103-e.html. Accessed 2 Dec 2011
23. Furuta S, Sumiya S, Watanabe H, Nakano M, Imaizumi K, Takeyasu M, Nakada A, Fujita H, Mizutani T, Morisawa M, Kokubun Y, Kono T, Nagaoka M, Yokoyama H, Hokama T, Isozaki T, Nemoto M, Hiyama Y, Onuma T, Kato C, Kurachi T (2011) Results of the environmental radiation monitoring following the accident at the Fukushima Daiichi nuclear power plant. JAEA-Review 2011–035, Japan Atomic Energy Agency (in Japanese with English abstract; available online)

24. Tokyo Metropolitan Government (2011) http://www.sangyo-rodo.metro.tokyo.jp/whats-new/measurement-kako.html. Accessed 2 Dec 2011 (in Japanese)
25. Ministry of Education, Culture, Sports Science and Technology (MEXT) (2007) SPEEDI System for prediction of environmental emergency dose information, Pamphlet of SPEEDI
26. Nagai H, Chino M, Yamazawa H (1999) Development of scheme for predicting atmospheric dispersion of radionuclides during nuclear emergency by using atmospheric dynamic model. J Atom Energ Soc Jpn 41:777–785 (in Japanese with English abstract)
27. Terada H, Nagai H, Furuno A, Kakefuda T, Harayama T, Chino M (2008) Development of worldwide version of system for prediction of environmental emergency dose information: WSPEEDI 2nd version. Trans Atom Energ Soc Jpn 7:257–267 (in Japanese with English abstract)
28. Grell GA, Dudhia J, Stauffer DR (1994) A Description of the fifth-generation Penn state/NCAR mesoscale model (MM5), NCAR Tech, Note NCAR/TN-3921STR, 122 pp
29. Terada H, Chino M (2008) Development of an atmospheric dispersion model for accidental discharge of radionuclides with the function of simultaneous prediction for multiple domains and its evaluation by application to the Chernobyl nuclear accident. J Nucl Sci Technol 45:920–931
30. Sehmel GA (1980) Particle and gas dry deposition: a review. Atmos Environ 14:983–1011
31. International Commission on Radiological Protection (ICRP) (1995) Age-dependent doses to members of the public from intake of radionuclides: part 4 inhalation dose coefficients. ICRP publication 71. Ann ICRP 25(3–4), Pergamon, Oxford
32. Furuno A, Terada H, Chino M, Yamazawa H (2004) Experimental verification for real-time environmental emergency response system: WSPEEDI by European tracer experiment. Atmos Environ 38:6989–6998
33. Terada H, Furuno A, Chino M (2004) Improvement of worldwide version of system for prediction of environmental emergency dose information (WSPEEDI), (I) new combination of models, atmospheric dynamic model MM5 and particle random walk model GEARN-new. J Nucl Sci Technol 41:632–640
34. Terada H, Chino M (2005) Improvement of Worldwide Version of System for Prediction of Environmental Emergency Dose Information (WSPEEDI) (II). Evaluation of numerical models by ^{137}Cs deposition due to the Chernobyl nuclear accident. J Nucl Sci Technol 42:651–660
35. KEK, High Energy Accelerator Research Organization (2011) measurement result of airborne nuclide and air radiation level in Tsukuba area. http://www.kek.jp/quake/radmonitor/index-e.html. Accessed 21 July 2011
36. Sportisse B (2007) A review of parameterizations for modelling dry deposition and scavenging of radionuclides. Atmos Environ 41:2683–2698
37. Japan Nuclear Energy Safety Organization (JNES) (2011) JNES-RE-2011-0002, JNESRE-report series. http://www.jnes.go.jp/content/000119740.pdf. Accessed 18 Nov 2011 (in Japanese)
38. Tokyo Electric Power Company (TEPCO) (2011) Influence to surrounding environment, archives. http://www.tepco.co.jp/en/nu/fukushima-np/f1/index2-e.html. Accessed 18 Nov 2011
39. Nuclear Safety Commission of Japan (NSC) (2011) Trial estimation of emission of radioactive materials (I-131, Cs-137) into the atmosphere from Fukushima Dai-ichi nuclear power station. http://www.nsc.go.jp/NSCenglish/geje/2011%200412%20press.pdf. Accessed 18 Nov 2011
40. Clark MJ, Smith FB (1988) Wet and dry deposition of chernobyl releases. Nature (Lond) 332:245–249
41. Nagai H, Chino M, Terada H, Katata G (2012) Atmospheric dispersion simulations of radioactive materials discharged from the Fukushima Daiichi nuclear power plant due to accident: consideration of deposition process. In: Proceedings of the first NIRS symposium on reconstruction of early internal dose in the TEPCO Fukushima Daiichi nuclear power station accident. NIRS-M-252, pp 137–149, National Institute of Radiological Sciences http://www.nirs.go.jp/publication/irregular/pdf/nirs_m_252.pdf. Accessed 12 Nov 2013
42. Torii T, Sugita T, Okada CE, Reed MS, Blumenthal DJ (2013) Enhanced analysis methods to derive the spatial distribution of ^{131}I deposition on the ground by airborne surveys at an early stage after the Fukushima Daiichi nuclear power plant accident. Health Phys 105:192–200

Part VII
Dose Assessment

Chapter 16
NIRS's Project for the Reconstruction of Early Internal Dose to Inhabitants in Fukushima After the Nuclear Disaster

Osamu Kurihara, Eunjoo Kim, Kumiko Fukutsu, Masaki Matsumoto, Soheigh Suh, Keiichi Akahane, and Kazuo Sakai

Abstract In 2012, National Institute of Radiological Sciences (NIRS) launched a project on the reconstruction of the early internal dose, namely the thyroid dose to inhabitants in Fukushima and adjacent prefectures from the intake of short-lived nuclides, mainly ^{131}I after the nuclear disaster. Limited human measurements make it difficult to estimate individual doses, and thus it is necessary to collect all information available and explore possible methods for dose reconstruction. As the first action of the project, a symposium was organized by NIRS on 10–11 July 2012. This chapter provides human or environmental measurement data collected and describes the current status of the project.

Keywords Dose reconstruction • Early internal dose • Fukushima • Inhabitants • Nuclear disaster • Thyroid dose

16.1 Introduction

The Tokyo Electric Power Company (TEPCO) Fukushima Daiichi Nuclear Power Station (FDNPS) accident triggered by the Tohoku Region Pacific Coast Earthquake on 11 March 2011 resulted in reactor core meltdown with several hydrogen explosion events, following an enormous release of radioactive materials into the environment [1]. Airborne surveys after this nuclear disaster have shown the spatial distribution of ambient dose rates and the Cs ground deposition on a regional scale,

O. Kurihara (✉) • E. Kim • K. Fukutsu • M. Matsumoto • S. Suh • K. Akahane • K. Sakai
Research Center for Radiation Emergency Medicine, National Institute of Radiological Sciences, 4-9-1 Inage-ku, Chiba-City, Chiba 263-8555, Japan
e-mail: osakuri@nirs.go.jp

S. Takahashi (ed.), *Radiation Monitoring and Dose Estimation of the Fukushima Nuclear Accident*, DOI 10.1007/978-4-431-54583-5_16,

revealing that heavily contaminated areas were generated mainly in a northwesterly direction from FDNPS [2]. It is thus of great importance to understand the magnitude of individual doses to populations in affected areas from the aspect of foreseeing health effects attributed to radiation exposure in the accident. Preliminary dose estimations for inhabitants in Fukushima Prefecture and the whole of Japan have been reported by the World Health Organization (WHO) [3].

The Fukushima government has also initiated dose estimations of the inhabitants inside the prefecture and results obtained are described as follows. External dose estimations of 228,512 inhabitants have been completed as of the end of October 2012, demonstrating that 99.6 % of these are 5 mSv in effective dose for the first 4 months after the accident [4]. These estimations have been performed using a system for calculating individual external doses based on time-series maps of ambient dose rates in Fukushima Prefecture and personal behavior records. Human measurements of the inhabitants with whole-body counters (WBCs) have been performed for estimating their internal doses. It has been reported that 26 of 90,050 subjects exceeded 1 mSv in the committed effective dose (CED) [5]. However, it should be noted that this result is for internal doses only from ^{134}Cs and ^{137}Cs. The early internal dose, which is expected to be received by the intake of short-lived nuclides (e.g., ^{131}I, ^{132}I, ^{132}Te) during the first few months after the accident, still remains unknown because of limited information available. Concern is thus raised concerning thyroid exposure to small children from the intake of radioiodine, as with situations found after Chernobyl accident [6].

In 2012, the National Institute of Radiological Sciences (NIRS) launched a project on the reconstruction of the early internal dose to the inhabitants in Fukushima and adjacent prefectures. As the first action of this project, the 1st NIRS symposium on “Reconstruction of early internal dose in the TEPCO Fukushima nuclear power station accident” was held on 10–11 July 2012. The main aims of this symposium were twofold: (1) to collect human and environmental measurement data available for estimating the early internal dose to the inhabitants and (2) to discuss methods for reconstructing the thyroid equivalent dose (hereinafter, thyroid dose) among invited experts from Japan and overseas. The proceedings of the symposium, including 17 peer-reviewed 17 papers and the summary of the discussion, have been published by NIRS [7]. Table 16.1 lists authors and titles of the papers included in the proceedings. The goals of the project this year are set as (1) to propose best methods for the internal dose estimation and (2) to estimate representative doses to the inhabitants of each area in Fukushima prefecture. This chapter briefly describes the current status of the project.

16.2 Measurement Data Collection

Main information on human and environmental measurements for reconstructing the thyroid dose to the inhabitants is described as follows.

Table 16.1 Contents of the proceedings of the 1st NIRS symposium on reconstruction of early internal dose in the TEPCO Fukushima Daiichi nuclear power station accident [7]

Authors	Title of paper
Part 1: Current status of internal does estimation	
(1) For responders	
C. Takada et al.	Results of whole body counting for JAEA staff members engaged in the emergency radiological monitoring for the Fukushima nuclear disaster
O. Kurihara et al.	Direct measurements of employees involved in the Fukushima Daiichi nuclear power station accident for internal dose estimates: JAEA's experiences
T. Nakano et al.	Direct measurements for highly-exposed TEPCO workers and NIRS first responders involved in the Fukushima NPS accident
N. Matuda et al.	Retrospective assessment of internal doses for short-term visitors to Fukushima within 1 month after the nuclear power plant accident
M. Miyazaki et al.	Lessons learned from early direct measurements at Fukushima medical university after the Fukushima nuclear power station accident
(2) For residents and visitors	
S. Tokomami et al.	Thyroid equivalent doses due to radioiodine-131 intake for evacuees from Fukushima Daiichi nuclear power plant accident
E. Kim et al.	Screening survey on thyroid exposure for children after the Fukushima Daiichi nuclear power station accident
T. Momose et al.	Whole-body Counting of Fukushima residents after the TEPCO Fukushima Daiichi nuclear power station accident
I. Yamaguchi et al.	Estimation of ingestion dose due to I-131 in the initial month by using food-monitoring data after the Fukushima nuclear disaster in Japan
Part 2: Measurement of radioactivity in the environment	
H. Tsuruta	Summary of atmospheric measurements and transport pathways of radioactive materials released by the Fukushima Daiichi nuclear power plant accident
T. Nakamura	Radiation and radioactivity monitoring in the surrounding environment after the Fukushima Daiichi nuclear power plant accident—Overview
Part 3: Atmospheric dispersion simulations for radionuclides	
M. Chino et al.	Reconstruction of the atmospheric releases of ^{131}I and ^{137}Cs resulting from the Fukushima Daiichi nuclear power plant accident
H. Nagai et al.	Atmospheric dispersion simulations of radioactive materials discharged from the Fukushima Daiichi nuclear power plant due to accident: consideration of deposition
T. Ohara and Y. Morino	Atmospheric transport and deposition modeling of radioactive materials: current status and future tasks
G. Sugiyama et al.	National atmospheric release advisory center dispersion modeling during the Fukushima Daiichi nuclear power plant accident
Part 4: Atmospheric dispersion simulations for radionuclides	
M. Balonov and I. Zvonava	Methodology and results of internal dose reconstruction in Russia after the Chernobyl accident: generic approach and thyroid dose
A. Bouville et al.	Dose reconstruction related to the nuclear weapons tests conducted by the US in the Pacific in the 1950s

16.2.1 Human Thyroid Measurements

Through the symposium, it was revealed that human thyroid measurement data of the inhabitants were much fewer in this accident compared to those collected in the Chernobyl accident. The total number of such measurements totals ~1,500 at most; the largest dataset was a screening survey on the thyroid exposure that was conducted for 1,080 children in late March 2011 [8]. The subjects of this screening survey were inhabitants of Kawamata Town, Iwaki City, or Iitate Village where only indoor evacuation was advised because it was outside the restricted zone (20-km radius of FDNPS). The results demonstrated that net readings of the devices used in the screening survey were 0 for 598 of the 1,080 subjects and also suggested that no one had a thyroid dose that exceeded 100 mSv. Kim et al. [9] first introduced the thyroid dose distribution of the 1,080 subjects, showing that the maximum thyroid dose was 43 mSv on the assumption of a chronic intake scenario. However, difficulty was recognized in evaluating the quantitative capability of the nonspectrometric devices being used under elevated levels of radiation background. On the other hand, Tokonami et al. [10] performed thyroid measurements with a NaI(Tl) scintillation spectrometer on 12–16 April 2011 of 62 subjects of Namie Town: 45 evacuees from coastal areas and 17 inhabitants in Tsushima district. Positive detection was found in 39 in the evacuees and 7 in the inhabitants. The maximum thyroid dose among the subjects was 23 mSv in the group less than 20 years old and 33 mSv in the group over 20 years old. Other human thyroid measurements were obtained from responders or workers in charge of emergency operations at FDNPS [11, 12].

16.2.2 Human Whole-Body (WB) Measurements

Although measurement data of WBCs directly give internal doses from Cs only, these data would be available for reconstructing the thyroid dose to the inhabitants if the intake ratio of I to Cs can be determined in some way. NIRS was in charge of the pilot survey as a part of Fukushima Health Management Survey [13]. This survey was performed for 122 inhabitants of pilot survey areas (Namie Town, Iitate Village, and Yamakiya district of Kawamata Town) from June 27 to July 16 in 2011 by means of the thyroid/WB measurements and urinalysis. Table 16.2 summarizes numbers of the subjects with positive detection in the thyroid/WB measurements. Only the WB measurements provided meaningful results, showing that neither ^{134}Cs nor ^{137}Cs was detected for about half the subjects. This result indicates that a median CED of the adult subjects was below 0.035 mSv, which was derived from the detection limit of the WB measurements based on an acute intake scenario via inhalation on 12 March 2011. The Japan Atomic Energy Agency (JAEA) subsequently started WB measurements of the inhabitants on 11 July 2011 at the request of the Fukushima government. The total number of the subjects (mainly children) reached 9,927 at the end of January in 2012. Momose et al. [14] have reported their analysis results of

Table 16.2 Thyroid and whole-body measurement results of subjects of the pilot survey (as of 10 July 2011) [13]

	4–7 years		8–12 years		13–17 years		≤18 years		All	
Target nuclide	Pos.[a]	No.[b]	Pos.[a]	No.[b]	Pos.[a]	No.[b]	Pos.[a]	No.[b]	Pos.[a]	No.[b]
^{131}I	0	9	0	14	0	6	0	80	0	109
^{134}Cs only	2		6		2		42		52	
^{137}Cs only	0		0		0		32		32	
^{134}Cs and ^{137}Cs	0		0		0		26		26	

Detection limits: 38 Bq for ^{131}I, 320 Bq for ^{134}Cs, and 570 Bq for ^{137}Cs
[a]Positive detection
[b]Subject number for each age group

the CED distributions of two age groups, 13–17 years old and older than 17 years. The median CED values of the two groups were evaluated to be 0.02 and 0.025 mSv, respectively. Here we note that all the individual CEDs were introduced based on the same intake scenario as described above for conservative estimations. Raw data of the WB measurements (e.g., the body content of Cs, measurement date, subject's age and sex, etc.) have not been published so far.

16.2.3 Environmental Measurements

Airborne sampling data are much needed because inhalation, rather than ingestion, is a main route of the intake by most of the inhabitants. However, such data were also rarely obtained in the first week after the accident. Continuous air sampling was performed only outside Fukushima Prefecture. Tsuruta et al. [15] have reported the gaseous/aerosol ratio of ^{131}I and the activity ratio of ^{131}I/^{137}Cs in air from their analyses on existing information. Both items are of importance for reconstructing the thyroid dose.

Figure 16.1 displays the relationship of the ^{131}I air concentration between gaseous and particulate forms at FDNPS, TPCO Fukushima Daini NPS (located 10 km south from FDNPS), and three sites of JAEA in Ibaraki Prefecture, showing that all the plots follow a common trend with a mean ratio of 0.5 in the ^{131}I concentration of higher than 10 Bq m^{-3}. This ratio significantly influences thyroid dose values because the dose coefficient for inhalation of ^{131}I in the elemental form becomes doubled compared to that in the particulate form (Table 16.3) [16]. Although little analysis has been performed on the chemical form of iodine in the accident, most of the iodine was assumed to exist in the methylated state.

The activity ratio of ^{131}I/^{137}Cs also varied with time and location. This ratio changed significantly with two orders of magnitudes (1–100). It became around 10 on March 15 and March 20–21 when large releases of the nuclides from FDNPS occurred and was calculated as 8 from the average air concentrations of ^{131}I and ^{137}Cs at the site of the Nuclear Fuel Cycle Engineering Laboratories of JAEA

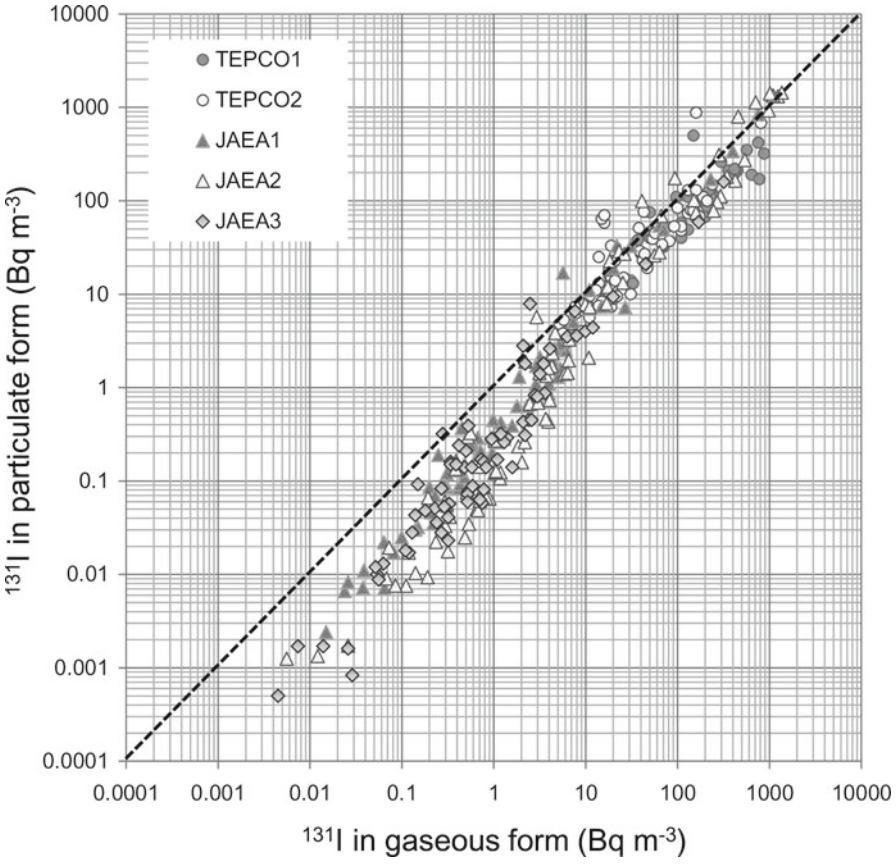

Fig. 16.1 Relationship of the physicochemical form of ^{131}I between gaseous and particulate forms. *TEPCO1* Fukushima Daiichi nuclear power station, *TEPCO2* Fukushima Daini nuclear power station

Table 16.3 Thyroid equivalent dose coefficient via inhalation for different age groups [16]

Physicochemical form	3 months	1 year	5 years	10 years	15 years	Adult
Methyl	2.6E–06	2.5E–06	1.5E–06	7.4E–07	4.8E–07	3.1E–07
Elemental	3.3E–06	3.2E–06	1.9E–06	9.5E–07	6.2E–07	3.9E–07
Particulate	1.4E–06	1.4E–06	7.3E–07	3.7E–07	2.2E–07	1.5E–07

Unit, Sv Bq^{-1}

(Table 16.4) [17]. These values seem to be consistent with a core inventory calculation. The activity ratio of $^{131}I/^{137}Cs$ on the ground surface shows a spatial distribution with higher ratios in a southerly direction and lower ratios in north and northwest directions from FDNPS, which is explained by the difference in metrological conditions at the time of the ground deposition. Details are described elsewhere.

Table 16.4 Dose contributions from various nuclides detected in air [17]

Nuclide	Averaged air concentration (Bq m^{-3})[a]	Adult (mSv)		1-year-old child (mSv)	
		Effective dose	Thyroid equivalent dose	Effective dose	Thyroid equivalent dose
^{129m}Te	1.5	1.9E–02	3.1E–02	1.8E–02	7.7E–02
^{132}Te	3.7	3.0E–02	4.4E–01	6.1E–02	1.1
^{131}I	12.0	3.8E–01	7.4	7.0E–01	14
^{132}I[b]	3.7	1.8E–03	2.1E–02	3.1E–03	5.1E–02
^{133}I	0.56	3.6E–03	6.8E–02	8.5E–03	1.7E–01
^{134}Cs	1.3	4.1E–02	1.3E–02	3.0E–02	7.6E–03
^{136}Cs	0.21	9.0E–04	3.2E–04	8.2E–04	2.9E–04
^{137}Cs	1.5	9.4E–02	1.1E–02	5.6E–02	6.1E–03
Total		0.57	7.9	0.88	15

[a]Average air concentration from March 12 to May 23, 2011
[b]Assuming the equilibrium state with ^{132}Te

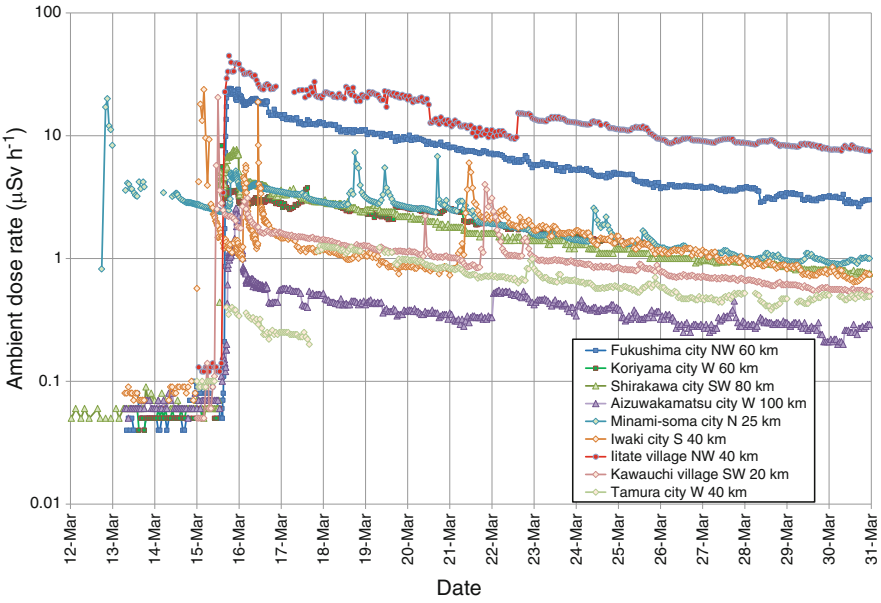

Fig. 16.2 Time trend of ambient dose rates at various locations in Fukushima Prefecture

Other short-lived nuclides such as ^{132}I, ^{133}I, or ^{132}Te were observed in the air sampling at several locations [17, 18]. Their contribution to the thyroid dose is estimated to be from 10 % to 20 %, although this may vary with assumed physicochemical forms of the nuclides and an intake period of the evaluation.

Figure 16.2 displays trends of ambient dose rates at various locations in the Fukushima prefecture. The first peak appears on March 15 at most of the locations

except for Minami-some city located north of FDNPS (on March 12). Thus, the first intake event for the inhabitants of the areas on the figure is also likely to occur on the same day. However, it is still difficult to know when and how the inhabitants, especially evacuees from the restricted zone, were exposed. Information on personal behavior records is needed: most of the evacuees moved outside the restricted zone before March 15. Atmospheric dispersion simulations for reproducing the behavior of enriched plumes may be also useful for this purpose.

16.3 Proposed Methods

Figure 16.3 displays proposed methods for reconstructing the thyroid dose to the inhabitants. The methods are classified into direct and indirect approaches: the former uses human data and the latter uses nonhuman data (including atmospheric dispersion simulations). The top priority in the dose reconstruction is placed on dose estimations from thyroid measurements. However, as mentioned earlier, such data are insufficient in terms of number and area. Thus, the direct approach utilizes available WB measurement data, which requires determining an appropriate intake ratio of I to Cs. Realistic scenarios of the intake are essential in the direct approach.

The dose estimation from the WB measurements is illustrated as follows. Here suppose the use of a CED value (^{134}Cs and ^{137}Cs) of the adult as the WB measurement data (currently available). Figure 16.4 displays a calculation flow from the CED of the adult to the thyroid doses to the children on the assumption that they both inhale the nuclides (^{131}I and Cs) with average ventilation rates for each age group under the same environment. The intake amounts of ^{134}Cs and ^{137}Cs giving a unit dose (1 mSv in the CED) are calculated as 90,000 Bq for each; here the existing ratio of ^{134}Cs/^{137}Cs is set as equal. When the intake ratio of ^{131}I/^{137}Cs is 1, the thyroid dose to the adult is 30 mSv, taking into account the gaseous/particulate ratio of ^{131}I and thyroid doses from nuclides other than ^{131}I. The thyroid doses to a 1-year-old child and a 10-year-old child are also calculated as 60 and 50 mSv, respectively. Note that these thyroid doses increase in proportion to the intake ratio of ^{131}I/^{137}Cs. For instance, when using a CED value of 0.025 mSv (from the average CED for the adult inhabitants in Fukushima) and an intake ratio of 10 (from the average existing ratio in air at the JAEA site), the thyroid dose to the 1-year-old child is calculated as 15 mSv ($=0.025\times60\times10$).

In the direct approach, internal doses received via inhalation or ingestion are separately estimated using materials on the figure. Dose estimation results from the indirect approach need to be compared with those from the direct approach for validation.

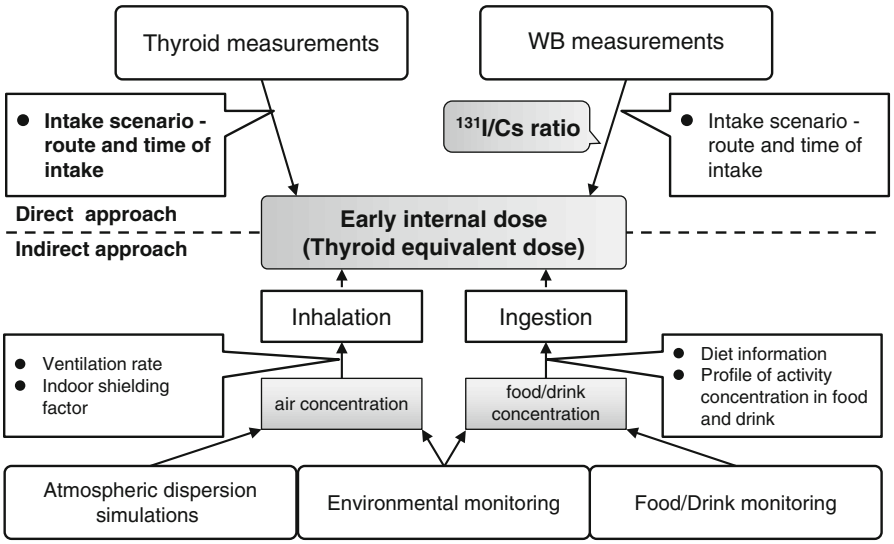

Fig. 16.3 Proposed methods for reconstruction of thyroid dose to inhabitants

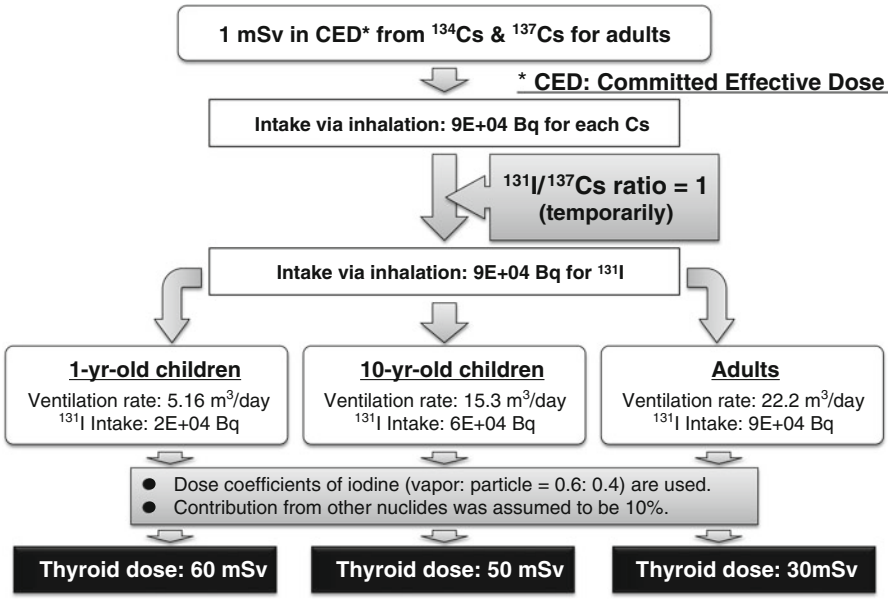

Fig. 16.4 Calculation flow of thyroid doses to different age groups from committed effective dose (CED) value of adult

16.4 Discussion and Future Tasks

The project has just started. Thus, discussion is provided only on the feasibility of the proposed methods for dose reconstruction.

In the direct approach, the WB measurements would compensate a relatively-small number of the thyroid measurements if appropriate intake ratios of ^{131}I/Cs can be determined. From an inverse estimation by the System for Prediction of Environmental Emergency Dose Information (SPEEDI), the discharge amount ratio of ^{131}I/^{137}Cs resulted in 10 [19]. On the other hand, the ground deposition ratio of ^{131}I/^{137}Cs is found to significantly vary with location [20], which suggests that it is difficult to make use of the relationship between Cs ground deposition and the thyroid doses to inhabitants [21]. The WB measurements of early responders to the accident have shown that estimated intake ratios of ^{131}I/Cs are considerably different between individuals [11]. Taking this fact into account, it would be necessary to carefully examine individual behavior.

In the indirect approach, the feasibility of atmospheric dispersion simulations for estimating the intake via inhalation is now under investigation. Figure 16.5 displays thyroid dose maps obtained from simulations by a worldwide version of SPEEDI (WSPEEDI-II) [22]. Note that these maps are given for hypothetical 1-year-old children and adults staying outside all the time from March 12 to March 31 in 2011. Thereby, these maps cannot be applied to persons moving during this period (e.g., the evacuees from the restricted zone), but would be useful for estimating thyroid doses to inhabitants on a regional scale. Preliminary calculations by WSPEEDI-II show reasonable overestimations for the thyroid dose in comparison to results of the

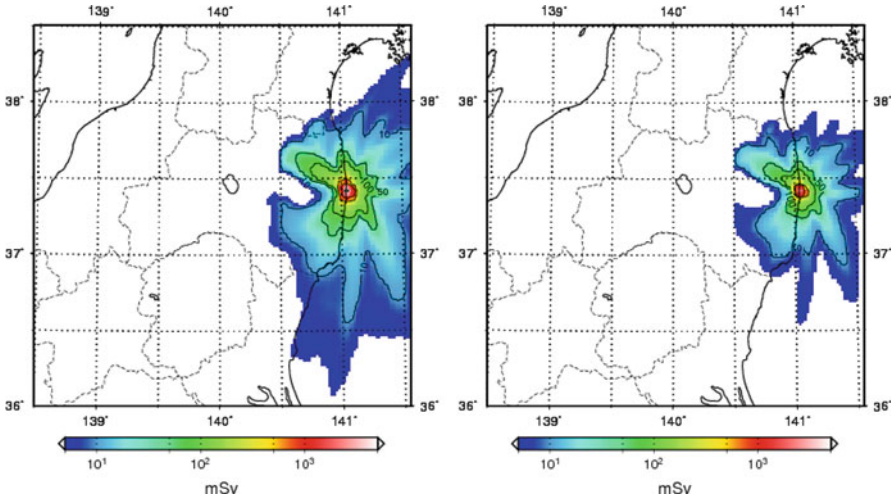

Fig. 16.5 Thyroid dose maps from inhalation of ^{131}I from the simulation by WSPEEDI-II (period of intake, March 12–31)

screening survey for the 1,080 children (data not shown here). Such a discrepancy would be minimized by adjusting parameters related to effects of indoor sheltering, a daily pattern of the ventilation rate, and so on.

Intake via ingestion in the accident is considered to be negligible for most of the inhabitants because of rapid action prohibiting the ingestion of contaminated food and water. In theory, the intake of the nuclides can be calculated using information on the diet intake and the concentration in food and water. However, this may not easy to perform. It is expected that the diet intake during the evacuation varies considerably from person to person and is more dependent on preserved foods than usual. Thereby, it is necessary to obtain information on the individual diet from personal interviews. This point was also stressed in the discussion of the last symposium.

Finally, future tasks for the dose reconstruction are listed as follows.

- To compile and validate all available data
- To track individual behavior for persons with human measurement data
- To analyze doses for each group with a similar behavior
- To determine appropriate intake ratios of ^{131}I/Cs
- To pursue investigations on the thyroid uptake of iodine in the Japanese

Acknowledgments This work has been conducted under the contract with Ministry of the Environment: Investigation on consequences of the nuclear disaster for 2012. Air concentration data from WSPEEDI-II were provided by Japan Atomic Energy Agency.

References

1. Prime Minister of Japan and his Cabinet (2011) Report of Japanese government to the IAEA ministerial conference on nuclear safety: the accident at TEPCO's Fukushima nuclear power station [Internet]. http://www.kantei.go.jp/foreign/kan/topics/201106/iaea_houkokusho_e.html. Accessed 13 Nov 2013
2. Nuclear Regulation Authority [Internet]. http://radioactivity.nsr.go.jp/ja/list/258/list-1.html (in Japanese)
3. World Health Organization (2012) Preliminary dose estimation from the nuclear accident after the 2011 great East Japan earthquake and tsunami. World Health Organization. Geneva, Switzerland
4. Fukushima Prefecture [Internet] (2012) http://www.pref.fukushima.jp/imu/kenkoukanri/241118kihontyosa.pdf (in Japanese). Accessed 13 Nov 2013
5. Fukushima Prefecture [Internet] (2012) http://www.pref.fukushima.jp/imu/wbc/20121206wbc_joukyou.pdf. (in Japanese). Accessed 13 Nov 2013
6. United Nations Scientific Committee on the Effects of Atomic Radiation (UNSCEAR) (2008) Health effects due to radiation from the Chernobyl accident. Source and effects of ionizing radiation, annex J

7. National Institute of Radiological Sciences (NIRS). NIRS-M-252 the 1st NIRS symposium on reconstruction of early internal dose in the TEPCO Fukushima Daiichi nuclear power station accident [Internet]. http://repo.nirs.go.jp/dspace/bitstream/918273645/330/1/nirs_m_252.pdf
8. Fukushima I (2012) Results of simplified survey for thyroid internal exposure of children in Fukushima and other surveys. Jpn J Health Phys 47:17–19
9. Kim E, Kurihara O, Suzuki T, Matsumoto M, Fukutsu K, Yamada Y, Sugiura N, Akashi M (2012) Screening survey on thyroid exposure for children after the Fukushima Daiichi nuclear power station accident. NIRS-M-252, Chiba, Japan, pp 59–66
10. Tokonami S, Hosoda M, Akiba S, Sorimachi A, Kashiwakura I, Balonov M (2012) Thyroid doses for evacuees from the Fukushima nuclear accident. Sci Rep 2:507
11. Takada C, Kurihara O, Kanai K, Nakagawa T, Tsujimura N, Momose T (2012) Results of whole body counting for JAEA staff members engaged in the emergency radiological monitoring for the Fukushima nuclear disaster. NIRS-M-252, Chiba, Japan, pp 3–12
12. Matsuda N, Kumagai A, Otsuru A, Morita N, Miura M, Yoshida M, Kudo T, Takamura N, Yamashita S (2012) Retrospective assessment of internal doses for short-term visitors to Fukushima within one-month after the nuclear power plant accident. NIRS-M-252, Chiba, Japan, pp 35–39
13. Fukushima Prefecture [Internet]. http://www.pref.fukushima.jp/imu/kenkoukanri/230724shiryou.pdf. (in Japanese)
14. Momose T, Takada C, Nakagawa T, Kanai K, Kurihara O, Tsujimura N, Ohi Y, Murayama T, Suzuki T, Uezu Y, Furuta S (2012) Whole-body counting of Fukushima residents after the TEPCO Fukushima Daiichi nuclear power station accident. NIRS-M-252, Chiba, Japan, pp 67–82
15. Tsuruta H, Takigawa M, Nakajima T (2012) Summary of atmospheric measurements and transport pathways of radioactive materials released by the Fukushima Daiichi nuclear power plant accident. NIRS-M-252, Chiba, Japan, pp 101–111
16. International Commission on Radiological Protection (ICRP) (2001) The ICRP database of dose coefficients; workers and members of the public. Elsevier, New York
17. Takeyasu M, Nakano M, Fujita H, Nakada A, Watanabe H, Sumiya S, Furuta S (2012) Results of environmental radiation monitoring at the nuclear fuel cycle engineering laboratories, JAEA, following the Fukushima Daiichi nuclear power plant accident. J Nucl Sci Technol 49:281–286
18. Nagaoka K, Sato S, Araki S, Ohta Y, Ikeuchi Y (2012) Changes of radionuclides in the environment in Chiba, Japan after the Fukushima nuclear plant accident. Health Phys 102:437–442
19. Chino M, Nakayama H, Nagai H, Terada H, Katata G, Yamasawa H (2011) Preliminary estimation of release amounts of ^{131}I and ^{137}Cs accidentally discharged from the Fukushima Daiichi nuclear power plant into the atmosphere. J Nucl Sci Technol 48:1129–1134
20. Nuclear Regulation Authority [Internet] (2011) http://radioactivity.nsr.go.jp/ja/contents/6000/5047/24/5600_110921_rev130701.pdf (in Japanese). Accessed 13 Nov 2013
21. Balanov MI, Bruk GY, Zvonova IA, Pitkevich VA, Bratilova AA, Jesko TV, Shutov VN (2000) Methodology of internal dose reconstruction for a Russian population after the Chernobyl accident. Radiat Prot Dosim 92:247–253
22. Katata G, Terada H, Nagai H, Chino M (2012) Numerical reconstruction of high rate zones due to the Fukushima Dai-ichi nuclear power plant accident. J Environ Radioact 111:2–12

Chapter 17
Internal Radiation Dose of KURRI Volunteers Working at Evacuation Shelters After TEPCO's Fukushima Daiichi Nuclear Power Plant Accident

Yuko Kinashi, Kouta Kurihara, Keiko Fujiwara, Eiko Kakihana, Tomohiro Miyake, Tomoyuki Takahashi, Tatsuya Yamada, Hiroshi Yashima, Hidehito Nakamura, Kenichi Okamoto, and Sentaro Takahashi

Abstract We report the radiation doses encountered by 59 Kyoto University Research Reactor Institute (KURRI) staff members who had been dispatched to screen refugees for radiation at emergency evacuation sites 45–80 km from the Tokyo Electric Power Co. (TEPCO) Fukushima Daiichi Nuclear Power Plant. From March 20 to April 30, 2011, 42 members were dispatched to the emergency evacuation sites located 45–80 km from the power plant to examine the radioactive contamination affecting refugees. Continuously, from May 10 to May 23, 2011, 17 members were dispatched to Fukushima Prefecture to establish the Kyoto University Radiation Mapping (KURAMA) system. Body burdens of radioactive nuclides were estimated using a whole-body counter. The first team dispatched showed 1,300–1,929 Bq internal radiation activity from cesium (including ^{137}Cs and ^{134}Cs) and 48–118 Bq ^{131}I. The internal doses of four members of the first team were estimated to be 24–39 μSv. The doses from internal exposure were almost similar to the cumulative external doses for the dispatch period (March 20–22, 2011) The external radiation doses of members dispatched after the second team had decreased from one third to less than one tenth of the external doses of the first dispatched team. The internal radiation doses of 55 members after the second team showed that 51 cases were undetectable and 4 cases showed doses of 2–15 μSv.

Keywords Cesium-134 • Cesium-137 • Internal radiation • Iodine-131 • Whole-body counter

Y. Kinashi (✉) • K. Kurihara • K. Fujiwara • E. Kakihana • T. Miyake • T. Takahashi • T. Yamada • H. Yashima • H. Nakamura • K. Okamoto • S. Takahashi
Research Reactor Institute, Kyoto University, 2-1010, Asashiro-nishi, Kumatori-cho, Sennan-gun, Osaka 590-0494, Japan
e-mail: kinashi@rri.kyoto-u.ac.jp

S. Takahashi (ed.), *Radiation Monitoring and Dose Estimation of the Fukushima Nuclear Accident*, DOI 10.1007/978-4-431-54583-5_17,

17.1 Background

On March 11, 2011, an earthquake and tsunami struck the Tohoku area of Japan, causing serious damage to the Tokyo Electric Power Co. (TEPCO) Fukushima Daiichi Nuclear Power Plant, and a significant amount of radionuclides was released into the surrounding environment (Fuyuno 2011; Butler 2011). The radioactive plume spread over Fukushima Prefecture toward the end of March 2011.

Fifty-nine members as the total number of man-teams of the Kyoto University Research Reactor Institute (KURRI) had been dispatched to the emergency evacuation shelters in Fukushima Prefecture 45–80 km from the power plant to help the local governments in screening the radioactivity level of refugees. From March 20 to April 30, 2011, 42 members in teams consisting of 2–4 staff were dispatched 13 times to nine emergency evacuation shelters. From May 10 to May 23, 2011, 17 members in teams consisting of 2–5 staff were dispatched six times to Fukushima Prefecture to establish the Kyoto University Radiation Mapping (KURAMA) system. All screening teams, especially the earlier one, risked internal radiation exposure because of the radioactivity in the environment.

Two volunteers of the initial team who had a high external and internal radiation dose were followed up 513 days after the first dispatch.

17.2 Methods

The external radiation dose for each staff member was measured using a personal dosimeter (ADM-112; Hitachi-Aloka Medical). For the internal radiation doses, body counters of radioactivity were determined using a whole-body counter consisting of an iron room, the 8 in. $\varphi \times 4$ in. t NaI (Tl) with four photomultiplier tubes (Fuji Denki), and a digital multichannel analyzer (MCA7600; Seiko EG&G) (Fig. 17.1). Body content of radioactivity was determined for 10 min using the whole-body counter, 3–4 days after returning from the dispatch. A spectral stripping method was used for the pulse amplitude analysis of ^{131}I, ^{134}Cs, and ^{137}Cs with the whole-body counter. The whole-body counter was calibrated using the human acryl phantom filled with KCl solution containing 40 kBq ^{40}K. The conversion from the measured radioactivity in the body to the committed effective dose by internal exposure was evaluated with the MONDAL 3 (monitoring to dose calculation ver. 3) from the National Institute of Radiological Science (NIRS). MONDAL is a user-friendly tool for internal dose calculation based on the ICRP biokinetic models, by which the committed effective dose can be calculated from the whole-body counter results (Ishigure 2004). Volunteers stayed in the local hotel 100 km from TEPCO's plant. They consumed served food without radioactive contamination during the screening work. The intake route of radioactive particles was considered to be inhalation. All the radioactivities were assumed to be taken by inhalation of 1.0-μm aerodynamic diameter particles in this calculation. The effective doses were calculated using the last working day as the acute inhalation of the radioactive particles.

Fig. 17.1 KURRI whole-body counter. *Left:* exterior. The iron walls, ceiling, and floor of the iron room are 20 cm thick, with the inner surfaces lined with 3-mm Pb sheet. *Right:* Interior. The 8 in. $\varphi \times 4$ in. t NaI (Tl) crystal scintillation counter and four photomultiplier tubes are 40 cm above the bed

17.3 Results

17.3.1 Initial Measurement of External Radiation and Internal Radiation Doses of Volunteers

The dispatch period, working place, and distance from TEPCO's plant, air dose rate, and external radiation doses of KURRI volunteers are listed in Table 17.1. The external radiation dose shows the 24-h doses for each volunteer using a personal dosimeter. As shown in Table 17.1, the data of screening teams 2–13, it is difficult to estimate the external exposure dose from the ambient dose rate because dose rate differs by place.

The internal radiation doses of ^{131}I and ^{134}Cs + ^{137}Cs are listed in Table 17.2. The spectral stripping method for the NaI whole-body counter cannot distinguish between ^{134}Cs and ^{137}Cs. We estimated that the ratio of ^{134}Cs–^{137}Cs was 1:1, on the basis of the data from the measurements of the protecting masks using a germanium detector (Table 17.3). Four volunteers in Screening Team 1 showed 1,929, 1,816, 1,469, and 1,300 Bq of radiocesium (^{137}Cs and ^{134}Cs) and 118, 72, 52, and 48 Bq of ^{131}I, respectively. The internal doses of radiocesium were estimated to be 28, 26, 21, and 19 μSv, and the internal doses of radioiodine were estimated to be 11, 7, 5, and 5 μSv, respectively.

Table 17.1 External radiation doses of KURRI volunteers

Group	Team members	Working day	Evacuation place	Evacuation site (distance from the plant in km)	Ambient dose rate (μSv/h)			[a]External exposure (μSv/day)
					Indoor	Under the eaves	Outdoor	
Screening team 1	A,B,C,D	March 20–22	Iwaki City Samekawa village Shirakawa City	62.7–79.2	1.5–2	–	2	16
Screening team 2	E,F,G,H	March 23–25	Fukushima City	67.9	–	0.11–0.13	–	1.5
Screening team 3	I,J,K,L	March 26–28	Fukushima City	67.9	–	0.08–0.1	–	2
Screening team 4	M,N,O	March 29–31	Fukushima City Kawamata cho	46.7–67.9	0.25	0.1	0.4–1.5	2
Screening team 5	P,Q,R	April 1–3	Fukushima City	67.9	0.07–0.13	0.08	0.35–0.43	5
Screening team 6	S,T	April 4–6	Sakuragawa City Fukushima City	59.9–67.9	0.05–0.09	0.08–0.1	0.29–0.43	1
Screening team 7	U,V,W	April 7–9	Fukushima City	67.9	0.04–0.05	0.07–0.08	0.32–0.36	1
Screening team 8	X,Y,Z	April 10–12	Fukushima City	67.9	0.04	0.07–0.1	0.32–0.33	3
Screening team 9	A1,A2,A3,A4	April 13–15	[b]Iwaki City Kawamata cho	44.6–46.7	0.1–0.15	0.26	0.3–1.5	2.5
Screening team 10	A,A5,A6	April 16–19	Kawamata cho	46.7	0.08–0.12	–	1.8–1.9	6
Screening team 11	A7,A8,A9	April 20–23	Minamisoma City	24.9	–	0.34–0.41	0.55–0.61	6
Screening team 12	B1,B2,B3	April 24–27	Minamisoma City Tanuma City	24.9–38.2	0.12–0.13	0.43	0.23–0.25	3
Screening team 13	A,B4,B5	April 28–30	Minamisoma City	24.9	0.12–0.18	0.44–0.45	–	3

[a]The maximum dose/day during the working days

[b]The shelter in Iwaki City of team 9 is the different shelter from that of team 1

Table 17.2 Internal radiation doses estimated with human counter at KURRI

Group	Volunteer's number	[a]Internal exposure caused by ^{137}Cs and ^{134}Cs		[a]Internal exposure caused by ^{131}I	
		(Bq)	(μSv)	(Bq)	(μSv)
Screening team 1	4	1,929	28	118	11
Screening team 2	4	[b]ND	0	ND	0
Screening team 3	4	ND	0	ND	0
Screening team 4	3	688	11	27	4
Screening team 5	3	ND	0	ND	0
Screening team 6	2	593	9	ND	0
Screening team 7	3	ND	0	18	2
Screening team 8	3	ND	0	ND	0
Screening team 9	4	ND	0	ND	0
Screening Team 10	3	ND	0	ND	0
Screening Team 11	3	ND	0	ND	0
Screening Team 12	3	ND	0	ND	0
Screening Team 13	3	ND	0	ND	0
KURAMA Team 1	4	ND	0	ND	0
KURAMA Team 2	2	ND	0	ND	0
KURAMA Team 3	2	ND	0	ND	0
KURAMA Team 4	2	594	9	ND	0
KURAMA Team 5	2	ND	0	ND	0
KURAMA Team 6	5	ND	0	ND	0

[a]The maximum internal dose of the each group
[b]*ND* not detected

Table 17.3 The cesium analysis of the protecting masks by a germanium semiconductor detector

Dispatched date	No of masks	Cs-134 (Bq/mask)	Cs-136 (Bq/mask)	Cs-137 (Bq/mask)
2011.3.20–3.22	11	2.2	0.2	2.5
2011.3.23–3.25	12	0.2	0	0.3

The doses from internal exposure were almost similar to the cumulative external doses for the dispatch period (March 20–22, 2011) when the radiation plumes following the explosions of Units 1 and 3 in TEPCO's Fukushima Daiichi nuclear plant had diffused over Fukushima City. The external radiation doses of the dispatched members after the second team decreased from one third to less than one tenth of the external doses of the first dispatched team. The internal radiation doses of 55 members after the second team was dispatched showed that 51 cases were undetectable and 4 cases showed doses of 2–15 μSv.

17.3.2 Follow-Up Data of Internal Doses for Two Volunteers

Two volunteers belonging the initial team (Screening Team 1) showed a rather high level of internal radiation dose because they visited Fukushima Prefecture three or more times. Volunteer A visited four times and volunteer B visited three times.

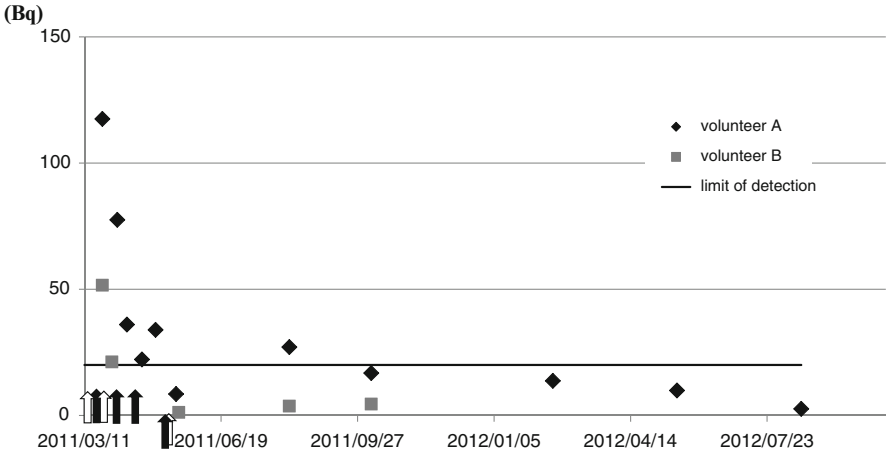

Fig. 17.2 Activity of ^{131}I measured by KURRI whole-body counter. *Diamond symbols* show the activity of ^{131}I of volunteer A. Volunteer A was dispatched joining in screening teams 1, 10, and 13 and KURAMA team 1. *Black arrows* show the dispatch period. *Square symbols* show the activity of ^{131}I of volunteer B. Volunteer B had stayed in Sendai City on 3/11–3/13/2011. He dispatched joining in screening team 1 and KURAMA team 1. *White arrows* show the dispatched period

Volunteer A was dispatched joining in Screening Teams 1, 10, and 13 and KURAMA Team 1. Volunteer B had stayed in Sendai City on 3/11-3/13/2011. He joined Screening Team 1 and KURAMA Team 1. We followed up their internal radiation doses for 6 months, to 2012/08/17. The activities of ^{131}I and ^{134}Cs + ^{137}Cs are shown in Figs. 17.2 and 17.3, respectively. Iodine-131 of volunteer A was detected until 2011/05/02, and iodine-131 of volunteer B was detected until 2011/03/31. Cesium-137 and -134 of volunteer A was detected until 2012/05/18, and cesium-137 and -134 of volunteer B was detected until 2011/08/08.

17.4 Discussion

The staff stayed in Fukushima prefecture for 3–4 days per dispatch, working at evacuation sites during the day and staying at a hotel near Fukushima City at night. As shown in Tables 17.1 and 17.2, Screening Team 1 had the largest accumulated dose from external exposure and internal exposure caused by iodine and cesium. Their dispatched period was the earliest; moreover, they used only simple masks with casual clothing so as not to make the evacuees anxious, so there was little difference in protection from internal exposure between staff members and evacuees. On the basis of the internal radiation dose of the first dispatched team, we gave the next dispatched team a warning to protect against internal exposure. The decrease in internal radiation doses after the second team was dispatched is attributable to the warning statement to the dispatched staff of KURRI regarding protection against internal radiation.

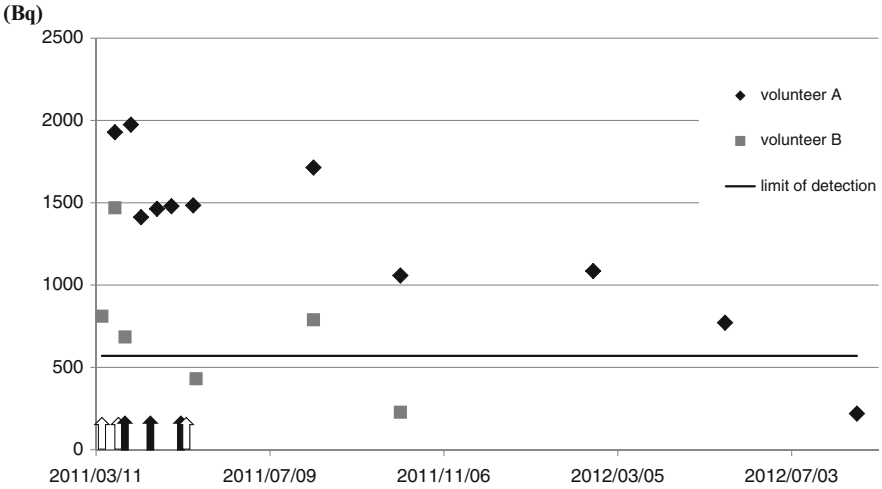

Fig. 17.3 The activity of $^{134}Cs + ^{137}Cs$ measured by KURRI whole-body counter. *Diamond symbols* show the activity of $^{134}Cs + ^{137}Cs$ of volunteer A. *Square symbols* show the activity of $^{134}Cs + ^{137}Cs$ of volunteer B. *Black arrows* show the dispatched period of Volunteer A. *White arrows* show the dispatched period of Volunteer B

Between September 2011 and March 2012, the internal radiation exposure of cesium in the 9,498 evacuated residents of Minamisoma, located 23 km north of the TEPCO plant, was measured. It was reported that the committed effective doses were less than 1 mSv in the 9,497 residents (Tsubokura 2012). We confirmed that internal exposure to cesium and iodine radiation soon after TEPCO's nuclear power plant accident was relatively low; that is, the largest effective dose was 39 μSv in the 59 dispatched KURRI volunteers. We are not aware of any published report on follow-up data of the internal exposure to cesium and iodine radiation measured with a whole-body counter in public after the early period following the TEPCO Fukushima Daiichi nuclear power plant accident.

The follow-up data of internal doses for two volunteers of the first dispatched team showed that the activity of iodine-131 was detected for 40 days in volunteer A and for 9 days in volunteer B after the last dispatch working day in Fukushima prefecture. Cesium-137 and -134 of volunteer A has been detected for 125 days and that in volunteer B for 56 days after the last dispatch working day in Fukushima.

The American Nuclear Society reported the initial measurements for residents who lived in areas associated with high doses of Fukushima Prefecture. Between June 27and July 16 in 2011, the activities of cesium-134, cecium-137, and iodine-131 were measured in 122 residents by whole-body counter. Cesium-134 was detected 47.7 % and cesium-137 at 29.4 %; the highest activity was 3,100 Bq of cesium-134 and 3,800 Bq of cesium-137. Iodine-131 was not detected. Based on this internal radiation measurement, the combined internal dose was less than 1 mSv for residents (ANS Committee Report 2012). Similar to the internal radiation data of the residents living near the high-dose area in Fukushima, the activity of iodine-131 in

two volunteers was not detected at the end of June 2011. The activities of cesium-137 and -134 of volunteer A and volunteer B on 2011/8/8 were measured as 1,714 and 789 Bq, respectively. It is reported that the half-life in the human body of episodic ingestion of cesium was 100 days. When a human intakes cesium chronically, cesium accumulates in the body and reaches equilibrium (ICRP Publication 2009). The activities of cesium of volunteer A continued rather higher 138 days after the initial dispatch because he had visited Fukushima several times in the earlier period following the TEPCO Fukushima Daiichi nuclear power plant accident.

References

1. Fuyuno I (2011) Quake shakes Japan's science. Nature 471:420
2. Butler D (2011) Radioactivity spreading in Japan. Nature 471:555–556
3. Ishigure N et al (2004) Development of software for internal dose calculation from bioassay measurements. Radiat Prot Dosim 109:235–242
4. Tsubokura M et al (2012) Internal radiation exposure after the Fukushima nuclear power plant disaster. JAMA 308:1621
5. American Nuclear Society (2012) A Report by The American Nuclear Society Special Committee on Fukushima, March 2012:15–18
6. ICRP Publication 111 (2009) Application of the commissions recommendations to the protection of people living in long-term contaminated areas after a nuclear accident or a radiation emergency: 20–22

Chapter 18
Probabilistic Assessment of Doses to the Public Living in Areas Contaminated by the Fukushima Daiichi Nuclear Power Plant Accident

Shogo Takahara, Masashi Iijima, Kazumasa Shimada, Masanori Kimura, and Toshimitsu Homma

Abstract Many residents are exposed to radiation in their daily lives in the areas contaminated by radioactive materials by the Fukushima Daiichi Nuclear Power Plant accident. To protect the people from radiation exposures adequately, dose assessment is necessary. The aim of this study is to provide the scientifically based quantitative information about a range of received doses to the people from the evacuation areas and the deliberate evacuation areas. To achieve this aim, we adopted a probabilistic approach that can provide the information about a range of doses and their likelihood of occurrence taking into account uncertainty and variability of input data. The dose assessment was performed based on the measurement data of the surface activity concentrations of ^{137}Cs and the results of actual survey on behavioral patterns of the population groups living in Fukushima Prefecture. As the result of assessment, the 95th percentile of the annual effective dose received by the inhabitants evacuated was mainly in the 1–10 mSv dose band in the first year after the contamination. However, the 95th percentile of the dose received by some outdoor workers and inhabitants evacuated from highly contaminated areas was in the 10–50 mSv dose band.

Keywords Behavioral pattern • Dose assessment • Exposure pathways • Fukushima Daiichi Nuclear Power Plant Accident • Measurement data • Probabilistic approach • Public exposure

S. Takahara (✉) • M. Iijima • K. Shimada • M. Kimura • T. Homma
Nuclear Safety Research Center, Japan Atomic Energy Agency,
2-4 Shirakata Shirane, Tokai-mura, Naka-gun, Ibaraki-ken, 319-1195, Japan
e-mail: takahara.shogo@jaea.go.jp

S. Takahashi (ed.), *Radiation Monitoring and Dose Estimation of the Fukushima Nuclear Accident*, DOI 10.1007/978-4-431-54583-5_18,

18.1 Introduction

After the Tohoku District Pacific Ocean Earthquake, large tsunamis struck the Fukushima Daiichi Nuclear Power Plant (1F Plant), which led to a nuclear accident that released a large amount of radioactive materials into the environment [1]. In the areas contaminated by the accident, many residents are now being exposed to radiation through various exposure pathways in their daily lives. To protect people from radiation exposures and manage the exposure situation appropriately, a suitable dose assessment is necessary [2]. The aim of this study is to provide preliminary results of the assessment of radiation doses received by the inhabitants of Fukushima Prefecture. This assessment is intended to be realistic and comprehensive. For this purpose, the doses are assessed by a probabilistic approach based on environmental monitoring data and realistic lifestyle habits in Fukushima prefecture.

18.2 Method

18.2.1 Scope

In the early phase of the accident, inhabitants were evacuated to prevent and reduce radiation exposure. The National Institute of Radiological Sciences (NIRS) suggested 18 evacuation scenarios according to the Fukushima health management survey [3]. These scenarios are listed in Table 18.1. Figure 18.1 shows the municipalities related to the evacuation scenarios and area classification of Fukushima Prefecture. Most people within the 20 km from the nuclear power plant were rapidly evacuated within a few days after the accident (evacuation scenario no. 1–12). However, some areas including Namie Town, Katsurao Village, Iitate Village, Minami Soma City, and Kawamata Town were later designated as "deliberate evacuation areas" based on environmental monitoring data (evacuation scenario no. 13–18).

Doses were assessed for the inhabitants evacuated, as well as for the inhabitants who continued to live in Fukushima City, Koriyama City, and Iwaki City after the contamination occurred. The doses were assessed for the population living in an urban environment, such as Fukushima City and Koriyama City, whereas the rural environment prevails in some municipalities in Fukushima Prefecture. Further assessments will be needed taking into account both urban and rural environments.

The dosimetric endpoints of the study are the effective doses received by adults in the first year after the contamination and over the inhabitants' lifetimes.[1] The total effective doses were calculated as the summation of those received by inhabitants in the municipalities listed in each evacuation scenario. The present study assumed that other protective actions such as sheltering and stable iodine uptake were not

[1] The integrated period is 60 years for adults.

Table 18.1 Evacuation scenarios for the population living in the evacuation area or the deliberate evacuation area based on the Fukushima health management survey [3]

Evacuation scenario no.	Municipality where the residence or evacuation facility is located and the length of stay during the period 11 Mar 2011 to 14 Mar 2012[a]		
1	Tomioka Town ~06:00, 12 Mar 2011	Kawachi Village ~10:00, 16 Mar 2011	Koriyama City ~14 Mar 2012
2	Okuma Town ~13:00, 12 Mar 2011	Tamura City ~14 Mar 2012	–
3	Futaba Town ~08:00, 12 Mar 2011	Kawamata Town ~10:00, 19 Mar 2011	Saitama Prefecture ~14 Mar 2012
4	Futaba Town ~16:00, 12 Mar 2011	Kawamata Town ~10:00, 19 Mar 2011	Saitama prefecture ~14 Mar 2012
5	Naraha Town ~13:00, 12 Mar 2011	Iwaki City ~10:00, 31 Mar 2011	Tamura City ~14 Mar 2012
6	Naraha Town ~13:00, 12 Mar 2011	Iwaki City ~10:00, 16 Mar 2011	Aizu Misato Town ~14 Mar 2012
7	Namie Town ~10:00, 15 Mar 2011	Namie Town ~10:00, 16 Mar 2011	Nihonmatsu City ~14 Mar 2012
8	Tamura City ~08:00, 12 Mar 2011	Tamura City ~10:00, 31 Mar 2011	Koriyama City ~14 Mar 2012
9	Minami Soma City ~10:00, 15 Mar 2011	Date City ~10:00, 31 Mar 2011	Fukushima City ~14 Mar 2012
10	Hirono Town ~08:00, 12 Mar 2011	Ono Town ~14 Mar 2012	–
11	Kawachi Village ~10:00, 13 Mar 2011	Kawachi Village ~10:00, 16 Mar 2011	Koriyama City ~14 Mar 2012
12	Katsurao Village ~10:00, 14 Mar 2011	Fukushima City ~14 Mar 2012	–
13	Namie Town ~10:00, 23 Mar 2011	Nihonmatsu City ~14 Mar 2012	–
14	Katsurao Village ~10:00, 21 Mar 2011	Fukushima City ~14 Mar 2012	–
15	Iitate Village ~10:00, 29 May 2011	Fukushima City ~14 Mar 2012	–
16	Iitate Village ~10:00, 21 June 2011	Fukushima City ~14 Mar 2012	–
17	Minami Soma City ~10:00, 20 May 2011	Minami Soma City ~14 Mar 2012	–
18	Kawamata Town ~10:00, 1 June 2011	Kawamata Town ~14 Mar 2012	–

[a]The dose assessment was performed with the assumption that the inhabitants stayed in the same municipality after movement to the final evacuation facility

implemented. Radiation exposure occurs through several pathways. The present study assessed the doses from external exposure to radionuclides deposited on the ground (hereafter referred to as groundshine) and to radionuclides in the radioactive cloud (hereafter referred to as cloudshine) as well as the doses caused by internal exposure through inhalation of radionuclides in the radioactive cloud.

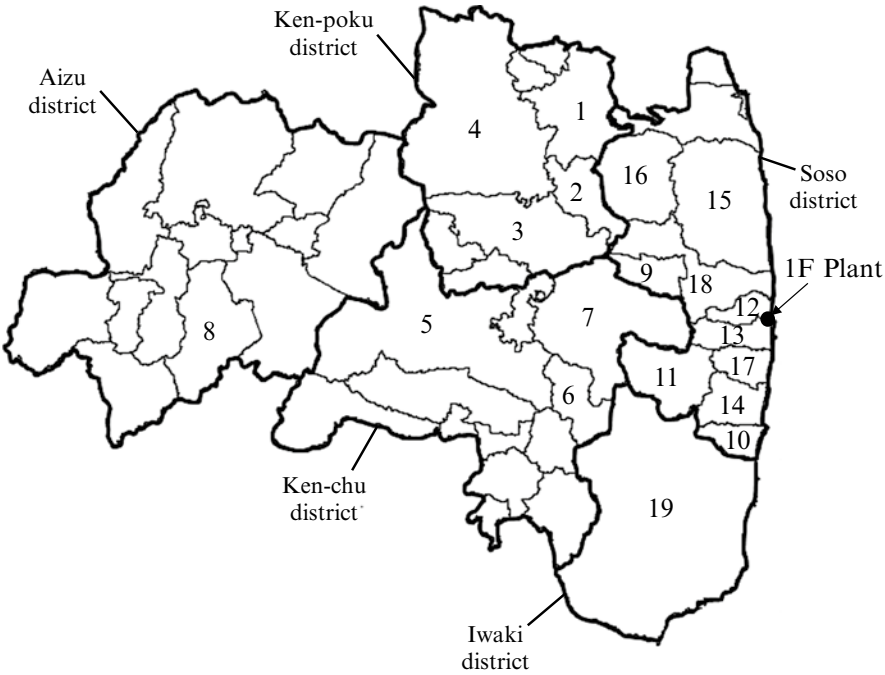

Fig. 18.1 Municipalities related to the 18 evacuation scenarios and area classification of Fukushima Prefecture. The numbers shown in this map represent municipalities listed in Table 18.5

The doses from inhalation of noble gases and radioactive materials resuspended from the ground surface were not included in the assessments. This assumption was adopted according to a World Health Organization (WHO) report [2], which mentions such inhalations are not expected to provide a significant contribution to radiation exposure. Also, the doses from cloudshine caused by noble gases cannot be considered in the present study. In addition, internal radiation doses from ingestion pathways were not included. The measurements of the doses resulting from the ingestion of contaminated food and water are being performed using a whole-body counter. The doses acquired from the ingestion pathway should be assessed with considerations about the results of measurements in the future.

18.2.2 Probabilistic Techniques in Radiation Dose Assessment

In the present study, we used a probabilistic approach to assess the doses to the public living in areas contaminated by radioactive materials released from the 1F Plant. Probabilistic approach in exposure assessments, which are a well-established

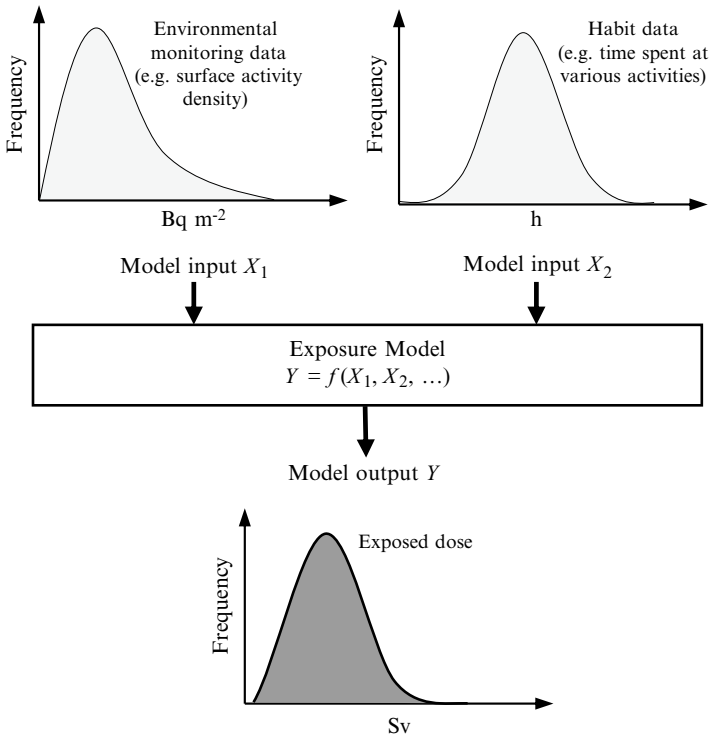

Fig. 18.2 Schematic illustrating the application of probabilistic approach to assess radiation doses

method to describe a diverse set of environmental hazards, can yield a fuller characterization of the information on the dose distributions in the population [4–8]. Application of this approach needs statistically characterized data on the contributors, such as the concentrations of radionuclides in environmental media data and habits data relevant to the exposure pathways [8].

Figure 18.2 illustrates the general process of applying a probabilistic approach to assess radiation doses. One sample from each input distribution is selected based on the statistical characteristics, and the set of samples is entered into the model. The process is repeated until the specified numbers of model iterations have been completed. As a result, it is possible to represent a distribution of the output of a model by generating sample values for the model input. In the present study, we used the probabilistic distributions of surface activity of ^{137}Cs and time the people spent outdoors as input of the calculations of doses.

Table 18.2 Parameters for location factors of cesium for an urban environment [11]

Type of location	$a_{l,1}$	$a_{l,2}$	T_l (years)
Virgin land	0.32	0.68	1.4
Dirt surface	0.50	0.25	2.2
Asphalt	0.56	0.12	0.9

18.2.3 Models for Assessing Doses from External and Internal Exposures

18.2.3.1 External Exposure to Deposited Radionuclides

The effective dose received by population group j from groundshine E_j^{gd} in each municipality listed in the evacuation scenarios is represented by

$$E_j^{gd} = \sum_l \left\{ \int f_l(t) \cdot \left\{ s_{gd} \cdot p_{l,in,j} + p_{l,out,j} \right\} \cdot \dot{E}_{\mathrm{v}}^{gd}(t) \mathrm{d}t \right\}, \tag{18.1}$$

where j is the index for population types; l is the index for location types; $\dot{E}_{\mathrm{v}}^{gd}(t)$ is the effective dose rate from groundshine at locations of virgin land in the urban environment (Sv h^{-1}); $f_l(t)$ is the location factor for urban locations of type l, $p_{l,\text{in (or out)},j}$ is the ratio of time spent indoors (or outdoors) at location type l to that of the assessment period; and s_{gd} is the shielding factor for groundshine.

The index l for location types represents virgin land, dirt surfaces, and asphalt, which are classified according to the characteristics of the ground surface [9–11]. The location factors are defined by dividing the dose rates at a given location by those at an open undisturbed field [9–11]. The location factors are represented as a function of the time elapsed after the contamination, as follows:

$$f_l(t) = a_{l,1} \cdot \exp\left(-\frac{\ln 2}{T_l} \cdot t \right) + a_{l,2}, \tag{18.2}$$

where $a_{l,1}$, $a_{l,2}$, and T_l are fitting parameters for the location factors of cesium. The values of these parameters are listed in Table 18.2; they were determined from data obtained from the Chernobyl accident [11].

The ratio of time spent at location type l for the assessment period was defined as a fraction of the average time spent in a day at location l, as follows:

$$p_{l,in(or\,out),j} = \frac{t_{l,in(or\,out),j}}{24}, \tag{18.3}$$

where $t_{l,\text{in(or out)},j}$ is the time spent indoors (or outdoors) in a day at location l by an individual of population group j.

In the present study, the calculations were performed for indoor workers, outdoor workers, and pensioners on the assumption that they live in the urban areas. It is assumed that indoor workers and pensioners spend all day in areas paved with asphalt. However, it is assumed that outdoor workers spend their working hours in areas classified as dirt surfaces in an urban environment.

The values of $t_{l,\mathrm{in(or\ out)},j}$ were determined by generating random numbers in accordance with the probabilistic distribution functions obtained from the surveys in Fukushima Prefecture. In the survey we measured time spent indoors and outdoors for the three population groups of indoor workers, outdoor workers, and pensioners. The indoor workers surveyed were from the Fukushima City office and the outdoor workers were from the Northern Fukushima affiliate of Contractors Association and Japan Agricultural Cooperatives. In the present study, data surveyed for the month of February, March, and April 2012 were used.

To determine the distribution form of time spent outdoors of each population group, normality tests were performed for time spent outdoors in a day and its logarithmic values. When the normality was examined for the logarithmic values of that of indoor workers, the results of the p values were more than 5 %. Log-normal distribution was thus assumed for the time spent outdoors by indoor workers. Hereafter, the significance level of 5 % is used to determine whether the null hypothesis is rejected. The results of similar analyses performed for time spent outdoors of the other population groups indicated that the distribution was normal for outdoor workers and log-normal for pensioners. The statistical values to determine the probabilistic distribution functions of $t_{l,\mathrm{in(or\ out)},j}$ are listed in Table 18.3.

The shielding factor s_{gd} for gamma radiation from deposited radionuclides is defined as the ratio of ambient doses inside a house to those outside. Figure 18.3 shows the correlation between the ambient dose rate measured inside and outside houses. The dosimetric surveys were made for 130 households in Fukushima Prefecture during a period between October 2 and November 11, 2012. The breakdown of building types is as follows: 124 one- or two-story wood frame houses, and 6 concrete houses with one or more stories. The calculations were performed using a shielding factor s_{gd} of 0.4. This value were determined conservatively based on the ratio of the ambient dose rate measured inside and those measured outside (Fig. 18.3).

The effective dose rate from groundshine at locations of virgin land is given by the following form:

$$\dot{E}_{\mathrm{v}}^{gd}(t) = r(t)\sum_{i}\left\{k_{gd,i}\cdot C_i\cdot A_{Cs137}(0)\cdot\exp\left(-\lambda_i\cdot t\right)\right\}, \tag{18.4}$$

where $r(t)$ is the attenuation function of dose rate from migration of ^{137}Cs into the soil; C_i is the ratio of the surface activity density of radionuclide i to that of ^{137}Cs; A_{Cs137} (0) is the initial value of the surface activity density of ^{137}Cs (Bq m^{-2}); λ_i is the decay constant for radionuclide i (h^{-1}); and $k_{\mathrm{gd},i}$ is the effective dose coefficient from surface density activity ((Sv h^{-1})/(Bq m^{-2})).

Table 18.3 Statistical values to determine the probabilistic distribution functions of time spent outdoors for each population group

Population group[a]	Distribution form	Mean (h)	Deviation
Indoor worker	Log-normal	0.57[b]	3.28[d]
Outdoor worker	Normal	6.97[c]	2.90[e]
Pensioner	Log-normal	1.27[b]	3.37[d]

[a]Indoor worker means Fukushima City office workers; outdoor worker includes construction workers and farmers
[b]GM
[c]AM
[d]GSD
[e]SD

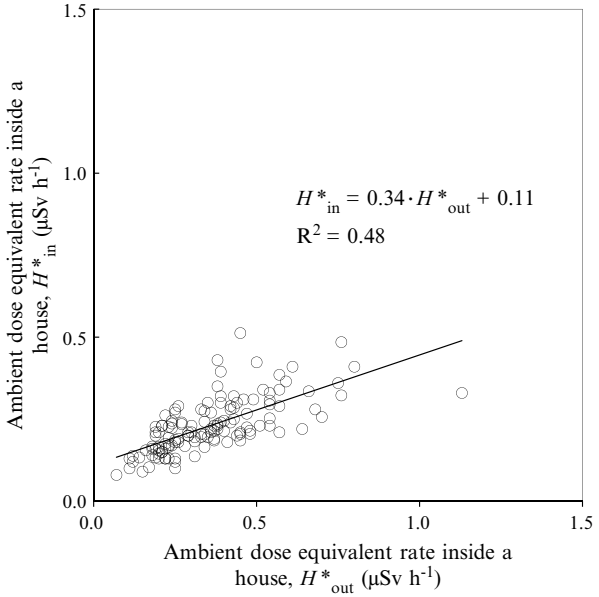

Fig. 18.3 Correlation between ambient dose equivalent rates measured inside and outside houses

The attenuation function $r(t)$ is given by the following equation [2, 9–12]:

$$r(t) = p_1 \cdot \exp\left(-\frac{\ln 2}{T_1} \cdot t\right) + p_2 \cdot \exp\left(-\frac{\ln 2}{T_2} \cdot t\right). \tag{18.5}$$

The parameter values were $p_1 = 0.34$, $p_2 = 0.66$, $T_1 = 1.5$ years, and $T_2 = 50$ years [2, 12].

Radioactive fallout and contamination in most of the contaminated areas of Fukushima Prefecture were estimated to have occurred on March 15 or 16, 2011 because the gamma dose rate in air suddenly increased over the background radiation rates during these days [13]. In the present study, the doses were assessed

Table 18.4 Composition of radionuclides deposited on March 15, 2011 [2]

Radionuclides	Deposited activity normalized by ^{137}Cs
^{131}I	11.7
^{132}I	–[a]
^{132}Te	8.0
^{134}Cs	0.94
^{136}Cs	0.2
^{137}Cs	1.0
^{140}Ba	0.1
^{140}La	–[a]
^{110m}Ag	0.01
^{129m}Te	1.5

[a]Activity of ^{132}I and ^{140}La was derived from that of the parent nuclide, i.e., ^{132}Te and ^{140}Ba, assuming radioactive equilibrium

with the assumption that the contamination occurred at 00:00 on March 15, 2011.[2] The ratio of the surface activity density of each radionuclide i to that of ^{137}Cs was determined according to the report of WHO [2]. The relative isotopic composition of deposited radionuclides is listed in Table 18.4.

Equation (18.4) was calculated using values of $A_{Cs137}(0)$ produced by the random number generator according to the distributions of the measured surface density of ^{137}Cs for each municipality listed in the evacuation scenarios. The distributions of the surface activity density of ^{137}Cs on March 15, 2011 were derived from the monitoring data measured by MEXT[3] [14]. The soil samples were collected from a 5-cm surface layer within 80 km of the 1F Plant.[4] In principle, the measurements were conducted at a single location per 2×2 km^2 grid for these areas. The details of the surface density of ^{137}Cs are discussed in Sect. 18.2.4. The effective dose coefficients were obtained from a U.S. Environmental Protection Agency (EPA) report [16].

18.2.3.2 External Exposure to the Radioactive Cloud

The effective dose received by population group j from cloudshine E_j^{cd} is represented by

$$E_j^{cd} = p_{in,j} \cdot s_{cd} \cdot E_{out}^{cd} + p_{out,j} \cdot E_{out}^{cd}, \tag{18.6}$$

[2] The data presented in this paper used Japan Time [i.e., Greenwich mean time (GMT) plus 9 h].

[3] MEXT is the abbreviation for the Ministry of Education, Culture, Sports, Science and Technology of Japan.

[4] The soil samples had been collected prior to the rainy season in Japan, from June 6 to June 14 and from June 27 to July 8, 2011, so that the level of contamination could be observed before any changes occurred on the soil surface [15].

where $p_{\mathrm{in},j}$ is the ratio of time spent indoors; $p_{\mathrm{out},j}$ is the ratio of time spent outdoors; $E_{\mathrm{out}}{}^{\mathrm{cd}}$ is the effective dose from cloudshine outdoors (Sv); and s_{cd} is shielding factor for cloudshine from radionuclides in the radioactive cloud.

The ratio of time spent indoors or outdoors was calculated as the total time spent indoors or outdoors in various locations per day. To calculate the external doses from the radioactive cloud, $E_{\mathrm{out}}{}^{\mathrm{cd}}$, it was necessary to convert the surface density of radionuclides to time-integrated activity concentrations in air. Noble gases, which do not deposit on the ground surfaces, were not included in the calculations.

The effective dose from cloudshine outdoors, $E_{\mathrm{out}}{}^{\mathrm{cd}}$, is represented as follows:

$$E_{out}^{cd} = \sum_i \left(\frac{C_i \cdot A_{Cs137}(0)}{V_i} \right) \cdot k_{cd,i}, \tag{18.7}$$

where V_i is the bulk deposition velocity of radionuclide i (m s^{-1}) and $k_{\mathrm{cd},i}$ is the effective dose coefficient for air submersion of radionuclide i (Sv/(Bq s m^{-3}).

The deposition velocity V_i is determined according to the method in the WHO preliminary report [2]. The areas in which the surface density of ^{137}Cs, A_{Cs137}, is higher than or equal to 30 kBq m^{-2} were treated as being contaminated through wet deposition, with deposition velocities of $V_{\mathrm{I\text{-}131}} = 0.07$ m s^{-1} for ^{131}I and $V_{\mathrm{other}} = 0.01$ m s^{-1} for other radionuclides. If the surface density A_{Cs137} is less than 30 kBq m^{-2}, then the contamination originated from dry deposition with deposition velocities of $V_{I\text{-}131} = 0.01$ m s^{-1} for ^{131}I and $V_{\mathrm{other}} = 0.001$ m s^{-1} for other radionuclides. The doses from cloudshine and inhalation were calculated using the surface densities of ^{137}Cs in the municipality where the inhabitants stayed while the radioactive plumes passed.

The value of 0.6 was used as the shielding factor s_{cd} for gamma radiation from the radioactive plume [17]. The effective dose coefficients $k_{\mathrm{cd,i}}$ were obtained from an EPA report [16].

18.2.3.3 Internal Exposure Through Inhalation of Radionuclides

The effective dose received by the population group j from internal exposure through inhalation of radionuclide i in the radioactive cloud E_j^{inh} is represented by

$$E_j^{inh} = p_{l,in,j} \cdot f \cdot E_{out}^{inh} + p_{l,out,j} \cdot E_{out}^{inh}, \tag{18.8}$$

where $E_{\mathrm{out}}^{\mathrm{inh}}$ is the effective dose from inhalation of radionuclide i in the radioactive cloud (Sv); f is the filtering factor for a house.

To prevent underestimation of doses in the calculation, the value of 1 was adopted for the filtering factor f. $E_{\mathrm{out}}^{\mathrm{inh}}$ is given as

$$E_{out}^{inh} = \sum_i \left(\frac{C_i \cdot A_{Cs137}(0)}{V_i} \right) \cdot B \cdot k_{inh,i}, \tag{18.9}$$

where B is the breathing rate for adults (L day^{-1}) and $k_{\mathrm{inh},i}$ is the effective dose coefficient for inhalation of radionuclides i (Sv Bq^{-1}).

The value of 22.2 L day^{-1} was adopted as the breathing rate of adults from the recommendation of the International Commission on Radiological Protection (ICRP) Publication 71 [18]. The effective dose coefficients for inhalation were also obtained from the same publication [18].

18.2.4 Input Monitoring Data of the Surface Activity Density of ^{137}Cs

To determine the distribution form of the surface density of ^{137}Cs, normality tests were performed for the logarithmic values of the surface density for each municipality. The data measured by MEXT [14] were used for the tests, which decay corrected to 0:00 on March 15, 2011. The p values of the tests for municipalities other than Fukushima City, Koriyama City, Nihonmatsu City, Tamura City, and Namie Town were higher than the significance level of 5 %, so the null hypothesis was not rejected.[5] The normality tests for Fukushima City and Namie Town yielded p values of 0.044 and 0.036, respectively. Because the values were close to 5 %, these two municipalities were treated in the same manner as those without normality rejection. Therefore, log-normal distribution was assumed for the surface density of ^{137}Cs for these municipalities.

The p values of the tests for the distributions for Koriyama City, Nihonmatsu City, and Tamura City were considerably lower than the significance level of 5 %. Thus, the null hypothesis for these tests was rejected. Although the following calculations assume log normality in the surface density distributions for municipalities including Koriyama City, Nihonmatsu City, and Tamura City, attention should be paid to the limitations already mentioned.

The geometric mean (GM) and geometric standard deviation (GSD) of the surface densities for each municipality of Fukushima Prefecture are listed in Table 18.5. Futaba Town, Okuma Town, and Namie Town are the most highly contaminated areas, and the values of the GM for the surface densities of ^{137}Cs are 1.53, 1.23, and 0.97 MBq m^{-2}, respectively. The next most highly contaminated municipalities are Iitate Village, Tomioka Town, and Katsurao Village, whose surface densities are 0.61, 0.60, and 0.26 MBq m^{-2}, respectively. The surface density levels of ^{137}Cs for the other municipalities of the Soso area, that is, Hirono Town, Kawauchi Village, Naraha Town, and Minami Soma City, are comparable to the levels for the municipalities in the Ken-poku and Ken-chu districts.

The surface densities of ^{137}Cs in municipalities in the Ken-poku and Ken-chu districts are about 0.1 and 0.02–0.07 MBq m^{-2}, respectively. The surface density of ^{137}Cs for the Iwaki City was the lowest among the values for the municipalities listed in the evacuation scenarios.

[5] In other words, it concludes that the surface density data for these municipalities are from a lognormal-distributed population.

Table 18.5 Surface density of ^{137}Cs for each municipality of Fukushima Prefecture

Area	Municipality		Sample size	GM (Bq m^{-2})	GSD
Ken-poku District	1	Date City	60	1.29E+05	1.94E+00
	2	Kawamata Town	38	1.40E+05	1.87E+00
	3	Nihonmatsu City	82	1.20E+05	2.00E+00
	4	Fukushima City	94	1.25E+05	2.13E+00
Ken-chu District	5	Koriyama City	118	6.76E+04	2.71E+00
	6	Ono Town	31	2.16E+04	1.48E+00
	7	Tamura City	109	3.78E+04	2.81E+00
Aizu District	8	Aizu Misato Town	2	1.22E+04	1.34E+00
Soso District	9	Katsurao Village	18	2.56E+05	1.94E+00
	10	Hirono Town	14	6.79E+04	1.77E+00
	11	Kawauchi Village	37	1.01E+05	2.42E+00
	12	Futaba Town	9	1.53E+06	3.67E+00
	13	Okuma Town	14	1.23E+06	3.90E+00
	14	Naraha Town	16	9.18E+04	2.61E+00
	15	Minami Soma City	78	1.06E+05	2.81E+00
	16	Iitate Village	53	6.08E+05	1.77E+00
	17	Tomioka Town	16	5.98E+05	2.90E+00
	18	Namie Town	38	9.66E+05	4.02E+00
Iwaki District	19	Iwaki City	266	2.15E+04	2.14E+00

18.3 Results and Discussion

18.3.1 Estimated Effective Doses

18.3.1.1 Effective Dose in the First Year After the Contamination Event

To assess doses, the set of values for time spent outdoors, $t_{l,\mathrm{out},j}$, and initial value of the surface activity density of ^{137}Cs, A_{Cs137} (0), was selected based on the statistical characteristics using the global sensitivity analysis code GSALab [19], which was developed by the Japan Atomic Energy Agency (JAEA). The calculations of doses were performed by 10,000 sets of sample values. Relative errors of these calculations were less than 0.05.

Table 18.6 lists the 50th and 95th percentiles of the effective doses in the first year after the contamination, which were obtained from the probabilistic assessment. The following discussions are based on the 95th percentile.

The effective doses received by the population groups of Namie Town and Iitate Village in the first year after the contamination were estimated to be in the 10–50 mSv dose band. Namie Town had two evacuation scenarios, nos. 7 and 13. In evacuation scenario 7, the inhabitants were rapidly evacuated on March 16, 2011. On the other hand, the evacuation of Namie Town according to scenario 13 was implemented 7 days after evacuation scenario 7. The difference in the annual effective doses

Table 18.6 Effective doses in the first year after the contamination[a] (mSv)

	Evacuation scenario no.		Pensioner	Indoor worker	Outdoor worker	WHO[b]
Tomioka Town	1	50th–95th percentile	1.3–5.4	1.3–5.0	1.8–8.1	–
		Groundshine (%)	91	90	94	
		Cloudshine (%)	1	1	0	
		Inhalation (%)	8	9	6	
Okuma Town	2	50th–95th percentile	0.74–3.3	0.71–3.0	1.0–4.8	–
		Groundshine (%)	89	88	92	
		Cloudshine (%)	1	1	1	
		Inhalation (%)	10	11	7	
Futaba Town	3, 4	50th–95th percentile	0.45–1.2	0.43–1.2	0.54–1.5	–
		Groundshine (%)	65	64	71	
		Cloudshine (%)	2	2	2	
		Inhalation (%)	33	34	27	
Hirono Town	10	50th–95th percentile	0.55–0.81	0.53–0.75	0.72–1.1	–
		Groundshine (%)	69	68	76	
		Cloudshine (%)	2	2	2	
		Inhalation (%)	29	30	22	
Naraha Town	5	50th–95th percentile	0.72–2.6	0.69–2.3	0.98–4.0	1–10
		Groundshine (%)	87	86	91	
		Cloudshine (%)	1	1	1	
		Inhalation (%)	12	13	8	
	6	50th–95th percentile	0.34–0.53	0.33–0.50	0.44–0.68	
		Groundshine (%)	63	61	71	
		Cloudshine (%)	3	3	2	
		Inhalation (%)	34	36	27	
Namie Town	7	50th–95th percentile	4.3–18	4.1–17	5.7–21	10–50
		Groundshine (%)	61	60	69	
		Cloudshine (%)	3	3	2	
		Inhalation (%)	36	37	29	
	13	50th–95th percentile	6.2–39	6.0–37	8.4–52	
		Groundshine (%)	79	78	84	
		Cloudshine (%)	1	1	1	
		Inhalation (%)	20	21	15	
Minami Soma City	9	50th–95th percentile	2.5–6.1	2.4–5.7	3.5–9.3	1–10
		Groundshine (%)	94	93	96	
		Cloudshine (%)	0	1	0	
		Inhalation (%)	6	6	4	
	17	50th–95th percentile	1.9–9.9	1.8–9.2	2.7–15	
		Groundshine (%)	93	93	95	
		Cloudshine (%)	1	0	0	
		Inhalation (%)	6	7	5	

(continued)

Table 18.6 (continued)

	Evacuation scenario no.		Pensioner	Indoor worker	Outdoor worker	WHO[b]
Iitate Village	15	50th–95th percentile	6.7–16	6.5–14	9.3–22	10–50
		Groundshine (%)	90	89	92	
		Cloudshine (%)	1	1	1	
		Inhalation (%)	9	10	7	
	16	50th–95th percentile	7.3–17	6.9–16	9.9–24	
		Groundshine (%)	90	90	93	
		Cloudshine (%)	1	1	1	
		Inhalation (%)	9	9	6	
Tamura City	8	50th–95th percentile	1.2–4.5	1.2–4.1	1.7–6.8	–
		Groundshine (%)	92	92	95	
		Cloudshine (%)	1	1	0	
		Inhalation (%)	7	7	5	
Kawamata Town	18	50th–95th percentile	2.5–6.8	2.3–6.3	3.5–9.5	–
		Groundshine (%)	94	93	95	
		Cloudshine (%)	0	1	0	
		Inhalation (%)	6	6	5	
Kawachi Village	11	50th–95th percentile	1.4–5.5	1.3–5.0	1.9–8.3	–
		Groundshine (%)	91	90	94	
		Cloudshine (%)	1	1	0	
		Inhalation (%)	8	9	6	
Katsurao Village	12	50th–95th percentile	2.2–7.5	2.0–6.5	3.1–11	1–10
		Groundshine (%)	94	93	96	
		Cloudshine (%)	0	1	0	
		Inhalation (%)	6	6	4	
	14	50th–95th percentile	3.0–7.2	2.8–6.7	4.1–11	
		Groundshine (%)	90	89	93	
		Cloudshine (%)	1	1	1	
		Inhalation (%)	9	10	6	
Fukushima City	–[c]	50th–95th percentile	2.2–7.5	2.1–6.9	3.1–11	–
		Groundshine (%)	94	94	95	
		Cloudshine (%)	0	0	0	
		Inhalation (%)	6	6	5	
Koriyama City	–[c]	50th–95th percentile	1.2–5.5	1.1–5.4	1.7–8.6	–
		Groundshine (%)	92	91	94	
		Cloudshine (%)	1	1	1	
		Inhalation (%)	7	8	5	
Iwaki City	–[c]	50th–95th percentile	0.55–1.3	0.53–1.2	0.72–1.9	1–10
		Groundshine (%)	78	77	84	
		Cloudshine (%)	2	2	1	
		Inhalation (%)	20	21	15	

[a]Contributions of exposure pathways were calculated using the arithmetic mean of the distributions of each pathway

[b]It is noted that the estimated values by WHO include contributions of internal exposures from ingestion of radionuclides in food and water

[c]The calculations of doses were performed with the assumption that the inhabitants had lived continuously in these cities during the first year after the contamination occurred

Table 18.7 Effective lifetime doses (60 years) (mSv)

	Pensioner 50th–95th percentile	Indoor worker 50th–95th percentile	Outdoor worker 50th–95th percentile
Fukushima City	5.2–18	4.9–16	9.3–34
Koriyama City	2.8–14	2.7–13	5.0–26
Iwaki City	1.1–3.0	1.1–2.8	1.8–5.8

between the rapid evacuation (scenario 7) and the deliberate evacuation (scenario 13) is almost double for each population group. This result indicates that the doses received by the population living in the highly contaminated area were significantly influenced by the delayed evacuation at the early phase after the contamination.

However, there was no significant difference among the evacuation scenarios for inhabitants living in Iitate Village. The entire population of Iitate Village was evacuated 2–3 months after the accident onset. Thus, most of the inhabitants had already been exposed to radiation before they were evacuated to Fukushima City. In our estimations, about 80 % of the effective doses received by the inhabitants living in Iitate Village throughout the first year were delivered before the evacuation was implemented.

In addition, the effective doses received by outdoor workers had the potential to be above 10 mSv for 1 year after the contamination in Minami Soma City, Katsurao Village, and Fukushima City. The effective doses received by the inhabitants evacuated according to scenarios 1–5, 8–12, 14, and 18 and to the inhabitants living in Koriyama City and Iwaki City were assessed to be in the 1–10 mSv dose band. The contributions to the annual effective dose from the doses received in the final evacuation facilities in the municipalities ranged from 60 % to 75 % for each scenario.

The effective doses reported by WHO [2] are shown in Table 18.6. The effective doses received by inhabitants living in Iitate Village and Namie Town in the first year after the accident are estimated to be in the 10–50 mSv dose band. At other locations considered in Fukushima Prefecture, the effective doses are estimated to be in the 1–10 mSv dose band. The range of the assessed values in this chapter corresponds approximately to that of the results reported by WHO [2]. In addition, NIRS [3] reported the external doses received by the evacuees during the 4 months after the accident. The results reported by NIRS cannot be compared directly with the assessed values in this chapter because the period subject to assessment is different. The results of this chapter, however, are consistent with the results reported by NIRS [3].

18.3.1.2 Effective Lifetime Doses

The lifetime doses received by the inhabitants of Fukushima City, Koriyama City, and Iwaki City are listed in Table 18.7. The values of the 95th percentile of the effective doses to the three population groups are 16–34, 13–26, and 2.8–5.8 mSv in Fukushima City, Koriyama City and Iwaki City, respectively. For each city, 20–30 % of the lifetime effective dose was delivered during the first year.

18.3.2 Contributions of Different Exposure Pathways

For evacuation scenarios 10, and the continuously living scenario of Iwaki City, the contributions of doses through inhalation range from 15 % to 30 %. Because the doses for these evacuation scenarios were calculated under the condition that radionuclides were deposited on dry property, the deposition velocities are less than those for average scenarios with a wet property. Thus, the dose contributions through inhalation are larger than those in average scenarios.

For evacuation scenarios 3 and 4, the inhabitants of Futaba Town were evacuated to Saitama Prefecture on March 19, 2011. The contamination level in Saitama Prefecture is considerably lower than that in Fukushima Prefecture. Therefore, the prolonged doses from groundshine after the evacuation to Saitama Prefecture are small. Consequently, the dose contributions through inhalation are larger than those in the other average scenarios.

The inhabitants of Namie Town were evacuated according to evacuation scenarios 7 and 13. These inhabitants received doses through internal exposure before evacuation from the highly contaminated area. Therefore, the doses through this pathway are larger than those through external exposure to groundshine in Nihonmatsu City after evacuation.

Contributions of the doses from groundshine and inhalation to the annual effective dose are 85–95 % and 5–15 %, respectively. The contributions from cloudshine are much less than those from groundshine and inhalation. For several evacuation scenarios, the contribution of inhalation is larger than that already mentioned.

18.4 Conclusions

The present study assessed radiation doses in the first year after the contamination and over inhabitants' lifetimes caused by external exposure to groundshine and cloudshine as well as those from internal exposures through inhalation. To assess the doses realistically and comprehensively, a probabilistic approach was employed using data that reflected realistic environmental trends and lifestyle habits in Fukushima Prefecture.

The 95th percentile of the estimated annual effective dose for most of the population living in the municipalities listed in the evacuation scenarios was in the 1–10 mSv dose band. However, the doses received by some outdoor workers living in Minami Soma City, Katsurao Village, and Fukushima City could exceed 10 mSv. In addition, the inhabitants of Namie Town and Iitate Village were exposed to radiation doses in the 10–50 mSv dose band. These results suggest that the doses received by the population living in the highly contaminated area were significantly influenced by the delay in evacuation in the early phase after the contamination.

Contributions of the groundshine and inhalation doses to the annual effective dose are about 85–95 % and 5–15 %, respectively. However, the contributions from

these pathways vary depending on deposition conditions, timing of evacuations, and differences in the contamination level of the ground surface.

In addition, the values of the 95th percentile of the lifetime effective doses received by the inhabitants of Fukushima City, Koriyama City, and Iwaki City are 16–34, 13–26, and 2.8–5.8 mSv. For each city, 20–30 % of the lifetime effective dose was delivered during the first year after the contamination.

It is noted that these calculations were performed on the basis of some important assumptions regarding the input data, assessment model, and model parameters. The doses must be assessed by iterative processes that reflect site-specific and realistic information derived from further investigations.

References

1. Nuclear Emergency Response Headquarters Government of Japan (2011) Report of Japanese government to the IAEA ministerial conference on nuclear safety [online]. http://www.kantei.go.jp/foreign/kan/topics/201106/iaea_houkokusho_e.html. Accessed 31 Oct 2012
2. WHO (2012) Preliminary dose estimation from the nuclear accident after the 2011 Great East Japan Earthquake and Tsunami. World Health Organization [online]. http://apps.who.int/iris/bitstream/10665/44877/1/9789241503662_eng.pdf. Accessed 31 Oct 2012
3. NIRS (2012) Estimation of doses from external exposure, website of Fukushima prefecture [online]. http://www.pref.fukushima.jp/imu/kenkoukanri/231213senryosuikei.pdf. Accessed 31 Oct 2012 (in Japanese)
4. IAEA (1989) Evaluating the reliability of predictions made using environmental transfer models, vol 100, International Atomic Energy Agency: safety series. International Atomic Energy Agency, Vienna
5. Finley B, Paustenbach D (1994) The benefits of probabilistic exposure assessment: three case studies involving contaminated air, water, and soil. Risk Anal 14:53–73
6. USEPA (1997) Guiding principles for Monte Carlo analysis. EPA/630/R-97/001. Risk Assessment Forum, Washington, DC
7. Cullen AC, Frey HC (1999) Probabilistic techniques in exposure assessment: a handbook for dealing with variability and uncertainty in models and inputs. Plenum, New York
8. ICRP (2006) Assessing dose of the representative person for the purpose of radiation protection of the public. ICRP publication 101. Part 1. Ann ICRP 36:5–62
9. Jacob P, Likhtarev I (1996) Pathway analysis and dose distributions. European Commission, Brussels
10. Golikov V, Balonov M, Erkin V, Jacob P (1999) Model validation for external doses due to environmental contaminations by the Chernobyl accident. Health Phys 77:654–661
11. Golikov VY, Balonov MI, Jacob P (2002) External exposure of the population living in areas of Russia contaminated due to the Chernobyl accident. Radiat Environ Biophys 41:185–193
12. Likhtarev IA, Kovgan LN, Jacob P, Anspaugh LR (2002) Chernobyl accident: retrospective and prospective estimates of external dose of the population of Ukraine. Health Phys 82:290–303
13. Fukushima Prefecture (2012) Results of radioactivity measurement in 7 districts of Fukushima prefecture [online]. http://wwwcms.pref.fukushima.jp/pcp_portal/PortalServlet?DISPLAY_ID=DIRECT&NEXT_DISPLAY_ID=U000004&CONTENTS_ID=27468. Accessed 31 Oct 2012

14. MEXT (2011) Readings of radioactive cesium concentration in soil, website of ministry of education, culture, sports, science and technology [online]. http://www.mext.go.jp/b_menu/shingi/chousa/gijyutu/017/shiryo/__icsFiles/afieldfile/2011/09/02/1310688_1.pdf. Accessed 31 Oct 2012 (in Japanese)
15. MEXT (2011) Preparation of distribution map of radiation doses, etc. Map of radioactive cesium concentration in soil by MEXT [online]. http://radioactivity.mext.go.jp/old/en/1750/2011/08/1750_083014.pdf. Accessed 31 Oct 2012
16. USEPA (1993) External exposure to radionuclides in air, water and soil. Federal Guidance Report No. 12
17. NSC (2007) Emergency preparedness of nuclear installations. Nuclear Safety Commission of Japan (in Japanese)
18. ICRP (1995) Age-dependent doses to members of the public from intake of radionuclides: inhalation dose coefficients: Part 4. Inhalation dose coefficients. ICRP publication 71. Ann ICRP 25
19. Liu Q, Homma T, Nishimaki Y, Hayashi H, Terakado M, Tamura S (2010) GSALab computer code for global sensitivity analysis. Japan Atomic Energy Agency, JAEA-Data/Code 2010–001 (in Japanese)

Chapter 19
Reduction of External Exposure for Residents from the Fukushima Nuclear Accident by Weathering and Decontamination

Hiroko Yoshida

Abstract External exposure for residents resulting from the Fukushima nuclear accident was measured in the Marumori and Kosugo regions for the period from September 2011 to March 2013 after the occurrence of the Fukushima nuclear accident. Marumori is a rural settlement, and Kosugo is a suburban city along a freeway. The initial substantial reduction in personal dose equivalent [Hp(10)] for Marumori residents, which was in accordance with the reduction in the air dose rate, was observed. Both values of the Hp(10) results and the air dose rates dropped and remained low during the heavy snow season. The values returned to previous levels and then followed a relatively faster reduction than the radioactive decay rate of ^{134}Cs and ^{137}Cs after the snow had thawed. These faster reductions are considered to be caused by weathering from snow melting or migration of radionuclides down the soil column. However, neither a drop resulting from an accumulation of snow nor faster reduction was observed in Hp(10) for Kosugo residents, except the reduction from the radiocesium decay, although the same reduction tendency as that in Marumori was observed in the air dose rates. The discrepancy between the air dose rate and Hp(10) for Kosugo residents might be caused by dose contributions from the fixed contamination in houses in the suburban environment. The effects of schoolyard decontamination on the Hp(10) values for schoolchildren in Kosugo have been observed in the readings recorded since October 2012, and dose reduction was evaluated as approximately 10–20 μSv/month on average.

Keywords Air dose rate • Decontamination • External exposure • Fukushima accident • Reduction • Residents • Weathering

H. Yoshida (✉)
Graduate School of Pharmaceutical Sciences, Tohoku University,
6-3 Aramaki-Aoba, Aoba-ku, Sendai, Miyagi 980-8578, Japan
e-mail: hiroko@m.tohoku.ac.jp

S. Takahashi (ed.), *Radiation Monitoring and Dose Estimation of the Fukushima Nuclear Accident*, DOI 10.1007/978-4-431-54583-5_19,

19.1 Introduction

The magnitude 9.0 earthquake and tsunami that occurred on 11 March 2011 in Japan resulted in severe damage to the Fukushima Daiichi nuclear power plant (NPP), and this disaster caused a month-long release of radioactive materials into the atmosphere. Aerial measurements reported by the Ministry of Education, Culture, Sports, Science and Technology, Japan (MEXT) survey showed that the major radioactive plumes spread in the northwest direction from the NPP, causing significant radionuclide deposition in that area. Marumori and Kosugo, which are located in Miyagi, a neighboring prefecture to Fukushima, are near the border between Miyagi and Fukushima. Marumori is located 46 km northwest of the NPP at the closest approach (Fig. 19.1). A distribution map of the radioactivity concentration in the soil [1] published by MEXT (Nuclear Regulation Authority after 1 April 2013) showed the presence of several radioactive plumes in this area, and the ^{137}Cs deposition level ranged from 100 to 300 kBq/m^2. After the decay of ^{131}I (with a half-life of 8 days), radiation doses since June can be primarily attributed to Cs nuclides. When an initial substantial reduction in the air dose rate is observed, which is expected to occur as a result of weathering, physical decay, and migration of radionuclides down the soil column [2–4], the dose for residents is expected to reduce in the same pattern. External exposure to radionuclides deposited in the environment was in many cases one of the dominant contributions to the total dose to the public after the accidental release of the radioactive material into the atmosphere. Internal exposure also contributed to the total dose. The main pathways of internal

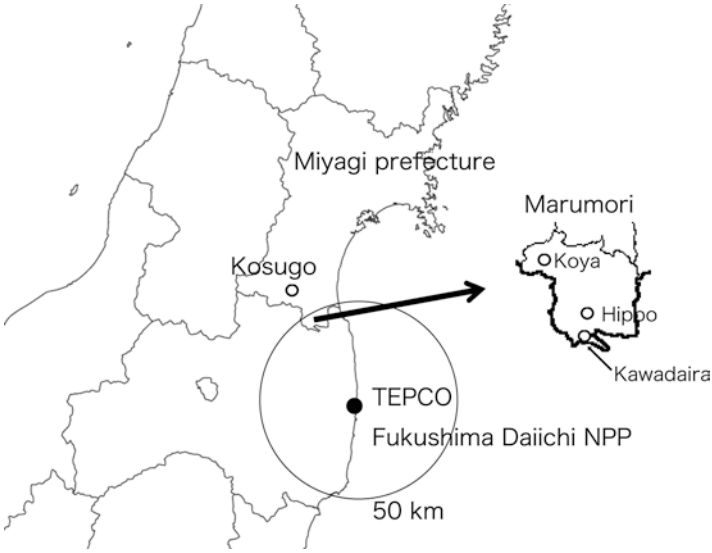

Fig. 19.1 Locations of Marumori and Kosugo. The territories studied in Marumori were geographically divided into three regions: Kawadaira, Hippo and Koya

exposure to residents were inhalation and ingestion. The environmental radioactivity level (fallout) [5] measured by the prefecture showed that the fallout (^{131}I, ^{134}Cs, and ^{137}Cs) was basically not detectable or that small amounts of radiocesium were sometimes detected in all prefectures including Fukushima from the end of June. Therefore, on 1 September 2011, when measurements were initiated, there was no longer a high possibility of being exposed to the source through inhalation.

In this study, the values of air dose rates (ambient dose equivalents [$H^*(10)$]) in Marumori and Kosugo regions were analyzed to investigate their temporal variation from Cs nuclides. The personal dose equivalent [$H_p(10)$] for residents in those regions was evaluated using optically stimulated luminescent (OSL) dosimeters. Then, the initial substantial reduction in personal dose for residents was compared with that in the air dose rate. The effect of school, nursery, and community center yard decontamination on the $H_p(10)$ values for residents was evaluated. For area monitoring of penetrating radiation such as gamma rays emitted from Cs nuclides, the ambient dose equivalent [$H^*(d)$], with $d = 10$ mm, which is written $H^*(10)$, is used as the operational quantity. The personal dose equivalent [$H_p(d)$] is the dose equivalent in the International Commission on Radiation Units and Measurements (ICRU) tissue at a depth d in a human body below the position where an individual dosimeter is worn. For monitoring effective dose, $d = 10$ mm is recommended, and $H_p(d)$ is written $H_p(10)$.

19.2 Methods

The $H_p(10)$ for 54 Marumori and 71 Kosugo residents was evaluated starting 1 September 2011 and 16 December 2011, respectively, until the end of March 2013. The numbers of residents increased to 60 and 90 for Marumori and Kosugo residents after 31 August and 29 October 2012, respectively (150 in total). The residents mainly consisted of preliminary-school children and preschool children, and a few of them were the adults in their families. The territories in Marumori for which data were collected were geographically divided into three regions, Kawadaira, Hippo, and Koya, because the ^{137}Cs deposition levels varied markedly in these regions [1]. The measurements were carried out using OSL personal dosimeters, and an OSL reader (InLight badge and microStar system; Nagase Landauer). In this study, readings were repeated three times. According to the specifications of the system, doses in excess of 100 μSv are measured within ±10 % standard deviation for an average value of three readings. Dosimeters were calibrated following the Japanese International Standard JIS Z 4511 [6]. The deviation in the energy-independent response for photons from 24 keV to 1.25 MeV is within ±10 %. The dosimeters that we used are small devices that can be worn on a neck strap. When worn close to the torso, they measure the radiation exposure of the entire body. Each dosimeter was used by an individual, one by one, and read out approximately every 2 months (1.3–2.9 months) to obtain readings. The correct way to wear the OSL dosimeter was explained to the residents, and dosimeters were distributed to those

who were willing to wear the dosimeters themselves or were willing to strap them onto their children. The residents were instructed to record their daily activities and to confirm that they followed the instructions for wearing the dosimeter correctly for the entire period of time that dosimeters were worn. The dosimeter data collected from individuals who did not follow the instructions were excluded from the analysis. All the procedures performed in this study are in accordance with the ethical guidelines for scientific studies, as stipulated by Tohoku University, and the personal information of the subjects has been carefully protected.

The data for air dose rates in the Marumori and Kosugo regions were acquired from the data that were recorded by the local governments [7, 8] through the use of an NaI scintillation survey meter over the same period from September 2011 to March 2013, and the temporal variations in the rates from Cs nuclides after the decay of ^{131}I were investigated.

The measurement data were reflective of the radiation from both the Fukushima Daiichi fallout and natural sources. Therefore, air dose rates and external exposure doses from natural radiations, which were estimated to be 0.51 and 0.63 mSv/y [9], respectively, in Japan (from cosmic radiation and natural terrestrial radiation), were subtracted from each measured value.

19.3 Results and Discussion

19.3.1 Air Dose Rates

In Fig. 19.2a, b, air dose rates (ambient dose equivalents [$H^*(10)$]) from 1 September 2011 to the end of March 2013 in the Marumori and Kosugo regions are shown. The territories studied in Marumori were divided into three regions, Kawadaira, Hippo, and Koya (Fig. 19.1) as mentioned above. In Fig. 19.2a, the values in three measurement locations of Kawadaira (blue diamonds), Koya (red triangles), and Hippo (green circles) are shown. The three measurement locations shown in Fig. 19.2b are the Kosugo elementary school (blue diamonds), a nursery school (red squares), and a community center (closed green triangles). The symbols are used indicate measured $H^*(10)$ values, and the calculated values obtained by Eq. (19.1) below are indicated by solid lines in the figures.

The air dose rate data were analyzed by comparing them with the calculated rates that accounted for the radioactive decay of ^{134}Cs and ^{137}Cs. The ^{134}Cs/^{137}Cs activity ratio for Fukushima is close to 1 in most published data [10]. The effective doses E(t) were calculated using Eq. (19.1):

$$E(t) = E(0) / 3.7 \times \left\{ 2.7 \times \exp\left(-\lambda_1 t\right) + \exp\left(-\lambda_2 t\right) \right\}, \tag{19.1}$$

where λ_1 and λ_2 are the decay constants of ^{134}Cs and ^{137}Cs, respectively. From the effective dose rate constants of radionuclides, which are listed in the *Table of*

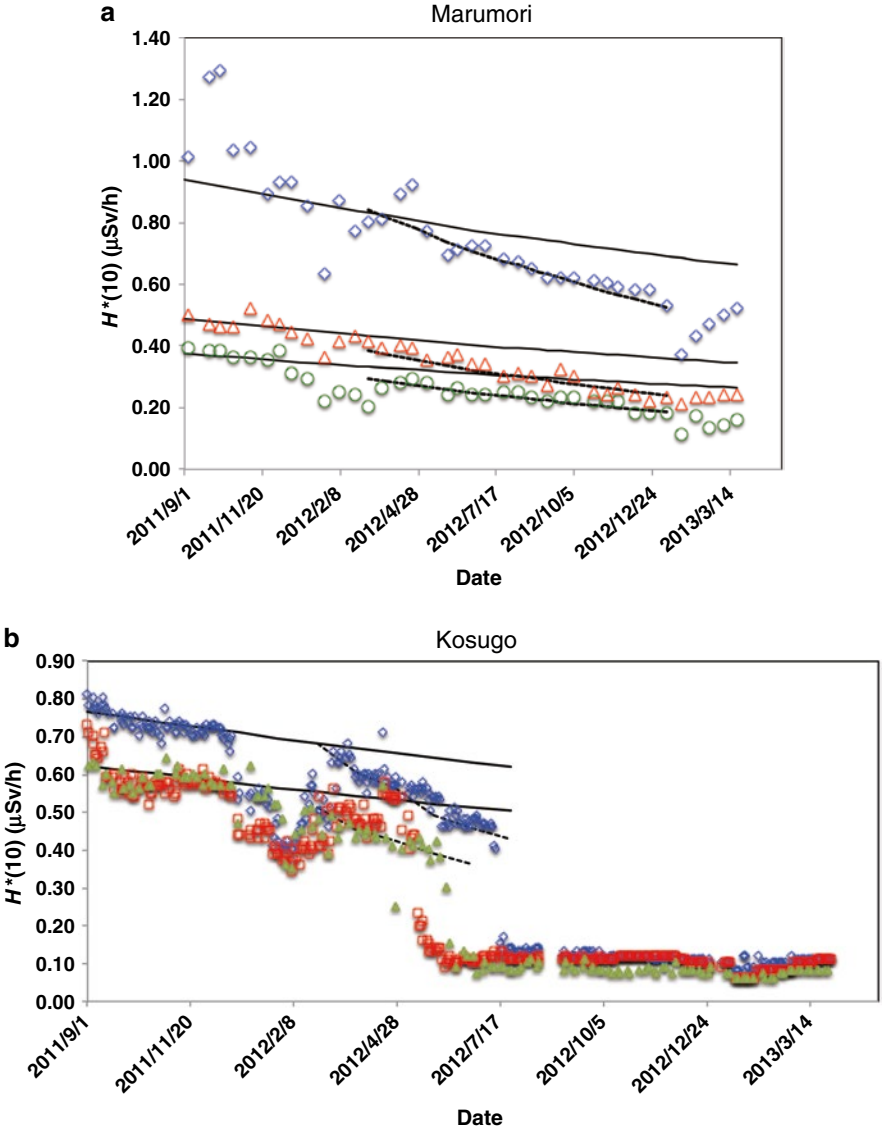

Fig. 19.2 Air dose rates (ambient dose equivalents [$H^*(10)$]) in Marumori (**a**) and Kosugo (**b**) regions. The values in three measurement locations of Kawadaira (*blue diamonds*), Koya (*red triangles*), and Hippo (*green circles*) are presented in **a**. Three measurement locations in **b** are the Kosugo elementary school (*blue diamonds*), a nursery school (*red squares*), and a community center (*closed green triangles*). Calculated values, which are obtained by Eqs. (19.1) and (19.2), are indicated by *solid* and *dotted lines*, respectively. A faster reduction than the radioactive decay of ^{134}Cs and ^{137}Cs appears after the thawing of snow in both regions

Isotopes, 10th edition [11], as 0.211 and 0.0779 for ^{134}Cs and ^{137}Cs, respectively, the proportion of ^{134}Cs that contributed to the total effective dose was calculated to be 2.7 times higher than that of ^{137}Cs. The value of E (0) was the measured value for each region, which represented the location factor. In settlements in urban and rural areas, the characteristics of the radiation field differ considerably from those over an open plot of undisturbed land, which is used as the reference site and starting point for calculation of external dose to people from deposited activity. These differences are attributable to varying source distributions as a result of deposition, runoff, weathering, and shielding. All such effects can be summarized by the term location factor [2].

The data plotted in Fig. 19.2 show similar patterns until air dose rates dropped at the three measurement locations in Kosugo after decontamination (Fig. 19.2b). The observed long-term decrease in the plotted values is in accordance with the predicted radioactive decay process of ^{134}Cs and ^{137}Cs from summer 2011 to December 2011. During the heavy snow season, air dose rates dropped and remained low from January to early March in 2012. After the snow thawed, the air dose rates returned to previous levels and then followed a relatively faster reduction than the radioactive decay rate of ^{134}Cs and ^{137}Cs. This reduction is considered to be caused by weathering from snow melting or migration of radionuclides down the soil column [2–4]. The half-lives of this faster reduction in the air dose rate were estimated to be the same at all three measurement locations of the Marumori and Kosugo regions, and only slight differences in half-lives were observed between the two regions; these were estimated as 450 and 300 days in Marumori and Kosugo, respectively, using Eq. (19.2):

$$E'(t) = E'(0) \times \exp(-\lambda_3 t), \tag{19.2}$$

where λ_3 is the decay constant. Values calculated using Eq. (19.2) are shown using dotted lines in the figures. In Fig. 19.2b, all the air dose rate values dropped sharply between May and July 2012 because of the decontamination carried out for the yards of the elementary school, nursery school, and community center in Kosugo. In Marumori, decontamination of school and nursery yards was conducted in July 2011 but had not been carried out at the three measurement locations during the time measurements were being taken.

19.3.2 Personal Dose Equivalent for Residents

In Fig. 19.3 the *H*p(10) of residents in Marumori and Kosugo regions are shown. The recorded *H*p(10) values for approximately 2 months (1.3–2.9 months) were converted into monthly dose. In Fig. 19.3a, average values of *H*p(10) for Kawadaira (blue diamonds), Koya (red triangles), and Hippo (green circles) residents are shown. The average values for Kosugo residents are indicated using circles in Fig. 19.3b. Error bars show 1 standard deviation for each value. The decrease in *H*p(10) for the residents of the Marumori and Kosugo regions differs significantly.

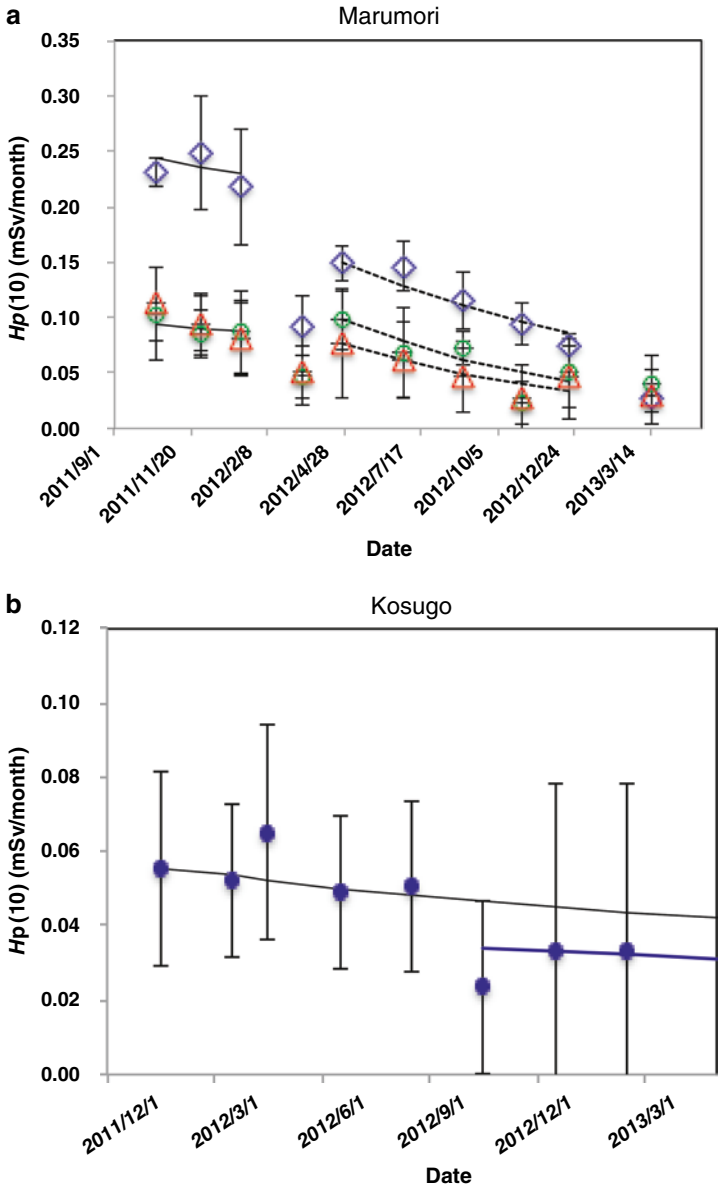

Fig. 19.3 *Hp*(10) of residents in Marumori (**a**) and Kosugo (**b**) regions. Each average value of *Hp*(10) for Kawadaira (*blue diamonds*), Koya (*red triangles*), and Hippo (*green circles*) residents is presented in **a**. The average value of Kosugo residents is shown as a *circle* in **b**. *Error bars* show 1 standard deviation for each value. Calculated values, which are obtained by Eqs. (19.1) and (19.2), are described as *solid* and *dotted lines*, respectively. Neither a drop caused by an accumulation of snow nor a faster reduction, except decontamination of the schoolyard, was observed in *Hp*(10) for Kosugo residents in **b**

The *H*p(10) of Marumori residents show a similar pattern to that observed in air dose rates: values drop during the heavy snow season, and faster reduction than the radioactive decay of ^{134}Cs and ^{137}Cs is observed after the thawing of snow (dotted line, Fig. 19.3a). The values of the half-lives of the rapid reductions in *H*p(10) were estimated to be 200–400 days according to Eq. (19.2); these values are consistent with the corresponding half-lives in air dose rates. For Kosugo residents, neither a drop caused by the accumulation of snow nor a faster reduction was observed in the *H*p(10) values, and only a decrease that could be attributed to the radioactive decay of ^{134}Cs and ^{137}Cs was observed (solid line, Fig. 19.3b), resulting in a slow decline in dose. The main difference between two regions is their living environment; the former is a rural settlement, whereas the latter is a suburban city along a freeway. In our previous study [12], we showed that the individual exposure dose depends on the indoor ambient dose equivalent rather than the outdoor ambient dose equivalent in each resident's dwelling. The discrepancy between the air dose rate and *H*p(10) for Kosugo residents might be caused by dose contributions from the fixed contamination in houses in the suburban environment of Kosugo. In Marumori, decontamination of school and nursery yards was conducted in July 2011 before *H*p(10) measurements for residents were initiated. Thus, no reduction on *H*p(10) values from the decontamination was observed in the readings during the measurements. In Kosugo, slow decontamination was carried out in July 2012, reducing the air dose rates in schoolyard from 0.46 to 0.19 μSv/h (Fig. 19.2b). Its effect on the *H*p(10) values for residents (preliminary-school children) was not observed in the readings recorded in September [13], but have been observed since October 2012 after school summer holidays ended (Fig. 19.3b), and dose reduction was evaluated as approximately 10–20 μSv/month on average. Figure 19.3b also shows that the *H*p(10) values for Kosugo residents have been declining in accordance with the radiocesium decay after decontamination as well.

References

1. Radiation Distribution Map by Nuclear Regulation Authority (2013) http://ramap.jmc.or.jp/map/mapdf/5640.html. Accessed 23 July 2013
2. IAEA (2006) Environmental consequences of the Chernobyl accident and their remediation: twenty years of experience. Report of the Chernobyl forum expert group 'Environment'. IAEA
3. Golikov VY, Balonov MI, Jacob P (2002) External exposure of the population living in areas of Russia contaminated due to the Chernobyl accident. Radiat Environ Biophys 41:185–193
4. Likhtarew IA, Kovgan LN, Jacob P, Anspaugh LR (2002) Chernobyl accident: retrospective and prospective estimates of external dose of the population of Ukraine. Health Phys 82:290–303
5. Nuclear Regulation Authority (2013) http://radioactivity.nsr.go.jp/ja/contents/3000/2372/view.html. Accessed 23 July 2013

6. Japanese Industrial Standards (JIS) (2005) Methods of calibration for exposure meters, air kerma meters, air absorbed dose meters and dose-equivalent meters. JIS Z 4511. Japanese Standards Association
7. Marumori Town Official Website (in Japanese) (2013) http://www.town.marumori.miyagi.jp/genpatsu/oshirasebacknumber.html. Accessed 23 July 2013
8. Shiroishi City Official Website (in Japanese) (2013) http://www.city.shiroishi.miyagi.jp/section/taisaku/etc/kekka.html. Accessed 23 July 2013
9. Nuclear Safety Research Association (NSRA) (2011) Seikatsu Kankyo Hosyasen, New edition. NSRA (in Japanese). Nuclear Safety Research Association, NSRA
10. KEK High Energy Accelerator Research Organization (2013) Measurement result of airborne nuclide and air radiation level in Tsukuba area. First–10th report 2011. KEK, JP (in Japanese). http://www.kek.jp/quake/radmonitor/. Accessed 23 July 2013
11. Japan Radioisotope Association (2001) Radioisotope pocket data book, 10th edn. Maruzen, Japan (in Japanese)
12. Yoshida-Ohuchi H, Hirasawa N, Kobayashi I, Yoshizawa T (2013) Evaluation of personal dose equivalent using optically stimulated luminescent dosemeters in Marumori after the Fukushima nuclear accident. Radiat Prot Dosim 154:385–390
13. Yoshida H, Saito J, Hirasawa N, Kobayashi I (2012) Initial substantial reduction in air dose rates of Cs origin and personal doses for residents owing to the Fukushima nuclear accident. In: Proceedings of environmental monitoring and dose estimation of residents after accident of TEPCO's Fukushima Daiichi nuclear power stations. The conference was held in Kyoto (Kyoto University), 2012